PODZOLS: ASPECTS OF THEIR CHEMISTRY AND DEVELOPMENT

A thesis
submitted in partial fulfilment
of the requirements for the degree
of
Doctor of Philosophy in Chemistry
in the
University of Canterbury

by

M. C. Taylor

University of Canterbury

1980

PHYSICAL
SCIENCES
LIBRARY
THESIS
copy 2

A B S T R A C T

Work for this thesis focussed on the complexing of iron (II) and iron (III) in aqueous solution with five polyphenolic ligands, gallic acid, pyrogallol, protocatechuic acid and tiron. These ligands were chosen as model compounds for the larger polymeric species known to be present in the soil system and thought to be important in the translocation of iron in podzol formation.

The iron (III)/polyphenol system was characterised by the formation of very stable 1:1 and 2:1 complexes in the pH range relevant to podzol formation (i.e. 3.0 - 7.0) and 3:1 complexes at higher pH. Ligands for which the standard reduction potential of the corresponding o-quinone was < 0.9 V underwent a redox reaction with Fe^{3+} at low pH (< 3.0). The formation of complexes with Fe^{3+} at higher pHs was critically dependant on dissolved oxygen concentration.

No complex formation, between Fe(II) and the ligands studied, was observed below pH 7. Stability constants have been determined for complexes between Fe^{2+} and the ligands gallic acid and catechol. Protonation constants for gallate and catecholate anions have also been determined.

The calculation of stability and protonation constants required accurately known hydrogen ion concentrations. For this reason a calibration relationship was established between pH, measured by the glass/calomel electrode assembly, and hydrogen ion concentration, calculated from buffer solutions of o-phthalic acid/potassium hydrogen phthalate.

The response of the glass/calomel electrode pair to various standard buffers over the pH range 1.7 - 12.5 has been characterised in terms of a "non-Nernstian" response throughout this pH range, with deviations attributed to the effect of the liquid-junction superimposed in the high and low pH regions (i.e. $3.5 > pH > 9.2$).

The status of an undeveloped podzolic soil on the West Coast, South Island, New Zealand, is discussed as background to the metal-ligand study. Thus, results are presented for various chemical and physical properties of the soil including important features of the clay mineralogy. The development of this soil as an agricultural unit has also been studied with data collected for important plant and animal nutrients over a period of 5 years.

A C K N O W L E D G E M E N T S

I am extremely grateful to Dr H.K.J. Powell, whose patient and thoughtful encouragement made an invaluable contribution to this work.

I am also thankful for the assistance of the technical staff of the Chemistry Department, especially Messers F Downing and B Reid; Messers R Lee and G Mew, of N.Z. Soil Bureau; Messers R Austin, E Cameron and B Bell of the Department of Lands and Survey; Messers A W Young and A S Campbell of the Soil Science Department, Lincoln College and Dr D A House of the Chemistry Department, University of Canterbury.

Lastly, I am grateful to my wife, Kathryn, who has faithfully supported me in the preparation of this thesis, especially in the many hours typing the manuscript.

This thesis is dedicated to

my parents

who have always encouraged

me to study

C O N T E N T S

INTRODUCTION

In the process of soil formation, the action of physical, chemical, and biochemical forces gives rise to a horizontal layering within the soil mass and a soil "profile" is developed. Such characteristics as texture, depth, colour and chemical properties distinguish the various soil "horizons" and help determine the agricultural value of the soil as a whole. Soil profiles are unique and their development depends on the particular combination of soil forming factors in the geographic region. Jenny [1] has described five such factors, namely: climate (especially temperature and precipitation), living organisms (especially the native vegetation), nature of the soil-parent material (its texture, structure, chemical and mineralogical composition), topography of the region, and the time over which parent materials are subjected to soil forming processes.

The Nature of Podzols

Because of their widespread occurrence and their unique chemical and physical features, the group of soils known as "podzols" has received considerable attention in soil studies. Podzolic soils develop most readily in moist temperate climates under forest or heath vegetation. As a result of intense weathering, in particular the vertical movement of soil constituents, profile layering in these soils is quite distinct. Podzols are often characterised by abundant surface accumulation of organic matter (horizon designated as A_0), that on decomposition yields organic acids and humic substances capable of mobilizing sesquioxides of iron and aluminium. Fungi are often the major microorganisms involved in the production of the humus. In podzols bacterial activity and earthworm population are at a minimum [2]. If vigorous podzolization is to occur sufficient moisture must be present to promote marked leaching. Leaching occurs when the acids of the organic horizons are carried downward through the mineral layers below, dissolving and removing any carbonates and other

soluble salts leaving the "A" horizons (topsoil) highly acidic (pH ca. 4.0 - 4.5). Colloidal complexes of this horizon are broken up and iron and aluminium removed in assoication with humic substances. These are carried down the soil profile and accumulate in the "B" horizons (subsoil). A drastically leached (eluvial) horizon (designated as A_2) is left in a highly acid, siliceous condition and often assumes a bleached, grey appearance. The term podzolization (from the Russian, *pod* meaning "under" and *zola*, "ash") is associated with these characteristic soil forming features.

The Mobilization of Iron and Aluminium in Podzolic Soils

The mobilization and translocation of iron and aluminium is a fundamental characteristic of podzol profile development. Several mechanisms have been proposed for this movement from the A horizons and subsequent deposition in the lower B horizons. The processes and reactions involved in these mechanisms are not fully understood, although it is generally accepted that soil organic matter is implicated. Stobbe and Wright [3] have described three possible mechanisms:

(1) Under strongly reducing acidic conditions, such as those found in "gleyed" or ground-water podzols, in which the soil is saturated with water for appreciable periods of the year, iron may be mobilized as the ferrous cation. Subsequent oxidation and precipitation as ferric-iron in the lower horizons could occur during periods of desiccation (and aeration).

(2) A more widely-held theory developed by Deb [4], involves the transport of iron and aluminium oxides as humus-protected sols. The mechanism of deposition in the B-horizon, assumed by earlier workers, required precipitation of the oxides by divalent cations. This was challenged by Deb who suggested that the processes governing precipitation are of a microbiological rather than colloidal or chemical nature.

(3) A third possible mechanism involves the transport of iron and aluminium as soluble metal-organic complexes.

Early work in this field indicated that sesquioxides of iron and aluminium are dissolved by organic acids, formed from the decomposition of soil organic matter. Jones and Wilcox [5] considered that iron and aluminium were associated with hydroxy-acids (R) forming salts of the type $Fe_2R_3 \cdot Fe_2O_3$. Rode [6] postulated, as one of four possible mechanisms for the movement of iron and aluminium oxides, the formation of soluble organo-mineral complexes of organic acids. He suggested that iron and aluminium were involved as part of the anionic complex of "fulvic" acid and to a lesser extent "humic" acid. Schnitzer [7] has suggested that fulvic acid is likely to be the most prominent humic compound in the "soil solution" and therefore involved in many of the important soil reactions, including those associated with podzolization. His investigations indicated that fulvic acid forms complexes with many divalent and trivalent metal ions, the most stable of which are with iron(III) and aluminium.

While soil humic matter is commonly regarded as being responsible for the translocation processes of podzolization, Bloomfield has suggested [8] that constituents of undecomposed plant material are far more important mobilizing agents, either as such or as the energy source for microbial action.

Schnitzer et al. [9] demonstrated that aqueous extracts of deciduous and coniferous leaves were capable of dissolving hydrous oxides of iron and aluminium. Bloomfield showed [10-16] that sterile aqueous extracts of the leaves and the bark of over thirty different tree species, including New Zealand rimu *(Dacrydium Cupressium)* and kauri *(Agathis Australis)*, were capable of dissolving significant amounts of ferric oxide. While other workers [17-21] have also noted the ability of aqueous extracts of fresh tree litter to dissolve iron and aluminium hydrous oxides, the mechanism of the corresponding soil processes has been the subject of considerable debate.

Bloomfield has suggested [16,22,23] that dissolution of ferric oxide by water-soluble organic compounds, leached from the overlying tree litter, is followed by reduction of the dissolved ferric iron to ferrous iron. The solution and reduction of ferric oxide is brought about by carboxylic acids and polyphenols, the latter being primarily responsible for the reduction process. Bloomfield reported the reduction of ferric ion even under aerobic conditions. The iron is apparently transported in a stable ferrous-organic complex.

Schnitzer and DeLong [24-26] have presented evidence that most of the iron mobilized from ferric hydroxide by either laboratory-prepared extracts, natural rainfall leachates of decomposing leaves or by rainfall dripping from the canopy of forest species, is in the ferric state. They also concluded that the active agent present in extracts and leachates of decomposing poplar leaves had characteristics of an acidic polysaccharide. Furthermore the process of mobilization was considered to be primarily one of peptization of the oxide by the acidic polysaccharides, a view supported by Loissant [17].

More recently Ellis [21] has distinguished between the mobilization of iron from hydrous and anydrous ferric oxides, the active agents being organic acids and phenolic compounds respectively.

Deposition of iron and aluminium in podzol B horizons has been variously explained. Jones and Wilcox [5] postulated the precipitation of sesquioxides as basic salts while others [4,27] maintain that microorganisms are responsible for the destruction of the organic compounds involved in the metal complex. Bloomfield noted that the immobilization of sesquioxides is associated with the sorption of the complexes on the mineral soil materials and suggested [28] that drying and/or aeration brought about the deposition reactions.

Chelation Reactions in Soil Development

Schwarzenbach [29] in classifying complexing agents described chelation complexes as mononuclear species formed with multidentate ligands; if charged these species are highly soluble in water. Agricultural interest in chelating agents has grown rapidly with most of the studies being focussed on synthetic metal chelates and their use in plant nutrition [30]. However, comparatively little attention has been devoted to the role of chelation as a natural phenomenon in the soil. In discussing soil development, Barshad [31] postulated that the translocation of iron and aluminium down the soil profile is due, in part, to chelation with certain organic substances. Swindale and Jackson [32] introduced the term "cheluviation" to explain a process that may contribute to podzolic soil formation. They described it as a "process in which minerals are decomposed by chelation in solution and eluviation." The process would remove "aluminium, iron and other strongly chelated elements faster than it would silicon and other weakly chelated elements."

The identification and characterization of chelated complexes in the soil has been difficult to establish and the evidence for chelation has largely been circumstantial. Atkinson and Wright [33] leached a column of calcareous soil material with a known chelating agent (EDTA) and showed that, under the right conditions, iron and aluminium were mobilized, transported and redeposited to give a podzol-like profile with well-defined horizons. Additional evidence, including the successful use of natural and synthetic chelating agents to extract metals and organic matter from the soil and data from titration curves of organic matter in the presence of various metals, has been reviewed by Mortensen [34].

Chelating Agents

The likely participation of metal chelation reaction in soil processes is further strengthened by the proven chelating properties of certain organic substances known to be present in the soil environment. Many organic

compounds have been isolated and identified in soil and plant extracts. Most of the principle chelating donor groups are represented in these compounds. In particular, amino, imino, keto, hydroxy, thioether, carboxylate and phosphonate groups are present in compounds which have been separated from soil organic matter [34]. It is likely that many of these chelating sites occur in polymers or mixtures of polymers such as lignin, polysaccharides, tannins and other polyphenols, proteins and quinones. Simple, low molecular weight amino acids, aliphatic and aromatic acids, monosaccharides and phenolics have also been identified in soil organic matter and aqueous leaf extracts [35-42].

In studies related to the mobilization of iron in soil development, attention has been largely focussed on the possible participation of iron-phenolic complexes. Bloomfield has suggested that polyphenols are the active chelating agents in aqueous leaf extracts [16] and Coulson et al.[43] have identified such compounds in leaves, litter and superficial humus. White [44] has suggested that tannin and tannin-like polymers, which are strong iron-chelating agents, are present in soil organic matter. Building blocks of polymeric phenolics, such as catechol, protocatechuic acid, gallic acid, ellagic acid, resorcinol and others have also been isolated [34]. McHardy et al.[45] used iron chelates of protocatechuic acid, catechol, resorcinol and pyrogallol in the study of the formation of iron oxides by decomposition reactions. They showed that these complexes can be decomposed to yield crystalline ferric oxides and postulated a possible inorganic decompostion mechanism for metal-organic chelates in the soil. They noted that, while such simple compounds probably have only a transitory existence in soils, they serve as useful models for the understanding of the properties of the more complex polymeric forms. Coulsen et al.[18] used the polyphenols, D- and epi-catechin (known to be present in leaf extracts) as model chelating agents in their study of the reduction and transport of iron in an artificial soil column,while Hingston [19] investigated the stability of iron complexes of tannic and gallic acids.

This Work

The aim of this work was to focus attention on the possible role of phenolic compounds in the mobilization of iron in soils where the podzolization process is important.

Part A of this thesis describes a detailed study of the acid-base properties of dilute aqueous solutions containing ferrous or ferric iron and various ortho-dihydroxy benzenes selected as simple model compounds of the more complex polyphenols thought to be among the active agents in podzolization. The five phenolic ligands used in this study are illustrated in figure 1. Potentiometric and spectrophotmetric data were used in the calculation of ligand protonation constants and metal ligand stability constants for two ferrous complexes and in studying the stoichiometry of ferric complexes. The sensitivity of the iron-phenolic systems to atmospheric oxygen (as a function of pH) was also investigated.

To complement this equilibrium study, a comprehensive survey was carried out on a gleyed podzol soil on the west coast of the South Island, New Zealand. The status of the soil in the region sampled was characterized in terms of its physical, chemical and mineralogical properties and the soil, water and herbage levels of certain plant and stock nutrients were monitored before and during agricultural development. This is the subject of part B.

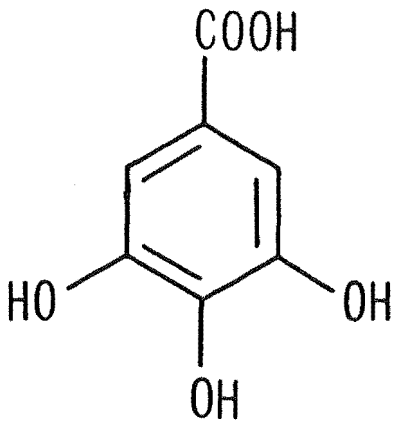

GALLIC ACID

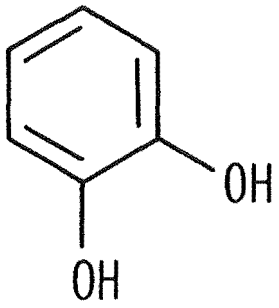

CATECHOL

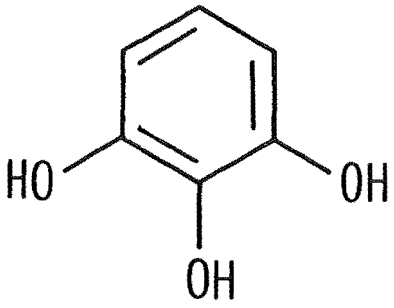

PYROGALLOL

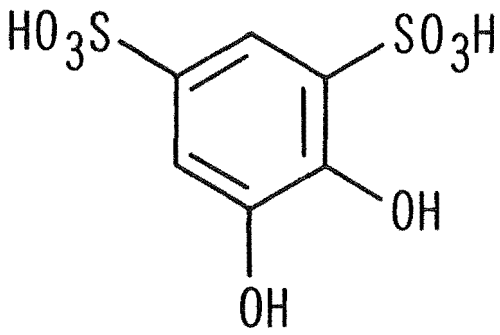

TIRON

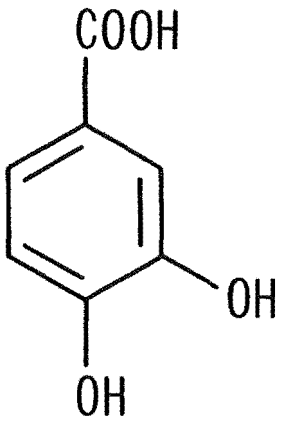

PROTOCATECHUIC ACID

Figure 1 Model Ligands

PART A

THE STUDY OF IRON COMPLEXES WITH ORTHO-DIHYDROXY BENZENES

CHAPTER 1

PREFACE TO PART A

1.1 Metal Ligand Complex Formation In Aqueous Solution

A complex has been defined as "a species formed by the association of two or more simpler species each capable of independent existence" [46]. When one of the simpler species is a metal ion, the resulting entity is known as a metal complex. The negative ion or polar molecule bound to the metal is known as a ligand. Some ligands are attached to the metal ion by more than one donor atom, forming a heterocyclic ring called a "chelate" ring.

The stability of a metal complex in solution is defined in terms of equilibria of the general type (charges are omitted for clarity):

$$M + nL \rightleftharpoons ML_n \qquad (1.1)$$

Applying the law of mass action to equation 1.1 the overall thermodynamic "stability constant" for the reaction may be written as:

$$\beta_n^\circ = \frac{a_{ML_n}}{a_M\, a_L^n} = \beta_n \cdot \frac{f_{ML}}{f_M\, f_L^n} \qquad (1.2)$$

where β_n represents the overall "concentration quotient" and is given by:

$$\beta_n = \frac{c_{ML_n}}{c_M\, c_L^n}$$

a_M is the activity, c_M the concentration, and f_M the activity coefficient of species M etc. Reaction 1.1 usually proceeds via a series of stepwise equilibria in which just one additional ligand is added to the complex, i.e.:

$$M + L \rightleftharpoons ML$$

$$ML + L \rightleftharpoons ML_2 \text{ ... etc.}$$

Stepwise thermodynamic stability constants K_n°, or concentration quotients K_n, are assigned to each of these equilibria and are related to β_n° and β_n as follows:

$$\beta_n^\circ = \Pi K_n^\circ \qquad (1.3)$$

$$\beta_n = \Pi K_n \qquad (1.4)$$

Conventionally, concentration quotients are also termed "stability constants ".

Where the ligand species is the conjugate base of a weak acid, various protonation equilibria must be considered also. For example:

$$nH + L \rightleftharpoons LH_n$$

for which

$$\beta_n^H = \frac{a_{LH_n}}{a_H^n \, a_L} \qquad (1.5)$$

These equilibria occur in competition with metal-ligand equilibria (see section 4.1.1).

Many different methods may be used to measure stability constants of metal ligand complexes [46]. Among them is a potentiometric method based on the use of an electrode reversible to hydrogen ions. This technique has been employed in this work. Knowledge of the various stability constants for a given system can provide valuable information about the equilibrium concentrations of metal ligand species in solution as well as predicting the conditions required for complete formation of a particular complex. This information has had application in analytical separation procedures, the rationalisation of kinetic and optical properties and, of special relevance to this work, the study of the role of metal chelates in natural systems.

1.2 Acid - Base Properties of Iron - polyphenol Systems

Ferrous iron forms complexes of comparatively low stability with phenolic ligands. Tyson and Martell [47] have reported the formation of

1:1 and 1:2 metal:ligand complexes between divalent transition metal ions (including ferrous) and o-dihydroxybenzene (catechol). The stepwise stability constants (expressed as concentration quotients in 1.0 mol dm^{-3} KNO_3 at 25 °C) were 7.95 and 5.54 for log K_1 and log K_2 respectively.

Tervalent iron on the other hand forms very stable coloured complexes with many hydroxybenzoic acids and polyphenols; stability constants K_1 are ca. 10^{19}. The marked affinity of ferric iron for oxygen-containing ligands and other electronegative ligands has prompted its classification, along with other small highly-charged metal ions such as Al^{3+}, Mg^{2+} and U^{4+}, as a "class A" acceptor ion [48,49]. The reaction between ferric iron and phenols with the associated formation of characteristic blue, purple or red solutions is well known and has been used as a qualitative test for the aromatic hydroxyl group. Spectrophotometric data for this reaction have been tabulated and discussed for a number of phenols [50,51]. In addition, quantitative colorimetric analyses for both iron and polyphenols, based on complexation reactions, have been used [52,53]. Other applications of the iron-phenol reaction have included the manufacture of writing inks (a reaction between Fe(III) and polyphenols such as gallic and tannic acids) and studies on the transport of iron in microorganisms [54,55].

Despite the long-standing interest in these reactions, the available data on the composition and stability of the complexes of iron (III) with phenolic ligands are far from complete. This may be attributed in part to difficulties associated with side reactions of the metal or ligand, or both, accompanying complex formation. Ferric ion undergoes extensive hydrolysis in aqueous solution forming such species as $FeOH^{2+}$, $Fe(OH)_2^+$ and $Fe_2(OH)_2^{4+}$. The hydrolytic processes involved are often slow reactions especially where polymerisation occurs [56].

Because of similar or lower reduction potentials of many polyphenol ligands relative to that of the Fe^{3+}/Fe^{2+} couple (E° = 0.749 V)[57]

equilibrium studies have been plagued by complicating redox processes. For example, some catechol-type ligands (ortho-dihydroxy benzenes) are thought to undergo oxidation to the corresponding ortho-quinone (qno) in the presence of Fe^{3+}: [58]

$$2Fe^{3+} + H_2cat \rightleftharpoons 2Fe^{2+} + qno + 2H^+$$

In addition, this redox process will be pH - dependant; but little work has been done to characterise the nature of this dependence, especially in relation to competitive pH - dependent complex formation between Fe^{3+} and the conjugate base of H_2cat.

A further complication is sometimes introduced when the polyphenol ligand in question is subject to (pH - dependent) oxidation by atmospheric oxygen in aqueous solution. Alkaline solutions of pyrogallol are well known for their ability to absorb oxygen and polyphenols such as gallic acid have been used as antioxidants [59].

Table 1.1 summarizes some of the properties of iron (III) - o-dihydroxy ligand systems.

Table 1.1 Properties of Iron (III) - o-dihydroxy Systems

Ligand (a)	Protonation Constants for Ligand Species (b)	Redox Reactions (c)	Iron(III) - Ligand Complexes		E° (f)
			Stability Constants (d)	Spectrophotometric Data (e)	
(1) 1,2 dihydroxy - 3,5-benzene disulphonic acid (Tiron), LH_2 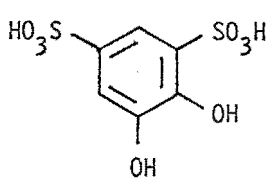	$\log k_1$ = 12.51 $\log k_2$ = 7.67 (0.1 M KNO_3 & $NaClO_4$) (60)	No redox reaction with Fe^{3+} (61)	$\log K_1$ = 17.6 $\log K_2$ = 14.9 $\log K_3$ = 11.2 (0.1 M KNO_3) (60) K_{f1} = 1.45 (1.0 M $NaClO_4$) (61)	1:1, λmax = 670 - 676 nm ε = 1900 2:1, λmax = 560 - 562 nm ε = 4570 3:1, λmax = 478 - 482 nm ε = 6200 (60)	0.955 V (62)
(2) 4-cyano - 1,2-dihydroxy-benzene, LH_2 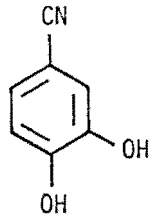		No redox reaction with Fe^{3+} (61)	K_{f1} = 2.05 (1.0 M $NaClO_4$) (61)	Data imply 1:1 complex formed with λ max somewhere in the region 635 - 700 nm (61)	0.924 V (62)

(3) 4-nitro -1,2-dihydroxybenzene, LH_2 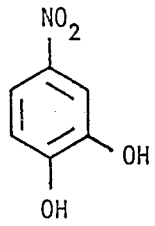	$\log k_1$ = 10.8 $\log k_2$ = 6.65 (27.1 °C, no background electrolyte) *(54)*		$\log K_1$ = 18.2 $\log K_2$ = 14.2 $\log K_3$ = 9.2 (27.1 °C, no background electrolyte) *(54)*		
(4) 3,4-dihydroxy-benzoic acid (Protocatechuic Acid), LH_3 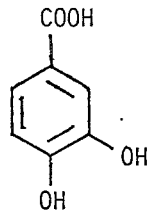	$\log k_1$ = 13.12 $\log k_2$ = 8.64 $\log k_3$ = 4.25 *(63)*	No redox reaction with Fe^{3+} *(61)*	$\log K_1$ = 19.0 $\log K_2$ = 14.3 $\log K_3$ = 10.1 *(63)* K_{f1} = 0.102 (1.0 M $NaClO_4$) *(61)*	1:1, λmax = 620 - 630 nm ϵ = 2380 2:1, λmax = 570 nm ϵ = 4300 3:1, λmax = 490 nm ϵ = 5700 *(63)*	0.885 V *(62)*
(5) 2,3 dihydroxy-benzoic acid, LH_3 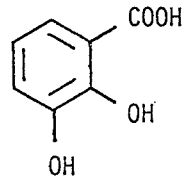	$\log k_1$ = 13.1 $\log k_2$ = 10.06 (27.1 °C, no background electrolyte) *(54)*		$\log K_1$ = 7.3 $\log K_2$ = 4.3 (27.1 °C, no background electrolyte) *(54)*		

(6) (-)-1-(3'4'-dihydroxyphenyl) -2-(methylamino) ethanol (Adrenaline), LH_4 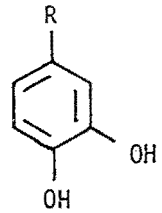 R = $CH_3NH_2CH_2CH(OH)$-	$\log k_1$ = ca. 13 $\log k_2$ = ca. 13 $\log k_3$ = 9.95 $\log k_4$ = 8.66 (0.1 M KCl) *(64)*	Ligand oxidised to o-quinone with Fe^{3+} *(61)*	K_{f1} = 0.069 (1.0 M $NaClO_4$) *(61)*	As for ligand 2	0.812 V *(62)*
(7) 3,4-dihydroxy-phenyl acetic acid, LH_3 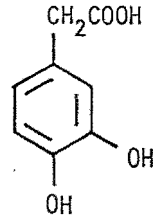	$\log k_1$ = 13.7 $\log k_2$ = 9.49 (27.1 °C, no background electrolyte) *(54)*		$\log K_1$ = 14.9 $\log K_2$ = 8.8 (27.1 °C, no background electrolyte) *(54)*		
(8) 3-(3,4-dihydroxyphenyl)-2-amino-propanoic acid (L-Dopa), LH_4 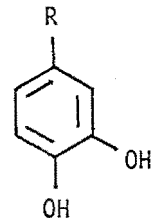 R = $HOOCCH(NH_2)CH_2$-	$\log k_1$ = 13.4 $\log k_2$ = 9.74 $\log k_3$ = 8.71 $\log k_4$ = 2.31 (1.0 M KNO_3) *(65)*	Ligand oxidised to o-quinone with Fe^{3+} *(61)*	K_{f1} = 0.051 (1.0 M $NaClO_4$) *(61)*	As for ligand 2	0.798 V *(62)*

(9) 1,2-dihydroxybenzene(Catechol), LH_2 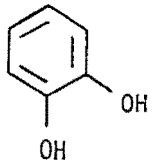	$\log k_1$ = 13.05 $\log k_2$ = 9.23 (1.0 M KNO_3) *(47)*	Ligand oxidised to o-quinone with Fe^{3+} *(58)* Redox reaction with Fe^{3+} below pH 2.3 reversible over short periods of time with addition of base *(54)*	$\log K_1$ = 20.0 $\log K_2$ = 14.7 $\log K_3$ = 9.1 (27.1 °C, no background electrolyte) *(54)* K_{f1} = 0.044 (1.0 M $NaClO_4$) *(61)*	1:1, λ max = 700 nm, ϵ = 1250 *(66)* 2:1, λ max = 570 nm, ϵ = 3330 3:1, λ max = 490 nm, ϵ = 4190 *(54)*	0.792 V *(62)*
(10) 3,4,5-trihydroxybenzoic acid (Gallic Acid), LH_4 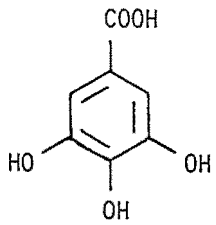	pk_1 = 11.30 pk_2 = 10.05 pk_3 = 8.54 pk_4 = 4.44 (0.1 M KCl) *(67)*	No redox reaction with Fe^{3+} reported *(67)*	$\log K_1$ = 18.05 $\log K_2$ = 7.96 $\log K_3$ = 7.15 (these data are for $Fe(LH)_n$ species) (0.1 M KCl) *(67)*	λ max = 550 nm, ϵ = 4130 This absorption associated with FeL^- species *(67)*	0.799 V (30 °C) *(68)*

(11)	4-t-butyl-1,2-dihydroxybenzene, LH_2 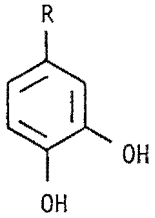 $R = (CH_3)_3C-$		Ligand oxidised to o-quinone with Fe^{3+} *(61)*	K_{f1} = 0.023 (1.0 M $NaClO_4$) *(61)*	As for ligand 2	0.753 V *(62)*
(12)	4-methyl-1,2-dihydroxybenzene, LH_2 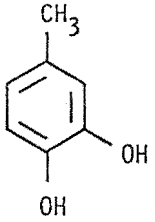		Ligand oxidised to o-quinone with Fe^{3+} *(61)*	K_{f1} = 0.028 (1.0 M $NaClO_4$) *(61)*	As for ligand 2	0.739 V *(62)*
(13)	1,2,3-trihydroxybenzene (Pyrogallol), LH_3 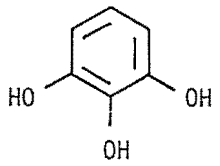	$\log k_1$ = 11.64 $\log k_2$ = 9.01 *(69)*	Rapid oxidation of ligand by atmospheric oxygen.		λ max = 515 nm (pH 8.0) stoichiometry not given *(70)*	0.713 V (30 °C) *(68)*

(14)	1,2-dihydroxynaphthalene-4-sulphonate, LH_2 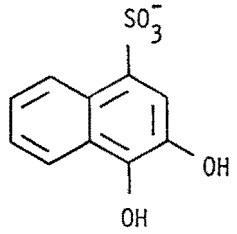	log k_1 = 12.66 log k_2 = 8.14 (0.1 M $NaClO_4$) *(71)*	Instantaneous oxidation below pH 2 to o-quinone in the presence of Fe^{3+}. Rapid oxidation by atmospheric oxygen above pH 2. *(71)*	log K_1 = 19.84 log K_2 = 15.11 (0.1 M $NaClO_4$) *(71)*	1:1 complex "green" 2:1 complex "blue" *(71)*	0.021 V *(71)*
(15)	1,3,5-tris(2,3-di-hydroxybenzoyl aminomethyl) benzene, LH_6 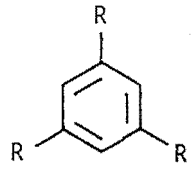 R = $-CH_2NHC(:O)C_6H_3(OH)_2$-o, m		No redox reaction with Fe^{3+} reported *(55)*	log β = 45.8* *(55)*	1:1, λ max = 492 nm e = 4700 *(55)*	

** (overall stability constant for the formation of Fe(III) complex with a hexadentate ligand, ie. FeL^{3-})*

Explanatory Notes for Table 1:1

(a) Systematic and common names for the ligands, LH_n, are given along with structural formulae.

(b) Protonation constants for the ligands are listed as log k_n, where k_n is the equilibrium constant for the following reaction:

$$H^+ + LH_{n-1} \rightleftharpoons LH_n$$

Where equilibrium constant determinations involved the use of background electrolytes to minimise changes in ionic strength (refer to section 4.1.3), relevant details are given in parentheses. Except where stated, the temperature at which measurements were made was 25 °C. (Care is required in the interpretation of protonation constants for L-Dopa and (-)-Adrenaline - refer to reference 72).

(c) Any reported redox reaction between the ligand and ferric ion or the ligand and oxygen is described.

(d) Stability constants of ferric-ligand complexes are listed as log K_n. For several ligands, K_{f1}, the "formation constant" of the metal:ligand 1:1 complex is also given. K_{f1} is the equilibrium constant for the following reaction:

$$M + LH_n \rightleftharpoons MLH_{n-2} + 2H^+$$

The comments made about background electrolytes and temperature in (b) above also apply to stability constant data given here.

(e) Spectrophotometric data for the visible region of absorption of the metal ligand complexes are given as λ max, wavelength of maximum absorption of the complex and ϵ, extinction coefficient at this wavelength (units of $cm^{-1} l\ mol^{-1}$). The particular complex is

described in terms of the ligand to metal ratio (ie. 1:1, 2:1 or 3:1).

(f) E° *values represent standard reduction potentials for the o-quinone/ligand couple.*

References are given throughout the table as italicised numbers in parentheses.

1.3 Scope of Part A

Potentiometric and spectrophotometric data for metal-ligand complexes were collected from titrations in a specially designed thermostatted cell. The method and other experimental aspects of this work are detailed in Chapter 2.

The significance of pH data furnished by commonly used electrode assemblies is discussed in Chapter 3 and results from the standardisation of a glass/calomel electrode pair are presented.

The methods used to calculate the stability constants of ferrous complexes and the protonation constants of the ligands concerned, required accurately known hydrogen ion concentrations. This work included a detailed study on the calibration of a glass electrode as a hydrogen ion "concentration probe". The method and results of this calibration are described in Chapter 4.

Protonation constants for the anions of 3,4,5-trihydroxybenzoic acid and 1,2-dihydroxybenzene are given in Chapter 5 along with qualitative data on the pH-dependant behaviour of these and other dihydroxybenzenes in the presence and absence of oxygen.

The acid-base properties of iron-ligand solutions and the influence of oxygen on metal-ligand equilibria in these solutions is the subject of Chapter 6. The ligands used were those listed in figure 1 of the Introduction. Data for ferrous systems included stability constant calculations for complexes with 3,4,5-trihydroxybenzoic acid and 1,2-dihydroxybenzene.

CHAPTER 2

EXPERIMENTAL

A. STANDARDISATION AND CALIBRATION OF pH ASSEMBLY

2.1 pH Electrode Assembly

2.1.1 pH Meter

Most pH measurements were made using a Beckman 101901 Research pH meter. This meter is of the null potentiometric type employing two series-connected mercury standard cells in the null-balance electrical circuit and has a quoted relative accuracy of ± 0.00099 pH unit (or 0.11 mV)[73]. Calibration of the instrument against the standard cells was performed daily prior to any pH measurements.

A Radiometer PHM64 Research pH meter was used in the latter part of this work. This meter is of the direct-reading type with a digital display and has a quoted relative accuracy of ± 0.001 pH unit (or 0.1 mV)[74]. The electrical zero-point of this meter may be adjusted, which facilitates standardisation of the pH assembly using two or more standard buffer solutions (see section 3.4.3).

2.1.2 Electrodes

The electrodes used in conjunction with the Beckman pH meter were as follows:

(1) A Beckman E-2 glass electrode, type 39004. This electrode, which may be recognised by its blue glass bulb, is a high sensitivity glass electrode, exhibiting minimum alkali metal response at high pH (e.g. 0.03 pH units in 0.1 M* NaOH at 25 °C)[75]. It has a silver-silver chloride internal element.

---

* *"M" denotes mol dm^{-3} (molar)*

(2) A Beckman calomel reference electrode, type 39071. This electrode has a frit liquid junction of pressed-sintered carborundum and glass pellets and has a saturated potassium chloride solution as the filling electrolyte.

In conjunction with the Radiometer pH meter, a Radiometer combination electrode, type GK2401C, was used. This combines a glass electrode with silver-silver chloride internal reference electrodes and exhibits moderate deviation at high pH (e.g. 0.25 pH units in 0.1 M NaOH at 20 °C)[76]. It has a porous pin liquid junction and uses saturated potassium chloride as the filling electrolyte.

In addition to these commercial electrodes, several silver-silver chloride reference electrodes were prepared. Silver electrodes, 1 cm^2 in surface area, were cathodised for ca. 45 min at 1.5 mA in 0.1 M HCl. They were then dipped in conc. HNO_3, rinsed, and soaked in conc. NH_3(aq) for 4 h, then distilled water for 1 - 2 days. The electrodes were anodised at 1.5 mA in 0.3 M HCl for varying lengths of time and soaked in distilled water overnight. They were then aged in 0.005 M KCl for ca. 24 h before use and stored in this solution when not in use. All reagents were analytical grade. It was found that (when used in conjunction with a glass electrode) silver electrodes anodised for more than ca. 20 min, proved to be unstable and prone to severe drifting (up to 0.001 pH unit/min). The best results were obtained using electrodes anodised for 10 min at 1.5 mA. Even so, drift was a significant part of their performance, (typically 0.0001 pH/min). Electrodes prepared in this way were selected for use from pairs which exhibited a maximum potential difference with respect to each other of 0.1 mV, as measured in .005 M KCl solution.

2.1.3 Titration Unit

The thermostatted titration cell and electrode housing, previously described by Hedwig[77], are shown diagramatically in fig 2.1. Titrant was added through a syringe needle(21-gauge) at the side of the titration

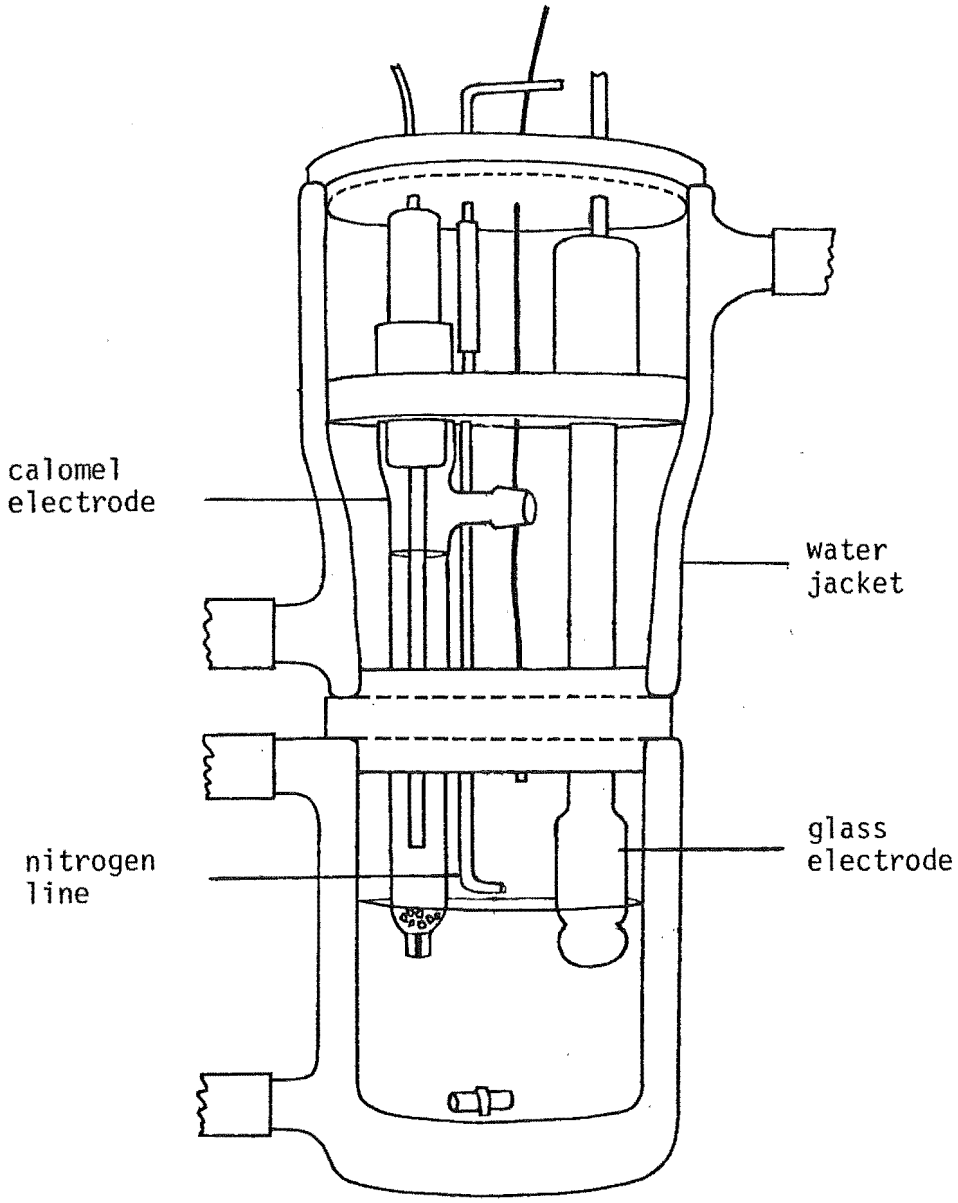

Figure 2.1 pH Titration Unit

unit. Water circulating through the unit was maintained at 25.0 ± 0.1 °C by a "Retostat" temperature controller.

2.2 Standardisation Against NBS Buffers

2.2.1 Preparation of Standard Buffer Solutions

Ten NBS* standard buffer solutions were used to characterize the response of the glass/calomel electrode assembly. These were: potassium hydrogen tartrate; potassium hydrogen phthalate; potassium dihydrogen phosphate/di-sodium hydrogen phosphate of molal+ ratios 1:1 and 1:3.5; borax; sodium bicarbonate/sodium carbonate (1:1); potassium tetroxalate (0.05 m); acetic acid/sodium acetate (1:1); tris(hydroxymethyl) aminomethane (or "tris")/"tris"-hydrochloride (1:1); and calcium hydroxide.

In addition to these, two other buffer systems, potassium tetroxalate (0.01 m) and a series of o-phthalic acid/potassium hydrogen phthalate solutions were prepared. The composition, preparation and assigned standard pH values, pH(S), of these solutions are given in Appendix 1.

In general, the buffer solutions were prepared by dissolving the indicated weight of pure dry buffer substance in 1 litre of distilled water, according to the methods outlined by Bates[78]. Where required, freshly-boiled distilled water (purged with N_2 during cooling to avoid dissolution of atmospheric carbon dioxide), pH = 6.1 - 7.1, was used. Analytical grade chemicals were used for all buffer solutions.

The following additional comments on the preparation and use of these buffers are relevant.

(a) Stability of Solutions. For accurate pH measurements, portions of buffer solutions used to standardise the electrode assembly were

---

* *"NBS" denotes National Bureau of Standards*

\+ *"molal" denotes moles/kg solvent ("m")*

discarded after each measurement. This meant that fresh solutions were being prepared regularly. The most frequently used buffers (viz phthalate, phosphate 1:1, borax, carbonate and tetroxalate) gave reproducible pH measurements relative to phosphate 1:1 up to at least 10 weeks after preparation. Solutions of potassium hydrogen tartrate, recommended by Bates to be replaced every few days[78], gave reproducible pH measurements relative to phosphate 1:1, up to at least six weeks after preparation. Tartrate buffers were stored as saturated solutions in contact with undissolved crystalline salt.

(b) Borax Buffer. Because of the propensity of crystalline borax to lose water of crystallization on standing, either freshly recrystallized borax prepared by the method of Vogel[79], or analytical grade borax from previously unopened reagent bottles, was used. Results showed that recrystallization produced no significant difference in the pH of the borax buffer.

(c) Acetate Buffer. A stock solution of ca. 1.2 M acetic acid, prepared from glacial acetic acid (ca. 17.4 M), was standardised against standard potassium hydroxide. Calculated amounts of acetic acid stock solution and sodium acetate salt were added to a known mass of freshly boiled distilled water to give a solution 0.01 molal in both acetic acid and acetate ion.

(d) Tris Buffer . Tris(hydroxymethyl)aminomethane and tris-hydrochloride were available commercially, but initially the hydrochloride salt was prepared by reaction of hydrochloric acid and tris(hydroxymethyl)aminomethane. The product was recrystallized from 70% propan-2-ol/30% water by Soxhlet extraction, dried under vacuum for ca. 2 h and stored in a dessicator.

(e) Tetroxalate Buffer (0.01 m). To give more information about the response of the glass electrode system in the low pH region, a 0.01 m potassium tetroxalate solution was prepared. The assignment of a standard pH value (pH(S) = 2.157), to this solution is discussed in Appendix 2 .

(f) o-Phthalic Acid /Hydrogen Phthalate Buffers. Potentiometric measurements on o-phthalic acid/potassium hydrogen phthalate solutions with potassium chloride as a background electrolyte has led to a series[80] of tabulated pH values for various buffer mixtures at 25 °C. A solution comprising, potassium hydrogen phthalate (0.00503 m), o-phthalic acid (0.0075 m) and KCl (0.00505 m) was prepared and assigned a standard pH value of 2.913 (see Appendix 2). Other phthalate buffers were generated in titrations between o-phthalic acid and potassium hydroxide. Use of these for standardisation in the pH range 4 - 7 is discussed in Appendix 2. The preparation of o-phthalic acid used in these buffer solutions is described in section 2.3.1.

(g) Buffers for use with silver-silver chloride electrodes. Five buffer solutions (viz phosphate 1:1, phthalate, carbonate, tetroxalate and tartrate), prepared in the normal fashion, were "spiked" with KCl solution for use with Ag/AgCl electrodes. Buffers prepared this way were 0.001 M in chloride ion. They gave identical results to the unspiked buffers when used with the glass/calomel electrode pair thus confirming previous observations made by McBryde [81].

2.2.2 Procedure for pH Measurements

Before any pH measurements, the electrodes and titration cell in use were carefully rinsed with small portions of distilled water and dried with absorbent tissue. A portion of test solution was introduced into the cell, the electrodes inserted and the pH recorded when equilibration was complete. If the test solution had been stored at 25 °C then equilibrium was reached in 3 - 5 minutes, otherwise 10 - 15 minutes were allowed.

The usual procedure for a series of pH measurements was firstly to set the pH indicated by the pH meter to 6.863 (the NBS value for the standard pH of the 1:1 phosphate buffer) while the electrodes were immersed in the phosphate buffer solution. Following rinsing of the

electrodes, the pH of one or more other standard buffer solutions was measured. The pH of the phosphate buffer was re-determined and any drift in pH was calculated, corrections being applied to measured pH values where necessary. Drifting in the system was usually of the order of 5×10^{-5} pH units/min (e.g. ΔpH = 0.006 over a typical 2-hour period). A detailed discussion on the response of the glass electrode assembly to the NBS standard buffers is given in chapter 3.

2.3 Calibration With o-Phthalic Acid

As introduced in chapter 1 and discussed in detail in chapter 4, a series of o-phthalic acid buffers was prepared and used to calibrate the pH-response of the glass electrode assembly in terms of hydrogen ion concentrations.

2.3.1 Preparation of o-Phthalic Acid Buffer Solutions

To prepare crystals of o-phthalic acid (benzene-1, 2-dicarboxylic acid), 50 g of analytical grade potassium hydrogen phthalate was dissolved in ca. 700 ml distilled water. Two 100 ml portions of concentrated hydrochloric acid (analytical grade) were added slowly with stirring. The second portion of HCl was added to the supernatant liquid after the white precipitate of o-phthalic acid was allowed to settle. When precipitation appeared complete the solution was filtered through a Buchner funnel and the precipitate was washed with ca. 400 ml of cold distilled water in 100 ml portions (yield > 95 %). The product was recrystallized twice from 400 ml of hot distilled water, air-dried in a dessicator, oven-dried at 40 °C for 5 h then vacuum dried for 1.5 h. o-Phthalic acid crystals prepared this way were stored in a dessicator. (Found: C, 58.0 %; H, 3.92 %. Calculated for $C_8H_6O_4$: C, 57.8 %; H, 3.60 %).

2.3.2 Acid, Base and Electrolyte Solutions

(a) Potassium Hydroxide. Analytical grade potassium hydroxide pellets, (ca. 36 g), from a previously unopened sealed container, were washed quickly with small portions of carbon dioxide-free distilled water and dissolved in 250 ml of water to give a solution of between 0.7 and 1.0 M.

The KOH solution was standardised by potentiometric titration against weighed amounts of potassium hydrogen phthalate. Repeated measurements gave an overall precision of 0.2 - 0.6 % in hydroxide ion concentration. Solutions of potassium hydroxide were found to be stable for up to 3 months after preparation. Determination of the endpoint in phthalate-standardisation is considered in section 2.8.2.

(b) Hydrochloric Acid. Analytical grade concentrated hydrochloric acid (180 ml) was diluted to 1 litre with distilled water to make a stock solution of ca. 2 M. The acid solution was standardised against borax, sodium carbonate (dried at 260 °C) and standard potassium hydroxide. Repeated measurements gave an overall precision of 0.17 % for borax, 1 % for carbonate, and 0.25 % for potassium hydroxide standardisation. Averaged results for sodium carbonate and potassium hydroxide agreed to within 0.5 % but those for borax were ca. 3 % low. Russell[82] also observed erroneous results for borax (ca. 2 % low) and recommended the use of freshly recrystallized borax as a primary standard. Determination of the endpoints in these standardisation titrations is discussed in section 2.8.2.

(c) Potassium Chloride. All titrations were performed in KCl solution, ionic strength 0 - 0.2 M, to ensure a constant ionic medium (see section 4.1.3). Analytical grade potassium chloride, dried at 120 °C for ca. 2 h, was used for the preparation of stock solutions or for direct addition to titration solutions.

2.3.3 Titration Procedure

From stock solutions of o-phthalic acid (ca. 8×10^{-3} M), working solutions of o-phthalic acid ($1 - 3 \times 10^{-3}$ M) and potassium chloride (0.039 - 0.197 M) were prepared in 250 ml volumes. A 50 ml aliquot of working solution was titrated with standard potassium hydroxide which was added in small increments (typically 0.005 ml) from a micrometersyringe (see section 2.9.2). The pH was recorded for each increment of titre, equilibration being established in 1 min and after suitable adjustments for drifting (see section 2.2.2) and/or liquid junction effects (see section 3.5.2) these data were used in subsequent calculations.

2.3.4 Density Measurements

Equilibrium data for the dissociation of o-phthalic acid have been reported in molal units[80,83]. However it was found convenient to prepare solutions on the molar scale and to calculate molality from the measured density. The density of o-phthalic acid/potassium chloride solutions was determined by accurately weighing portions of the buffer solution at 20 °C in a calibrated density bottle (volume ca. 50 ml). The density of potassium hydroxide solution was determined by interpolation from tabulated data[84]. The density bottle was calibrated by weighing distilled water and using published density data[85].

B. LIGAND AND METAL - LIGAND TITRATIONS

2.4 Preparation of Solutions

2.4.1 Ligand Solutions

(a) Gallic Acid (3,4,5 - trihydroxybenzoic acid). Reagent grade gallic acid was used without further purification. (Found: C, 44.9 %; H, 4.15 %. Calculated for $C_7H_6O_5 \cdot H_2O$: C, 44.7 %; H, 4.28 %). Analysis by potentiometric titration with standard alkali is considered in section 2.8.2.

(b) Catechol (1,2-dihydroxybenzene). Reagent grade catechol was used without further purification. (Found: C, 65.6 %; H, 5.44 %. Calculated for $C_6H_6O_2$: C, 65.45 %; H, 5.49 %).

(c) Protocatechuic Acid (3,4-dihydroxybenzoic acid), Tiron (1,2-dihydroxybenzene-3,5-disulphonic acid), Pyrogallol (1,2,3-trihydroxybenzene). Reagent grade chemicals were used for each of these ligands and only semi-quantitative experiments performed.

Ligand solutions were prepared by dissolving appropriate weights of solid material in freshly-boiled distilled water to give stock solutions of ca. 5×10^{-3} - 1×10^{-2} M. For catechol and pyrogallol, a known volume of standard hydrochloric acid solution was added to ensure the ligand solutions were stored at $pH < 3.5$. Ligand solutions were kept in well-stoppered flasks and out of direct exposure to sunlight. These two measures were taken to minimise slow oxidation processes known to take place in aqueous solutions of o-dihydroxy-benzene compounds[65]. Solutions of gallic acid were observed to be stable for up to 10 days when a yellowing of solution became apparent, whereas solutions of catechol remained colourless for up to 5 weeks.

2.4.2 Metal Solutions

(a) Ferric Chloride ($FeCl_3 \cdot 6H_2O$). Analytical grade ferric chloride was used from a previously unopened container. A portion of the solid was quickly weighed and transferred to a 100 ml volumetric flask containing 50 ml of ca. 2 M HCl, and made up to the mark. This method was adopted because ferric chloride is appreciably hygroscopic and hydrolyses rapidly in weakly acidic or neutral solutions. Stock solutions of 0.2 M were prepared.

(b) Ferrous Sulphate ($FeSO_4 \cdot 7H_2O$). Analytical grade ferrous sulphate was used to prepare stock solutions of ca. 0.2 M by dissolving the required weight of ferrous sulphate in 50 ml of 2 M HCl and making up to 100 ml. Acid suppresses the atmospheric oxidation of Fe(II) to Fe(III) which is rapid in neutral or alkaline conditions. Russell[86] found that Fe(II) solutions that were 0.01 M in HCl were stable ([Fe(III)]/[Fe(II)] $\leqslant$ 0.03) for approximately two weeks. A slowly-intensifying yellow colour in solution after this time indicated the oxidation of Fe(II) to Fe(III). Therefore fresh stock solutions of ferrous sulphate were prepared regularly.

2.5 Measurement and Control of Oxygen Concentration

2.5.1 Oxygen Probe

Because of the propensity of certain ligands to undergo oxidation, and the rapid conversion of Fe(II) to Fe(III) in neutral or basic conditions in the presence of atmospheric oxygen, some titrations were performed in nitrogen atmospheres.

The concentration of dissolved oxygen was monitored with a Beckman 100802 Fieldlab oxygen analyser coupled with a Beckman 39550 polarographic oxygen electrode. The oxygen-sensitive electrode detects the partial pressure of dissolved oxygen by a polarographic method. Oxygen dissolved in the test solution diffuses through a gas-permeable teflon membrane to

the electrode assembly (a rhodium cathode and silver/silver chloride anode). A potential of 0.53 V is applied between the electrodes. The oxygen is reduced at the cathode according to the following reaction;

$$2\ H_2O\ +\ O_2\ +\ 4e\ \longrightarrow\ 4\ OH^-$$

and a current flows which is proportional to the partial pressure of oxygen in the bulk solution. Kee [87] has shown that the response of the oxygen sensor is linear with the concentration of dissolved oxygen up to air saturation. The oxygen analyser was standardised before use with air-saturated distilled water ($[O_2]$ = 8.48 ppm at 25 °C) [88] and oxygen-free distilled water (water purged with oxygen-free nitrogen, and any residual oxygen removed by reaction with sodium sulphite). For titration solutions (ionic strength ca. 0.1 M KCl) an empirical adjustment for the varying oxygen solubility with changing ionic strength was made according to the manufacturer's manual [88]. It was found necessary to replace the teflon membrane every 4 - 6 weeks during regular operation.

Factors important to the reliable and reproducible performance of the oxygen analyser were: (1) the speed at which the bulk solution was stirred, (2) the depth of the semi-permeable membrane in solution, (3) deterioration of the membrane itself, and (4) cleanliness of the tip of the rhodium electrode.

2.5.2 Titration Unit

A thermostatted titration cell was designed to meet the demands of a system requiring rigorous exclusion of oxygen, accurate pH titration data, and the monitoring of dissolved oxygen levels, as well as affording the possibility of direct spectrophotometric measurements. A diagram of the apparatus appears in figure 2.2. The cell had a total volume of ca. 185 ml and was fitted with a lid and sealed by means of a ground-glass flange on the upper face of the cell and the underside rim of the lid. Ground-glass ports were located in the lid. Three B 19 ports accommodated

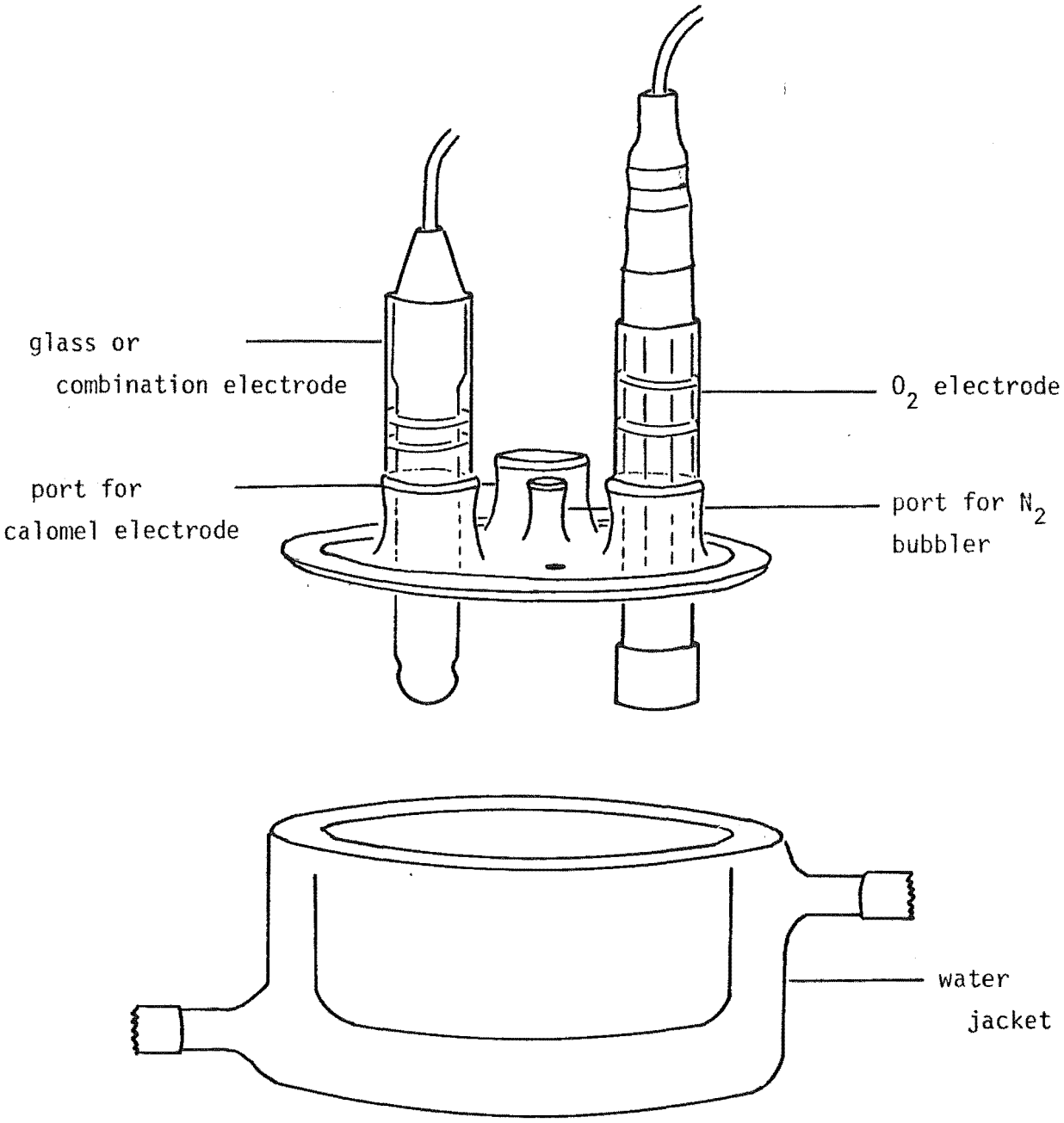

Figure 2.2 Modified pH Titration Unit

any electrodes used and one B 7 port was used for the nitrogen gas line. Electrodes were sealed within glass sleeves fitted with ground-glass cones by means of two rubber o-rings. Three small holes (diameter 6 mm) in the lid enabled addition or removal of solution (e.g. titrant) via plastic tubing or syringe needles (inserted in size 5 rubber bungs).

This cell design enabled easy removal of electrodes for cleaning or storage purposes. Standardisation of the pH-electrodes before and after a titration involved simply transferring the lid, with electrodes in place, to another identical cell containing a standard buffer solution.

To ensure that the titration unit was airtight, ground-glass joints were smeared with a thin coating of I.C.I. silicon M949 grease. Care was taken to ensure that grease did not come in contact with the sensitive electrode surfaces or liquid junction interfaces.

Purified nitrogen was passed through the titration solution by means of a 'bubbler unit' (fig. 2.3) designed to allow nitrogen gas to enter and leave via the same port. Earlier designs for the titration unit allowed nitrogen gas to escape from the cell through narrow spaces in rubber sleeves securing the electrodes to the unit or through a glass capillary tube mounted on top of the cell. These methods were found to be unsatisfactory for rigorous exclusion of oxygen.

2.5.3 Deoxygenation Procedure

(a) Principle. To purge titration solutions of dissolved oxygen, purified nitrogen gas was bubbled through the test solution (thus reducing the partial pressure of oxygen above the liquid and thereby the concentration of dissolved oxygen in solution). Because of the comparative inefficiency of nitrogen purging, the oxygen-level in solution was monitored by the oxygen analyser.

(b) Oxygen-free Nitrogen. Purified nitrogen gas was prepared by bubbling commercial nitrogen through a concentrated solution (ca. 6 M) of

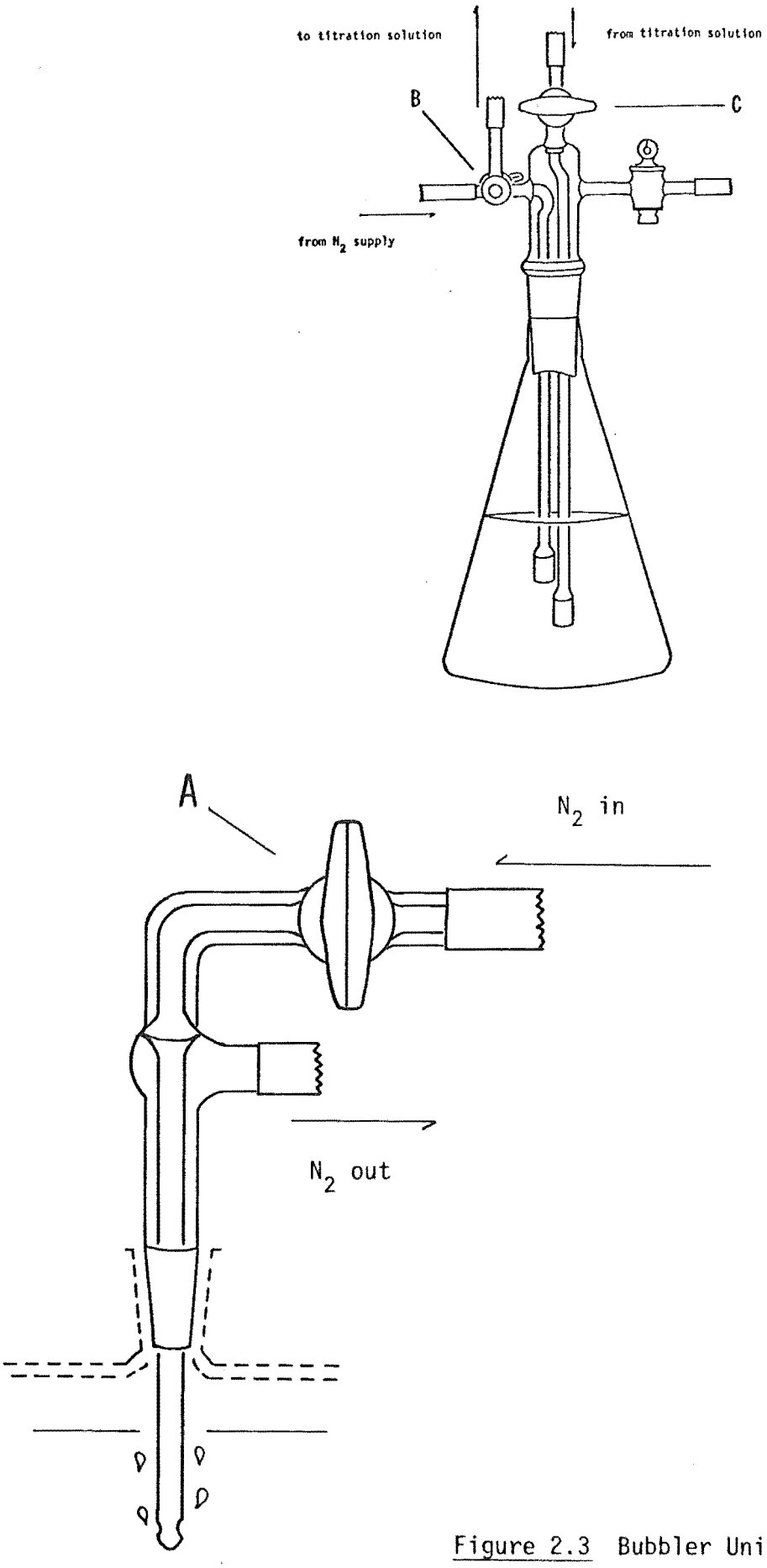

Figure 2.3 Bubbler Unit and Conical Gas Bottle

sodium hydroxide to remove traces of carbon dioxide and then through an acidic vanadium(II) solution over a zinc amalgam.

(c) Preparation of Zinc Amalgam. A 2 % solution of mercuric chloride was prepared by dissolving ca. 4 g of mercuric chloride in ca. 100 ml of 1 M hydrochloric acid. 50 g of zinc pellets were stirred in this solution for a few minutes until a shiny coating of mercury appeared on the surface of the zinc. The zinc amalgam was washed with several portions of distilled water.

(d) Stock Vanadyl Sulphate Solution. A stock solution of vanadyl sulphate was prepared by dissolving 4.5 g $VOSO_4.2\ H_2O$ in 500 ml of 2 M sulphuric acid.

(e) Vanadium(II) solution. Acidic vanadyl solution (100 ml) was added to the zinc amalgam in a gas bottle, the solution completely covering the amalgam. Nitrogen was bubbled vigorously through the solution until the colour changed from blue (VO^{2+}), to green (V^{3+}), to violet (V^{2+}).

The gas bottle was sealed off from the atmosphere when not in use but it was found necessary to replace the zinc amalgam/vanadium(II) solution every 3 - 4 months.

Commercially available "oxygen-free nitrogen" was also used but was found to give no significant improvement in the deoxygenation of titration solutions.

(f) Oxygen-free titrations. The required volumes of metal and/or ligand stock solutions, weighed amounts of potassium chloride and any additional distilled water were added to the titration cell. Purified nitrogen was bubbled through the stirred solution until the oxygen sensor registered an oxygen concentration near zero (typically 0.00 - 0.05 ppm). This took between two and three hours. When deoxygenation was complete, the nitrogen supply was closed off from the titration unit (stopcock A in fig. 2.3) and diverted through a 1 litre conical gas bottle containing 500 ml of water (i.e. via stopcock B). During deoxygenation, nitrogen

passing through the test solution was also returned to the gas bottle and bubbled through the water reservoir via stopcock C. With this method, once the titration unit was sealed off to incoming gases, it was open only to a length of line filled with purified nitrogen between the top of the unit and the water reservoir. It was found that, once the titration unit was sealed off in this manner, no increase in the oxygen concentration of the test solution occurred in the 1 - 2 hours duration of a typical metal-ligand titration.

2.5.4 Titration Procedure

For the titration proper, standard potassium hydroxide was added incrementally to the metal-ligand or ligand solution and corresponding pH data were recorded according to the method described in section 2.3.3. If information about the metal ligand system in the presence of oxygen was required, then air was allowed to diffuse back into the cell or compressed air was bubbled through the test solution.

2.6 Determination of Iron

2.6.1 Ferric

To monitor the progress of various oxidation-reduction processes thought to be occurring in many of the metal-ligand systems, iron as Fe(III) was determined quantitatively by spectrophotometric measurement as the $Fe(NCS)(H_2O)_5^{2+}$ complex.

One millilitre samples of the test solution were withdrawn by syringe from the titration cell and quickly added to 1 ml of 1 M HCl in a 10 ml volumetric flask, effectively quenching any further redox process. 1 ml of ammonium thiocyanate (ca. 2 M) was added and distilled water was added to the mark. The deep red thiocyanate-iron(III) complex was measured immediately at 480 nm and compared with a standard calibration curve which was linear in the concentration range used (viz 0 - 6 x 10^{-5} M Fe(III)).

2.6.2 Ferrous

Because of the relatively high reduction potential of the ferric-o-phenanthroline/ferrous-o-phenanthroline couple,

$$Fe(o\text{-phen})_3^{3+} + e \longrightarrow Fe(o\text{-phen})_3^{2+} \quad E^\circ = 1.14\ V,^{89}$$

the presence of mild reducing agents such as gallic acid, catechol etc., (E° = ca. 0.8 V) will interfere with the quantitative determination of ferrous ion as the $Fe(o\text{-phen})_3^{2+}$ complex. Therefore ferrous iron was determined by difference, between known total iron and Fe(III) determined as above.

2.7 Spectrophotometric Measurements

2.7.1 Instruments

Ultraviolet and visible absorption spectra were recorded on a Varian SuperScan 3 flat-bed recorder spectrophotometer, or, in the case of Fe(III) determinations, a Varian Techtron 635 spectrophotometer.

2.7.2 Cells

(a) Static. Static measurements were made using either 1 mm or 10 mm U.V. silica spectrophotometer cells.

(b) Flow. Several attempts were made to record spectral data for the oxygen-sensitive metal-ligand titration solutions. These measurements involved the use of either (1) aliquots of titration solution withdrawn via syringe and transferred to spectrophotometer cells, (2) a peristaltic pump linked to a specially designed 10 mm flow-cell and the titration cell proper by 3 mm plastic tubing or (3) a specially designed 1 mm flow-cell linked directly to the titration cell via 1 mm plastic tubing through which test solution was 'bled' from the titration cell and led off to waste after passing through the spectrophotometer cell.

The latest model of each of the flow cells is depicted in figure 2.4.

Use of the first method allowed oxygen to diffuse into solution and was used for qualitative work only. In the case of 10 mm flow-cell, it was not possible to lower the oxygen concentration below about 0.2 ppm during pumping, with the equipment being used. So this system was used for collecting spectrophotometric data where elaborate deoxygenation procedures were not required.

The flow of solution through the 1 mm cell was aided by a small back pressure which existed if a continuous passage of nitrogen through the titration unit was allowed. This system was used where more rigorous exclusion of oxygen was required and some useful preliminary data were collected this way. However results suggested that further modifications might be necessary before a completely air-tight system could be achieved.

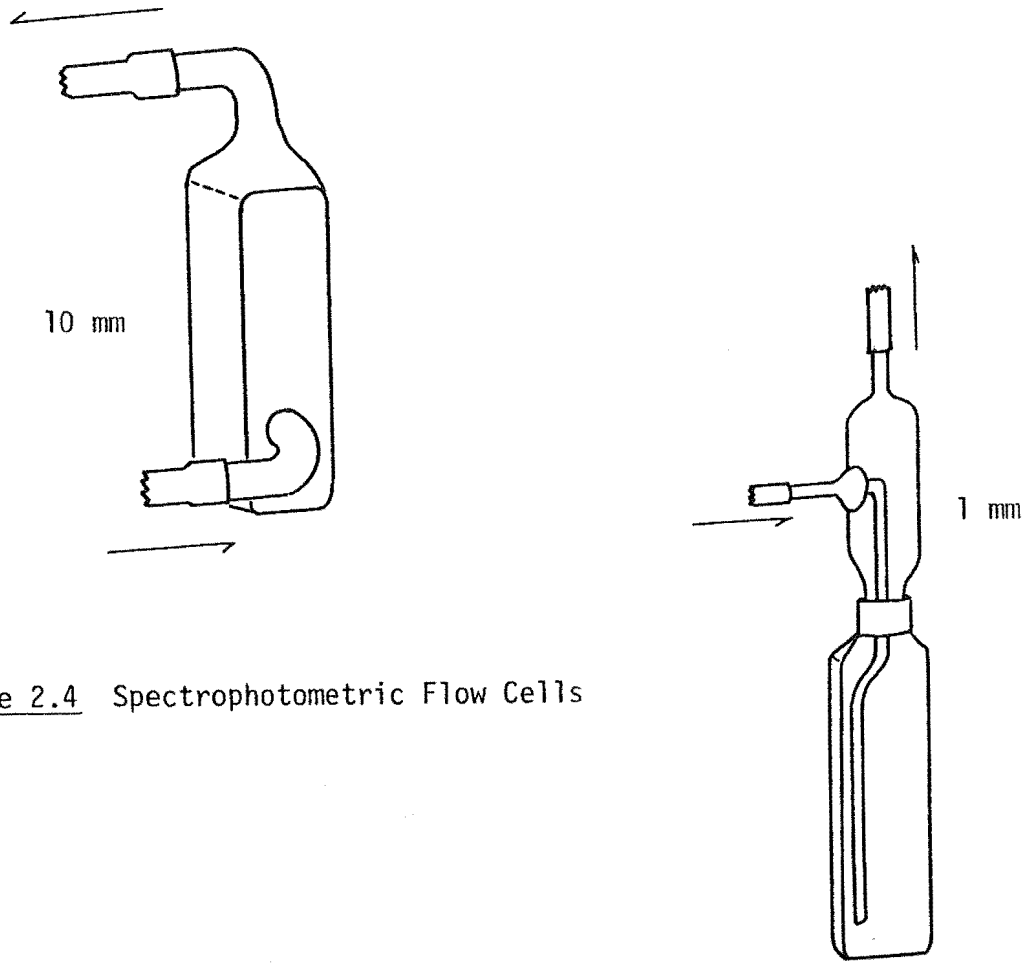

Figure 2.4 Spectrophotometric Flow Cells

C. MISCELLANEOUS

2.8 Analytical Procedures

2.8.1 Microanalyses

Microanalyses of o-phthalic acid, gallic acid and catechol for carbon and hydrogen were performed by Dr A. Campbell at the Microanalytical Laboratory, University of Otago, Dunedin.

2.8.2 Endpoint Determinations

(a) Differential plots. In the standardisation of potassium hydroxide with potassium hydrogen phthalate a plot of $\Delta pH/\Delta titre$ vs. titre was found to fix the endpoint to within .06 % (graphical error). Similarly in the standardisation of hydrochloric acid, a precision of .04 % was achieved with standard alkali and .06 % with borax. Determination of the endpoint by differential plots was considered adequate for the standardisation of potassium hydroxide.

(b) Gran's analysis. When sodium carbonate was used to standardise hydrochloric acid, and when endpoints in titrations of gallic acid and o-phthalic acid with potassium hydroxide were required, Gran's graphical analysis technique was used. This technique can be illustrated in the titration of a diprotic acid H_2A with a strong base.

(1) Before the first endpoint:

$$K_1 = \frac{[HA][H]}{[H_2A]} = \frac{V_B[H]}{(Ve_1 - V_B)}$$

$$K_1(Ve_1 - V_B) = [H]V_B$$

where K_1 = first dissociation constant

Ve_1 = volume at first equivalence point

V_B = volume of base added

[H], [H_2A], [HA] = concentrations of individual species present in solution.

Hence a plot of $10^{-pH} \cdot V_B$ versus V_B should produce a straight line intersecting the abscissa at $V_B = Ve_1$.

(2) After the first endpoint:

$$K_2 = \frac{[H][A]}{[HA]} = \frac{(V_B - Ve_1)}{(Ve_2 - V_B)} [H]$$

$$K_2(Ve_2 - V_B) = (V_B - Ve_1)[H]$$

where K_2 = second dissociation constant

Ve_2 = volume at second equivalence point

[A] = concentration of completely dissociated acid.

Hence a plot of $10^{pH} \cdot (Ve_2 - V_B)$ vs. V_B should produce a straight line, also intersecting the abscissa at $V_B = Ve_1$. (An approximate value of Ve_2 is assumed for this plot).

Similarly, plots of:

(3) $10^{-pH}(V_B - Ve_1)$ vs. V_B ..... before the 2nd endpoint

(4) $10^{pH}(V_A + V_B)$ vs. V_B ..... after the 2nd endpoint

where V_A = total initial volume, intersect the abscissa at $V_B = Ve_2$

When the pK values of the diprotic acid are well separated (3 log units or more) there is no difficulty in locating the equivalence points by Gran's plot and the titration curve resembles that of two monoprotic acids. However if the pK values are closely spaced (less than 3 log units) the titration curve resembles that of a monoprotic acid and the first equivalence point cannot be located by Gran's analysis. The straight line segments intersect above the x-axis because, in the derivation of these lines, non-overlapping equilibria are assumed.

In the titration of sodium carbonate and hydrochloric acid, intersection of individual Gran's plots on each side of the two equivalence points agreed to within 2 % for the first equivalence point and 0.6 % for the second.

Similarly, in the titration of gallic acid and potassium hydroxide the first endpoint (pH 6.3) was located within 0.4 % and the second within 3 % . The pKs of gallic acid are separated by 4.4 log units (pK_1, pK_2) and 2.8 log units (pK_2, pK_3) respectively.

However for o-phthalic acid it was not possible to accurately determine the first endpoint (pH 4.0) as the straight line segments intersected above the x-axis. The pKs of o-phthalic acid are separated by 2.6 log units.

2.9 Volumetric Equipment

2.9.1 Glassware

(a) Pipettes used in quantitative work were calibrated by weighing the volume of distilled water delivered at a known temperature using published density data[85].

(b) Volumetric flasks. The tolerances assumed for standard volumetric flasks were those given by Vogel[91].

2.9.2 Micrometer Syringes

The addition of titrant in electrode calibaration and metal-ligand titrations was effected by a Gilmont micrometer syringe, capacity 2.5 ml, calibrated in 0.0001 ml divisions.

Additions of small volumes of metal stock solutions to titration solutions were made by an Agla micrometer syringe (Burroughs Wellcome and Co.), capacity 0.5 ml, calibrated in 0.0001 ml divisions.

A calibration by Hedwig[92] showed the volume delivered by the Agla syringe to be within 0.06 % of the indicated volume.

CHAPTER 3

STANDARDISATION OF THE pH ELECTRODE ASSEMBLY

A. THE THEORY OF pH MEASUREMENT

3.1 Basic Concepts of pH

3.1.1 Acidity

Water is the medium for the chemical reactions of animal and plant life. Because of its amphoteric character, water can undergo rapid proton-transfer reactions with many of the substances involved in these biochemical reactions. For example:

$$HA + H_2O \rightleftharpoons A^- + H_3O^+ \qquad (3.1)$$

The extent to which HA, an "acid", is converted to A^- is a measure of the acidity of HA in solvent H_2O and is determined by the "active mass" of H_3O^+.* The problem of the concept of acidity is the search for a definition of this "active mass" of hydrogen ions and of experimental methods for its determination.

The unique influence of the hydrogen ion concentration on biochemical reactions led Sorensen, in 1909, to propose a scale of acidity [93]. At that time it was thought that the "active mass" of hydrogen ion (or of any other species) in solution was adequately expressed by its concentration. In the solutions of interest, c_H, the concentration of hydrogen ions in units of mol dm^{-3}, is frequently a very small number. For this reason Sorensen proposed the "hydrogen ion exponent", which came to be known as "pH", and was defined as:

$$pH \equiv -\log c_H \qquad (3.2)$$

---

* *Hereafter, for sake of simplicity, H_3O^+ will be denoted by H^+ or just H.*

3.1.2 Activity

The mass law constant for reaction 3.1 can be expressed in the form:

$$K = \frac{c_H\, c_A}{c_{H_2O}\, c_{HA}} \cdot \frac{f_H\, f_A}{f_{H_2O}\, f_{HA}}$$

$$= K' \cdot \frac{f_H\, f_A}{f_{H_2O}\, f_{HA}} \qquad (3.3)$$

It was originally thought that equilibrium constants for such reactions were expressible simply in terms of the concentrations of the species concerned (i.e. K'). However, K' was found to vary with the composition of the solution. The factors "f" in equation 3.3, called "activity coefficients", were introduced by Lewis [94] to produce a constant product.

The "active mass" of solution species thus came to be known as "activity" and was arbitarily related to concentrations as follows:

$$a_H = c_H f_H \quad \text{... units of mol dm}^{-3}\ (M) \qquad (3.4)$$

$$\text{or} \quad a_H = m_H y_H \quad \text{... units of mol kg}^{-1}\ (m) \qquad (3.5)$$

The arbitary convention adopted is that activity coefficients tend to unity as the composition of the solution tends to that of the pure solvent. This relationship expresses the non-ideal behaviour of solution species due to interionic forces which reduce their "effective concentration".

The relationship applies formally to ions; however, the activity coefficients of individual ions cannot be uniquely measured. Only certain quotients or products of single ionic activity coefficients can be determined exactly, since any thermodynamic property derived from a measurement on an electrolyte solution is a function of both anion and cation species. Nevertheless, it is advantageous to express certain thermodynamic properties in terms of hypothetical or "conventional" single ion activity coefficients. These activity coefficients can be calculated

theoretically for concentrations so low that the interionic forces depend primarily on the charge, radius, and distribution of the ions, and the dielectric constant of the medium, rather than on the chemical properties of the ions.

eg. Hückel form of the Debye-Hückel equation:

$$-\log y_i = \frac{A z_i^2 I^{\frac{1}{2}}}{1 + B a_o I^{\frac{1}{2}}} + \beta I \qquad (3.6)$$

where I = "ionic strength" $= \frac{1}{2} \Sigma m_i z_i^2$

a_o = "ion size parameter" or mean distance of closest approach,

m_i = concentration of ionic species i in units of mol kg^{-1},

z_i = charge of ionic species i,

A,B = constants dependant on temperature and dielectric constant of the solvent.

(a_o, β are empirically chosen parameters dependant on the chemical nature of the ions involved).

3.1.3 Measurement of pH With Electrochemical Cells

Along with Sorensen's first proposals for a scale of acidity came his assertion that electromotive force (e.m.f.) measurements on certain galvanic cells gave a direct measure of hydrogen ion concentration. The electrochemical cell used by Sorensen to measure pH, can be represented thus:

$$\text{Pt; } H_2\text{, soln. X} \;\Big|\; \begin{matrix}\text{Salt Bridge} \\ \text{eg. KCl(satd)}\end{matrix} \;\Big|\; \text{Calomel electrode} \qquad (3.7)$$

The cell reaction is written:

$$\tfrac{1}{2}H_2(g) + \tfrac{1}{2}Hg_2Cl_2 \rightleftharpoons Hg\ (l) + H^+\ (\text{soln X}) + Cl^- \pm \text{ ion transfer} \qquad (3.8)$$

It is now realised that the e.m.f. of a galvanic cell is a function of activity rather than concentration. Furthermore, no simple relationship

exists between the activity of the hydrogen ion and the quantity derived from e.m.f. measurements from cells of the type used by Sorensen.

The formal relationship between the hydrogen ion activity and the e.m.f. is given by:

$$E_{cell} = E^{\circ}_{cell} - \frac{RT}{F} \ln a_H a_{Cl} + E_j \qquad (3.9)$$

where E_j is the algebraic sum of the potentials across the liquid-liquid boundaries and E° is the e.m.f. of a hypothetical cell of type 3.7, corrected for liquid junction potential, in which each of the reactants and products of the cell reaction is present at unit activity. An exact determination of a_H would require a knowledge not only of the liquid junction potentials but also of the activity coefficient of chloride ion. There is no completely rigorous means of obtaining either of these quantities.

The e.m.f. of a galvanic cell of this sort measures a quantity that could be designated $m_H y'$ where y' is a complicated quantity depending on transference numbers of the ions (which relates to the liquid junction potentials), ionic strength and ionic environment in solution.

By using a silver/silver chloride reference electrode, a cell without a liquid junction can be employed. For example:

$$Pt;\ H_2\ ,\ soln\ X,\ Cl^-,\ AgCl;\ Ag \qquad (3.10)$$

Although the standard potential, E°, of this cell is known over a wide range of temperatures, the indeterminant activity coefficient of the chloride ion prevents the exact evaluation of a_H.

3.1.4 Establishing a pH Scale

Realising the response of galvanic cells to changes in activities rather than of concentration, Sorensen and Linderstrom-Lang [95], in 1924, proposed a new pH unit, termed "pa_H":

$$pa_H \equiv -\log a_H = \log m_H y_H \qquad (3.11)$$

Other pH scales have been proposed, for example:

$$p(a_H y_{Cl}) \equiv -\log (m_H y_H y_{Cl}) \qquad (3.12)$$

Some of these scales are essentially the same as pa_H while others, such as $p(a_H y_{Cl})$, although physically definable at all ionic strengths, do not adequately reflect changes in hydrogen ion activity or concentration.

The problem of pH thus becomes a search for a scale of acidity which attempts to maximise the measurable physical possibilities as well as the ascribed theoretical significance. Bates [96] has summarized it thus: "As yet there has been devised no practical experimental method sufficiently convenient and versatile to supplant the electromotive determination of acidity by the Sorensen cell (3.7) and its counterpart with a glass electrode and a saturated calomel electrode...The experimental method is so firmly established however, that the selection of a pH scale is in actuality a search for the hydrogen ion function most nearly consistent with the e.m.f. response of this particular cell that is used so widely".

The scale most widely accepted and referred to hereafter, is $pa_H \equiv -\log a_H$, where a_H is a conventional hydrogen ion activity. Although the pa_H value thus determined has, in itself, no unique physical definition, it is useful for reproducible comparisons of acidity and under ideal experimental conditions affords the possibility of a limited amount of theoretical interpretation.

3.2 NBS Conventions for Standardising the pH Scale

3.2.1 Operational Definition of Measured pH

The great majority of practical pH determinations depend on the measurement of the e.m.f. of cells of the type:

$$\text{Pt; } H_2 \text{ (g), Soln. X} \;\big|\; \text{KCl (satd)} \;\big|\; \text{Reference electrode} \qquad (3.13)$$

The glass electrode is commonly used in place of the hydrogen gas electrode and the calomel electrode is the most useful reference electrode. The e.m.f.

is usually measured by a "pH meter".

From equation 3.9 the relationship between pa_H of solution X and the e.m.f. of a cell of the type shown above in 3.13 is:

$$pa_H \equiv -\log a_H = \frac{[E - (E^{\circ\prime} + E_j)]F}{RT \ln 10} \qquad (3.14)$$

where $E^{\circ\prime} = E^{\circ} - \frac{RT}{F} \ln a_{Cl}$ (3.15)

The selection of values for $E^{\circ\prime} + E_j$ is all that is necessary to permit conventional pH values or conventional hydrogen ion activities to be derived from the e.m.f. of this cell. However, this procedure has been found to be impractical for modern pH measurements, particularly when glass electrodes are being used. The value for $E^{\circ\prime} + E_j$ may differ appreciably from one cell assembly to another; it may also vary considerably with time. Hence a redetermination of $E^{\circ\prime} + E_j$ at frequent intervals is preferred. This standardisation is accomplished by the measurement of E_s, the e.m.f. of cell 3.13 with a "standard solution" (whose pa_H is denoted pH(S)) replacing solution X in the cell. If the value of $E^{\circ\prime} + E_j$ remains unchanged on replacement of the standard solution by the unknown then:

$$pH\,(X) = pH\,(S) + \frac{(E_x - E_s)F}{RT \ln 10} \qquad (3.16)$$

This then becomes the operational definition of the measured pH.

In the standardisation of commerical pH assemblies, day-to-day changes in the cell potential are compensated by a manual adjustment of resistances in the meter circuit. In this way, the instrument is made to indicate the correct pH(S) of the standard solution, and the value of $E^{\circ\prime} + E_j$ need not be ascertained.

The purpose of establishing pH standards is twofold; first, to provide a common basis for all pH measurements, in order that pH numbers obtained will be truly reproducible; and second, to permit the measured pH to assume as much quantitative meaning (in terms of chemical equilibria) as possible.

3.2.2 Assignment of pH(S) Values to Standard Buffer Solutions

The determination of pH values from measurements on galvanic cells requires the precise definition of a conventional acidity scale and the assignment of pH(S) values to one or more selected standard solutions. The NBS (National Bureau of Standards) method for assigning such pH(S) values involves e.m.f. measurements for certain carefully chosen buffer solutions, in cells without liquid junction, and a conventional definition of the activity coefficient of the chloride ion.

The "primary standard" pH scale is defined in terms of the conventional pa_H of seven reference solutions. These solutions were selected to give satisfactory stability with respect to accidental contamination, changes in concentration or temperature, as well as for their reproducibility and ease of preparation. Each has an ionic strength not in excess of 0.1 mol kg^{-1} in order that maximum possible theoretical significance can be attributed to the measured pH values. The seven solutions cover the intermediate pH range, 3.5 - 10.0, within which considerable uniformity of the liquid junction potential and e.m.f./pH slope is to be expected.

The steps by which NBS assigned pH(S) values to these primary standards were as follows:

(1) Determination of $p(a_H y_{Cl})$ for three or more portions of the buffer solution with different small concentrations of added soluble chloride, by measurement of the e.m.f. of the hydrogen-silver chloride cells without liquid junction:

$$Pt;\ H_2,\ \text{Buffer solution},\ Cl^-,\ AgCl;\ Ag \qquad (3.17)$$

Values of $p(a_H y_{Cl})$ were obtained unambiguously from the measured e.m.f. and known values of the standard e.m.f, E°, of the cell by:

$$p(a_H y_{Cl}) = \frac{(E - E^\circ)F}{RT\ln 10} + \log m_{Cl} \qquad (3.18)$$

(2) Evaluation of $p(a_H y_{Cl})^\circ$, the limit approached by $p(a_H y_{Cl})$ as the concentration of added chloride in the buffer solution approached zero, thus eliminating any specific ion interaction due to chloride ions.

(3) Computation of pa_H from $p(a_H y_{Cl})^\circ$ by introduction of a conventional individual ionic activity coefficient:

$$pa_H = p(a_H y_{Cl})^\circ + \log y_{Cl} \qquad (3.19)$$

The "Bates-Guggenheim" convention, applicable to solutions of ionic strengths not exceeding 0.1, was used to evaluate $\log y_{Cl}$:

$$\log y_{Cl} = \frac{-AI^{\frac{1}{2}}}{1 + 1.5\, I^{\frac{1}{2}}} \qquad (3.20)$$

(4) Identification of the pa_H of the selected reference solutions with pH(S). For these few solutions:

$$pH(S) \equiv pa_H \qquad (3.21)$$

Table 3.1 lists the NBS primary standards with their assigned pH(S) values at 25 °C.

Table 3.1 Standard pH(S) Values for NBS Primary Buffers

STANDARD BUFFER SOLUTION	pH(S)	Reference
KH tartrate (satd. at 25 °C)	3.557	*(97)*
KH_2 citrate (m = 0.05)	3.776	*(97)*
KH phthalate (m = 0.05)	4.005	*(98)*
KH_2PO_4 (m = 0.025), Na_2HPO_4 (m = 0.025)	6.863	*(99)*
KH_2PO_4(m = 0.0087), Na_2HPO_4 (m = 0.0304)	7.415	*(99)*
Borax (m = 0.01)	9.183	*(99)*
$NaHCO_3$ (m = 0.025), Na_2CO_3 (m = 0.025)	10.014	*(99)*

3.2.3 Secondary Standards

Although the standard scale represented by pH(S) possesses a satisfactory degree of internal consistency in the intermediate region of the pH scale, at high acidities and high alkalinities the highly mobile hydrogen and hydroxyl ions alter the value of the liquid junction potential (and hence $E^{\circ\prime} + E_j$) significantly. The resultant deviations in measured pH from pa_H determined from cells without liquid junction are not a function of pH alone, unfortunately, and accordingly cannot be corrected by a suitable standardisation of the pH cell. For this reason primary standardisation of the pH cell is limited to the intermediate region of the pH scale. To affirm the proper functioning of the pH cell, additional secondary standards of pH outside the intermediate range are desirable. Even within the intermediate pH range, secondary standards prove convenient if they are more easily prepared or more stable than the primary standards.

NBS have prepared and assigned pH(S) values at 25 °C to four secondary standards. These are listed in Table 3.2. (The assignment of these pH(S) values was made in the same way as for the primary standards.)

Table 3.2 Standard pH(S) Values for NBS Secondary Buffers

STANDARD BUFFER SOLUTION	pH(S)	Reference
K tetroxalate (m = 0.05)	1.679	*(100)*
Tris (m = 0.05), Tris. HCl (m = 0.05)	8.173	*(100)*
Tris (m = 0.01667), Tris. HCl (m = 0.05)	7.699	*(100)*
$Ca(OH)_2$ (satd. at 25 °C)	12.454	*(100)*

3.3 Limitations of the pH Scale and Possible Interpretation

3.3.1 Internal Consistency of the Primary Standards

The seven NBS primary standards fix a "working" scale which shows a satisfactory internal consistency from pH 3.7 to 9.2. This means that the pH furnished by a cell of type 3.13 with a properly designed liquid junction is nearly the same regardless of which of these seven solutions is chosen as a standard. Measurements made on these standards, with cells possessing liquid junctions, show that the five standards of pH(S) 3.7 to 9.2 appear to be consistent among themselves to ± 0.006 pH unit at 25 °C *[101]*.

Deviation of pH(measured) values of individual standard solutions from the "working acidity scale" (fixed by pH(S) values as a group), is a function of:

(1) the limitations of the Bates-Guggenheim convention for estimating the indeterminant activity coefficient of the chloride ion.

(2) experimental limitations in obtaining $p(a_H y_{Cl})$, $p(a_H y_{Cl})^\circ$ and ionic strength I in the determination of pH(S).

(3) any lack of uniformity of the liquid junction potential where cells with liquid junctions are being used.

(4) the reproducibility in the compositions of the standard buffer solutions.

(5) the accuracy of the pH meter in the determination of e.m.f.s.

3.3.2 Uncertainties in the Measured pH of Test Solutions

The measured pH of test solutions suffers the same limitations as the measured pH of standard buffers (see 3.3.1 above). In particular, the practical pH, the number furnished by the electrode-assembly adjusted to the "working" acidity scale, approaches the dimensions of this conventional scale only under certain ideal conditions. By comparison of the operational definition of pH (eqn 3.16) with equation 3.14, it can be seen that the necessary condition for the measured pH to fall on the scale defined by the activity standards is for $E^{\circ\prime} + E_j$ to remain unchanged when the standard solution is replaced by the unknown. This condition is approximately fulfilled only when the unknown is a fairly dilute (< 0.2 M) aqueous solution of simple solutes and its acidity matches closely that of the standard solution selected. Unfortunately, the great majority of test solutions will not meet these stringent conditions and the measured pH will never fall exactly on the conventional activity scale defined by the pH standards.

Furthermore, because the standard electrode potential of the

hydrogen electrode is defined as zero at all temperatures, we have, inescapably, several different pH scales and the pH at one temperature has no quantitative meaning relative to that at another.

3.3.3 Conclusions

The modern definition of pH is an operational one. pH is not a theoretical concept. Experimentally determined pH can never be an exact measure of either the concentration or the activity of the hydrogen ion, and affords only limited interpretation under ideal conditions.

A summary of the problem of pH is illustrated in Figure 3.1.

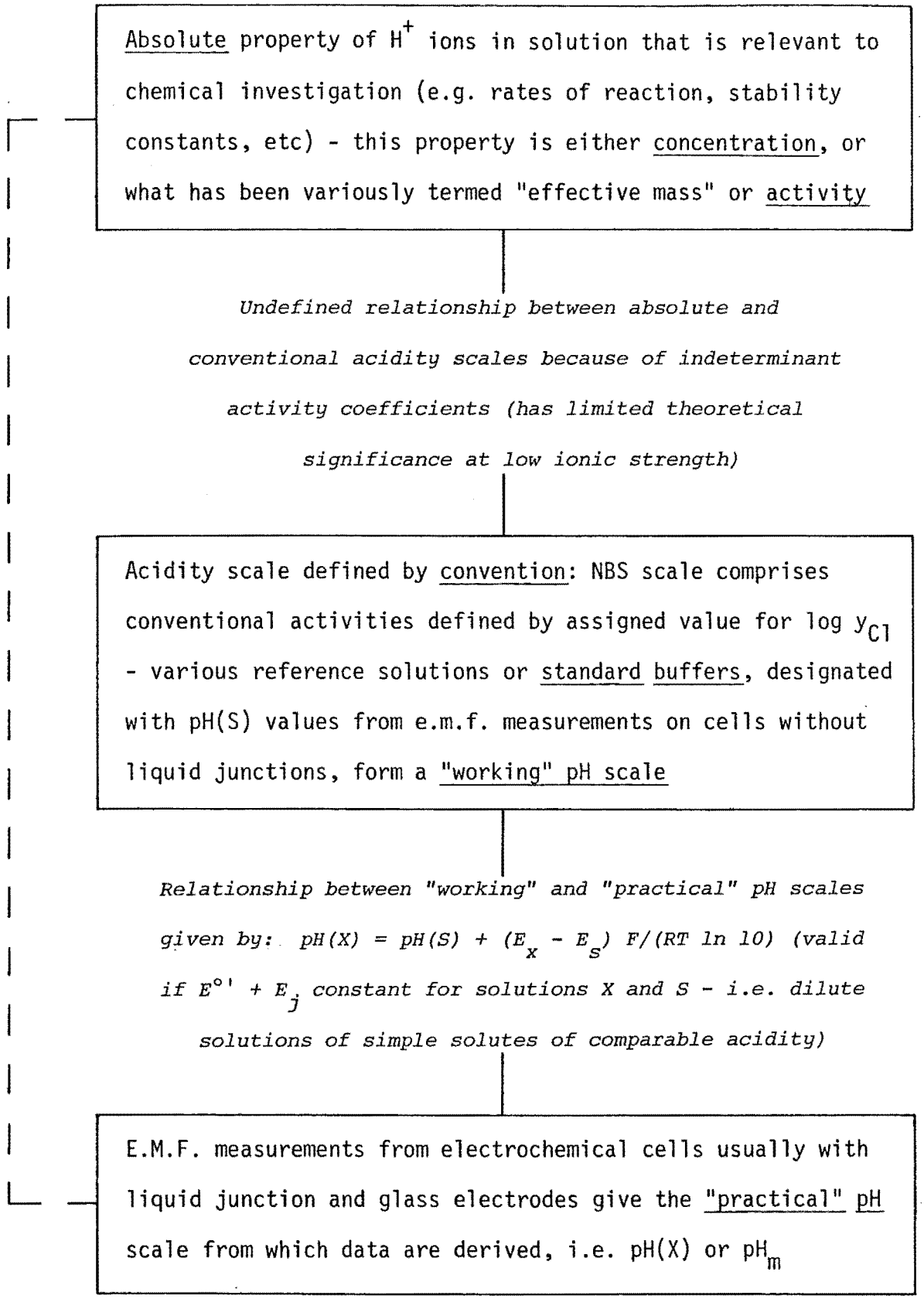

Figure 3:1 The Problem of pH Illustrated

B. THE RESPONSE OF THE GLASS/CALOMEL ELECTRODE ASSEMBLY TO NBS BUFFERS

Results from a detailed study of the behaviour of the Beckman glass/calomel electrode pair in 15 standard buffer solutions are presented in this section. The pH range 1.7 - 12.5 was covered and the non-ideal response of the electrode assembly is discussed.

3.4 Response of the Glass Electrode

3.4.1 Theory of the Glass Electrode

The most widely used measuring electrode is the "glass electrode".

(a) The Glass Electrode Potential

When a thin membrane of glass is interposed between two aqueous solutions, an electrical potential difference, the so-called "glass-electrode potential", is observed across the glass. This potential is related to the ionic activities in the solutions in a reproducible manner; and, depending on the composition of the glass, may represent a response chiefly to hydrogen ions or to other cations such as sodium, potassium, ammonium, silver or calcium.

Until recently the origin of potentials in glass electrodes was not well understood. It now seems certain that the glass electrode behaves as a perfect cation-exchange membrane whose electrode potential represents the sum of two major contributions: the "boundary potential", which results from the ion exchange equilibrium at the boundary between the hydrated surface layer of the glass and the solution; and the "diffusion potential" which results from the interdiffusion of ions within the surface layer. Thus the contribution of a particular ion to the electrode potential is a function of both its mobility within the

glass and the relative strength with which it is bound to the glass. Equations have been developed that account well for the response of glass electrodes to the hydrogen ion and other cations[102].

(b) Measurement of the Response of the Glass Electrode

The response of a hydrogen ion electrode is given by:

$$E_2 - E_1 = \frac{RT \ln 10}{F} . (pH_2 - pH_1) \quad (3.22)$$

or

$$R_{pH} \equiv \frac{E_2 - E_1}{pH_2 - pH_1} \quad (3.23)$$

Where E_1 and E_2 represent the e.m.f.s of test solutions of pH equal to pH_1 and pH_2 respectively. The ideal pH response is shown by a glass electrode behaving in exactly the same manner as the standard hydrogen gas electrode, that is:

$$R_{pH} = (RT \ln 10)/F \ (=59.16 \text{ mV/pH unit at } 25 \ ^\circ C) \quad (3.24)$$

Unfortunately, no glass electrode yet constructed shows ideal response in all types of test solutions and over the entire practical pH range. The potential of the glass electrode is usually a linear function of pH in the intermediate pH range, 3 - 10, but the response (R_{pH}) usually differs from the theoretical. This difference can be expressed as the "electromotive efficiency", βe: .

$$\beta e = \frac{R_{pH} \text{ glass electrode}}{R_{pH} \text{ hydrogen electrode}} \quad (3.25)$$

Electromotive efficiencies of glass electrodes are usually greater than 0.95.

3.4.2 Results for Buffers of Intermediate pH

Table 3.3 presents results for the response of the Beckman E-2 glass/calomel assembly to several buffer solutions in the intermediate pH range 3.5 - 9.2. Figure 3.2 presents these results graphically along with results obtained for buffers in the high and low pH range (see also section 3.5.2).

Results obtained for the primary NBS buffers, tartrate, phthalate and the two phosphate solutions indicated a linear response of the glass electrode in the pH range 3.5 - 7.4. While the buffer solutions generated from acetic and o-phthalic acids are not formal standards by the NBS definition, they did furnish data which were consistant with the four primary standards already mentioned. The borax primary buffer and the tris secondary buffer gave values of pH_m (measured pH) that were consistently higher and lower, respectively, than expected. The use of recrystallized material in each case gave no significant improvement.

Although the response of the glass/calomel electrode assembly appears to be linear in this intermediate pH range the slope of the graph of pH_m - pH(S) vs pH(S) is clearly non-zero. (Note: the Beckman pH meter used had no provision for slope adjustment).

In order to record all pH measurements relative to the standard scale fixed by the NBS buffers, values of pH_m in this pH range were standardised by the following empirical equation:

$$\text{pH (standardised)} = pH_m - \delta \qquad (3.26)$$

where

$$\delta = -6.993 \times 10^{-3}\, pH_m + 0.048 \qquad (3.27)$$

Table 3.3 Response of the Glass/Calomel Assembly to Buffers of Intermediate pH

Buffer Solutions	pH(S)	pH_m (a)	s (b)	n	pH_m - pH(S)
(1) NBS Primary Standards					
K H tartrate	3.557	3.577	.002	15	+ .020
K H phthalate	4.005	4.029	.004	15	+ .024
KH_2PO_4, Na_2HPO_4 (1:1)	6.863	6.863	-		0 .000
KH_2PO_4, Na_2HPO_4 (1:3.5)	7.415	7.412	.005	3	- .003
Borax	9.183	9.178	.008	19	- .005
(2) NBS Secondary Standards					
Tris, Tris HCl (1:1)	8.173	8.136	.009	4	- .037
(3) Other Buffers Used					
0.01 M acetic acid,					
0.01 M Na acetate	4.718 (c)	4.730	.001	2	+ .012
o-phthalic acid/KOH	5.063	5.076	.008	4	+ .013
titrations (d)	5.238	5.253	.006	4	+ .015
	5.360	5.380	.002	3	+ .020

(a) pH (measured) values determined as the average of a number of measurements with the glass/calomel cell (n); each relative to phosphate 1:1 primary standard.

(b) "s" represents one standard deviation from the mean of n measurements. These figures may be taken as an estimate of the reproducibility associated with the pH measurements of the buffer concerned.

(c) pH(S) assigned by reference to pa_H values given in reference 78, p11.

(d) details of the determination of pH(S) and pH_m values for these buffers are given in Appendix 2.

Equation 3.27 is the equation of the line of estimated best fit on the graph of pH_m - pH(S) *vs* pH(S) (see figure 3.2). The non-zero slope of this line was attributed to a non-ideal or "non-Nernstian" response of the glass electrode (see section 3.4.1*b*).

A measure of this non-ideality can be made by determining pH_m values for two or more standard buffer solutions *viz* $pH(X_1)$, $pH(X_2)$. From equation 3.23:

$$R_{pH} \text{ glass electrode} = \frac{E_2 - E_1}{pH_2 - pH_1}$$

where pH_1 and pH_2 are the standard pHs of these buffers. Since the pH meter is set to convert e.m.f. to measured pH values by a constant factor of RT ln 10/F, equation 3.23 may be written:

$$R_{pH} \text{ glass electrode} = \frac{[pH(X_2) - pH(X_1)](RT \ln 10)/F}{pH_2 - pH_1}$$

Combining with equations 3.24 and 3.25:

$$\frac{R_{pH} \text{ glass electrode}}{R_{pH} \text{ hydrogen electrode}} = \frac{pH(X_2) - pH(X_1)}{pH_2 - pH_1} = \beta e$$

By inspection of equations 3.26 and 3.27 it can be seen that the right hand side of this expression for βe is just 1 + s where s is the slope of the plot pH_m - pH(S) *vs* pH(S).

Thus, βe for the Beckman electrode used in this work was *ca*. 0.993.

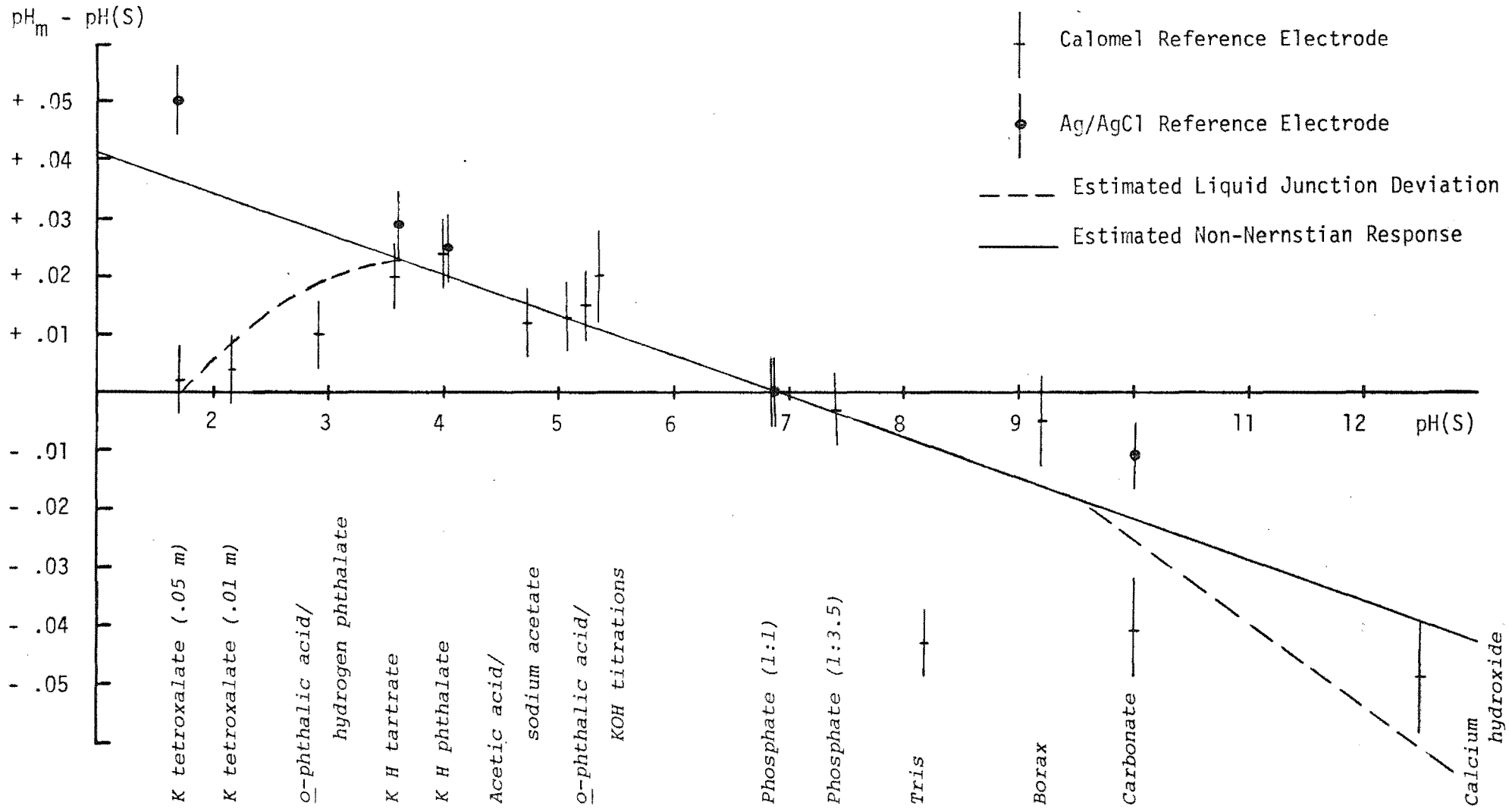

Figure 3.2 Standardisation of the Practical pH Scale With Reference Buffer Solutions

3.4.3 Two-Buffer Standardisation

Because of the non-ideal response of most glass electrodes, some modern pH meters are equipped with a slope adjustment facility. The pH meter is essentially a voltmeter equipped in such a way that values of e.m.f. of test solutions are properly converted into pH units on the scale of the instrument. On the Radiometer pH meter used in part of this work, an ISO-PH [74,103] knob was used to control the scale position by effectively altering the electrical zero of the instrument, while a SENSITIVITY control altered the slope or scale length. In practice, standardisation of the instrument assembly was made by setting the ISO-PH control to the pH(S) of the standard phosphate buffer (1:1). The instrument was adjusted to read 6.863, by means of the linear BUFFER control, while the electrodes were immersed in the phosphate buffer. The electrodes were then placed in a second standard buffer, usually phthalate, and any non-Nernstian response of the glass electrode was compensated for by adjusting the SENSITIVITY control. Simple two-buffer standardisation of the electrode assembly was thus effected, eliminating the need for empirical corrections, such as equation 3.26, to measured pHs in the intermediate pH range.

3.5 Liquid Junction Effects

3.5.1 Liquid Junction and the pH Scale

The relationship between pa_H of a test solution and the e.m.f. of a commonly used pH cell which has a liquid junction is given by:

$$-\log a_H = \frac{(E - E^{\circ\prime} + E_j)\,F}{RT \ln 10}$$

E_j is the algebraic sum of the potentials across the liquid junction

between the test solution and the filling solution of the reference electrode (often saturated potassuim chloride). The liquid junction is a complicated function of the activities and transference numbers of the several ionic species in the transition layers[104]. Since calculations of E_j itself requires knowledge of indeterminant single ion activity coefficients, log a_H remains physically immeasurable.

The necessary condition for the measured pH to fall on the scale defined by the pH standards is that $E^{\circ\prime} + E_j$ remain constant when the standard solution is replaced by another buffer or test solution (see section 3.3.2). This is seldom the case. In particular, when buffers of high or low pH are included the residual liquid junction potential may be significantly greater than zero. This is mainly due to the high mobility of hydrogen and hydroxyl ions. This residual potential manifests itself as an error in the measured pH. By comparing pH_m of a number of buffer solutions using cells with and without liquid junction, Bates et al[105] monitored deviations in the practical pH scale from pH 1 - 13. They found that deviations due to liquid junction effects, represented by $pH(lj) - pa_H$ values, were between 0.00 and -0.05 for $pH > 9$ and up to -0.035 for $pH < 3.0$. A few positive deviations, up to +0.03, were also reported.

Subsequent work[106] suggested an approximately linear deviation above pH 9.18 of about -0.01 pH per pH unit (eg. -0.034 for the NBS hydroxide buffer, pH(S) 12.454). Standardisation of the pH electrode assembly at high pHs in this linear fashion was suggested, although the determination of deviations associated with particular liquid junctions being used was advised.

3.5.2 Results for Buffers of High and Low pH

Table 3.4 presents results for the response of the Beckman glass/calomel assembly to several buffer solutions in the high pH range (pH >9.2) and the low pH range (pH < 3.5). Figure 3.2 presents these results graphically along with results for buffers in the intermediate pH range (see also section 3.4.2).

In the low pH region (pH< 3.5), significant deviation from linearity was apparent in the response of the glass/calomel assembly. In particular pH_m for the NBS secondary buffer, tetroxalate, was approximately 0.035 pH units lower than the linear response fixed by standard buffers of intermediate pH. To detail the electrode response in the pH range between NBS buffers, tetroxalate and tartrate, pH(S) 1.679 and 3.557 respectively, two other buffers were prepared. These were 0.01 m tetroxalate and o-phthalic acid/phthalate (see section 2.2.1). Although these were not strictly standard buffers, data from the pH response to these two solutions confirmed the pronounced deviation from linearity observed for NBS .05 m tetroxalate.

At high pHs (pH > 9.2) deviations from linearity were also observed, but of a less well defined nature. Only two buffers, namely NBS hydroxide and carbonate, were suitable for characterising the electrode response in this pH range. Carbonate was, on average 0.013 and hydroxide 0.010 pH units lower than the linear scale of the intermediate buffers. These two buffers, along with borax and tris (1:1), showed the lowest measure of reproducibility of all the standard solutions used.

Deviations from linearity at high and low pH were assumed to arise from liquid junction effects. To check the validity of this assumption, the response of the glass electrode, used in conjunction with a silver/silver chloride reference electrode, to five of the NBS buffers was

Table 3.4 Response of the Glass/Calomel Assembly to Buffers of High and Low pH

Buffer Solution	pH(S)	pH_m (a)	s (b)	n	pH_m - pH(S)
(1) NBS Primary Standards					
$NaHCO_3$, Na_2CO_3 (1:1)	10.014	9.973	.008	10	- .041
(2) NBS Secondary Standards					
K tetroxalate (0.05 m)	1.679	1.681	.006	15	+ .002
$Ca(OH)_2$ (satd.)	12.454	12.405	.010	7	- .049
(3) Other Buffers Used					
K tetroxalate (0.01 m)	2.157 *(c)*	2.161	.001	2	+ .004
o-phthalic acid/hydrogen phthalate	2.913 *(c)*	2.923	.001	2	+ .010

(a), (b) see respective notes for table 3.3

(c) details of the assignment of pH(S) given in Appendix 2

investigated. The buffers used and the corresponding values for pH_m - pH(S) were: tetroxalate (0.05 m), + .050; tartrate, + .029; phthalate, + .025; phosphate, 0.000; carbonate, -.011. These data, determined in a cell without a liquid junction, represented deviations consistent with the non-Nernstian response of the glass electrode alone, even at high and low pH (see figure 3.2). This suggested that deviations from linearity associated with the use of the calomel electrode were primarily a function of the liquid junction.

In order to standardise all pH measurements relative to a linear pH scale that matched the working pH scale (fixed by pH(S) values) as closely as possible, corrections were applied to pH measurements at high and low pHs. These corrections were made somewhat arbitarily, based on the assumption that deviations due to liquid junction effects are basically a function of pH and follow the pattern set by standard buffers at each end of the pH scale (the curved lines in figure 3.2). This assumption will be only approximately fulfilled for dilute aqueous solutions of simple solutes. These corrections are presented in tabular form in Appendix 3.

In practice pH measurements were standardised firstly by applying liquid junction corrections for pHs above 9.2 and below 3.5 and secondly by adjustment for non-Nernstian response of the glass electrode, according to equation 3.26, throughout the pH range.

3.5.3 Conclusions

In order that the practical pH scale, as represented by day to day measurements on the pH meter, corresponds as closely as possible to the conventional acidity scale, as fixed by pH(S) values of NBS standard buffers, standardisation of the electrode assembly is required throughout the pH range to be used. Two important factors in this process emerge. Firstly, for cells utilizing a glass electrode, the departure of the electrode's response relative to that for the hydrogen electrode needs to be compensated for. This "non-Nernstian" behaviour can be characterised by reference to the expected linear response of the electrode assembly to standard buffers in the intermediate pH range (eg. 3.5 - 9.0). Secondly, for cells utilizing a liquid-liquid junction, departures from linearity at high and low pH can be approximately compensated for by reference to the response to standard buffers in these regions. It

should be noted that this second adjustment to pH_m values is approximate only since the magnitude of these liquid junction effects is a function of, not only the structure of the particular liquid junction being used and the pH of solution, but also the concentration and type of ions present in the test solution compared with those of the standards. For this reason the measured pH will seldom fall exactly on the conventional acidity scale defined by the pH - standards. (Note: if a low sensitivity glass electrode is used, additional corrections to the measured pH may have to be made to compensate for response of the electrode to alkali metals at high pH).

Where pH_m values are directly calibrated in terms of known hydrogen ion concentrations (eg. pc_H) of certain reference solutions, many assumptions about the behaviour of the electrode assembly are bypassed. This relationship is represented by the dotted line in figure 3.1. The practical pH scale becomes simply a useful, if only arbitary, reference scale to which all pH_m values can be reproducibly related. Calibration of the electrode assembly in terms of hydrogen ion concentration is the subject of chapter 4.

CHAPTER 4

CALIBRATION OF THE pH ELECTRODE ASSEMBLY AS A HYDROGEN ION CONCENTRATION PROBE

A. USE OF THE pH METER TO DETERMINE HYDROGEN ION CONCENTRATION

The calculation of many acid/base or metal/ligand equilibrium constants requires accurately known hydrogen ion concentrations. Readily available pH data are often used in these calculations but there are fundamental limitations in the interpretation of these data in terms of hydrogen ion concentration. Many of these limitations can be avoided by calibrating the measuring electrode assembly with solutions of known hydrogen ion concentrations. Calibrations of this sort have been effected with solutions of strong acids and bases (covering the low and high pH range respectively) as well as many buffer systems (for the intermediate pH range). In order to use buffer solutions as calibrants, well defined equilibrium concentration quotients of the relevant weak acid or base must be known or readily calculable.

In this chapter data are presented that extend the calibration of the pH electrode assembly by use of buffer solutions comprising o-phthalic acid/hydrogen phthalate and hydrogen phthalate/phthalate, covering the pH range 2.8 - 5.3. Concentration quotients for these buffer systems have been calculated from thermodynamic equilibrium constants and empirical expressions for single ion activity coefficients. The calibration relationship between measured pH and hydrogen ion concentration, determined in KCl media of ionic strength 0.04 - 0.2 M at 25 °C, has also been defined at high and low pH.

4.1 The Determination of Equilibrium Constants Using pH Data

4.1.1 Equilibrium Constants

Equilibrium constants of two main types have been the focus of numerous calculations involving data from commercial pH-electrode assemblies. The first type includes association constants of weak acids or bases and certain hydrolysis constants. For example, consider the equilibrium reaction of a weak acid HA (charges omitted for clarity):

$$A + H^{+} \rightleftharpoons HA \qquad (4.1)$$

The thermodynamic equilibrium constant for this reation is given by:

$$k^{\circ} = \frac{a_{HA}}{a_H a_A} = \frac{c_{HA}}{c_H c_A} \cdot \frac{f_{HA}}{f_H f_A} \qquad (4.2)$$

Hence, if values of pH_m (the measured pH) are considered to represent -log a_H, then acidity constants such as k° can in principle be determined from equilibrium activities of the acid and its conjugate base. Since the latter require knowledge of indeterminant single ion activity coefficients, many workers have chosen to measure the "mixed" constant, k'_{HA}, defined as:

$$k'_{HA} = c_{HA}/(c_A a_H) \qquad (4.3)$$

The second type of equilibrium constant includes the formation constants of metal-ligand complexes. When the ligand is the conjugate base of a weak acid, protons may be released on formation of the complex. The competition between metal ions and protons for the co-ordination sites of the ligand is a function of the association constants of the acidic groups and the stability constant of the metal complex. For example, consider a metal M, and an acid-ligand LH_2, forming a 1:1 complex ML, by displacing both protons from the ligand:

$$M + LH_2 \rightleftharpoons ML + 2H^+ \qquad (4.4)$$

for which the "formation constant" K°_{f1} may be written:

$$K^\circ_{f1} = \frac{a_{ML}(a_H)^2}{a_M\, a_{LH_2}}$$

$$= \frac{a_{ML}}{a_M a_L} \cdot \frac{a_L(a_H)^2}{a_{LH_2}}$$

$$= K^\circ_1 / (k^\circ_1 k^\circ_2) \qquad (4.5)$$

Where competition between protons and metal ions exists, the extent of formation of ML is a function of pH. Bjerrum has shown that stepwise equilibrium constants of the type K°_{f1} may be determined from pH data of solutions containing known total concentrations of metal and acid ligand [107].

4.1.2 The Validity of Using pH Data in Equilibrium Constant Calculations.

The main limitations in determining equilibrium constants of the types defined in equations 4.2, 4.3 and 4.5 using pH data are simply those of the identification of the measured pH with the true activity of the hydrogen ion.

Firstly, there is the limitation inherent in the association of measured pH with -log a_H, the conventionally defined acidity scale. As has been discussed in section 3.3.2, the necessary condition for measured pH to correspond to the working acidity scale, defined by pH(S) values of standard buffers, is the constancy of the term $E^{\circ\prime} + E_j$ (see equation 3.14). The medium used for the determination of equilibrium constants is often a complex one involving several ionic species some of which are present in concentrations of >1 mol dm^{-3}, whereas that used to define pH(S) values involved simple solutes in concentrations typically 0.02 - 0.05 M.

Further problems exist where mixed solvents are used. In examples such as these, where the residual liquid junction potential will be nonzero, pH_m can not be accurately identified with the conventional activity.

The second limitation, more fundamental in nature, concerns the adopted acidity scale, pa_H. Because this scale is a conventional one, with only limited physical significance in ideal conditions of dilute solutions of simple solutes, it cannot strictly be identified with the true activity of the hydrogen ion (see section 3.1.4).

4.1.3 Equilibrium Concentration Quotients

Equations 4.2 and 4.5 may be rewritten as:

$$k = \frac{c_{HA}}{c_H c_A} \qquad (4.6)$$

and

$$K_{f1} = \frac{c_{ML}(c_H)^2}{c_M c_{LH_2}} = K_1/(k_1 k_2) \qquad (4.7)$$

where k, K_{f1} and K_1 are "concentration quotients". While the thermodynamic constants k°, K°_{f1} and K°_1 depend on temperature, pressure, the scale of concentration and the chosen standard state, the corresponding concentration quotients will also vary with the ionic strength and composition of the medium. For this reason concentration quotients are commonly determined in "constant ionic media". These media usually contain some inert background electrolyte such as sodium or potassium salts. The relatively concentrated neutral salt medium is relied upon to "swamp out" changes in the activity coefficients of the charged species when small changes in concentration occur and to equalise the activity coefficients of ions of like charge present at small concentrations. In

general complete swamping of activity coefficient variations is not achieved and care in the design of the measurement system is essential if meaningful results are to be obtained [108].

In conjunction with expressions of the type given in equations 4.6 and 4.7, a series of "mass balance" equations involving the known stoichiometric concentrations of metal (T_M), ligand (T_L) and titratable protons (T_H) may be set up as follows:

$$T_M = c_M + c_{ML} + c_{ML_2} + \ldots + c_{ML_n} \quad (4.8)$$

$$T_L = c_{ML} + 2c_{ML_2} + \ldots + nc_{ML_n} + c_L + c_{LH} + \ldots + c_{LH_x} \quad (4.9)$$

$$T_H = c_H + c_{LH} + 2c_{LH_2} + \ldots + xc_{LH_x} - c_{OH} \quad (4.10)$$

By appropriate substitutions for the equilibrium concentrations of the various species in equations 4.8 - 4.10, in terms of equilibrium constants k and K, an equation of the following general form can be derived:

$$T_L = fn(K_1, K_2 \ldots K_n, k_1, k_2 \ldots k_x, T_M, T_H, c_H) \quad (4.11)$$

If the protonation constants k_1, $k_2 \ldots k_x$ are known then, in principle, determination of metal-ligand stability constants K_1, $K_2 \ldots K_n$ only requires appropriate values for c_H, the equilibrium hydrogen ion concentration.

4.2 Measurement of Hydrogen Ion Concentration

4.2.1 Use of Single Ion Activity Coefficients

In order to calculate hydrogen ion concentrations, a common approach [109] has been to convert the measured pH according to the following relation:

$$pc_H = pH_m + \log f_H \qquad (4.12)$$

The hypothetical single ion activity coefficient, f_H, is estimated from an empirical relation such as the Davies equation [110]:

$$-\log f_H = 0.5\, z^2 \,(I^{\frac{1}{2}} / (1 + I^{\frac{1}{2}}) - 0.20\, I) \qquad (4.13)$$

Two important assumptions are involved in this approach.

(1) Values of pH_m are assumed to measure the true activity of the hydrogen ion in solution. This assumption is therefore subject to the same limitations inherent in the calculation of activity constants described in section 4.1.2.

(2) An additional limitation is the assumption that an empirical equation such as 4.13 accurately defines f_H at a given ionic strength. However, for a mixed electrolyte system, the value of f_H will depend on all the specific ionic interactions in solution, for which the individual coefficients are often not known. A fuller treatment of the limitations involved in using the Davies equation is given by Hedwig [111].

4.2.2 Calibration of Cells With Liquid Junctions

Hydrogen ion concentrations have also been determined from pH measurements by means of empirically-derived calibration relationships. This method has been used for cells without liquid junctions [81, 112]. However, since most pH data, including those presented in this work, are recorded from electrode assemblies employing a salt bridge as a liquid-liquid junction, discussion will be confined to this type of cell.

From equation 3.16 we have the operational definition of measured pH:

$$pH\,(X) = pH(S) + \frac{(E_x - E_s)F}{RT \ln 10}$$

The condition for the measured pH, pH(X), to fall on the conventionally defined activity scale, pa_H, is the constancy of $E^{\circ\prime} + E_j$. In particular the residual liquid junction potential, $\Delta E_j = E_j^X - E_j^S$, must be close to zero. In reality, however, the measured pH differs from the "actual" hydrogen ion activity a_H, by a quantity related to the residual junction potential:

$$pH(X) = pa_H + \frac{\Delta E_j F}{RT \ln 10} \qquad (4.14)$$

and

$$pH(X) = pc_H + \frac{\Delta E_j F}{RT \ln 10} - \log f_H \qquad (4.15)$$

or, at constant ionic strength:

$$pH(X) = pc_H - A \qquad (4.16)$$

Values of A have been determined from measurements on a variety of acid-base systems in constant ionic media [113], and have been used to convert measured pH to hydrogen ion concentrations. A was found to be constant for individual salt media, over a range of pH up to 5.3, apparently indicating the effectiveness of the medium in reducing variations in the residual liquid junction potential and the activity coefficient, f_H.

McBryde [81] calibrated several glass/calomel assemblies using solutions of a strong acid in media of constant ionic strength. Values of pH_m were plotted against the negative logarithm of the known hydrogen ion concentration and a least squares fit to a straight line was calculated. An empirical relationship of the general form

$$pH_m = M\ pc_H + C \qquad (4.17)$$

was derived, where M = slope and C = intercept. Results for 0.1 M sodium chloride medium, for example, averaged over three electrode

assemblies gave:

$$pH_m = 0.994\ pc_H + 0.1046$$

McBryde also determined the ratio , Γ_H , between 10^{-pH_m} and c_H. This was observed to be constant in the range 10^{-2} to 10^{-4} M hydrogen ion concentration. The following relationship was used in the conversion of pH data to hydrogen ion concentrations:

$$c_H = 10^{-pH_m} / \Gamma_H \qquad (4.18)$$

This calibration was later extended to the alkaline region with a linear relationship being observed between 10^{pH_m} and c_{OH} (equation 4.19), in the approximate range 10^{-2} to 10^{-4} M hydroxide ion concentration [112].

$$c_{OH} = 10^{pH_m} / \Gamma_{OH} \qquad (4.19)$$

Values of Γ_H computed from Γ_{OH} and estimated K_{cw}, the ionic concentration product for water, agreed to $\leqslant$ 3 % of Γ_H calculated in the acid region.

Another important extension of this work required the definition of these empirical relationships in the intermediate pH ranges. This was made possible by the titration of certain buffer solutions with a strong base or acid. The buffer solutions used were those for which accurate concentration quotients were known or could be derived. For example, Powell and Curtis [114] titrated ethylenediamine with perchloric acid in sodium perchlorate solutions, ranging in ionic strength from 0.04 to 0.35 M. Plots of pH_m against -log c_H (pc_H), at each ionic strength, were found to be colinear. (Theory requires them to be parallel; see equation 4.16). A similar result was found [115] for titrations of hydrochloric acid, acetic acid and ethylenediammonium chloride with sodium hydroxide in sodium chloride solutions (0.04 to 0.20 M ionic strength). The data were again colinear within experimental error and the following relationship derived:

$$pH_m = 0.9951\ pc_H + 0.088$$

Avdeef and Bucher [116] calibrated a Beckman combination electrode to read hydrogen ion concentrations by titrating various mixtures of the buffers potassium acetate, potassium dihydrogen phosphate, ethylenediammonium chloride and borax, with standard acid and/or alkali in a KCl medium. This calibration covered the pH range 1.5 to 12.5 and ionic strength range 0.05 to 0.20 M. They found that the relationship between pc_H and pH_m was a function of ionic strength. Empirical terms accounting for liquid junction effects were included in the calculations. These parameters were found to be quite variable for different buffer compositions and were disregarded in the final derivation of a pc_H/pH_m relationship covering all the data. This relationship was expressed as:

$$pH_m = S'pc_H + \Delta'$$

where S' and Δ' were fitted to quadratic functions of I, the ionic strength.

The advantages of a calibration method of determining hydrogen ion concentration are:

(1) the limitations of associating pH_m with the conventional activity scale, where a significant residual liquid junction potential is often encountered, are avoided,

(2) the assumption concerning the identification of the conventional activity scale with the "true" activity scale are bypassed, and

(3) no empirical expression is required for f_H to convert pH_m values to pc_H.

The reader is referred again to figure 3.1 for an illustration of the principles being discussed here. The dotted line in the figure

represents the direct calibration of the pH meter in terms of hydrogen ion concentration.

The method does, however, rely on some assumptions. These are that the constant background ionic medium (1) ensures the constancy of the activity coefficient of hydrogen ions, and (2) minimises the residual liquid junction potential between solutions of known c_H and the test solutions. Under these conditions an operational definition of pc_H can be stated as:

$$pc_H(X) = pc_H(S) + \frac{(E_X - E_S)\,F}{RT \ln 10} \qquad (4.20)$$

where X and S refer to the test and calibrant solutions respectively. The second of these assumptions can be eliminated by using a cell without a liquid junction but this is generally found to be less convenient. Calibration of any one electrode assembly is made relative to the response to standard buffers. These serve as a reproducible reference scale to which subsequent pH measurements are also related.

4.2.3 Development of the Calibration Method

This work extends the buffer calibration method to enable use of o-phthalic acid in a potassium chloride medium in the pH range 2.8 - 5.3. o-Phthalic acid can be easily prepared in pure crystalline form (see section 2.3.1) and hence could be preferred to acetic acid (which requires standardisation) for calibration procedures in the weakly acidic to neutral pH range.

B CALIBRATION OF THE GLASS/CALOMEL ASSEMBLY WITH o-PHTHALIC ACID BUFFERS

4.3 Determination of Concentration Quotients For o-Phthalic Acid

4.3.1 First and Second Dissociation Constants For o-Phthalic Acid

In order to use a weak acid or base in the calibration of the electrode assembly accurate concentration quotients must be known. Although these were not available for o-phthalic acid, precise empirical relationships for the relevant single ion activity coefficients have been established by Hamer et al. [80, 83]. These expressions, along with the first and second thermodynamic dissociation constants (designated K_1 and K_2 respectively) determined by Hamer et al. in a potassium chloride medium, enabled calculation of the corresponding concentration quotients at various ionic strengths.

Galvanic cells without liquid junctions used in the determination of K_1 and K_2 were of the type:

$$Pd;\ H_2(g),\ \text{Buffer solutions}\ (m_1,\ m_2),\ KCl\ (m_3),\ AgCl(s);\ Ag(s) \qquad (4.21)$$

where m_3 was the concentration of potassium chloride in mol kg^{-1} (molality). The buffer solutions used in the determination of the second dissociation constant were mixtures of potassium hydrogen phthalate (KHPh), molality m_1 and dipotassium phthalate (K_2Ph), molality m_2; o-phthalic acid (H_2Ph), molality m_1 and KHPh, molality m_2 were used for the first dissociation constant. For cell 4.21 used in the determination of the second dissociation constant:

$$[(E - E^\circ) / (\ln 10\ RT / F) + \log (m_3\ m_1 / m_2)] +$$

$$\log (y_{Cl} y_{HPh} / y_{Ph}) = -\log K_2 = pK_2 \qquad (4.22)$$

The extended Debye-Hückel equation was used to evaluate activity coefficients, y_i and equation 4.22 was rewritten in terms of the variables E, T, m_1, m_2, m_3 and I (the ionic strength). Also included was an empirical expression, which allowed for corrections to m_1 and m_2 as determined by additional equilibria involving H_2Ph, HPh^- and $Ph^=$ species. This required the use of an assumed value for K_1 , the first dissociation constant. A similar procedure was used in the determination of K_1. Equations of the general form:

$$pK'_n + \beta I = pK_n \qquad (4.23)$$

were derived, where pK'_n was a complex function of the variables listed above, n = 1 or 2, and β represented a combination of $\beta_i m_i$ terms arising from the Debye-Hückel equation. Values of pK'_n were plotted against I and extrapolated to I = 0 to determine pK_1 and pK_2.

4.3.2 Calculation of Concentration Quotients

In an aqueous solution of o-phthalic acid the essential equilibria are:

$$HPh^- + H^+ \rightleftharpoons H_2Ph \qquad (4.24)$$

$$Ph^= + H^+ \rightleftharpoons HPh^- \qquad (4.25)$$

The association constants for these two equilibria can be written (charges omitted for clarity):

$$k_1^\circ = a_{H_2Ph} / (a_H\, a_{HPh}) = k_1 \cdot y_{H_2Ph} / (y_H\, y_{HPh}) \qquad (4.26)$$

$$k_2^\circ = a_{HPh} / (a_H\, a_{Ph}) = k_2 \cdot y_{HPh} / (y_H\, y_{Ph}) \qquad (4.27)$$

where k_1 and k_2 are the concentration quotients. In order to convert the known values of k_1° and k_2° to k_1 and k_2 for a given ionic medium, activity coefficients, y , must be estimated. (k_1° and k_2° are simply $1/K_1$ and $1/K_2$ respectively in terms of the designations used by Hamer et al.)

In the calculation of K_1 and K_2, Hamer et al. determined values for β (a function of β_i m_i). The individual ion parameters β_i were then derived by a least squares method. This enabled the estimation of single ion activity coefficients using the extended form of the Debye-Hückel expression, viz:

$$-\log y_i = A z_i^2 I^{\frac{1}{2}} / (1 + B a_i I^{\frac{1}{2}}) + \beta_i m_i \qquad (4.28)$$

In this work k_1 and k_2 were calculated using equations of the type 4.28 substituting values of β_i and a_i as given by Hamer et al. The constants A and B were taken from Manov et al. [117] ; I and m_i were calculated from the solution stoichiometry. A list of values used for these empirical parameters, including values for K_1 and K_2, is given in table 4.1. Calculated values for k_1 and k_2, at I = 0.1 M are included in table 4.2.

Table 4.1 Constants Used in the Calculation of Concentration Quotients for the Protonation of o-Phthalic Acid Species.

K_1	1.123×10^{-3} mol kg^{-1}	a_i	3.76×10^{8} cm
K_2	3.906×10^{-6} mol kg^{-1}	β_{HPh}	-0.023 mol^{-1} kg
A	0.5085	β_{Ph}	-0.38 mol^{-1} kg
B	0.3281×10^{-8} cm^{-1}		

4.4 Calibration Results

4.4.1 Calculation of Hydrogen Ion Concentration in o-Phthalic Acid Buffer Systems

The following electrochemical cell was used in the calibration procedure:

glass electrode	o-phthalic acid buffer system, KCl (0.04 - 0.20 M), KOH (v ml)	KCl (satd.), Hg_2Cl_2;Hg	(4.29)

The o-phthalic acid buffer system comprised a series of aqueous solutions of weighed amounts of o-phthalic acid and potassium chloride to which standard potassium hydroxide was added incrementally, (see section 2.3.3). The concentrations of o-phthalic acid and KCl were chosen to give solutions of ionic strength 0.04, 0.10, 0.15 and 0.20 mol dm^{-3}.

Equilibrium constants for o-phthalic acid were determined by Hamer et al. on the "molal" scale (i.e. mol/kg solvent; molality of species X represented by "m_X"). It was considered desirable, therefore, to retain the use of molal units throughout the bulk of the calculations. Concentrations of o-phthalic acid/KCl and KOH solutions prepared on the "molar" scale (i.e. mol dm^{-3}; molarity of species X represented by "c_X") were converted to molal units using measured or tabulated density data (see section 2.3.4). Since subsequent determinations of protonation and stability constants were to be made in molar units, hydrogen ion concentrations calculated at first on the molal scale were converted back to molar units (pc_H) for calibration purposes.

In the calculation of hydrogen ion concentration (m_H), two parameters, T_B, total base species and T_H, total acid species, were established:

$$T_B = m_{Ph} + m_{HPh} + m_{H_2Ph} \quad (4.30)$$

$$T_H = m_H + m_{HPh} + 2m_{H_2Ph} \quad (4.31)$$

Expressions for the concentration quotients k_1 and k_2 are:

$$k_1 = m_{H_2L} / (m_H \, m_{HPh}) \quad (4.32)$$

$$k_2 = m_{HL} / (m_H \, m_{Ph}) \quad (4.33)$$

Combining equations 4.24 - 4.27:

$$k_1k_2m_H^3 + (k_1k_2(2T_B - T_H) + k_2) \, m_H^2 + (k_2(T_B - T_H) + 1) \, m_H - T_H = 0 \quad (4.34)$$

T_B and T_H were calculated from the known initial solution composition and the titre (v) of added KOH, concentration c_{KOH}:

$$T_H = 2 \, m^\circ_{H_2Ph} \, Q - v \, c_{KOH} / S + m_{OH} \quad (4.35)$$

$$T_B = m^\circ_{H_2Ph} \, Q \quad (4.36)$$

where $m^\circ_{H_2Ph}$ = initial concentration of o-phthalic acid, Q = dilution due to added alkali and S = total mass of solvent after v ml alkali added. The last term in the expression for T_H (equation 4.35) represents the contribution of hydrolysis reactions of the type:

$$Ph^{2-} + H_2O \rightleftharpoons HPh^- + OH^- \quad (4.37)$$

In practice the hydrolysis contribution was negligible as the maximum pH for which data were collected was ca. 6.

A FORTRAN program was written to calculate pc_H data for this buffer solution as a function of alkali titre, v (see Appendix 4). Pairs

of data points comprising v, pH_m values were fed into the program along with various data relating to solution stoichiometry, parameters for activity coefficient calculations etc. Two sets of titration data at each ionic strength were included. Approximate values of m_{HPh}, m_{Ph} (from estimated solution stoichiometry) and m_H ($m_H = 10^{-pH_m}$) were determined.

The ionic strength of the solution was then calculated using the following expression:

$$I = m_{KCl} + 3m_{Ph} + m_{HPh} \qquad (4.38)$$

Initial values of k_1 and k_2, the concentration quotients, were found as described in section 4.3.2. Equation 4.34 was solved for m_H using the Newton-Raphson method for solving a polynominal. Hence new values of m_{HPh} and m_{Ph} could be determined using expressions derived from equations 4.30 - 4.33, viz:

$$m_{HPh} = k_2 m_H T_B / (1 + k_2 m_H + k_1 k_2 m_H^2)$$

$$m_{Ph} = T_B / (1 + k_2 m_H + k_1 k_2 m_H^2)$$

An improved value for I, the ionic strength, was then found and m_H was recalculated, as the values for k_1 and k_2 depended on the values ascribed to I. The iteration process continued until the change in ionic strength due to modification of m_H was less than 0.0005 mol kg^{-1}.

Representative data, from the titration of o-phthalic acid with standard potassium hydroxide at an overall ionic strength of 0.1 M, are given in table 4.2. Included in this table are values of the concentration quotients calculated for o-phthalic acid and activity coefficients for the ions HPh^-, Ph^{2-} and H^+. Representative data from titrations of o-phthalic acid with KOH at ionic strengths 0.04, 0.15 and 0.20 M are given in Appendix 7.

Table 4.2 Representative Data From a Titration of o-Phthalic Acid With Standard Potassium Hydroxide at 25 °C, Ionic Strength 0.10 M.

Titre (ml) *(a)*	pH' *(b)*	pc_H	y_H	y_{HPh}	y_{Ph}	I (mol kg^{-1})	k_1 (mol^{-1} kg x 10^2)	k_2 (mol^{-1} kg x 10^4)
0.0000	2.9882	2.9134	0.7664	0.7662	0.3446	0.09965	5.228	8.824
0.0100	3.0315	2.9602	0.7663	0.7661	0.3445	0.09968	5.228	8.822
0.0200	3.0859	3.0111	0.7663	0.7661	0.3445	0.09972	5.227	8.821
0.0300	3.1493	3.0671	0.7662	0.7661	0.3444	0.09976	5.227	8.819
0.0400	3.2117	3.1290	0.7662	0.7660	0.3443	0.09981	5.226	8.817
0.0500	3.2802	3.1985	0.7661	0.7660	0.3443	0.09986	5.226	8.815
0.0550	3.3165	3.2366	0.7661	0.7660	0.3442	0.09989	5.225	8.814
0.0600	3.3567	3.2775	0.7660	0.7659	0.3442	0.09992	5.225	8.813
0.0650	3.4071	3.3214	0.7660	0.7659	0.3441	0.09995	5.224	8.812
0.0700	3.4574	3.3689	0.7660	0.7659	0.3441	0.09999	5.224	8.811
0.0750	3.5168	3.4205	0.7659	0.7659	0.3441	0.1000	5.224	8.809
0.0800	3.5793	3.4769	0.7659	0.7658	0.3440	0.1001	5.223	8.808
0.0850	3.6488	3.5390	0.7659	0.7658	0.3439	0.1001	5.223	8.806

0.1300	4.4725	4.3570	0.7652	0.7652	0.3429	0.1009	5.214	8.779
0.1350	4.5641	4.4476	0.7651	0.7651	0.3427	0.1011	5.213	8.774
0.1400	4.6457	4.5334	0.7650	0.7650	0.3425	0.1012	5.211	8.769
0.1450	4.7202	4.6151	0.7649	0.7649	0.3423	0.1014	5.210	8.764
0.1500	4.7897	4.6934	0.7648	0.7648	0.3421	0.1015	5.208	8.759
0.1550	4.8622	4.7693	0.7647	0.7647	0.3419	0.1017	5.207	8.753
0.1600	4.9327	4.8437	0.7646	0.7646	0.3417	0.1018	5.205	8.748
0.1650	5.0082	4.9173	0.7644	0.7644	0.3415	0.1020	5.204	8.743
0.1700	5.0888	4.9913	0.7643	0.7643	0.3413	0.1022	5.202	8.737
0.1750	5.1713	5.0664	0.7642	0.7642	0.3411	0.1023	5.200	8.732
0.1800	5.2599	5.1438	0.7641	0.7641	0.3408	0.1025	5.199	8.726
0.1850	5.3506	5.2248	0.7640	0.7640	0.3406	0.1026	5.197	8.721
0.1900	5.4402	5.3113	0.7638	0.7638	0.3404	0.1028	5.196	8.716

(a) *Cumulative volume of 0.8893 M KOH added to 49.93 ml of titration solution, initially comprising o-phthalic acid (1.9960×10^{-3} M), KCl (0.09799 M).*

(b) *pH' corresponds to measured pH (pH_m) corrected for liquid junction deviations (see section 4.4.3).*

4.4.2 Other Calibrant Solutions Used

(a) Hydrochloric Acid. Calibration of the glass/calomel assembly was extended to low pH by the titration of hydrochloric acid/potassium chloride solutions with standard KOH at ionic strengths of 0.04, 0.10, 0.15 and 0.20 M. The pH range 1.8 - 3.0 was covered by titration of solutions ca. 0.02 M in HCl concentration. Hydrogen ion concentrations were calculated from the known solution composition, and tabulated along with corresponding pH_m data. The FORTRAN program used for these calculations is given in Appendix 5.

Representative data from titrations at 0.10 M ionic strength are given in table 4.3. Data from titrations at the remaining ionic strengths are given in Appendix 8.

(b) Potassium Hydroxide. Extension of the calibration procedure to high pH was effected by the titration of potassium chloride solutions with standard KOH, at the same ionic strengths used for hydrochloric acid and o-phthalic acid titrations. This calibration covered the pH range 10.8 - 12.0. Hydrogen ion concentrations were calculated from the ionic activity product of water K_w (as defined by equation 4.39) and the known hydroxide ion concentration. The FORTRAN program used for these calculations is given in Appendix 6.

$$K_w = a_H a_{OH} / a_{H_2O} = m_H m_{OH} \cdot (f_H f_{OH} / a_{H_2O}) \quad (4.39)$$

The term in parentheses in equation 4.39 was determined by an empirical relationship [118] as a function of ionic strength. Details of this relationship are given in Appendix 10. K_w was taken to be 1.008×10^{-14} at 25 °C [118].

Representative data from titrations at 0.10 M ionic strength are given in table 4.4. Data from titrations at remaining ionic strengths are given in Appendix 9.

Table 4.3 Representative Data From a Titration of HCl with Standard Potassium Hydroxide at 25 °C, Ionic Strength 0.10 M.

Titre (ml) *(a)*	pH' *(b)*	pc_H
0.000	1.7868	1.7005
0.050	1.8070	1.7208
0.150	1.8483	1.7643
0.250	1.8966	1.8125
0.350	1.9500	1.8664
0.400	1.9782	1.8960
0.450	2.0094	1.9278
0.500	2.0426	1.9620
0.550	2.0708	1.9990
0.600	2.1181	2.0393
0.650	2.1624	2.0838
0.700	2.2118	2.1331
0.750	2.2682	2.1888
0.800	2.3306	2.2524
0.850	2.4041	2.3269
0.900	2.4937	2.4166
0.950	2.6065	2.5296
1.000	2.7586	2.6824
1.050	3.0003	3.9195

(a) *Cumulative volume of 0.8893 M KOH added to 49.93 ml of titration solution initially comprising HCl (1.993×10^{-2} M), KCl (0.0800 M).*

(b) *pH' corresponds to measured pH (pH_m) corrected for liquid junction deviations (see section 4.4.3).*

Table 4.4 Representative Data From a Titration of KCl Solution With Standard Potassium Hydroxide at 25 °C, Ionic Strength 0.10 M.

Titre (ml) *(a)*	pH' *(b)*	pc_H
0.080	10.9736	10.8931
0.090	11.0260	10.9441
0.100	11.0733	10.9896
0.110	11.1126	11.0309
0.120	11.1539	11.0685
0.140	11.2213	11.1350
0.160	11.2817	11.1927
0.200	11.3784	11.2889
0.250	11.4771	11.3849
0.300	11.5567	11.4632
0.350	11.6241	11.5292
0.400	11.6825	11.5863
0.450	11.7339	11.6366
0.500	11.7792	11.6815
0.600	11.8587	11.7589
0.700	11.9252	11.8242

(a) Cumulative volume of 0.7826 M KOH added to 49.93 ml of titration solution, comprising KCl (0.0950 M).

(b) pH' corresponds to measured pH (pH_m) corrected for liquid junction deviations (see section 4.4.3).

4.4.3 pc_H / pH_m Relationships

A simple least squares analysis (using FORTRAN program ORGLS [119]) was performed on pc_H / pH_m* data at each ionic strength. Results are presented as the coefficients M, C of the general equation 4.17, along with various measure of uncertainty and "goodness of fit" associated with the fitting of a calculated straight line to the experimental data points. These are: σ_m, σ_c, standard deviations associated with variations in the parameters M and C; σ, a measure of the average deviation of individual data points from the least-squares fitted straight line, and R, the "crystallographic" R-factor [120, 121]. Table 4.5 gives results from HCl, H_2Ph and KOH calibrations combined. Data from each pH region were found to be colinear within the stated experimental errors. Only data from the well-buffered regions, (viz: pH < 3.0, 2.8 - 5.3, > 11.0), were considered and all data points were given unit weighting.

Results showed that pc_H, pH_m lines were parallel and close to unit slope as required by theory (equation 4.16). The intercept, C, increased with increasing ionic strength.

In these calibration relationships, where no account has been taken of possible liquid junction effects, some curvature was noted in the pc_H vs. pH_m plot (pc_H, pH_m values plotted as x,y coordinates respectively). This was manifest as downward curvature of experimental points from the calculated line of best fit in the extremes of the pH range. This deviation was of the order of .02 - .04 pH units and was observed at each ionic strength used.

---

* *pH_m data were corrected for the "non-Nernstian response" of the glass electrode as described in section 3.4.2.*

Table 4.5 pc_H / pH_m Calibration Relationships

Ionic Strength (mol dm^{-3})	M (a)	σ_m (b)	C (a)	σ_c (b)	σ (c)	n (d)	R (%) (c)
0.04	0.9966	0.0004	0.064	0.002	0.016	154	0.26
0.10	1.0010	0.0005	0.075	0.003	0.020	162	0.34
0.15	1.0010	0.0008	0.085	0.004	0.024	159	0.51
0.20	0.9990	0.0009	0.103	0.004	0.025	128	0.53

Table 4.6 pc_H / pH' Calibration Relationships

Ionic Strength (mol dm^{-3})	M (a)	σ_m (b)	C (a)	σ_c (b)	σ (c)	n (d)	R (%) (c)
0.04	0.9957	0.0004	0.086	0.002	0.015	155	0.25
0.10	1.0010	0.0003	0.087	0.002	0.013	162	0.22
0.15	1.0000	0.0005	0.098	0.002	0.015	159	0.32
0.20	0.9983	0.0006	0.113	0.003	0.017	129	0.36

(a) *M,C are parameters from the general equation:*

pH_m *(or pH')* $= M\ pc_H + C$

(b) σ_m, σ_c *are the standard deviations associated with variations in M and C*

(c) σ *, R have been defined by Russell* [120]

(d) *n is the number of data points*

In order to compensate for possible liquid junction errors at high and low pH, pH_m values were corrected according to the procedure outlined in section 3.5.2. Table 4.6 presents pc_H / pH' relationships, where pH' represents the measured pH corrected for liquid junction deviations. When corrections for liquid junction effects were included, the intercept, C, was increased on average by 0.014 pH units. The fit of the calculated straight line to the experimental data improved and deviations at high and low pH were reduced. For example, average values of σ and R, both measures of the "goodness of fit", decreased from 0.021 to 0.015 and 0.41 % to 0.29 % respectively. The slope of each line was again close to unity and lines were parallel for different ionic strengths.

The calibration relationship pc_H / pH',defined at 0.1 M ionic strength, was used in subsequent calculations of ligand protonation constants (chapter 5) and metal-ligand stability constants (chapter 6).

4.5 Conclusions

Results presented here show that pc_H vs. pH_m calibration of the glass/calomel electrode assembly with o-phthalic acid, hydrochloric acid and potassium hydroxide in a potassium chloride medium gives rise to a series of parallel lines of near unit slope with intercepts that depend on ionic strength. At 0.1 M ionic strength the relationship between pc_H and pH' was found to be:

$$pH' = 1.001\ pc_H + 0.087 \qquad (4.40)$$

The slope and intercept of this line is similar to that determined by Hedwig and Powell [115] for 0.1 M NaCl medium, (slope, 0.9951; intercept, 0.088), McBryde [81], 0.1 M NaCl medium (0.994, 0.105) and Avdeef and Bucher [116], 0.1 M KCl medium (0.998, 0.110). It should be noted however, that the coefficients in an empirical relationship such as

this will be partly a function of the particular electrode assembly used. Each of the examples quoted above involved the use of a cell with a glass electrode and a liquid junction. (The glass/calomel system used in this work closely matched that used by Hedwig and Powell).

Solutions of strong acids and strong bases make poor standards for pH measurements due to their significant contribution to the liquid junction potential. It is known that constant ionic media stabilize the liquid junction potential to a certain extent [122], especially in the intermediate pH range, 3 - 9. Results presented here show that, outside this pH range, deviation from linearity of up to .04 pH units can occur. Although aberrations in the pH scale due to liquid junction effects are likely to be less in constant ionic media than those observed for standard buffer solutions [122], approximate corrections derived from the latter have been used in this calibration work. Corrected pH_m data, pH', showed an improved fit to the least-squares calculated line and this combined with the observed deviation mentioned already was taken as justification for working with pH' data in subsequent calculations of protonation and stability constants.

It should also be noted that the previously observed colinearity of the calibration lines for NaCl systems [114,115] of different ionic strengths was not found in this work. Avdeef and Bucher [116] also found an ionic strength dependence of C, the intercept, in KCl media. The colinearity observed in NaCl media, was attributed to the compensating effect that the change in log f_H had on the change in residual liquid junction potential as each varied with ionic strength (see equation 4.15). Apparently, in KCl media, the increase in -log f_H is greater than the corresponding decrease in E_j, in the ionic strength range 0.04 - 0.20 M. Since, however, it is expected that -log f_H will pass through a maximum as the ionic strength increases beyond 0.20 M [123], a range of ionic strengths may be found for which pc_H/pH_m relationships in a KCl medium

are colinear as observed for NaCl. This is also suggested by figure 4.2 which shows the relationship between $pH_m - pc_H$ (Δ pH) (calculated at $pc_H = 7.00$ from pc_H vs. pH_m relationships with liquid junction corrections included) and I, ionic strength. (Note: figure 4.2 includes a datum point derived from a single titration of o-phthalic acid, 9.973×10^{-4} M, with no added KCl, i.e. I ca. 0.001 M).

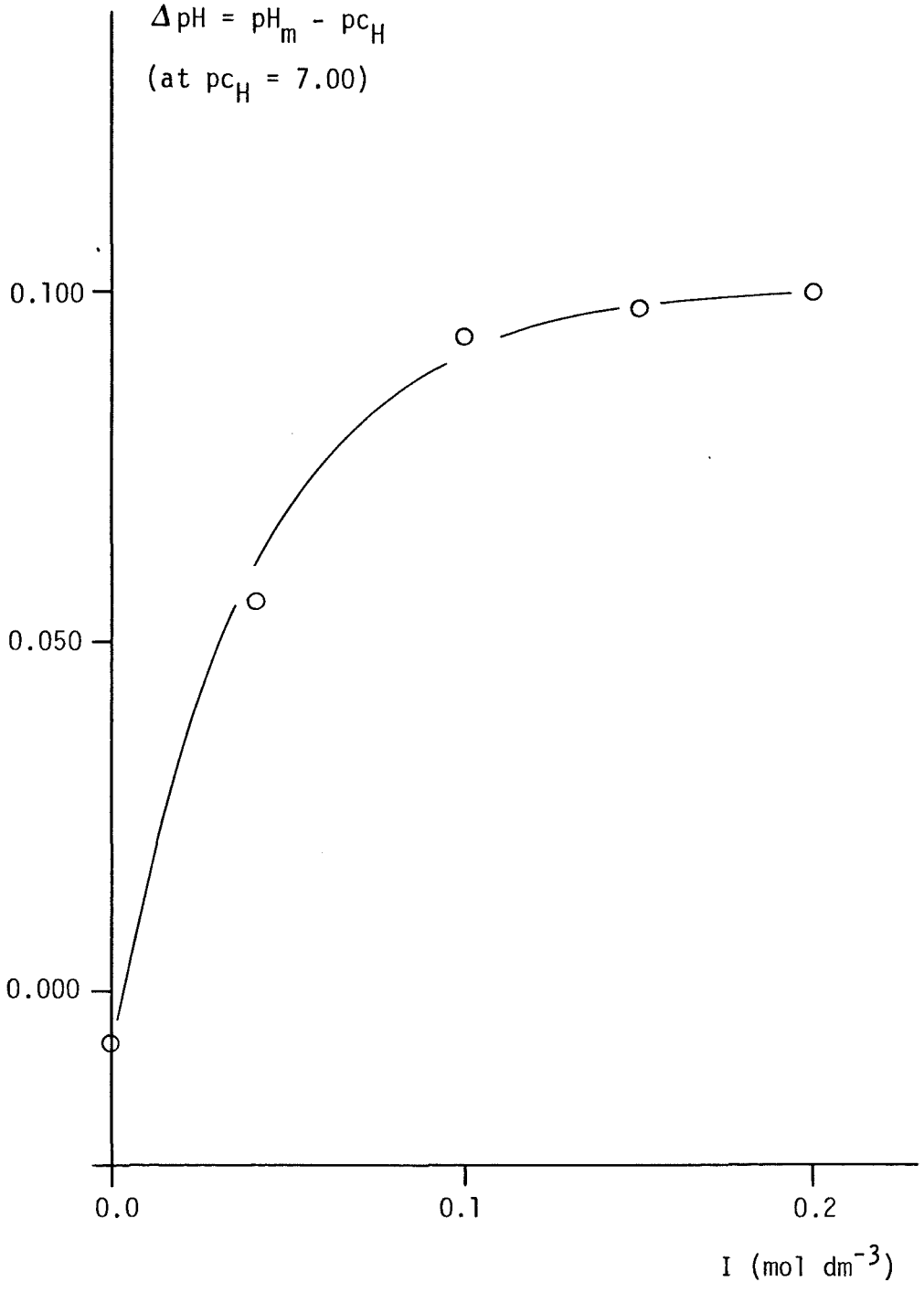

Figure 4.1 Δ pH vs. I

CHAPTER 5

ACID-BASE PROPERTIES OF o-DIHYDROXY SUBSTITUTED BENZENE LIGANDS

Ligand protonation constants for two of the five model phenolic ligands used in this study (gallic acid and catechol) have been determined in a potassium chloride medium (0.1 mol dm^{-3}) at 25 °C (data in the literature for the acidity constants of gallic acid are incomplete; catechol has been more thoroughly studied). Spectrophotometric data for the ultra-violet region are presented for gallic acid and oxidation of this ligand by atmospheric oxygen is discussed. Results for the other three ligands (pyrogallol, protocatechuic acid and tiron) are limited to semi-quantitative data which are evaluated as background to the metal-ligand study presented in chapter 6.

The electrochemical cell used in this part of the work can be represented thus:

$$\text{Glass electrode} \;\Big\|\; \begin{matrix}\text{Ligand solution, KCl(0.1 M)} \\ \text{KOH(v ml)}\end{matrix} \;\Big|\; \text{KCl(satd.), } Hg_2Cl_2(s); \text{ Hg(l)}$$

A. EQUILIBRIUM PROTONATION CONSTANTS

5.1 Potentiometric Data

Gallic acid (3,4,5-trihydroxybenzoic acid) and catechol (1,2-dihydroxybenzene) were titrated with standard potassium hydroxide solution according to the procedures outlined in chapter 2. Potassium chloride was added to the titration solution to give an overall ionic strength of 0.1 mol dm^{-3}. The experimentally measured pH was corrected for the "non-Nernstian" response of the glass electrode and for liquid junction effects

at high and low pH, as described in chapter 3. Hydrogen ion concentrations were calculated from the empirical relationship given by equation 4.40.

5.1.1 Gallic Acid

Representative potentiometric data from a titration of gallic acid with standard potassium hydroxide solution are listed in table 5.1. Figure 5.1 presents these data graphically. This and other titrations of gallic acid were carried out in a nitrogen atmosphere to prevent atmospheric oxidation of the ligand in alkaline solution.

Two main buffer regions were apparent in the pH titration curve. The first of these, which occurred below pH ca. 5.0, was terminated by a sharp endpoint, pH ca. 6.5, corresponding to the addition of 1 mole of alkali per mole of ligand. This observation is consistent with the titration of the acidic carboxyl proton in this region, i.e.:

$$LH_4 + OH^- \rightleftharpoons LH_3^- + H_2O \qquad (5.1)$$

A second buffer region was observed between pH 8.0 and 9.2 and a poorly defined endpoint occurred at pH ca. 9.6 after the addition of 2 moles of alkali per mole of ligand. One of the three hydroxy protons is titrated in this buffer region, i.e.:

$$LH_3^- + OH^- \rightleftharpoons LH_2^{2-} + H_2O \qquad (5.2)$$

Above pH 9.6 further buffering occurs, but the buffering effect of the solvent masks any further inflexions in the pH curve, i.e.:

$$LH_n + H_2O \rightleftharpoons LH_{n+1} + OH^- \qquad (5.3)$$

The gallic acid solution was colourless throughout the pH range investigated.

Table 5.1 Representative Data From a Titration of Gallic Acid With Standard Potassium Hydroxide at 25 °C, Ionic Strength 0.10 M

Titre (ml) *(a)*	pc_H *(b)*	$\bar{n}_H$ *(c)*	Titre (ml) *(a)*	pc_H *(b)*	$\bar{n}_H$ *(c)*
0.000	3.229	3.881	0.760	9.365	2.128
0.100	3.738	3.716	0.790	9.632	2.060
0.200	4.166	3.492	0.820	9.943	2.001
0.350	4.981	3.132	0.850	10.212	1.951
0.400	6.075	3.010	0.880	10.389	1.904
0.410	6.813	2.986	0.920	10.601	1.857
0.440	7.559	2.912	0.980	10.803	1.787
0.470	7.859	2.838	1.040	10.949	1.723
0.500	8.062	2.764	1.090	11.048	1.677
0.530	8.225	2.690	1.210	11.233	1.580
0.560	8.369	2.616	1.370	11.408	1.474
0.620	8.628	2.468	1.580	11.576	1.370
0.670	8.848	2.345	1.880	11.745	1.256
0.700	8.993	2.272	2.300	11.902	1.081
0.730	9.162	2.199	3.050	12.077	0.699

(a) *Cumulative volume of 0.8569 M KOH added to 69.76 ml of titration solution, initially comprising gallic acid (4.966×10^{-3} M) and KCl (0.085 M).*

(b) *Hydrogen ion concentrations derived from the measured pH as described in chapter 4.*

(c) $\bar{n}_H$ *corresponds to the observed "average degree of protonation of the ligand" as defined by equation 5.12 in the text.*

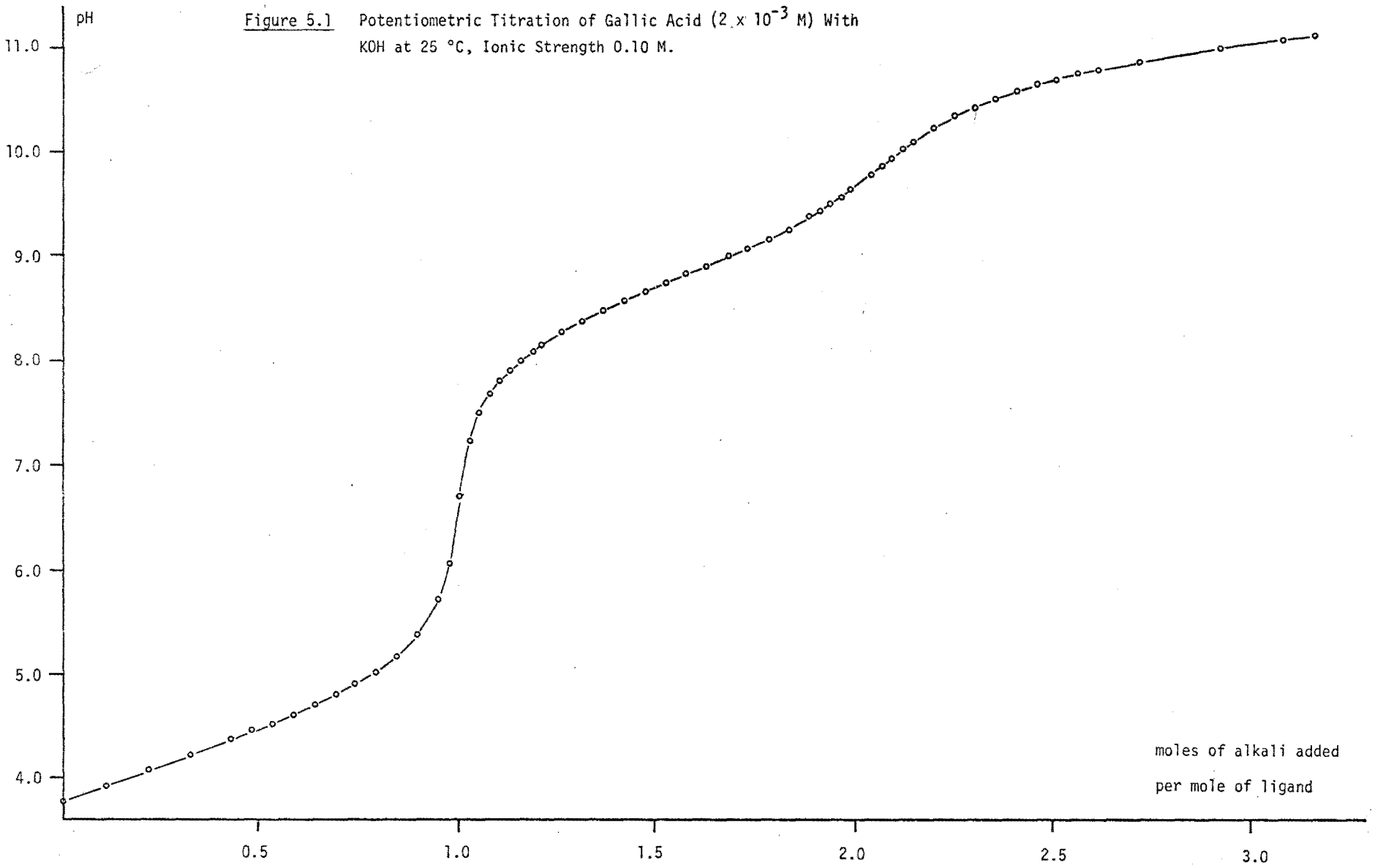

Figure 5.1 Potentiometric Titration of Gallic Acid (2×10^{-3} M) With KOH at 25 °C, Ionic Strength 0.10 M.

THE LIBRARY
UNIVERSITY OF CANTERBURY
CHRISTCHURCH, N.Z.

5.1.2 Catechol

Representative data from a titration of catechol with standard potassium hydroxide solution in an oxygen-free atmosphere are listed in table 5.2. Figure 5.2 presents these data graphically.

The sharp endpoint around pH ca. 6 corresponds to the neutralization of excess acid added originally to the catechol stock solution to minimise atmospheric oxidation of this ligand. A shallow inflexion in the titration curve was observed in the pH region 9.9 - 10.5, corresponding to the addition of 1 mole of alkali per mole of ligand. In the intervening buffer region the titration of one of the hydroxy protons was considered to take place. Above pH 10 the titration curve resembled that for gallic acid; the removal of the second hydroxy proton was at least partially effected in this region.

5.2 Method of Calculation of Protonation Constants

5.2.1 Calculation of the Secondary Concentration Variable, $\bar{n}_H$

In the determination of the protonation constants of gallate species, LH_n, the following equilibria and the corresponding concentration quotients, k_n, were considered:

$$L^{4-} + H^+ \rightleftharpoons LH^{3-} \quad ; \quad k_1 = c_{LH} / (c_L \, c_H) \qquad (5.4)$$

$$LH^{3-} + H^+ \rightleftharpoons LH_2^{2-} \quad ; \quad k_2 = c_{LH_2} / (c_{LH} \, c_H) \qquad (5.5)$$

$$LH_2^{2-} + H^+ \rightleftharpoons LH_3^- \quad ; \quad k_3 = c_{LH_3} / (c_{LH_2} \, c_H) \qquad (5.6)$$

$$LH_3^- + H^+ \rightleftharpoons LH_4 \quad ; \quad k_4 = c_{LH_4} / (c_{LH_3} \, c_H) \qquad (5.7)$$

(The charges have been omitted from concentration quotient expressions for clarity). The species LH_3^-, LH_2^{2-}, LH^{3-} and L^{4-} were also considered

Table 5.2 Representative Data From a Titration of Catechol With Standard Potassium Hydroxide at 25 °C, Ionic Strength 0.10 M

Titre (ml) *(a)*	pc_H *(b)*	$\bar{n}_H$ *(c)*
0.345	8.026	1.927
0.355	8.468	1.855
0.365	8.711	1.784
0.375	8.886	1.713
0.385	9.036	1.643
0.395	9.167	1.574
0.405	9.293	1.507
0.415	9.403	1.440
0.425	9.518	1.377
0.435	9.633	1.317
0.445	9.752	1.263
0.455	9.873	1.215
0.465	9.994	1.176
0.475	10.112	1.147
0.485	10.222	1.128

(a) *Cumulative volume of 1.179 M KOH added to 145.00 ml of titration solution, initially comprising catechol (1.089×10^{-3} M) and KCl (0.096 M).*

(b) *Hydrogen ion concentrations derived from the measured pH as described in chapter 4.*

(c) $\bar{n}_H$ *corresponds to the observed "average degree of protonation of the ligand" as defined by equation 5.12 in the text.*

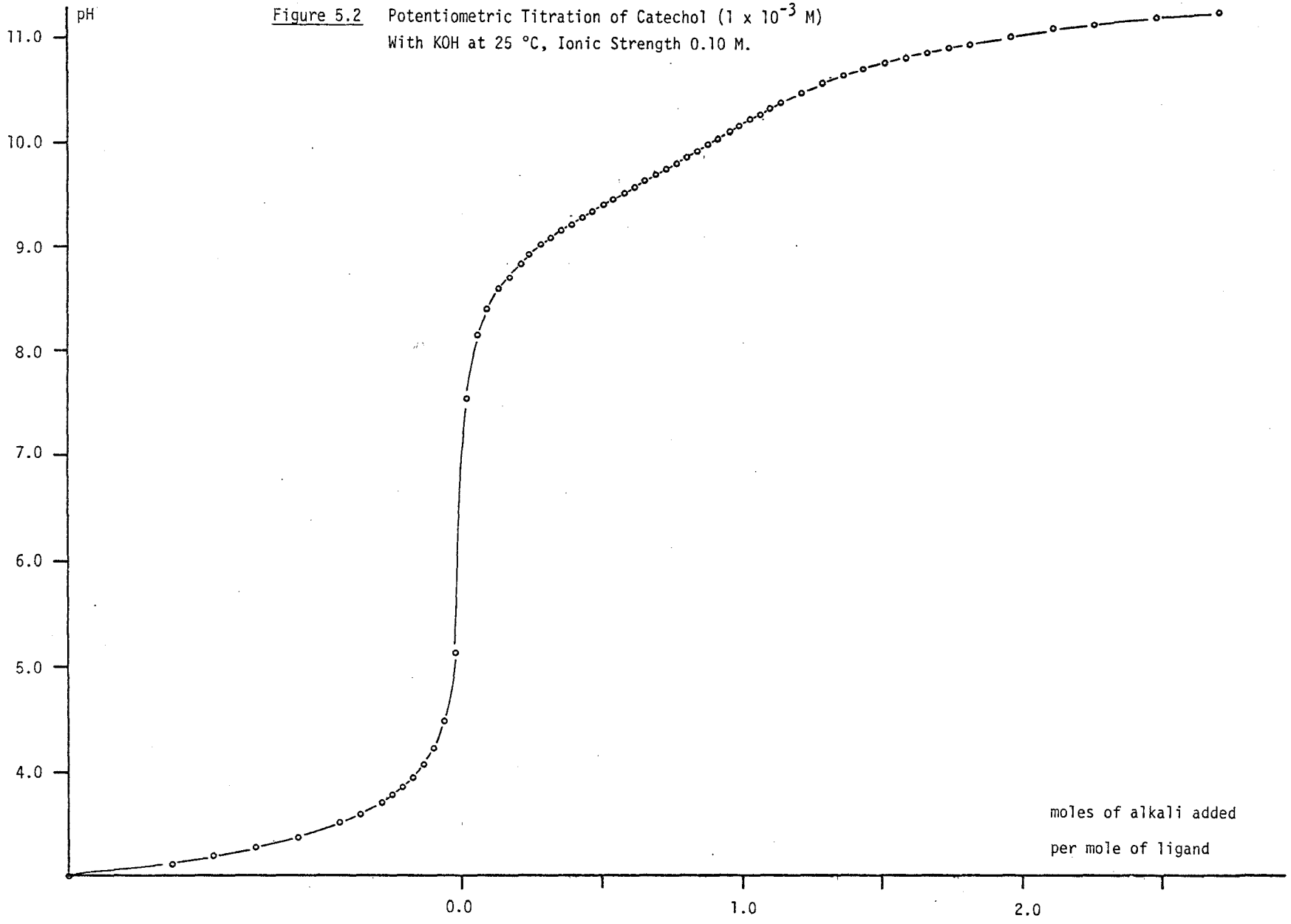

Figure 5.2 Potentiometric Titration of Catechol (1×10^{-3} M) With KOH at 25 °C, Ionic Strength 0.10 M.

to undergo hydrolysis reactions of the general type given by equation 5.3. The mass balance equations describing T_L, the total concentration of ligand species and T_H, the total concentration of ionisable protons are given by:

$$T_L = c_L + c_{LH} + c_{LH_2} + c_{LH_3} + c_{LH_4} \quad (5.8)$$

$$T_H = c_H + c_{LH} + 2c_{LH_2} + 3c_{LH_3} + 4c_{LH_4} - c_{OH} \quad (5.9)$$

The last term in equation 5.9 arises from the general reaction 5.3 and was calculated from the ionic activity product of water using the procedure described in section 4.4.2.

Values for T_H were determined for each increment of added alkali, v, according to the relation:

$$T_H = 4T_L' - v\, c_{KOH} / (V + v) \quad (5.10)$$

where V was the total initial volume of solution and c_{KOH} was the concentration of standard alkali. The value of T_L' was the total initial concentration of ligand (T_L) adjusted with an appropriate dilution factor, i.e.:

$$T_L' = T_L\, V / (V + v)$$

The secondary concentration variable, $\bar{n}_H$[124], which describes the average degree of protonation of the ligand, is defined as the concentration of ligand-bound protons divided by the total ligand concentration, i.e.:

$$\bar{n}_H = (c_{LH} + 2c_{LH_2} + 3c_{LH_3} + 4c_{LH_4}) / T_L' \quad (5.11)$$

Combining this with equation 5.9 gives:

$$\bar{n}_H = (T_H - c_H + c_{OH}) / T_L' \quad (5.12)$$

With the use of equilibrium expressions 5.3 - 5.7 and equations 5.8 and 5.11, $\bar{n}_H$ can also be written as a function of the protonation constants k_n:

$$\bar{n}_H = \frac{k_1 c_H + 2k_1k_2 c_H^2 + 3k_1k_2k_3 c_H^3 + 4k_1k_2k_3k_4 c_H^4}{1 + k_1 c_H + k_1k_2 c_H^2 + k_1k_2k_3 c_H^3 + k_1k_2k_3k_4 c_H^4} \qquad (5.13)$$

or

$$\bar{n}_H = \sum_{i=1}^{4} i \beta_i c_H^i / (1 + \sum_{i=1}^{4} \beta_i c_H^i) \qquad (5.14)$$

where β_i is a cumulative protonation constant defined by:

$$\beta_i = \prod_{n=1}^{i} k_n \qquad (5.15)$$

5.2.2 Calculation of Protonation Constants by Least Squares Refinement

From known values of T_H and T_L and corresponding values of the hydrogen ion concentration (derived from the measured pH), an experimental value of $\bar{n}_H$, ($\bar{n}_H$ (obs)), was determined for each point in the titration (equation 5.12). Calculated values of $\bar{n}_H$, ($\bar{n}_H$ (calc)), as defined by equation 5.13, were also obtained, using trial values for the equilibrium constants k_n. The least squares method involved the variation of the trial parameters k_n in the determination of $\bar{n}_H$ (calc), such that the sum of the squares of the residuals over all data points,

$$\Sigma (\bar{n}_H \text{ (obs)} - \bar{n}_H \text{ (calc)})^2,$$

was minimised. Unit weighting was assigned to each datum point. FORTRAN programs were written to calculate $\bar{n}_H$ (obs) and $\bar{n}_H$ (calc). These were in the form of subroutines to the least squares program ORGLS [119] and are listed in Appendix 11.

A similar procedure was used for the calculation of protonation constants for catechol. In this case two equilibria, (analogous to 5.4

and 5.5), were considered and expression 5.10 was modified as follows:

$$T_H = 2T_L' + A - v\, c_{KOH} / (V + v)$$

where A represents the concentration of added standard acid (initially included in stock solutions of catechol to minimise oxidation by atmospheric oxygen). The FORTRAN subroutines used in the calculation of catecholate protonation constants are given in Appendix 12.

5.3 Results

5.3.1 Gallic Acid

Figure 5.3 depicts the formation curve, $\bar{n}_H$ vs. pc_H for gallic acid as well as computed ionic concentrations of all ligand species throughout the pH range investigated. Table 5.3 lists the protonation constants determined for this ligand. Data in this table represent average values of log k_n over 6 individual potentiometric titrations, with total initial ligand concentrations of between 2×10^{-3} and 5×10^{-3} M. Errors listed in table 5.3 represent one standard deviation of the mean value of log k_n over 6 replications. Each titration yielded between 78 and 98 data points. Data above pH ca. 12.1 were not included in calculations as extensive hydrolysis in this pH region dominated any changes in $\bar{n}_H$. Values for the "R-factor"[120,121] ranged from 0.4 to 1.5 %.

Values determined for log k_1 are the least precise. This might be expected from the larger uncertainty associated with pH measurements in strongly alkaline solutions and the importance of hydrolysis reactions above pH ca. 10.5. It was found in this work that accurate values for log k_n could only be determined by least squares analysis if all four parameters were included, usually as variables. (In some calculations, one or more parameters were held constant. For example, in dilute solutions

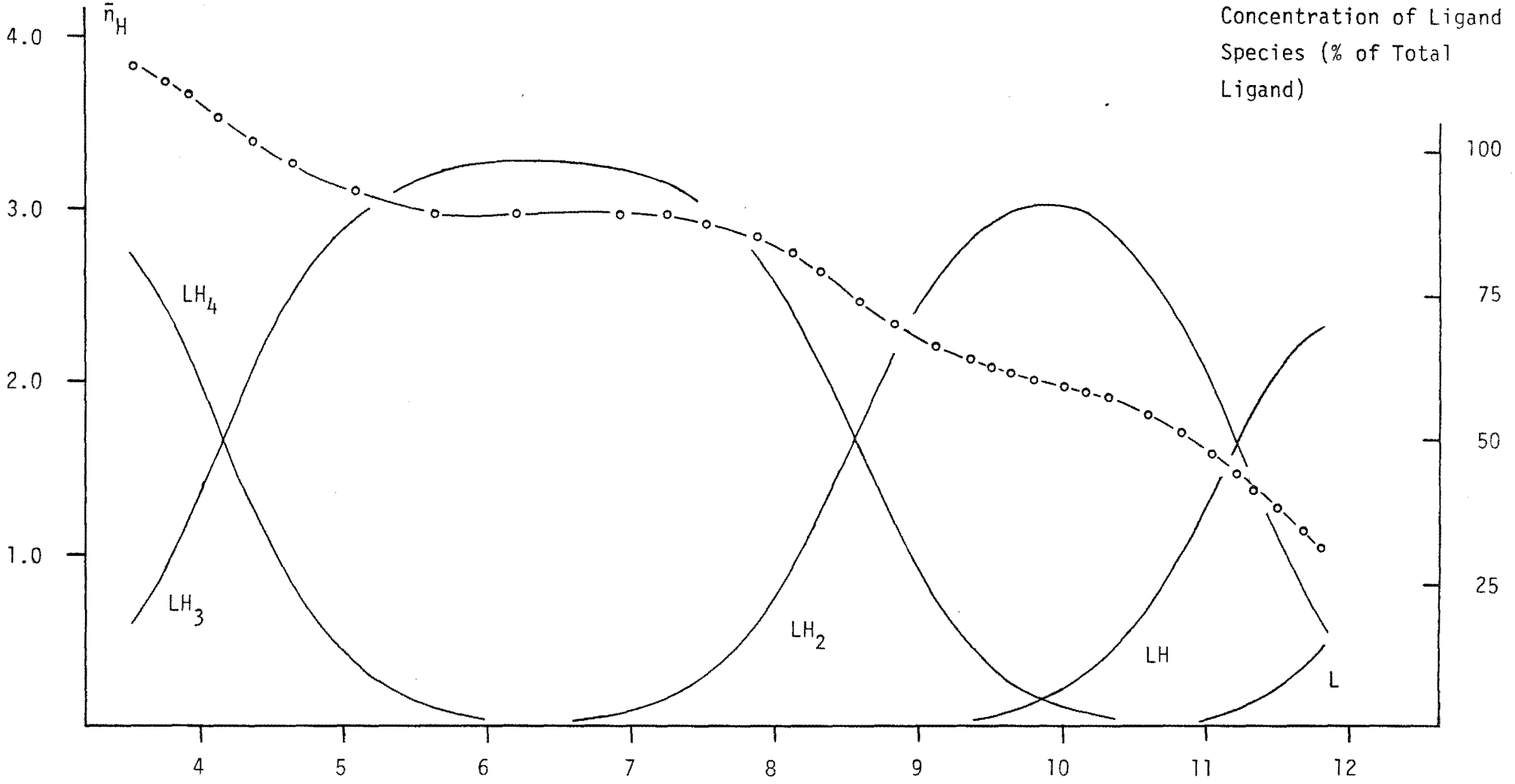

Figure 5.3 Formation Curve for Gallic Acid (LH_4)

Table 5.3 Protonation Constants for 3,4,5-Trihydroxybenzoic Acid Tetra-anion at 25 °C, 0.10 M KCl Solution

log k_1	12.8	± 0.4 *(a)*	(-OH)
log k_2	11.4	± 0.1	(-OH)
log k_3	8.55	± 0.01	(-OH)
log k_4	4.16	± 0.02	(-COOH)

(a) Errors estimated as described in text.

of ligand, k_1 was assigned a fixed value and k_2, k_3, k_4 were varied. This was to avoid large errors entering the calculations from less reliable data in the high pH region. Errors associated with these data were largest for the more dilute solutions of ligand). Previous work on the protonation of gallic acid species in aqueous solution is summarized in table 5.4. Determinations of log k_n values for gallic acid have resulted in a wide spectrum of results. Where log k_1 has previously been determined, values of 11.3 and 10.25 have resulted. Observations and calculations made in this work would not support these low values for this equilibrium constant.

Table 5.4 Previous Data for the Protonation of Gallate Species

log k_1	log k_2	log k_3	log k_4	Medium (temperature)	Reference
-	-	8.85	4.33	I < 0.011 M (30 °C)	*(125)*
-	11.19	8.69	4.22	not specified	*(126)*
11.3	10.05	8.54	4.44	0.1 M KCl (25 °C)	*(67)*
10.25	8.75	7.05	4.50	0.1 M $NaClO_4$ (28 °C)	*(127)*
12.8	11.4	8.56	4.16	0.1 M KCl (25 °C)	*(This work)*

5.3.2 Catechol

Figure 5.4 depicts the formation curve for catechol, while data for the second protonation constant are given in table 5.5 along with results from other workers. Two titrations, at total ligand concentrations of 1×10^{-3} and 5×10^{-4} M respectively, were used to determine a value for k_2.

No attempt was made to accurately determine k_1. Titration data from catechol solutions were collected primarily as background to the metal ligand study (discussed in chapter 6) and consequently insufficient data in the high pH region were available. Hence a value for log k_1 of 13.05 was selected from the literature [47] for the least squares refinement of k_2 (this value appeared to be consistent with determinations of log k_1 for other hydroxy-benzenes; see also table 5.6).

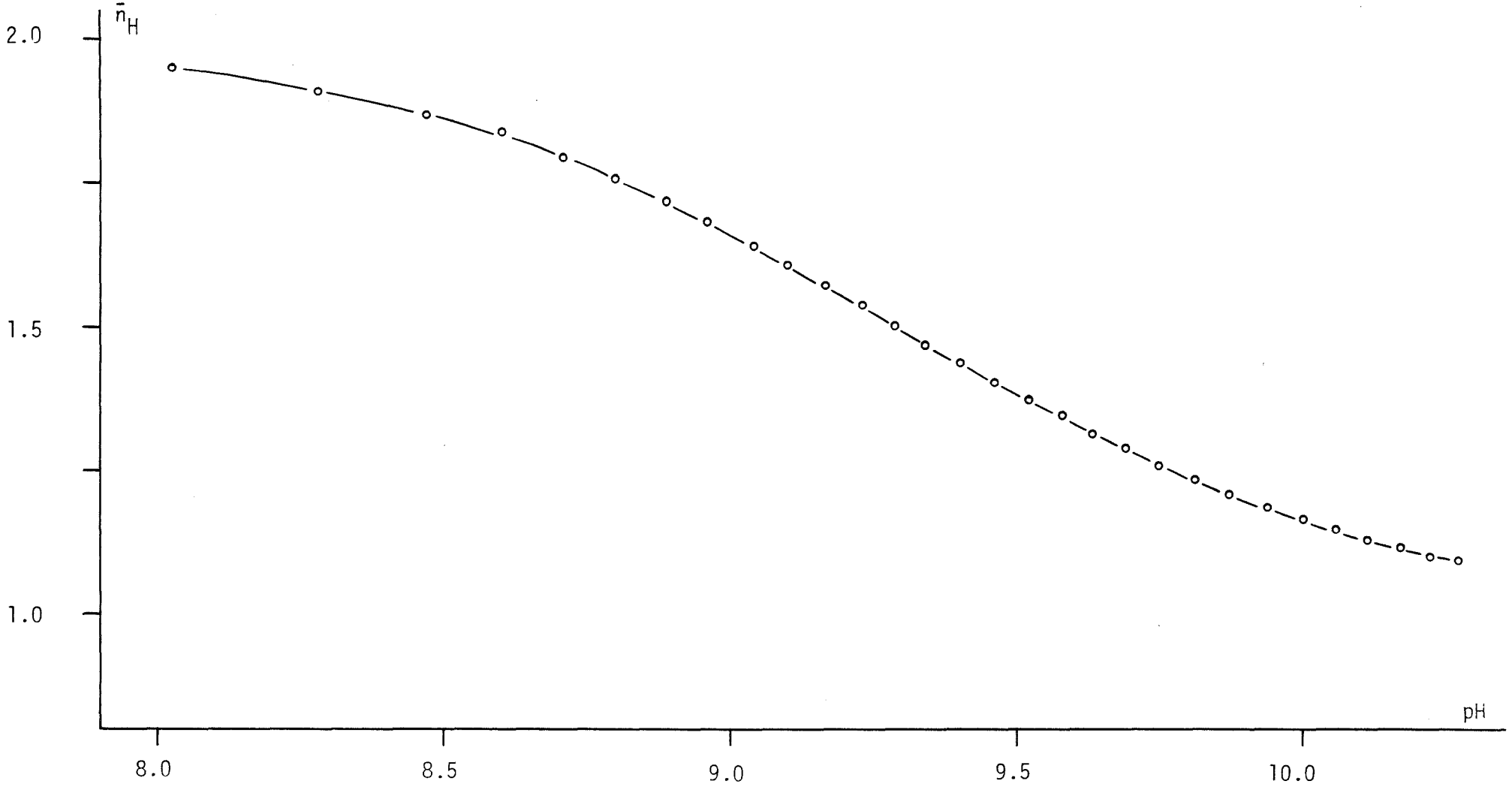

Figure 5.4 Formation Curve for Catechol (LH_2)

Table 5.5 Protonation Constants for 1,2-Dihydroxybenzene Di-anion

log k_1	log k_2	Medium (temperature)	Reference
11.59	9.13	0.1 M KNO_3 (30 °C)	*(128)*
12.8	9.37	0.1 M KCl (25 °C)	*(64)*
11.93	9.20	0.1 M KNO_3 (25 °C)	*(129)*
13.05	9.23	1.0 M KNO_3 (25 °C)	*(47)*
13.00	9.22	<0.1 M (27 °C)	*(54)*
-	9.28 ± 0.02	0.1 M KCl (25 °C)	*(this work)*

5.4 Discussion

Protonation constants for a series of hydroxy-benzenes are summarized in table 5.6. Removal of the first phenolic proton is somewhat easier for gallic acid (pk_3 8.56) and protocatechuic acid (pk_2 8.64) than for pyrogallol (pk_3 9.05) and catechol (pk_2 9.28) respectively. This may be attributed to the strong electron withdrawing action of the carboxylate group involving resonance interaction. This suggests that for gallic and protocatechuic acids preferential

deprotonation of the para-hydroxy group occurs to give the resonance stabilized bivalent anion:

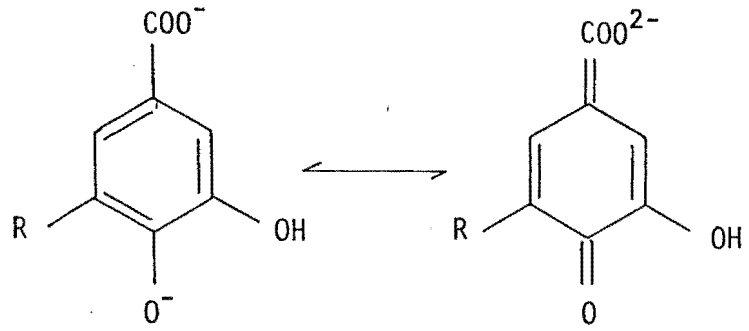

R = H : protocatechuic acid

R = OH : gallic acid

In support of this it is noted that pk_1 for para-carboxyl-substitution of phenol (viz 9.13) is lower than that for meta-substitution (pk_1 9.78). This effect does not appear to carry over to the removal of the second phenolic proton.

In the case of tiron, two strongly electron-withdrawing sulphonate groups reduce pk_2 to 7.67. Potentiometric data presented in this work for hydroxy-benzenes show that the carboxyl proton (where present) and one phenolic proton are easily dissociable in separate steps. The second phenolic proton is only appreciably acidic (i.e. $pk_2<12$) in the tri-hydroxy substituted benzenes (e.g. gallic acid pk_2 11.4; pyrogallol pk_2 11.19 cf. catechol pk_1 13.0). The additional acidity of the second hydroxy group in these examples may arise from the electron-withdrawing properties of the third hydroxy group.

Table 5.6 Protonation Constants for Hydroxy-Benzenes

Hydroxy-Benzene	log k_4	log k_3	log k_2	log k_1	Reference
Phenol				9.62	
Catechol			9.28	13.05	*(47, this work)*
Hydroquinone			9.91	12.04	*(69)*
Tiron			7.67	12.51	*(60)*
Pyrogallol		9.05	11.19	ca.14	*(130)*
Gallic Acid	4.16	8.56	11.4	12.8	*(this work)*
Protocatechuic Acid		4.25	8.64	13.12	*(63)*
p-Hydroxybenzoic Acid			4.29	9.13	*(69)*
m-Hydroxybenzoic Acid			3.90	9.78	*(69)*
Benzoic Acid				4.20	*(69)*

B GENERAL ACID-BASE AND REDOX PROPERTIES

5.5 Acid-Base Properties of Other Model Ligands

3,4-dihydroxybenzoic acid (protocatechuic acid), 1,2,3-trihydroxybenzene (pyrogallol) and 1,2-dihydroxybenzene-3,5-disulphonic acid (tiron) were titrated with standard potassium hydroxide solution in a nitrogen atmosphere. Data collected from these titrations are presented in graphical form in figures 5.5 - 5.7 respectively.

(a) Protocatechuic Acid. The sharp end-point in the pH titration curve at pH ca. 6.5, corresponding to the addition of 1 mole of alkali per mole of ligand, is consistent with the removal of the carboxylate proton. A shallow inflexion in the pH region 9.5 - 10.0 was attributed to the titration of one of the hydroxy protons.

(b) Pyrogallol. The titration curve for pyrogallol resembled that for protocatechuic acid except, in this case, the sharp endpoint around pH 6.5 corresponds to the titration of excess acid initially added to stock solutions of the ligand to minimise atmospheric oxidation.

(c) Tiron. The titration curve for tiron was markedly depressed with respect to the other ligands studied (including gallic acid and catechol). Well-defined endpoints at pH ca. 5.6 and 9.3, corresponding to 1 and 2 moles of alkali added per mole of ligand respectively, were observed. Both hydroxy protons of tiron are titrated in this pH range.

5.6 Oxidation of the Ligands

In the presence of dissolved oxygen, a distinct lime-green colour developed in gallic acid solutions of pH ca. 7.0; i.e. immediately past the first endpoint. Substantial downward drifting in pH was observed in this region and polarographic measurements made on the oxygen

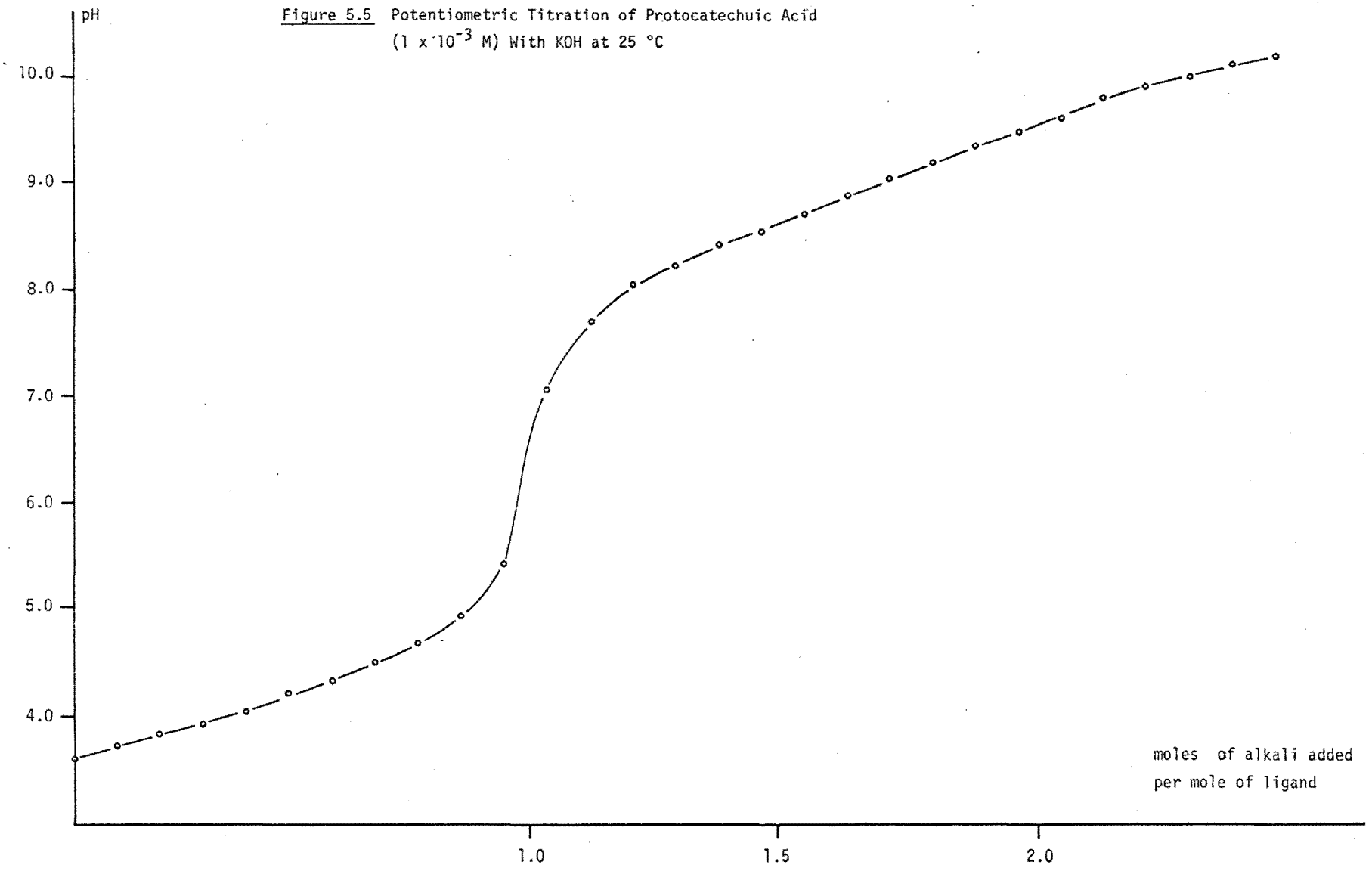

Figure 5.5 Potentiometric Titration of Protocatechuic Acid (1×10^{-3} M) With KOH at 25 °C

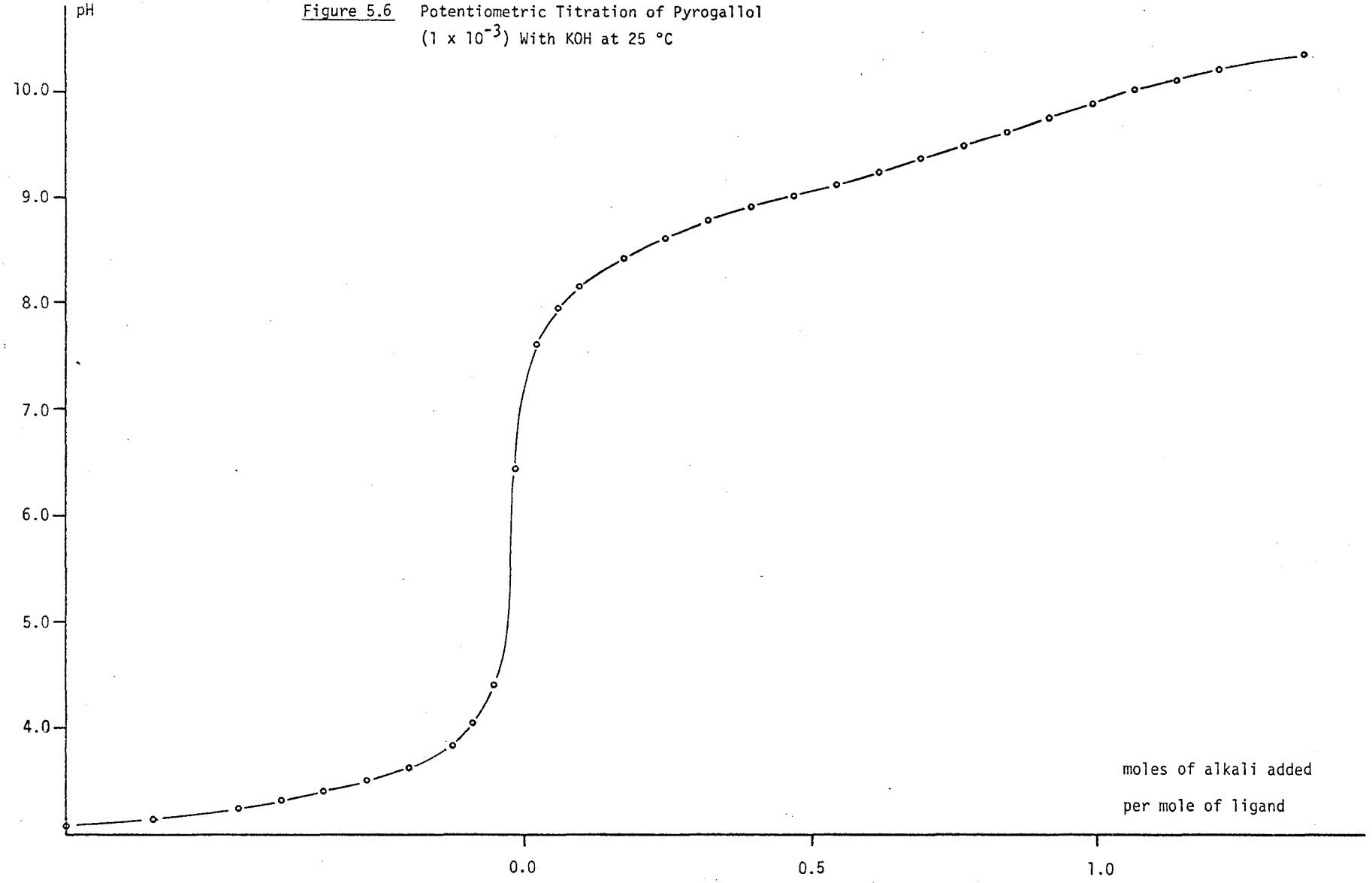

Figure 5.6 Potentiometric Titration of Pyrogallol (1×10^{-3}) With KOH at 25 °C

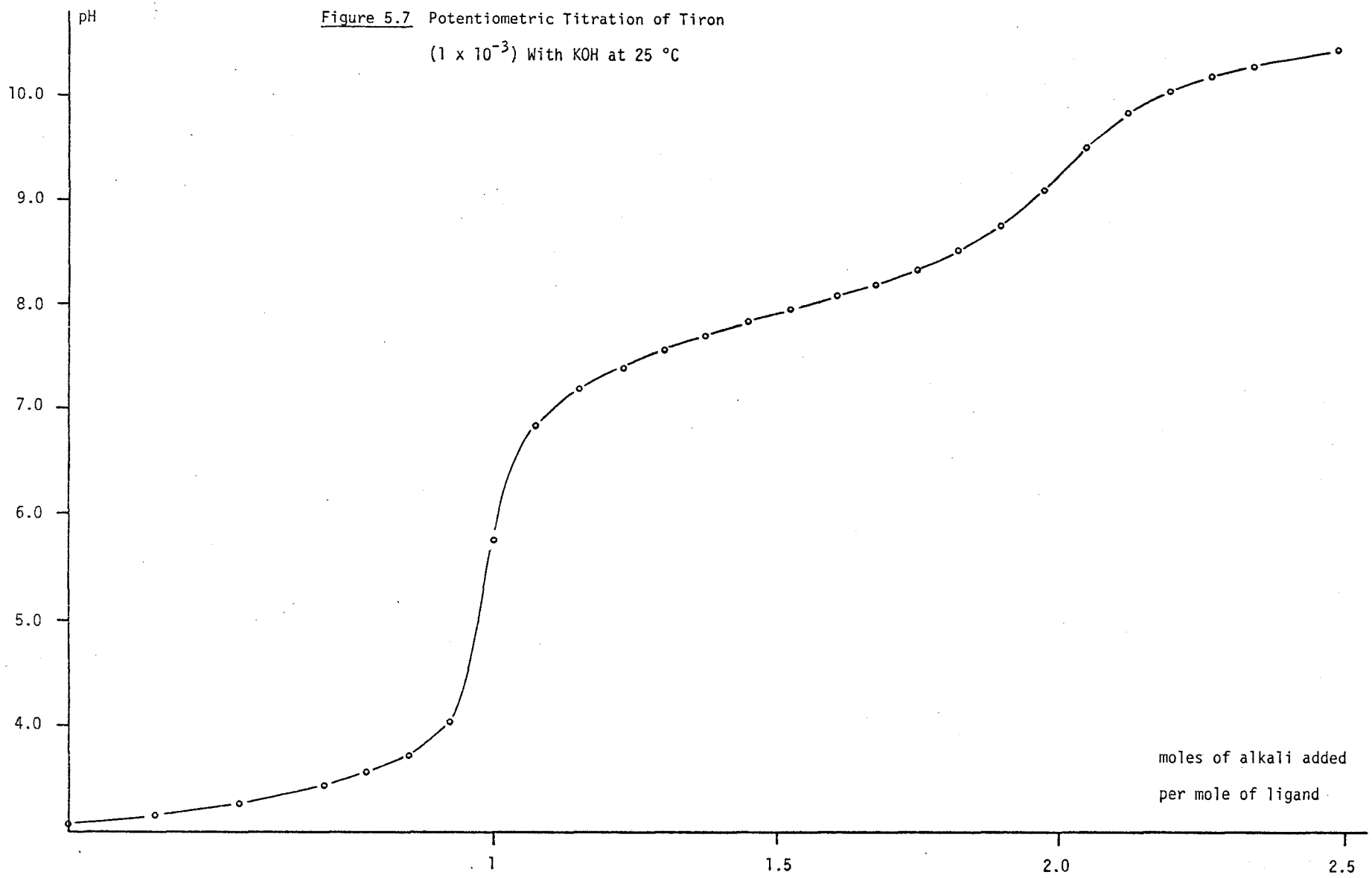

Figure 5.7 Potentiometric Titration of Tiron (1×10^{-3}) With KOH at 25 °C

concentration in solution, showed a steady consumption of oxygen as the pH was increased. At higher pH the green colour intensified and alkaline solutions of gallic acid left overnight became grey-brown.

Gallic acid is known to be readily oxidised in acidic and alkaline solutions [131]. Ball and Chen [68] have measured the standard reduction potential of the following reaction:

$$2e + QH_2 + 2H^+ \rightleftharpoons LH_4 \quad ; \quad E^\circ = 0.799 \text{ V } (30\ ^\circ C)$$

where QH_2 represents a quinone species. They noted that secondary reactions involving the oxidised product were apparent especially at "physiological" pH and above. Their measurements involved the use of a stopped flow technique designed to overcome this problem.

Grimshaw et al [132] have identified a yellow-green product (I) from the atmospheric oxidation of gallic acid in alkaline solution. They suggested the initial formation of the intermediate (II) via a semiquinone radical.

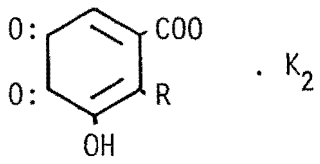

$\cdot K_2$

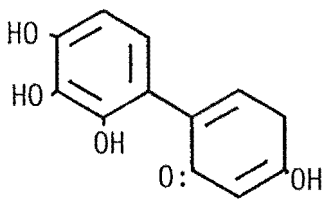

R = CH_2 C(:O) CH_2 C(:O) COO

(I) (II)

Tiron and protocatechuic acid were relatively stable to atmospheric oxidation. Acidic solutions of catechol developed a yellow tinge after about 5 weeks in a stoppered flask while acidic solutions of pyrogallol remained colourless for less than 7 days.

The redox potentials of these and other similar ligands are summarized in table 1.1. It is apparent from these potentials and observations presented in this work that trihydroxy-substituted benzenes

are readily oxidised in alkaline conditions and would be expected to undergo a rapid redox process with ferric ion in solution. This latter observation was especially relevant to this work where Fe(III)-ligand complexes were studied. Tiron and protocatechuic acid ($E° > 0.8$) might be expected to be stable in the presence of Fe^{3+} while catechol may be involved in a redox equilibrium.

The atmospheric oxidation of gallic acid and other related polyphenols appears to be a complex process involving phenolic coupling reactions and the formation of quinone species. Phenolic oxidation in the presence of ferric iron is discussed in more detail in chapter 6.

5.7 Spectrophotometric Data for Gallic Acid

Spectrophotometric data for the ultra-violet region recorded during the titration of gallic acid with potassium hydroxide, are recorded in figure 5.8 and summarized in table 5.7. The spectra of gallic acid in the pH range 2.6 - 9.6 show the existence of three distinct species with well-defined absorption maxima, the occurrence of which coincided with observed inflexions in the pH titration curve. Well-defined isosbestic points confirmed the presence of simple two-component equilibria in this pH region (i.e. equations 5.6 and 5.7).

The intense absorption at 219 nm is a "benzoid" band associated with a $\pi \longrightarrow \pi^*$ transition in the benzene ring [133]. At a longer wavelength (269.5 nm) the second major absorption of gallic acid occurs and arises from an electron transfer (E.T.) from the p-orbital of the carbonyl-oxygen to the aromatic π-system [134]. This band shifted to shorter wavelength as the carboxyl proton was titrated with alkali. Both these absorptions were displaced to longer wavelengths as the first hydroxyl proton was removed between pH 6.5 and 9.6.

Table 5.7 Spectrophotometric Data for Gallic Acid in 0.1 M KCl Solution at 25 °C

pH	Description	Wavelength (nm)	ε (cm^{-1} l mol^{-1})	Species Involved
2.6	absorption maximum	269.5 ± 1.0	9370 ± 50	LH_4
"	"	219 ± 1	13 320 ± 75	"
2.6 - 6.5	isosbestic point	260 ± 1	7910 ± 50	LH_4/LH_3^-
6.5	absorption maximum	257 ± 1	7780 ± 60	LH_3^-
"	"	219 ± 1	13 530 ± 100	"
6.5 - 9.6	isosbestic point	268 ± 1	6180 ± 100	LH_3^-/LH_2^{2-}
"	"	242 ± 1	5770 ± 200	"
9.6	absorption maximum	294 ± 2	9000 ± 100	LH_2^{2-}
"	"	229 ± 1	14 000 ± 100	"

Above pH 9.6 a more complex picture was observed. The benzoid band became more intense and shifted to longer wavelength (ca. 240 nm) while the E.T. band weakened steadily and moved to slightly shorter wavelength (ca. 290 nm). Isosbestic points were observed at 314 ± 1 nm and 264 ± 2 nm between pH 9.6 and 12.5. In this pH region a weaker absorption developed at 320 - 340 nm. Significant absorption occurred in the visible part of the spectrum (see figure 5.8) giving rise to the pale lime-green colour in solution noted in the previous section. Solutions for which spectrophotometric data were collected could not be rigorously purged of oxygen (see section 2.7.2). Hence it is thought that the absorption pattern above pH 9.6 reflected a combination of absorptions due to LH_2^{2-}, LH^{3-}, L^{4-} and oxidised ligand species.

pH			
1	2.60	4	4.87
2	3.38	5	4.80
3	3.86	6	5.33

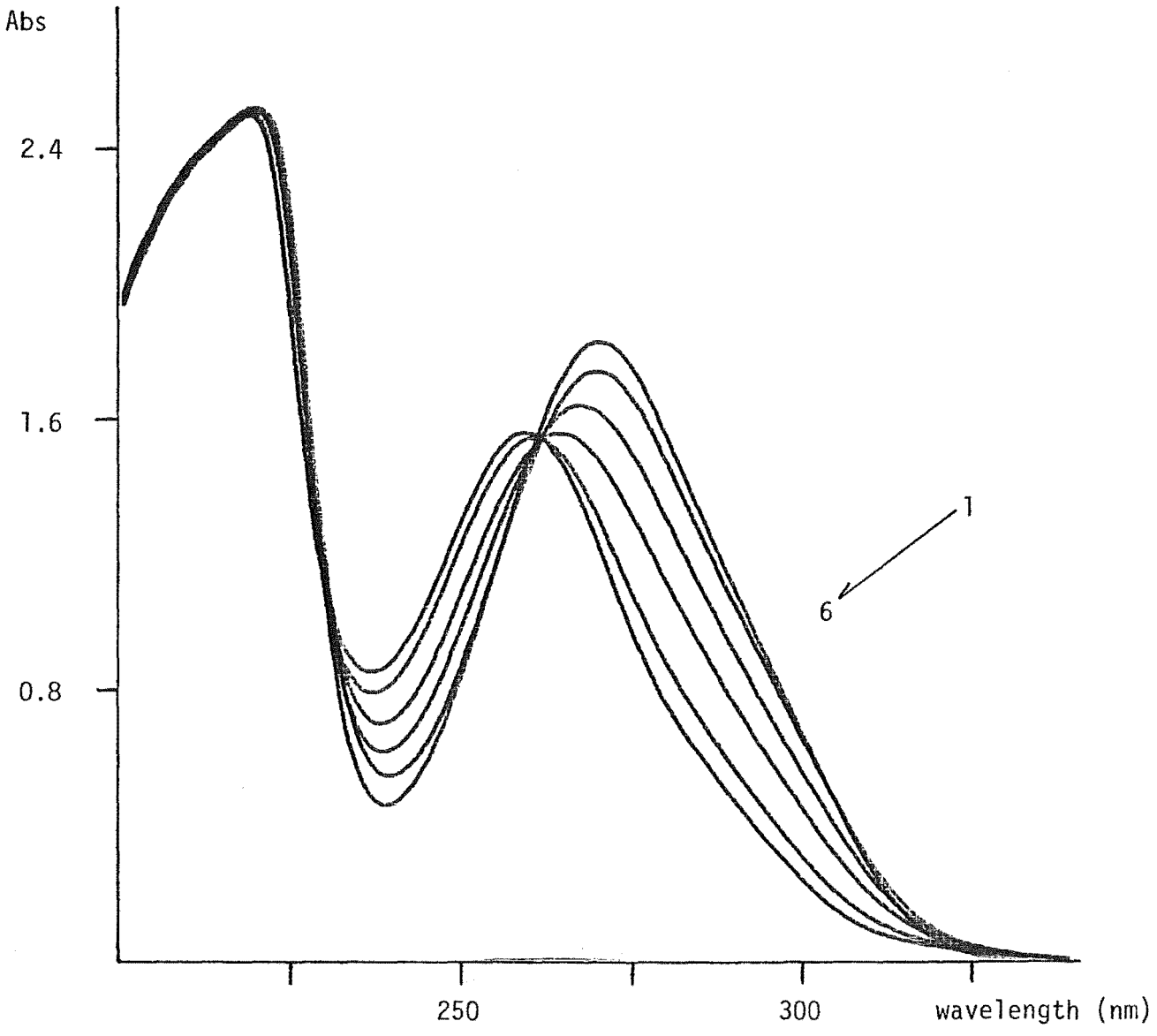

Figure 5.8 Spectrophotometric Data from Solutions of Gallic Acid (2×10^{-4} M) at 25 °C, 10 mm Cell

pH					
1	5.34	4	7.71	7	8.92
2	6.42	5	8.03	8	9.23
3	7.06	6	8.48	9	9.76

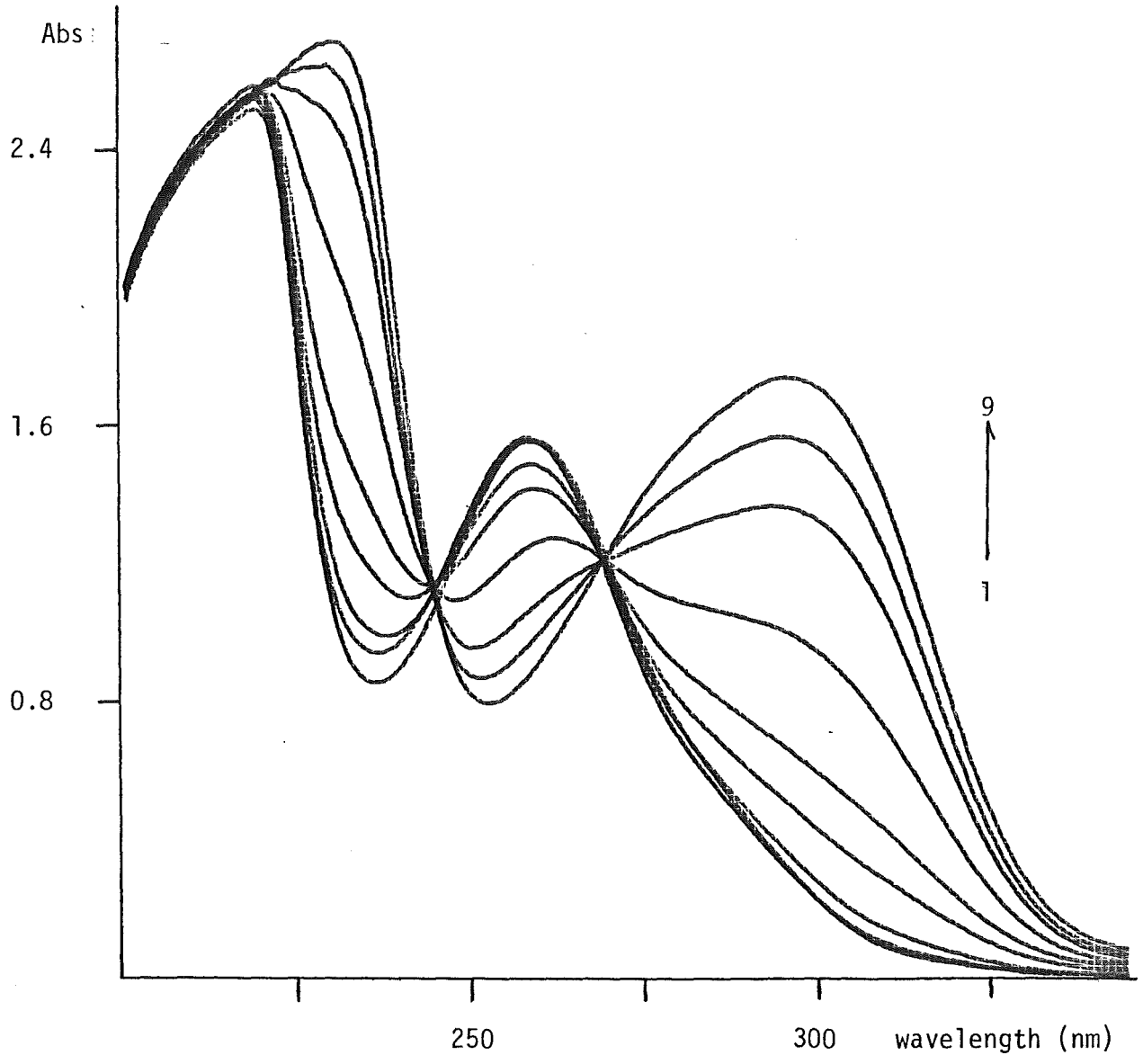

Figure 5.8 (continued)

pH							
1	9.75	4	10.98	7	12.17	10	12.69
2	10.08	5	11.49	8	12.32	11	12.87
3	10.55	6	12.01	9	12.50		

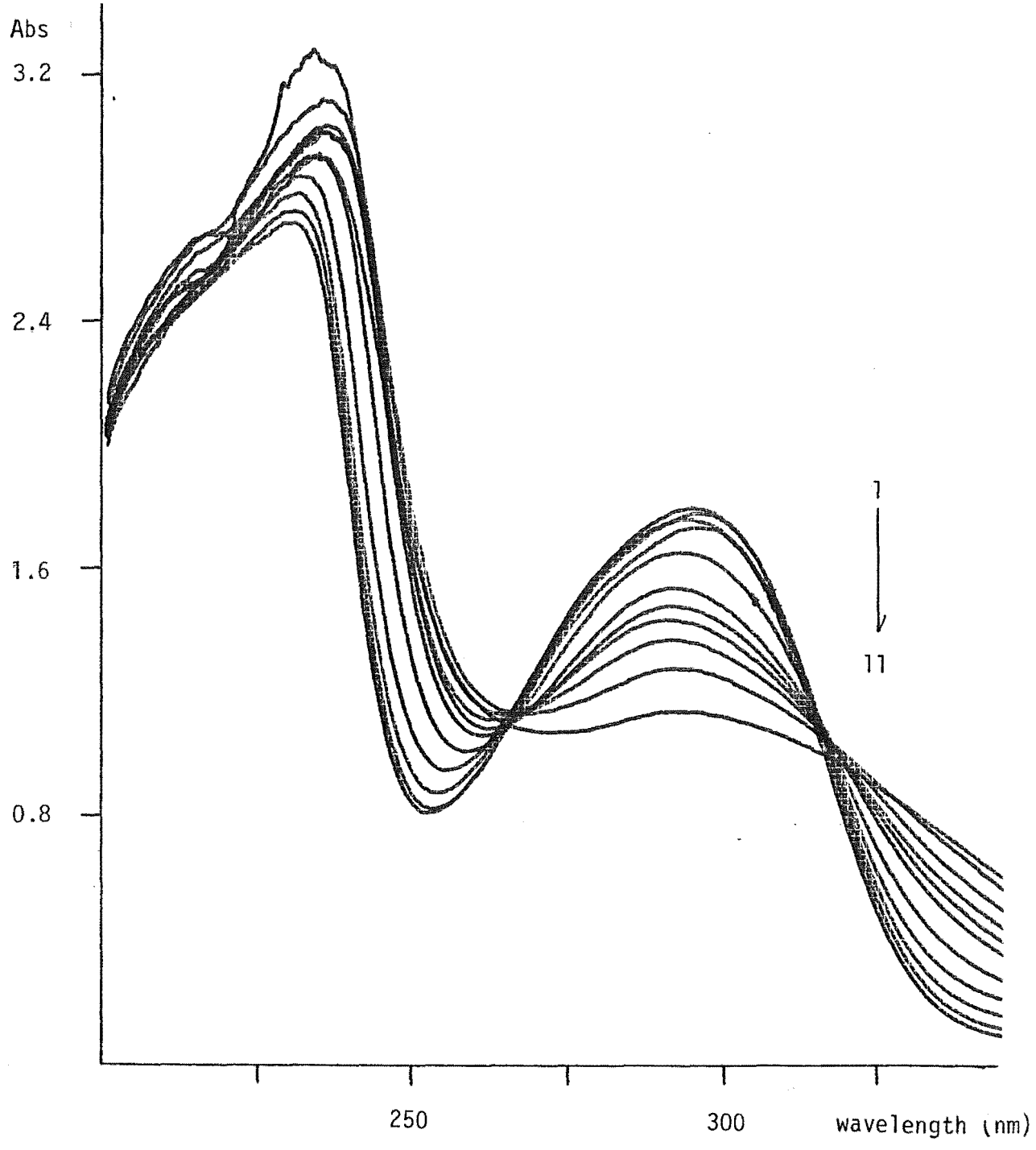

Figure 5.8 (contined)

CHAPTER 6

COMPLEXES OF IRON WITH o-DIHYDROXY SUBSTITUTED BENZENES

The behaviour of five model ligands in solutions containing ferrous or ferric ion is discussed in this chapter. These ligands were expected to range from easily oxidised (pyrogallol) to stable (tiron) in the presence of ferric ion (see section 5.6).

Results are presented from potentiometric and spectrophotometric titrations of dilute metal-ligand solutions (10^{-4} - 10^{-3} M) with standard potassium hydroxide. Potassium chloride was added to titration solutions where an overall ionic strength of 0.1 M was required. Stability constants for ferrous complexes with two ligands, gallic acid and catechol, have been determined.

Obtaining accurate data characteristic of Fe(II)-phenolic systems depended critically on rigorous exclusion of oxygen from the titration solution. Because of the marked insolubility of ferric hydroxide and the stable nature of ferric complexes with phenolics, traces of dissolved oxygen oxidised Fe(II) to Fe(III) even in moderately acidic solution. The oxygen concentration in solution was therefore carefully controlled, using the methods described in section 2.5.

Stability constants were not determined for ferric complexes, but from potentiometric and spectrophotometric titrations, the stoichiometries of Fe(III)-polyphenol interactions were characterized and the oxygen sensitivity of their solutions studied (In the description of titration curves "a" represents "moles of added alkali per mole of metal ions").

A. FORMATION OF FERROUS COMPLEXES WITH GALLIC ACID AND CATECHOL

6.1 Gallic Acid

6.1.1 Potentiometric Data

Representative potentiometric data from the titration of alkali against Fe(II)-gallic acid solution, with an initial ligand-metal ratio of 3:1 are given in table 6.1. Results from a 1:1 titration are presented graphically in figure 6.1. Titrations with initial ligand-metal stoichiometrics of 1:1 and 2:1 were also performed. Titrations were carried out in oxygen-free solutions in a nitrogen atmosphere to prevent oxidation of either the ligand or the metal.

A sharp inflexion in each pH titration curve occurred after the addition of 1 mole of alkali per mole of ligand (pH ca. 6.5), consistent with the titration of the carboxylate proton. Complex formation above pH 6.8 was evidenced by the depression of these curves relative to that of the ligand only (see figure 6.1). A buffer region was observed in each titration curve between pH 7.5 and 9.0. In this pH region, a distinct wine-red colour developed in solution and gradually intensified at higher pH.

Solutions of ferrous ion and gallic acid were essentially colourless below pH 6.8. A very pale blue colour which sometimes appeared between pH 4.0 and 6.8 was attributed to traces of ferric ion in solution. (Ferric complexes with gallic acid are intensely coloured; see section 6.4).

A broad, poorly defined inflexion in each of the titration curves was recorded at pH ca. 9.5 corresponding to the addition of 2 moles of alkali per mole of ligand plus 1½ moles of alkali per mole of metal ions. This stoichiometry is consistent with the formation of the complex $Fe_2(LH)_2(OH)$.

Table 6.1 Representative Data From a Titration of Gallic Acid and Ferrous Ion With Standard Potassium Hydroxide at 25 °C, L/M 3:1, Ionic Strength 0.10 M

Titre (ml) *(a)*	pc_H *(b)*	Titre (ml) *(a)*	pc_H *(b)*
0.800	7.316	0.950	8.173
0.810	7.442	0.970	8.261
0.820	7.543	0.980	8.306
0.830	7.624	0.990	8.349
0.840	7.693	1.000	8.397
0.850	7.750	1.010	8.448
0.860	7.804	1.020	8.497
0.870	7.854	1.030	8.552
0.880	7.885	1.040	8.610
0.890	7.931	1.050	8.663
0.900	7.969	1.060	8.723
0.910	8.007	1.070	8.783
0.920	8.047	1.080	8.843
0.930	8.088	1.090	8.907
0.940	8.132	1.100	8.971

(a) *Cumulative volume of 0.8951 M KOH added to 160.00 ml of titration solution, initially comprising gallic acid (1.501×10^{-3} M), ferrous ion (5.003×10^{-4} M), HCl (2.789×10^{-3} M) and KCl (0.0956 M).*

(b) *Hydrogen ion concentrations derived from the measured pH as described in chapter 4.*

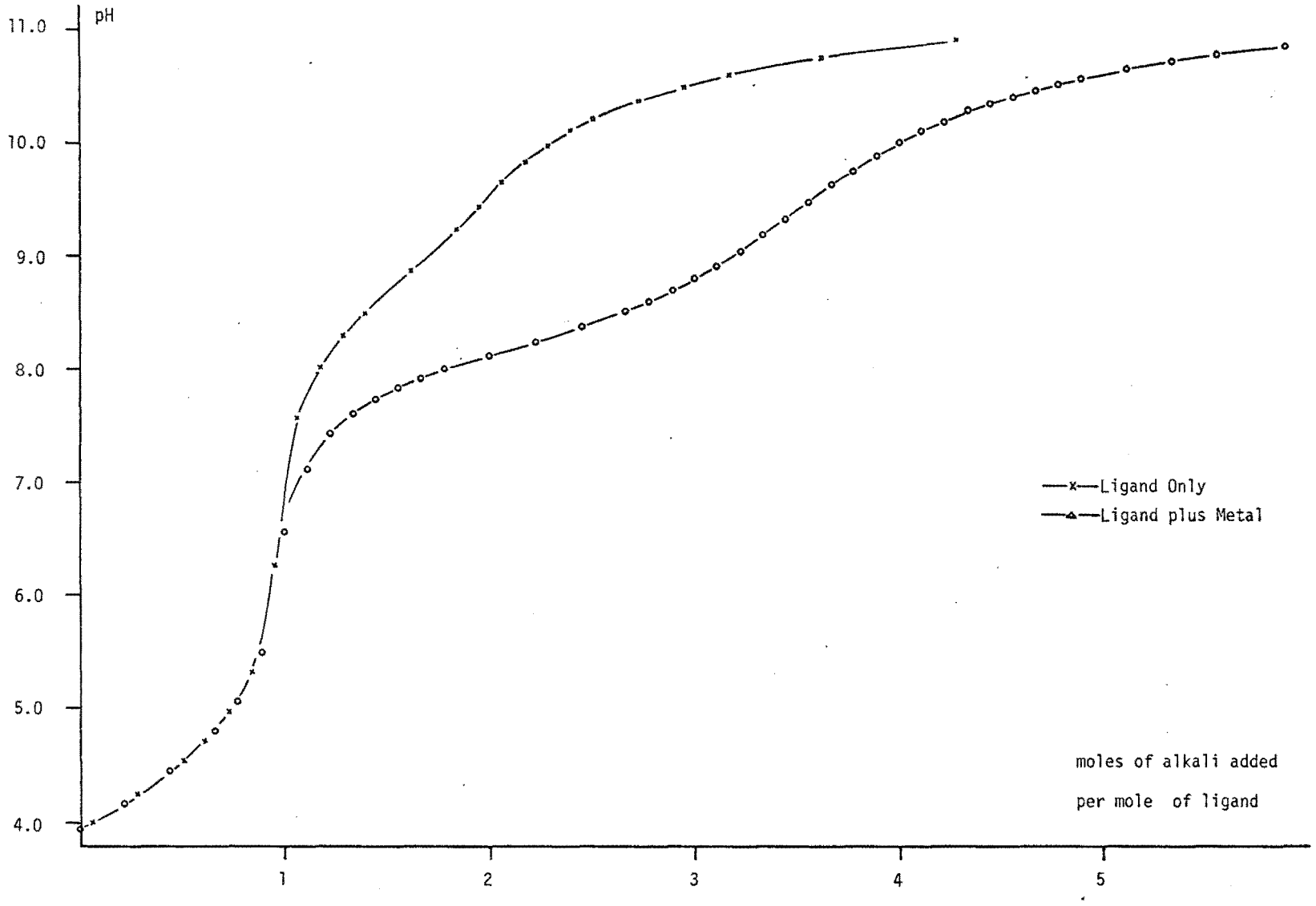

Figure 6.1 Potentiometric Data From Solutions of Gallic Acid (2.5×10^{-4} M) / Ferrous Ion at 25 °C, L/M 1:1, Ionic Strength 0.10 M

6.1.2 Spectrophotometric Data

The equipment described in section 2.7 was used to obtain some preliminary spectrophotometric data from ferrous-gallic acid solutions as a function of pH.

An absorption at ca. 520 nm was observed at pH > 8.0 for solutions with 1:1, 2:1 and 3:1 ligand-metal ratios. This absorption intensified at higher pH with little change in the wavelength of maximum absorbance below pH 9.5. Suspected contamination with Fe^{3+} at higher pH prevented quantification of this absorption, but initial results gave an extinction coefficient of about 1500 l mol^{-1} cm^{-1} (pH 9.5). This suggests a charge transfer transition involving ligand and metal ion.

6.1.3 Discussion

Potentiometric and spectrophotometric data from solutions of ferrous ion and gallic acid indicate complex-formation above pH 7. Endpoint stoichiometries from solutions of varying ligand-metal ratios suggest the formation of the hydroxy-species $Fe_2(LH)_2(OH)$. This complex is envisaged to be a bridged species with the coordination of the metal occurring via two ortho-O^- functions:

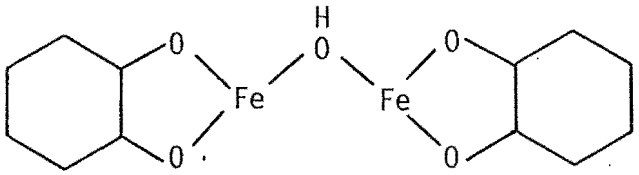

That a bridged species is formed is further supported by figure 6.2 which illustrates the relationship between ΔV and pH. ΔV represents the difference in volume of alkali required to bring solutions containing gallic acid (of a given concentration), with and without ferrous ion, to

Figure 6.2 ΔV versus pH for Solutions of Gallic Acid and Ferrous Ion, L/M 1:1, 2:1. 3:1

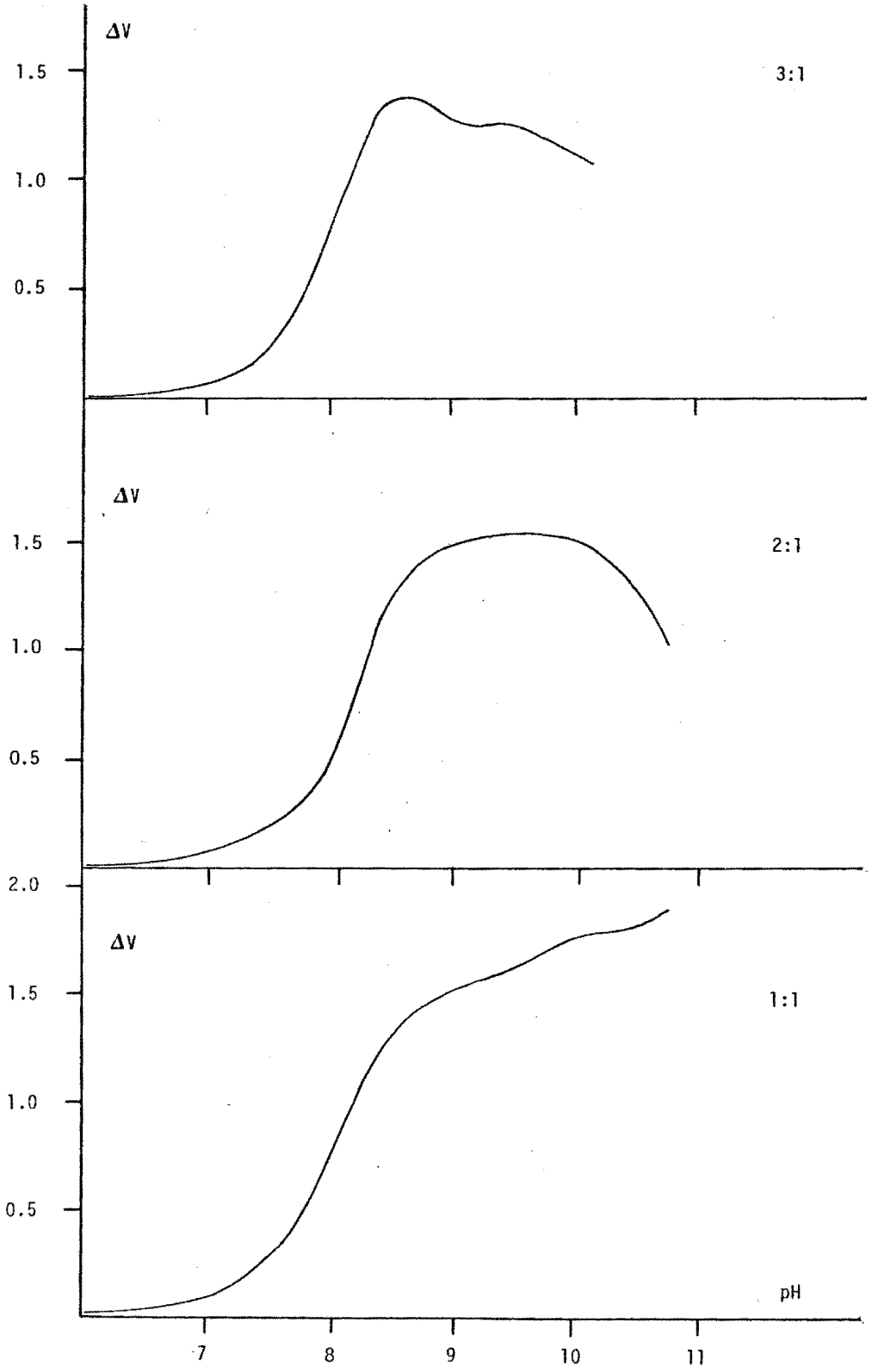

a specified pH, i.e.:

$$\Delta V_i = (V_{Fe/ligand} - V_{ligand})_{pH_i}$$

For each ligand-metal stoichiometry a distinct inflexion in these plots is noted at $\Delta V = 1.5$, close to the pH for which an endpoint occurred in the corresponding potentiometric titration curve. Data from the curve representing a 1:1 ligand-metal ratio, indicate that further deprotonation is associated with the metal ion above pH 9.5. This suggests the following equilibrium may occur:

$$Fe_2(LH)_2(OH)(H_2O) \rightleftharpoons Fe_2(LH)_2(OH)_2 + H^+$$

6.2 Catechol

6.2.1 Potentiometric Data

Representative potentiometric data from the titration of alkali against Fe(II)-catechol solutions, with an initial ligand:metal ratio of 2:1 are given in table 6.2. These results are presented graphically in figure 6.3. An additional titration was also performed with an initial ligand:metal stoichiometry of 1:1. These titrations were carried out under similar conditions to those used for Fe(II)/gallic acid.

Solutions of ferrous ion and catechol were essentially colourless up to pH 7.8. The well-defined endpoint which occurred around pH 7.0 corresponded to the titration of excess acid initially present in both iron and ligand solutions (see section 2.4). Above this pH a pale wine-red colour developed in solution similar to that observed for ferrous ion and gallic acid. Spectra were not recorded but this colour appeared to intensify slowly as the pH was increased. Further evidence for complex formation was found in the depression of the titration curves relative to that for the ligand alone above pH 7.8 (see figure 6.2).

Table 6.2 Representative Data From a Titration of Catechol and Ferrous Ion With Standard Potassium Hydroxide at 25 °C, L/M 2:1, Ionic Strength 0.10 M

Titre (ml) *(a)*	pc_H *(b)*
0.340	8.586
0.350	8.694
0.360	8.792
0.370	8.889
0.380	8.982
0.390	9.081
0.400	9.192
0.410	9.313
0.420	9.439
0.430	9.573
0.440	9.705
0.450	9.835
0.460	9.953

(a) *Cumulative volume of 0.8951 M KOH added to 160.00 ml of titration solution, initially comprising catechol (5.023×10^{-4} M), ferrous ion (2.376×10^{-4} M), HCl (1.6657×10^{-3} M) and KCl (0.0904 M).*

(b) *Hydrogen ion concentrations derived from the measured pH as described in chapter 4.*

Figure 6.3 Potentiometric Data From Solutions of Catechol (5×10^{-4} M)/Ferrous Ion at 25 °C, L/M 2:1, Ionic Strength 0.10 M

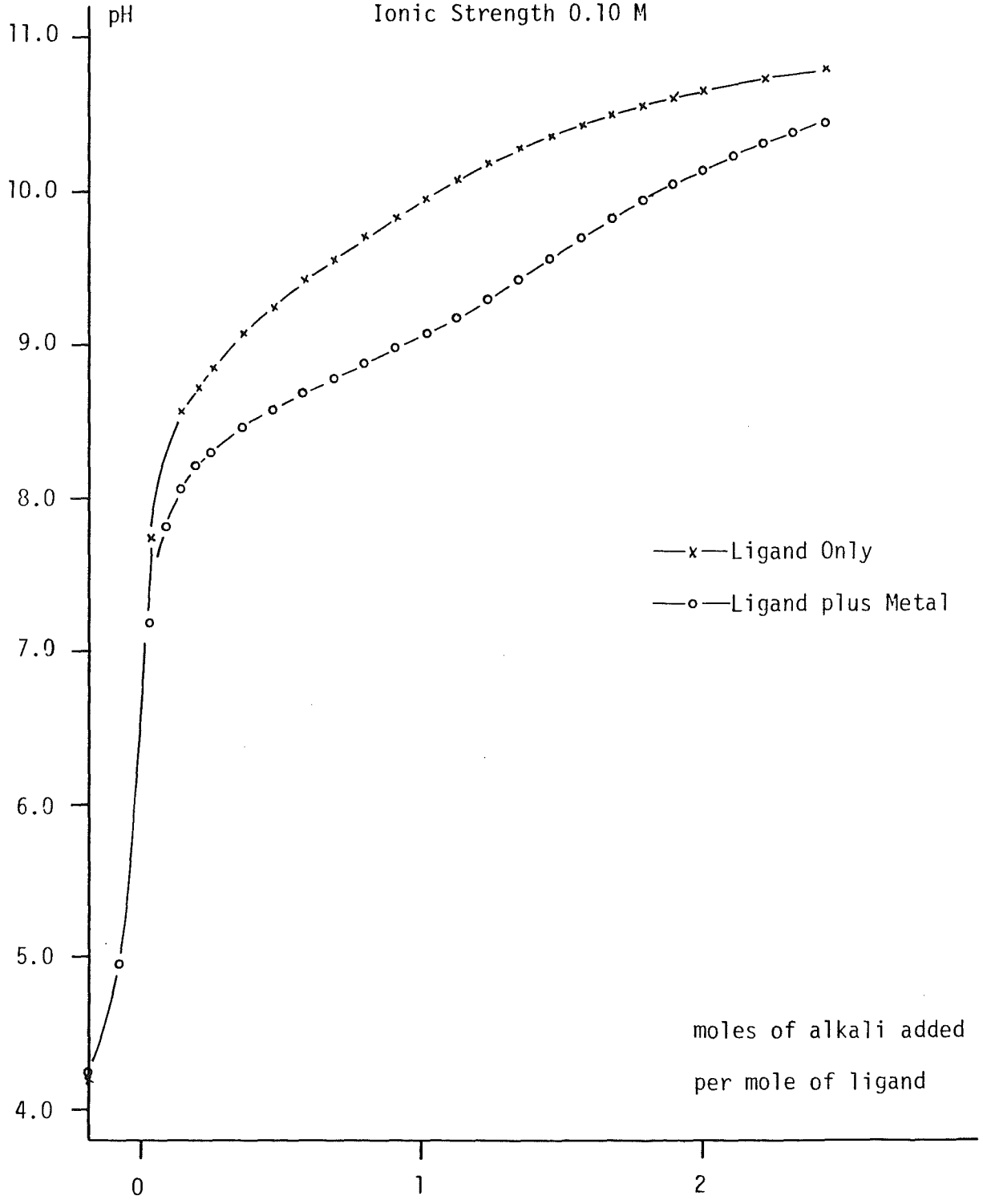

Slight downward drift in pH measurements accompanied by turbidity, which developed in solution at high pH, were attributed to precipitation of possibly a catechol-ferrous complex or ferrous hydroxide. Precipitation occurred at pH 8.8 for the 1:1 titration (initial ferrous ion concentration ca. 5×10^{-4} M) and pH 9.4 for the 2:1 titration (initial ferrous ion concentration ca. 4.5×10^{-4} M). Precipitation was not observed below pH 10.0 for a 2:1 titration in which the initial ferrous ion concentration was ca. 2.4×10^{-4} M. These observations suggest that the precipitate is $Fe(OH)_2$.

In the 2:1 titration an orange-red colour became apparent above pH 9.5. No distinct endpoints were observed in these titrations although there was some evidence for a shallow inflexion in the 2:1 titration curve after the addition of 1 mole of alkali per mole of ligand plus 1½ moles per mole of metal ions (see figure 6.2). This would be consistent with formation of the complex Fe_2L_2OH, analogous to the species formed in gallic acid solutions.

6.3 Stability Constants

6.3.1 Method of Calculation

Three different models were used in the calculation of stability constants for ferrous-polyphenol complexes. The first of these consisted of equilibria involving FeL and FeL_2 species, while the second had FeL and FeLOH species only. In addition to the fact that the endpoint stoichiometry from the potentiometric titration curves was not strictly consistent with either of these models, least squares analysis of the observed volume, pH data in many cases revealed a poor fit with calculated values.

For the third model, involving the bridged hydroxy-species $Fe_2(LH)_2(OH)$ (in the case of gallic acid) and Fe_2L_2OH (catechol), the

following equilibria were considered (the example is for gallic acid, LH_4):-

$$Fe^{2+} + LH^{3-} \rightleftharpoons FeLH^{-} \qquad (6.1)$$

$$K_1 = \frac{c_{FeLH}}{c_{LH}\, c_{Fe}}$$

$$2Fe^{2+} + 2LH^{3-} \rightleftharpoons Fe_2(LH)_2(OH)^{3-} + H^{+} \qquad (6.2)$$

$$K_b = \frac{c_{Fe_2(LH)_2(OH)}\, c_H}{c_{Fe}^2\, c_{LH}^2}$$

$$2Fe^{2+} + 2LH^{3-} \rightleftharpoons Fe_2(LH)_2(OH)_2^{4-} + 2H^{+} \qquad (6.3)$$

$$K_d = \frac{c_{Fe_2(LH)_2(OH)_2}\, c_H^2}{c_{Fe}^2\, c_{LH}^2}$$

$$Fe^{2+} \rightleftharpoons FeOH^{+} + H^{+} \qquad (6.4)$$

$$K_h = \frac{c_{FeOH}\, c_H}{c_{Fe}}$$

In addition, the relevant ligand protonation equilibria (e.g. equations 5.4 - 5.7), were also considered.

Combining equations 5.4 - 5.7 and 6.1 - 6.4 the following expressions were derived for T_L (total concentration of ligand species), T_M (total concentration of metal species) and T_H (total concentration of titratable protons):

$$T_L = k_2k_3k_4\, c_{LH}\, c_H^3 + k_2k_3\, c_{LH}\, c_H^2 + k_2\, c_{LH}\, c_H + c_{LH} / (k_1\, c_H) + K_1\, c_{Fe}\, c_{LH} + 2\, K_b\, (c_{Fe}\, c_{LH})^2 / c_H + 2\, K_d\, (c_{Fe}\, c_{LH} / c_H)^2 + c_{LH} \qquad (6.5)$$

$$T_M = c_{Fe} + K_1 c_{LH} c_{Fe} + K_h c_{Fe} / c_H + 2K_b c_{Fe}^2 c_{LH}^2 / c_H + 2K_d (c_{Fe} c_{LH} / c_H)^2 \quad (6.6)$$

$$T_H = 4k_2k_3k_4 c_{LH} c_H^3 + 3k_2k_3 c_{LH} c_H^2 + 2k_2 c_{LH} c_H + c_{LH} + K_1 c_{Fe} c_{LH} + K_b (c_{Fe} c_{LH})^2 / c_H + c_H - c_{OH} - K_h c_{Fe} / c_H \quad (6.7)$$

A trial value for c_{LH}, the equilibrium concentration of the co-ordinating form of the ligand (c_L for catechol), was estimated, enabling equation 6.6 to be solved for c_{Fe}, the equilibrium concentration of free metal. (Trial values of K_1, K_b and K_d were estimated). The hydrogen ion concentration, c_H, was determined from pH'_m data, (the measured pH corrected for liquid junction effects) using the methods outlined in chapters 3 and 4. K_h the hydrolysis constant for ferrous hydroxide, was taken to be $10^{-8.3}$ [135]. (This choice is evaluated in section 6.3.2). T_M, the total concentration of metal species, was calculated from the known initial concentration of ferrous ion in solution modified by an appropriate dilution factor, Q, to compensate for the addition of alkali.

A new value for c_{LH} was then found by solving equation 6.5. (T_L, the total concentration of ligand species, was calculated in an analogous fashion to T_M, and values for k_1 - k_4, the ligand protonation constants, were taken from calculations described in chapter 5.) Successive refinement in the calculation of c_{Fe} and c_{LH} was continued until the change in c_{LH} due to modification of c_{Fe} was less than 0.5 %.

Equation 6.7 was then solved for T_H, the total concentration of titratable protons, using the refined values of c_{Fe} and c_{LH}. (The term, c_{OH}, arising from ligand hydrolysis reactions (see equation 5.3) was

calculated from the ionic product for water, K_w, as described in section 4.4.2*(b)*.) This value of T_H was designated "T_H (calc)" to distinguish it from "T_H (obs)"; the latter was determined from the known solution stoichiometry thus:

$$T_H \text{ (obs)} = (4T_L + A)\, Q - v\, c_{KOH} / (V + v) \qquad (6.8)$$

where A = initial concentration of added acid (originating from the solution containing ferrous ion), v = volume of added potassium hydroxide solution of concentration, c_{KOH}, and V = total volume of solution.

The above calculations were repeated for each datum point from the potentiometric titration giving a series of T_H (obs), T_H (calc) values for the trial estimates of stability constants K_1, K_b and K_d. FORTRAN programs were written to calculate T_H (obs) and T_H (calc) (Appendix 13). These were in the form of subroutines to the least squares program ORGLS [119]. The parameters were varied until the function $\Sigma (T_H \text{ (obs)} - T_H \text{ (calc)})^2$ was minimised over all data points (i.e. a least squares refinement).

6.3.2 Results for Gallic Acid

Data from six individual titrations, of ligand-metal stoichiometries 1:1 (2), 2:1 (1) and 3:1 (3), were analysed. Table 6.3 summarizes the results. The fairly narrow range of values for K_1 and K_b for a wide range of ligand-metal stoichiometries is consistent with the chosen model for complex formation.

As mentioned in the previous section, data from 1:1 titrations suggested an additional metal-ligand species forming at high pH. Detailed analysis of titration data in the high pH region was not carried out, but

Table 6.3 Stability Constants for Ferrous-Gallic Acid Complexes

Metal-Ligand Complex	Stability Constant
$FeLH^-$	$\log K_1 = 7.00 \pm 0.02$ *(a)*
$Fe_2(LH)_2OH^{3-}$	$\log K_b = 9.04 \pm 0.11$ *(a)*
$Fe_2(LH)_2(OH)_2^{4-}$	$\log K_d = -1.75$ *(b)*

(a) *Errors estimated from spread of K-values over six titration results. Values of the R-factor ranged from 0.3 - 1.0 %.*

(b) *This value is approximate only; see text for details.*

preliminary results indicated a value of ca. -1.75 for the constant log K_d was consistent with the titration curve for 1:1 ligand-metal solutions.

A wide range of values for the hydrolysis constant, K_h, have been reported in the literature [57]. A value of $10^{-8.3}$ was chosen, rather arbitarily, for calculations in this work. Least squares analyses were also performed in which K_h was included as a parameter. Results from four such analyses gave an average value for log K_h of - 8.2 ± 0.4.

6.3.3 Results for Catechol

Data from only one titration involving Fe^{2+} and catechol were analysed using the same model for complex formation proposed for gallic acid. Estimates of the stability constants K_1 and K_b are listed in table 6.4. Tyson and Martell [47] analysed data from ferrous-catechol solutions using a complexing model involving the species FeL and FeL_2^{2-}. Values of the respective stability constants K_1 and K_2 were reported to be 7.95 and 5.54. No evidence was found for the formation of a bis-(diphenolate)-iron(II) complex in this work.

Table 6.4 Stability Constants for Ferrous-Catechol Complexes

Metal-Ligand Complex	Stability Constant
FeL	$\log K_1 = 8.4$
$Fe_2L_2OH^-$	$\log K_b = 10.9$

B. FORMATION OF FERRIC COMPLEXES WITH GALLIC ACID, PYROGALLOL, CATECHOL, PROTOCATECHUIC ACID AND TIRON

6.4 Gallic Acid

6.4.1 Potentiometric Data

(a) Titrations in Air. Potentiometric data for the titration of Fe(III) - gallic acid solutions with standard potassium hydroxide solution (initial ligand to metal ratio of 3:1) are shown in figure 6.4.

On mixing solutions of ferric ion and gallic acid (LH_4) in acidic conditions (pH < 3.5), a dark inky-blue colour developed immediately. In the space of a few minutes, however, this blue colour faded leaving a very pale yellow-green solution. A small rise in the pH of the solution was noted. When the solution was titrated with alkali it became progressively more grey in colour and a blue tinge was noted around pH 3.5. This developed into a very dark purple-blue by pH 7.4, where a distinct inflexion occurred in the pH titration curve corresponding to the addition of 7 moles of alkali per mole of metal ions (i.e. a = 7). Depression of the titration curve in this region, relative to that of the ligand only, was evidence of proton-releasing reaction(s) (see figure 6.4). These observations are consistent with the following net reaction:

$$Fe^{3+} + 2LH_4 + 6OH^- \longrightarrow Fe(LH)_2^{3-} + 6H_2O \qquad (6.9)$$

Titration of the excess ligand would consume the additional mole of alkali as the carboxyl proton is neutralized below pH 6.5 (see section 5.1.1).

The titration solution developed an intense red colour as the pH was increased beyond 7.4, becoming red-brown by pH 11.0. Further

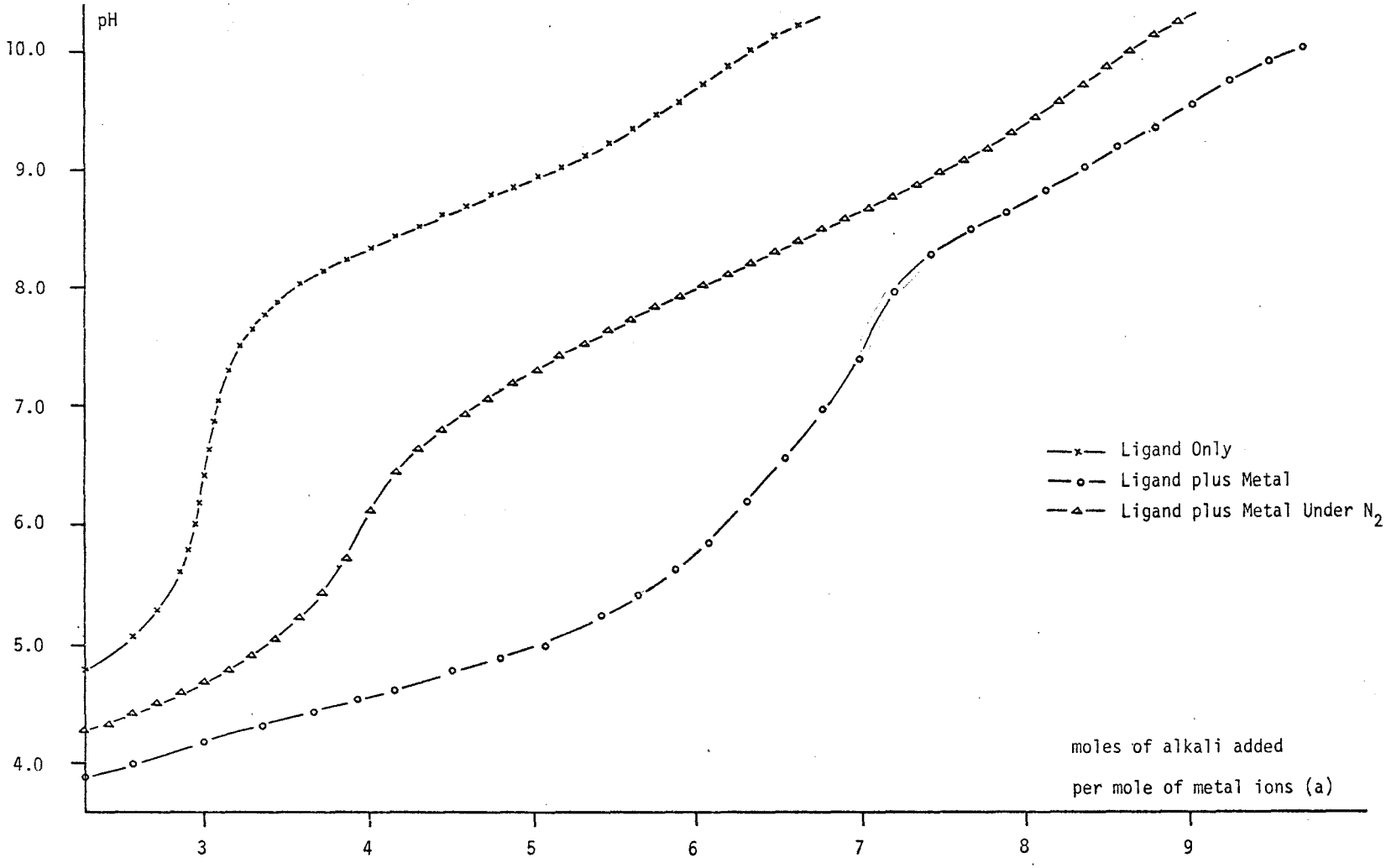

Figure 6.4 Potentiometric Data From Solutions of Gallic Acid (2×10^{-3} M) and Ferric Ion at 25 °C, L/M 3:1

buffering was observed in the pH range 8.2 - 9.0 with a very shallow inflexion occurring around pH 9.4 corresponding to a = 8.5 - 9.0. This was initially thought to indicate the formation of a ligand-metal complex of stoichiometry 3:1, i.e.:

$$Fe^{3+} + 3LH_4 + 9OH^- \longrightarrow Fe(LH)_3^{6-} + 9H_2O \qquad (6.10)$$

Figure 6.5 gives data for solutions with initial ligand to metal ratios of 2:1 and 1:1. For 2:1 stoichiometry a rather broad inflexion occurred at pH 7.6 - 8.8 corresponding to a = 6 - 6.5. In the buffer region observed below pH ca. 7.0 an intense purple-blue colour developed, similar to that observed in 3:1 titrations. These observations suggested the formation of a bis complex as per equation 6.9.

For solutions with ligand-metal ratios of 1:1 the titration curve showed a distinct inflexion at pH ca. 8.0, corresponding to a = 4. The colour of the solution at this pH was a dark reddish purple. A broad buffer region occurred below pH 6.0 with a slight inflexion in the titration curve evident at pH 5.0 (a = 3). Below this pH the titration solution was intensely purple in colour. The inflexions at a = 3 and 4 were initially thought to indicate the formation of FeLH and FeLH(OH) species respectively. At pHs above ca. 5.0 significant downward drift in pH readings was observed.

(b) Titrations in Nitrogen. To determine the role of redox processes involving oxygen, potentiometric titrations were carried out in an atmosphere of nitrogen. For an initial ligand:metal stoichiometry of 3:1 a distinct inflexion in the pH titration curve occurred around pH 6.0, corresponding to the addition of 1 mole of alkali per mole of ligand plus 1 mole per mole of metal ions (figure 6.4). Buffering occurred below pH 6.0 and the colour of solution changed from very pale yellow-green at pH$<$3.5 to grey at the end of the buffer region.

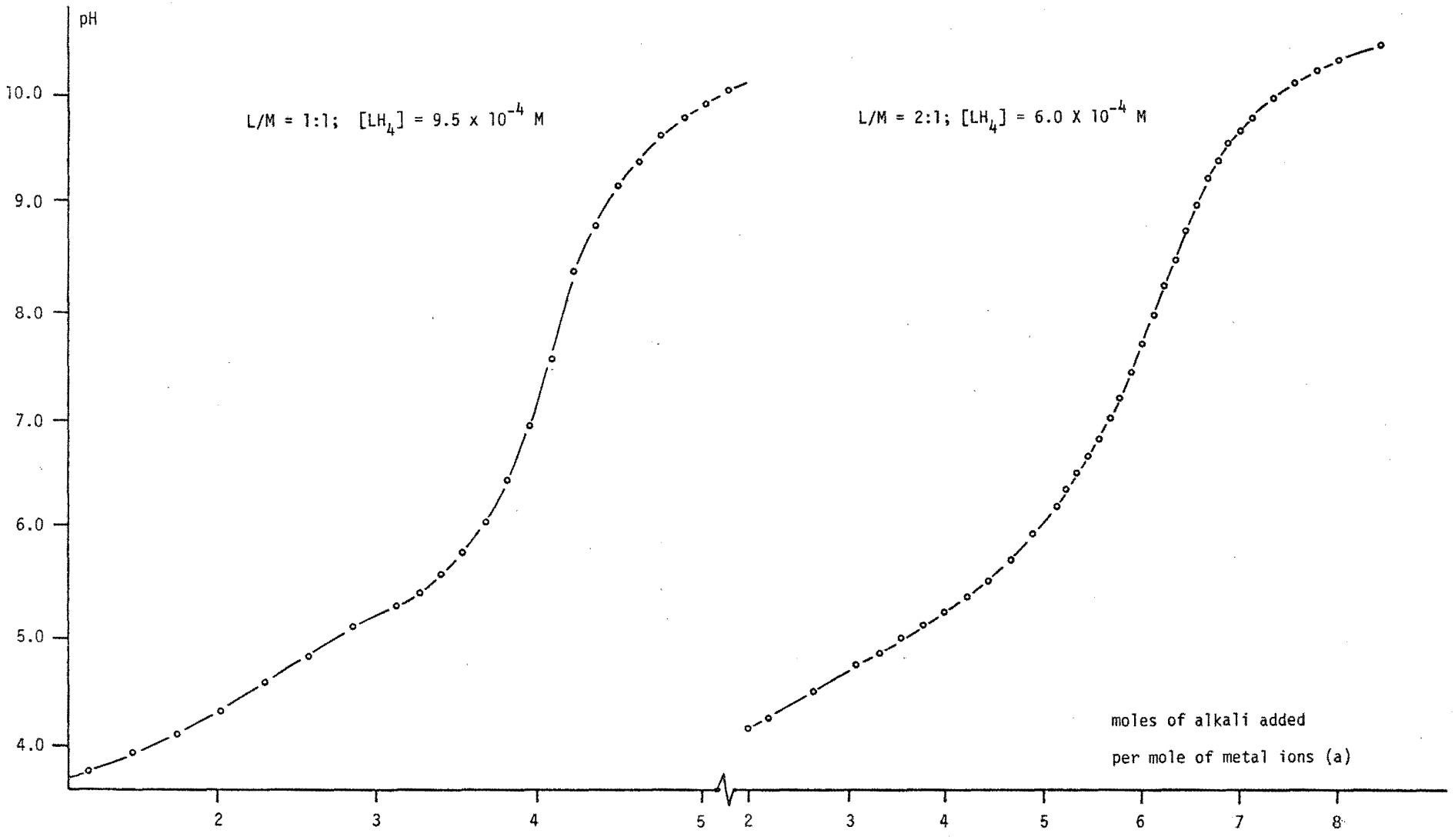

Figure 6.5 Potentiometric Titration of Gallic Acid and Ferric Ion at 25 °C, L/M 1:1 and 2:1

A wine colour developed above pH 6.7, similar to that observed for ferrous-gallic acid solutions, and this intensified at higher pH.

Titrations where oxygen was introduced into the system at a pH ca. 6.0 showed a rapid lowering of the pH and the development of an intense blue colour in solution. As the pH was increased further the titration curve followed that of the aerobic system. These observations are discussed further in section 6.4.6.

6.4.2 Spectrophotometric Data

Evidence of an initial redox process involving Fe^{3+} and gallic acid was obtained from the visible/ultraviolet spectra of solutions of the ligand to which small concentrations of ferric ion were added incrementally in the presence of atmospheric oxygen. These spectra were measured at pH 2.3 - 2.7. (Solutions containing Fe^{3+} and gallic acid for titration with alkali had pHs in this range when prepared). As ferric ion was added the electron-transfer band of gallic acid at 270 nm decreased in intensity accompanied by a gain in intensity of the benzoid transition at 219 nm. This latter absorption also moved to shorter wavelength (215 nm) as ferric solution was added. In the visible region of the spectrum a broad peak at ca. 385 nm developed, maximum intensity being reached after the addition of ca. 2 moles of Fe^{3+} per mole of gallic acid. Isosbestic points at 300 nm and 254 nm indicated the presence of two distinct species. This absorption at the high-energy end of the visible spectrum was responsible for the pale yellow-green colour of solutions of ferric ion and gallic acid already noted (section 6.4.1). It occurred at a wavelength expected for an o-quinone species [136].

Table 6.5 summarizes spectrophotometric data from the titration of potassium hydroxide against solutions of ferric ion and gallic acid in the presence of atmospheric oxygen (ligand-metal stoichiometry = 3:1).

Table 6.5 Spectrophometric Data For Solutions of Gallic Acid and Ferric Iron (Ligand-Metal Ratio = 3:1)

pH	Description	Wavelength (nm)	ε (cm^{-1} l mol^{-1})	Species Involved *(a)*
3.5	absorption maximum	385 ± 5	1340 ± 100	QH_2
5.0	absorption maximum *(b)*	560 - 580		Fe(LH) (?)
7.5	absorption maximum	548 ± 3	4370 ± 50	$Fe(LH)_2^{3-}$
7.5 - 10.5	isosbestic point	570 ± 5		$Fe(LH)_2^{3-}$ / $Fe(LH)_3^{6-}$
10.5	absorption maximum	499 ± 2	5750 ± 100	$Fe(LH)_3^{6-}$

(a) *These conclusions were reached after additional consideration of other data (refer to section 6.4.6).*

(b) *A poorly-defined absorption of low intensity.*

Figure 6.6 presents these results graphically. The absorptions in the visible region of the spectrum at 548 and 499 nm (giving rise to purple-blue and red colours respectively) reached maximum intensity at pHs consistent with the endpoints observed in the potentiometric titration curve (see section 6.4.1).

For an initial ligand-metal stoichiometry of 2:1 a similar pattern was observed up to pH 7.5 while at higher pHs the wavelength of

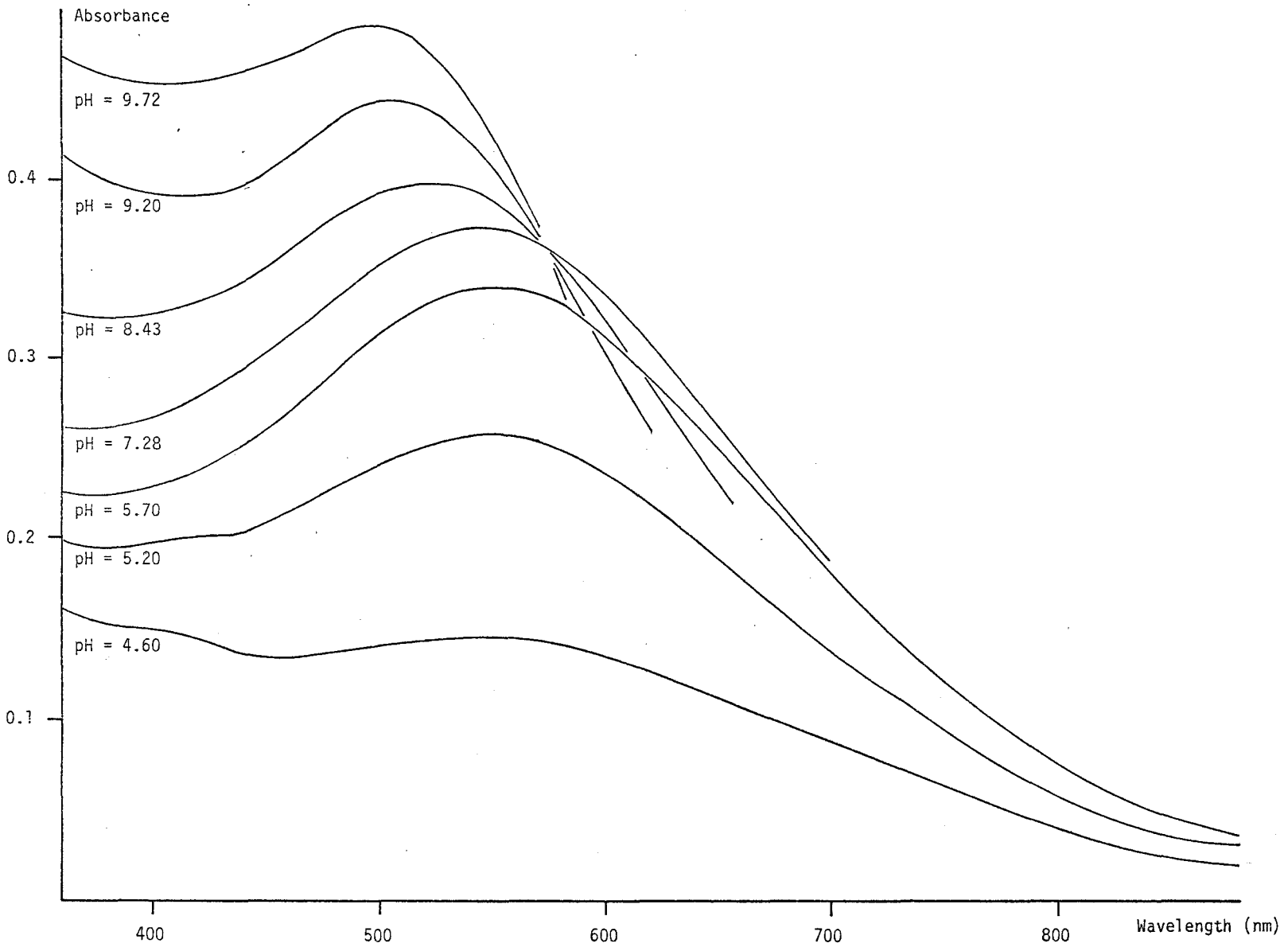

Figure 6.6 : Spectrophotometric Data From Solutions of Gallic Acid (2.6×10^{-4} M) and Ferric Ion, L/M 3:1

maximum absorption decreased, accompanied by a slight decrease in intensity.

In a 1:1 titration an absorption maximum developed at 546 nm (pH ca. 6.3, ϵ = 2400 l mol^{-1} cm^{-1}). This peak shifted to shorter wavelength above pH 6.3 with little change in intensity.

Few definitive conclusions about the coordinated form of the ligand could be made from the UV region of the spectrum (see also section 5.7). Above pH ca. 7.5, solutions of metal-ligand stoichiometry 1:1 and 2:1, in which all the ligand was expected to be coordinated to Fe^{3+}, showed absorptions in the UV region consistent with LH_2^{2-} or LH^{3-} species.

6.4.3 Vareille Plots

From the optical density or absorbance (A) of a solution an "extinction coefficient" (ϵ) may be calculated for a specified wavelength, viz.:

$$\epsilon = A / cl$$

where c = concentration of absorbing species and l = optical path length. Plots of ϵ vs. pH, so called Vareille plots [137], are useful for defining the pH ranges of stepwise complex formation reactions. They may also give some indication of the composition of complexes present. Figure 6.7 shows one such plot, for a ligand-metal ratio of 3:1, at 500, 570 and 650 nm. These wavelengths were chosen to highlight changes in the absorption spectra throughout the pH range investigated. Plateau regions at pH 6.0 - 7.0 and pH >10.5 indicated that formation of single complexes was completed at those pHs.

6.4.4 Job Variation Plots

The method of "continuous variations" or "isomolar solutions"

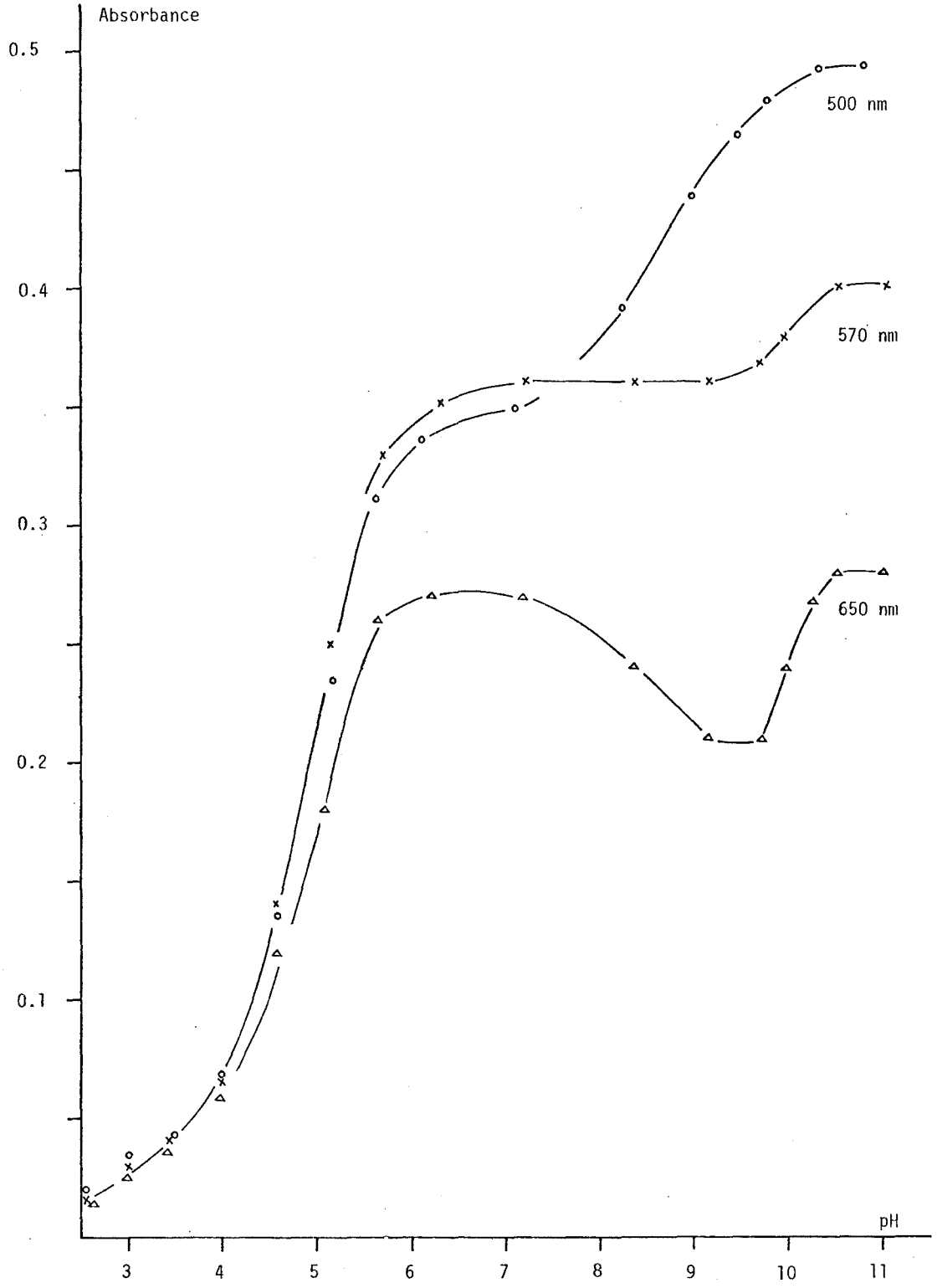

Figure 6.7 Vareille Plots for Gallic Acid (2.6×10^{-4} M) and Ferric Ion, L/M 3:1, 10 mm cell

introduced by Job [138] is widely used in investigations of complex formation in solution. One of the specific applications of this method is the determination of the stoichiometric composition of metal-ligand complexes. The theory behind such plots is outlined in Appendix 14.

The assumptions implicit in this method are[139] :

(1) Each of the reactants is of known composition (i.e. is not involved in competing equilibria).

(2) The law of mass action is valid in terms of concentrations.

(3) The reactants form only one complex (when other complexes are present the maximum in a Job plot is displaced from the stoichiometric point).

Job variation plots have been drawn for an isomolar series involving ferric ion and gallic acid with a total solution composition of 3.45×10^{-4} mol dm^{-3}. Plots were made from data at 600 nm (pH 7.5) and 500 nm (pH 10.5) (figure 6.8). These wavelengths were chosen to minimise any overlap between the principle absorption maxima, whilst retaining meaningful information about the absorbing species.

These plots were drawn from data at fixed pH in order to fulfill the condition stated in assumption (1) above, since the ligand is subject to competing protonation equilibria. Condition (2) was fulfilled by using KCl as a background salt medium, thus providing solutions of constant ionic strength. By choosing data from pH regions corresponding to an inflexion in the titration curve, i.e. where a complexing reaction is complete, condition (3) was satisfied.

Results showed that maxima in the isomolar plots occurred at $x = 0.67$ for pH = 7.5 and $x = 0.75$, pH = 10.5, indicating the presence of 2:1 and 3:1 complexes respectively. These pHs correspond to plateau regions in the Vareille plot (described in the previous section) and inflexions in the potentiometric titration curve (section 6.4.1).

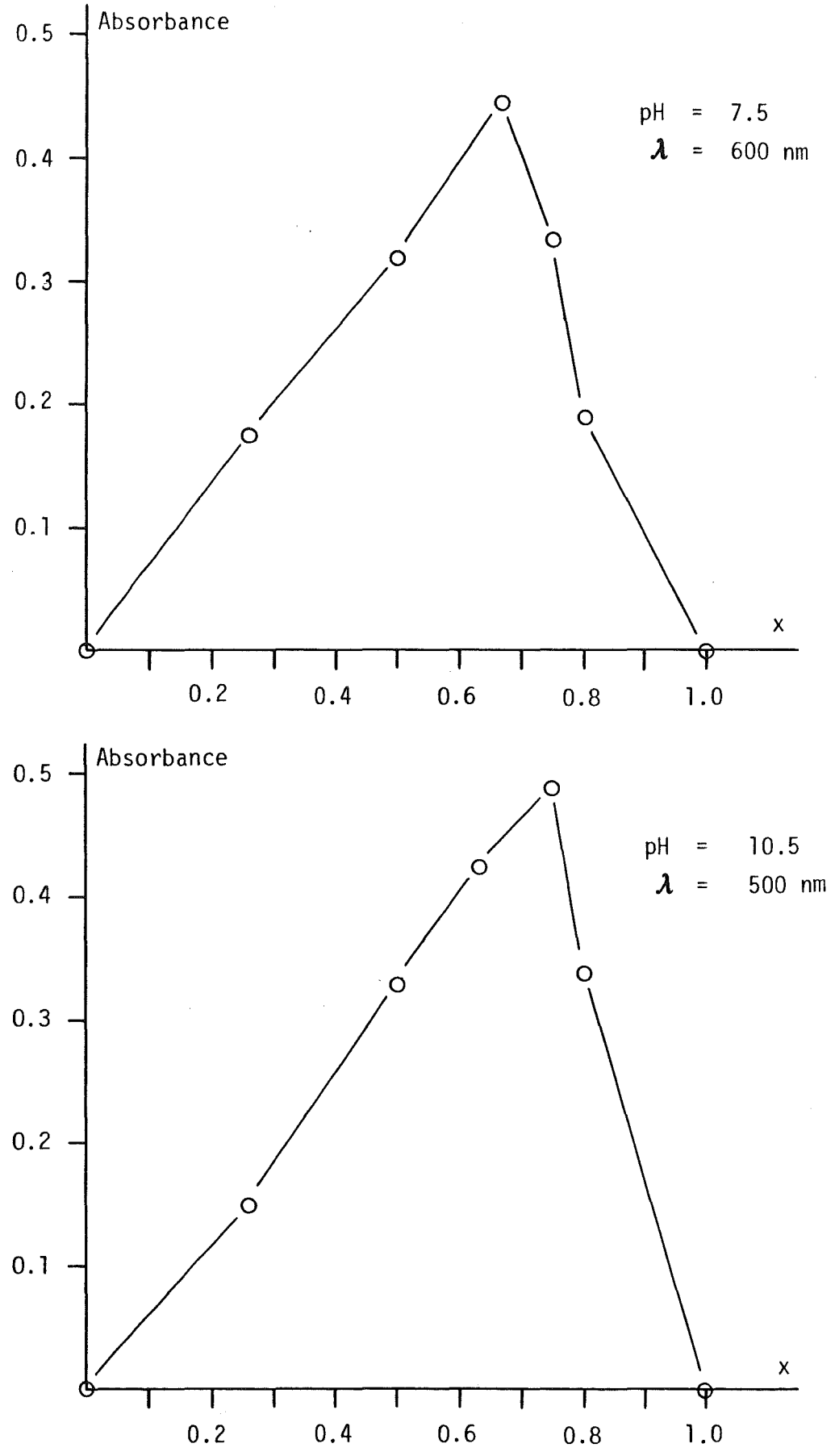

Figure 6.8 Job Variation Plots for Solutions of Ferric Ion and Gallic Acid, (Total Molar Concentration 3.45×10^{-4})

6.4.5 Analytical Results

To determine the nature of redox reactions thought to be occurring between ferric iron, gallic acid and oxygen, a quantitative determination of Fe(III) at various stages of metal-ligand titrations was made (see section 2.6.1). For these titrations,solutions were exposed to the atmosphere. Results showed that for solutions of Fe^{3+} and gallic acid (ligand:metal ratio $\geqslant 1.0$) in the pH region 2.0 - 3.0, less than 5 % of the total iron was present as Fe(III) whereas above a pH ca. 5.0 only Fe(III) species existed.

6.4.6 Discussion

The similarity in reduction potentials of ferric ion (0.749 V) and the o-quinone of gallic acid (0.799 V at 30 °C) suggests the possibility of a direct redox reaction in solutions containing Fe^{3+} and gallic acid. Indeed, experimental evidence presented here, confirmed this. In the low pH region, (2.0 - 3.0) Fe^{3+} was rapidly reduced to Fe^{2+} by half a mole of gallic acid per mole of metal ions, giving rise to a pale yellow-green solution absorbing at ca. 385 nm, consistent with quinone formation. The overall equilibrium reaction is as follows:

$$Fe^{3+} + \tfrac{1}{2}LH_4 \rightleftharpoons Fe^{2+} + \tfrac{1}{2}H_2qno + H^+ \qquad (6.11)$$

where LH_4 denotes gallic acid and H_2qno the corresponding o-quinone. This stoichiometry was confirmed by metal-ligand titrations performed in the absence of oxygen, where an inflexion in the potentiometric curve around pH 6.5 indicated the removal of 1 proton per metal ion in addition to the removal of the carboxylate proton.

The transitory blue colour observed in the preparation of Fe^{3+}-gallic acid solutions at low pH is possibly due to a metal-ligand complex

intermediate of the form $FeLH_2^+$. The observed rise in pH which accompanied the disappearance of this colour from solution could be accounted for in the following step:

$$FeLH_2^+ + H^+ \rightleftharpoons Fe^{2+} + \tfrac{1}{2}H_2qno + \tfrac{1}{2}LH_4 \qquad (6.12)$$

Laurence and Ellis[140] detected a blue complex intermediate in the oxidation of ascorbic acid (AH_2) by ferric ion. They suggested that following a complex-formation process resulting in the species $FeAH^{2+}$, an intramolecular electronic transfer from ascorbate to ferric ion takes place. The reduced metal complex then dissociates to produce Fe^{2+} and an ascorbate radical. This radical undergoes further rapid reaction with another Fe^{3+} to yield, overall, two moles of Fe^{2+} and one of dehydroascorbic acid, for every mole of ascorbic acid oxidised:

$$Fe^{3+} + \tfrac{1}{2}AH_2 \rightleftharpoons Fe^{2+} + \tfrac{1}{2}A + H^+$$

Metal-ligand complexes have also been detected as intermediates in the redox reactions of Fe^{3+} with catechol derivatives [58]. The mechanism proposed in this case involved intermediate semiquinone radical ($LH^{\cdot}$) formation as the rate-determining step followed by oxidation of $LH^{\cdot}$ to the o-quinone (qno) as follows:

$$Fe^{3+} + LH_2 \longrightarrow Fe^{2+} + LH^{\cdot} + H^+$$

$$Fe^{3+} + LH^{\cdot} \longrightarrow Fe^{2+} + qno + H^+$$

Where oxygen was excluded from Fe(III)-gallic acid solutions, in this work, no complexing was evident below pH 6.5. Above this pH a wine-red coloured ferrous complex with gallic acid was observed. For solutions where oxygen was reintroduced during the course of a titration rapid oxidation of Fe^{2+} to Fe^{3+} was observed above pH 4.0.

In solutions exposed to the atmosphere and with pH > 3.5,

Fe^{2+} was oxidised by dissolved oxygen to Fe^{3+}:

$$Fe^{2+} + \tfrac{1}{4}O_2 + H^+ \rightleftharpoons Fe^{3+} + \tfrac{1}{2}H_2O \qquad (6.13)$$

a reaction which was favoured by the formation of stable Fe(III)-gallate complexes. Indeed a ferrous-gallic solution titrated with alkali in the presence of oxygen resulted in a pH titration curve similar to that from ferric systems. Observed colour changes were also similar , the only major difference in spectrophotometric data recorded was the absence of the o-quinone absorption at low pH.

The weak absorption observed at 560 - 580 nm below pH 5.0 in spectra from 3:1 and 2:1 titrations may indicate the presence of a 1:1 metal-ligand complex but no supporting evidence was found for this.

Job variation and Vareille plots showed that in the region pH< 7.5, a bis -(gallate)-iron(III) complex is formed. This complex absorbed in the visible region of the spectrum at 548 nm giving rise to a dark blue solution. The endpoint in the pH titration curve (for a ligand:metal ratio of 3:1) indicated the titration of 1 proton per ligand plus 4 protons per metal ion in a single buffer region:

$$Fe^{3+} + 3LH_4 + 7OH^- \longrightarrow Fe(LH)_2^{3-} + LH_3^- + 7H_2O \quad (6.14)$$

Coordination of the metal to two $-O^-$ functions forming a five-membered chelate ring is envisaged, i.e.:

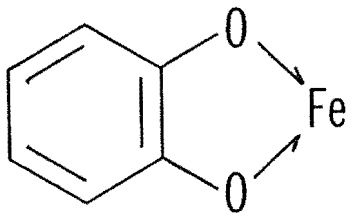

Spectrophotometric data for 3:1 solutions in the pH region 7.5 to 10.0, suggested the formation of a tris complex, red-purple in colour, with an absorption in the visible region of the spectrum at 500 nm. Potentiometric data in this region appeared to be consistent with the complex formation reaction 6.10. However, since the quinone initially formed by reaction 6.12 does not appear to be reduced at higher pH, approximately 1/6 of the ligand species represented by LH_4 in equation 6.10 will have the o-quinone form. Hence, equation 6.10 is not strictly valid. The possibility of coordination between Fe^{3+} and the o-quinone at high pH has a precedent in the formation of complexes between Fe^{3+} and kojic acid, log K_1 = 9.2 [57] . In this case an O^- / carbonyl chelating pair is responsible for binding Fe^{3+}. A further possible complication is introduced by the fact that above pH ca. 6.5 uncoordinated gallic acid will tend to be oxidised by dissolved oxygen (see section 5.6). To what extent this reaction competes with complex formation suggested by equation 6.10 remains undefined.

Potentiometric and spectrophotometric data from 2:1 titrations were consistent with the formation of a bis complex below pH 7.5, but a poorly-defined endpoint at a = 6 - 6.5 suggests a more complex picture. Data from a titration performed at metal-ligand stoichiometry of 1:1 were also not readily interpreted. It is possible that competing complexation, redox and hydrolysis reactions are responsible for the complex picture observed (see also section 6.6.4).

Loginova et al [66] have studied the coordination of gallic acid and ferric iron. They reported stability constants for a wide range of metal-ligand complexes, the most stable of which was FeL^-. A broad absorption at 550 nm with an extinction coefficient of 3900 l mol^{-1} cm^{-1} was assigned to this complex. Other data are summarized in table 1.1. All experiments were "conducted in an atmosphere of nitrogen" and no

redox reactions between Fe^{3+} and ligand were reported. Data presented in this work do not support many of the conclusions of Loginova *et al* and it is the opinion of this writer that a complex system involving Fe(II) as well as Fe(III) has been analysed erroneously.

6.5 Pyrogallol

6.5.1 Potentiometric Data

Titration solutions comprising ferric iron and 1,2,3-trihydroxybenzene (pyrogallol) had an initial ligand-metal ratio of 3:1. Potentiometric data from these titrations along with those from a ligand-only titration, are shown in figure 6.9.

(a) Titrations in Air. As potassium hydroxide solution was titrated against Fe^{3+} and pyrogallol, three buffer regions were observed, *viz*: pH < 3.7, 4.9 - 5.4, > 8.4. A shallow inflexion at a = 1 (pH *ca*. 4.2) and a broad inflexion at a = 4 (pH *ca*. 7.2) separated these buffer regions. As was the case for Fe^{3+} and gallic acid, depression of the titration curve relative to that of the ligand only indicated the presence of proton-releasing reaction(s).

Solutions of ferric ion and pyrogallol when mixed in acid conditions, (pH < 3.0), gave a bright orange-brown solution. When the solution was titrated with alkali the colour became grey-brown, then purple-grey at pH *ca*. 5.0. The colour of the solution at the end of the second buffer region was very dark purple-grey. For pH > 7.0 significant downward drift in pH readings occurred. The solution developed a red-purple colour in this pH region.

(b) Titrations in Nitrogen. Titration curves for Fe(III)-pyrogallol solutions, purged of oxygen, exhibited distinct inflexions

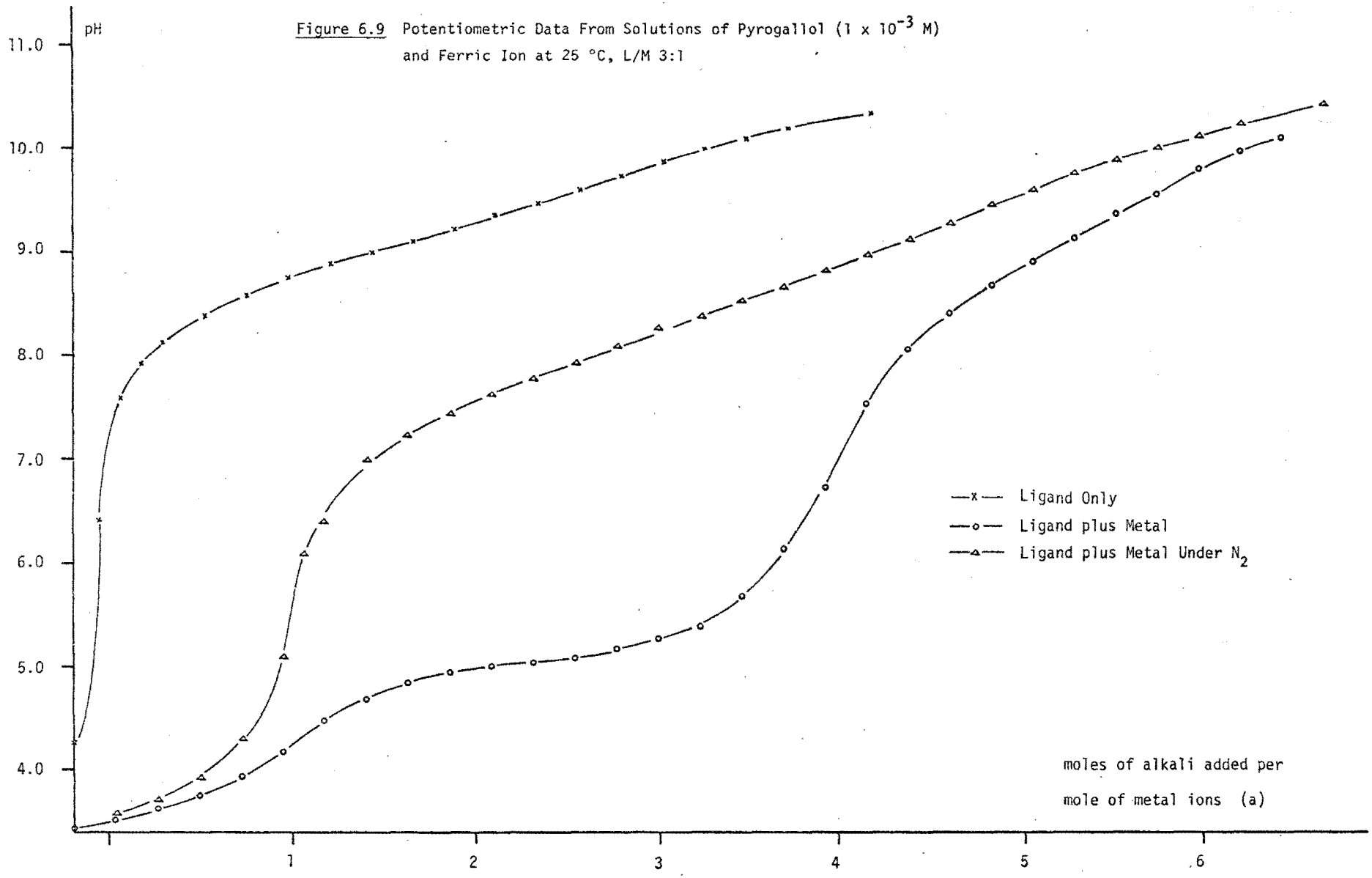

Figure 6.9 Potentiometric Data From Solutions of Pyrogallol (1×10^{-3} M) and Ferric Ion at 25 °C, L/M 3:1

around pH 5.7 corresponding to a = 1 (see figure 6.9). In the pH range, 3.0 - 5.0, the colour of solution changed from orange-brown to grey-brown. Above pH 7.2 a pale wine-red colour developed, intensifying at higher pHs.

6.5.2 Spectrophotometric Data

Solutions of pyrogallol and ferric ion, exposed to air, at pH < 3.0, exhibited a sharp maximum at 372 nm with a shoulder at ca. 400 nm. In the pH range 4.5 - 7.2, a broad absorption developed at 560 nm. Maximum absorbance occurred at pH 7.2 consistent with the observed endpoint in the potentiometric titration. An extinction coefficient of ca. 3900 cm^{-1} 1 mol^{-1} was measured at this point.

At higher pH the position of the absorption maximum shifted to shorter wavelength and became very broad (see figure 6.10). A poorly-defined isosbestic point was observed at 670 ± 10 nm between pH 7.2 and 10.0.

6.5.3 Analytical Data

Fe(III) was determined quantitatively in solutions of pyrogallol and ferric ion at various pHs. A plot of Fe(III) concentration vs. pH, for a titration solution exposed to the atmosphere, is given in figure 6.11. Reduction of Fe(III) to Fe(II) occurred below pH 3.0 with a gradual conversion back to Fe(III) at higher pHs.

6.5.4 Discussion

Pyrogallol, (E° = 0.713 V at 30 °C)[68], is immediately oxidised by ferric ion in solution at low pH. An orange brown product is formed with an absorption maximum in the visible spectrum at 372 nm. A reaction analogous to 6.12 for gallic acid, involving the formation of an o-quinone

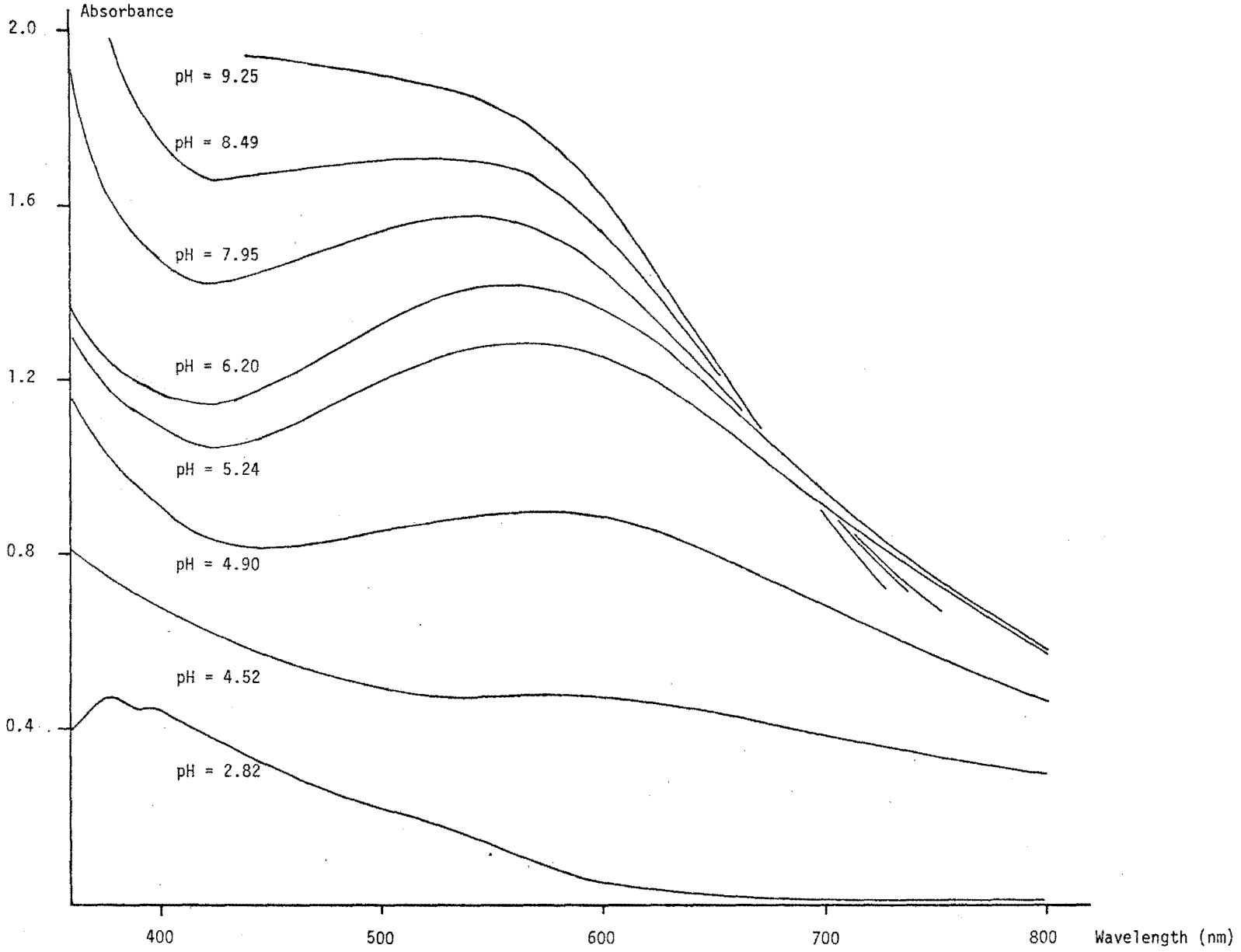

Figure 6.10 Spectrophotometric Data From Solutions of Pyrogallol (1×10^{-3} M) and Ferric Ion, L/M 3:1

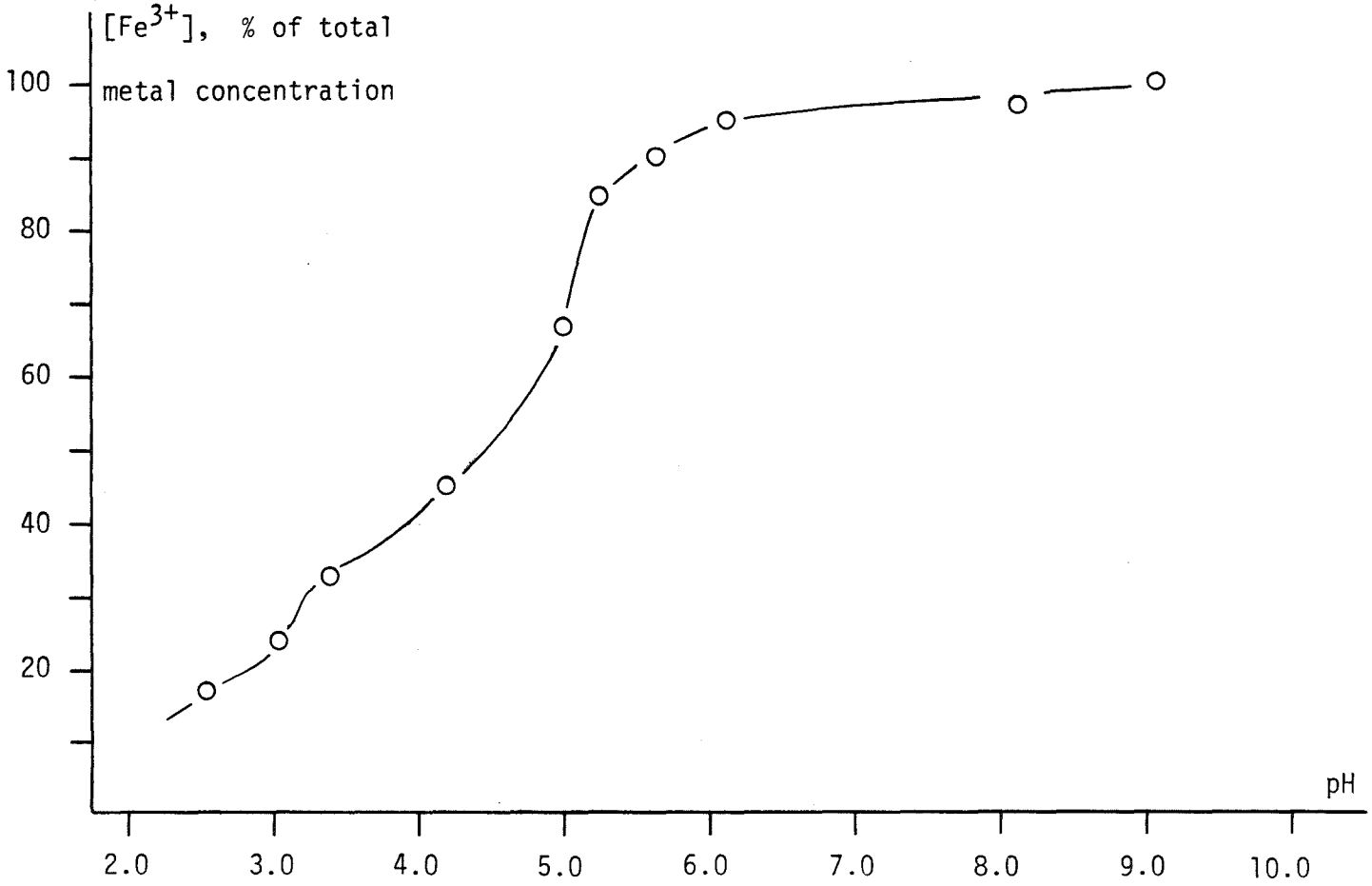

Figure 6.11 Ferric Ion Concentration in Solutions of Pyrogallol (1×10^{-3} M) Versus pH, L/M 3:1

is postulated:

$$Fe^{3+} + \tfrac{1}{2}LH_3 \rightleftharpoons Fe^{2+} + \tfrac{1}{2}Hqno + H^+ \qquad (6.15)$$

In the absence of oxygen, the proton released by reation 6.15 is titrated at pH 5.7. Above this pH, complexes of Fe^{2+} and the unoxidised ligand form. The pH range for Fe^{2+} complex formation is similar to that for gallic acid and catechol (see sections 6.1 and 6.2).

In the presence of oxygen, Fe^{2+} is oxidised to Fe^{3+}, the latter forming complex(es) with pyrogallol. The poorly defined endpoint at a = 1 in these titrations is consistent with the titration of the proton released from reaction 6.15 . The inflexion in the titration curve corresponding to 4 moles of alkali added per mole of metal ions suggests the following overall complexation reaction in the pH range 3.0 - 7.2:

$$Fe^{3+} + 2LH_3 \rightleftharpoons Fe(LH)_2 + 4H^+ \qquad (6.16)$$

This bis - (pyrogallate) - iron(III) complex would be responsible for the purple colour of the solution and the absorption maximum at 560 nm.

For pH $>$ 7.2, significant oxidation of the uncoordinated ligand by atmospheric oxygen is likely. This process may account for the drifting associated with pH measurements. However, a change in solution colour and an indication of an isosbestic point in the visible spectrum, in this pH region, may indicate the formation of a tris complex or an hydroxy species such as $Fe(LH)_2(OH)$.

6.6 Catechol

6.6.1 Potentiometric Data

Potentiometric data for the titration of Fe(III) - catechol solutions, with an initial ligand-metal ratio of 3:1, are shown in

figure 6.12, along with data from a ligand-only titration.

(a) Titrations in Air. The addition of ferric ion to solutions of catechol at low pH (<3.0) produced a blue-green colour in solution which faded slowly leaving a pale yellow colour. Titration of alkali against a solution of ferric ion and catechol (ligand:metal = 3:1) generated three separate buffer regions. In the first buffer region, pH < 4.8, a dark sea-green colour developed in solution. An inflexion in the titration curve was observed at a = ca. 1.5. Between pH 4.8 and 7.2 the colour of solution changed to a deep blue. At a = 4 a second more distinct endpoint was noted. At higher pH a third buffer region occurred with a shallow inflexion in the pH-titration curve at pH ca. 9.5, corresponding to a = 6. The colour of the solution in this region was red-purple.

(b) Titrations in Nitrogen. In the absence of dissolved oxygen, an inflexion was observed in the titration curve at a = 1, pH ca. 5.0 (initial ligand-metal ratio = 3:1). The solution was very pale grey-green at this pH. A second sharp endpoint occurred, close to the first inflexion, after the addition of a further ½ mole of alkali per mole of metal ions (see figure 6.12). The colour of the solution was pale purple-grey at the second inflexion. Above pH 7.7 a broad buffer region was observed and a distinct wine-red colour developed, intensifying at higher pH. This colour was similar to that observed in solutions of Fe(II) and catechol (see section 6.2).

Introduction of oxygen into the system caused a rapid lowering of the pH and the development of an intense green, blue or red-purple colour in solution depending on the amount of alkali previously added. Subsequent addition of alkali yielded a potentiometric curve identical to that of an initially aerated Fe(III)-catechol solution. The dissolved

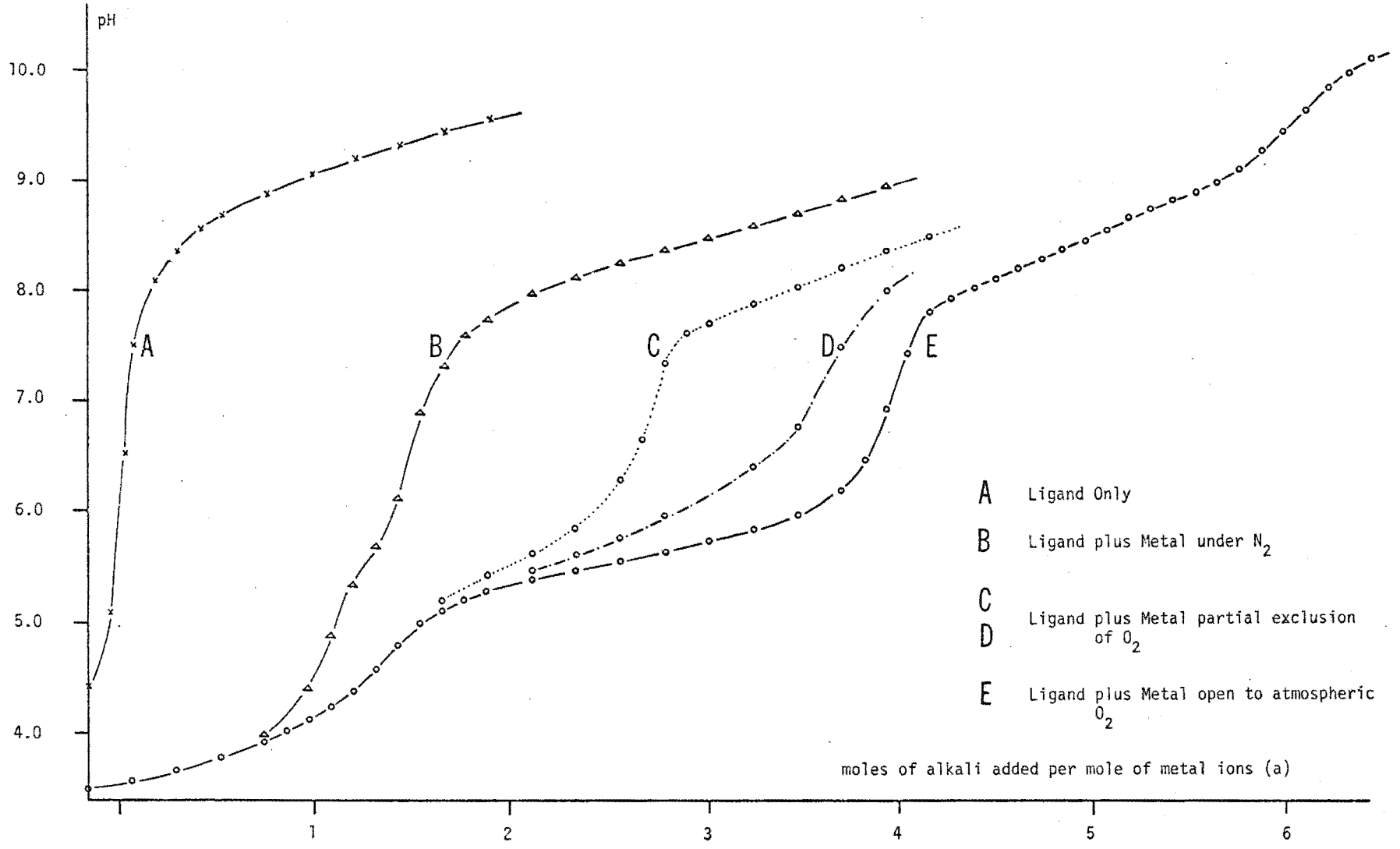

Figure 6.12 Potentiometric Data From Solutions of Catechol (1×10^{-3} M) and Ferric Ion at 25 °C, L/M 3:1

oxygen concentration was found to have a significant effect on the position of the titration curve. Titrations, for which only small concentrations of oxygen were allowed to remain in solution, gave results different from both the fully aerobic and anaerobic systems. The more oxygen present in solution the more complexing as evidenced by the suppression of the titration curve and position of the second endpoints in particular. Curves C and D in figure 6.12 illustrate results obtained when oxygen was partially excluded.

6.6.2 Spectrophotometric Data

Figure 6.13 gives spectrophotometric data (visible region) for solutions of catechol and ferric iron (L:M = 3:1) exposed to the air. Table 6.6 summarises these data.

Evidence of an initial redox process involving Fe^{3+} and catechol was found in the presence of an absorption in the visible spectrum at 388 nm in solutions of pH < 3.0. The absorptions in the visible region of the spectrum at 573 and 473 nm (giving rise to deep blue and red-purple colours respectively) reached maximum intensity at pHs consistent with the endpoints observed in the potentiometric titration curve (see section 6.6.1 *(a)*).

6.6.3 Analytical Data

Figure 6.14 shows a plot of Fe(III) concentration against pH for a ferric-catechol titration exposed to the atmosphere. A gradual increase in the concentration of Fe(III) with pH was observed up to a pH of ca. 7.0. At this pH close to 100 % of iron in solution was present as Fe(III). At pH ca. 4.8, the pH at which the first endpoint occurred, approximately 50 % of iron in solution was in the ferric state.

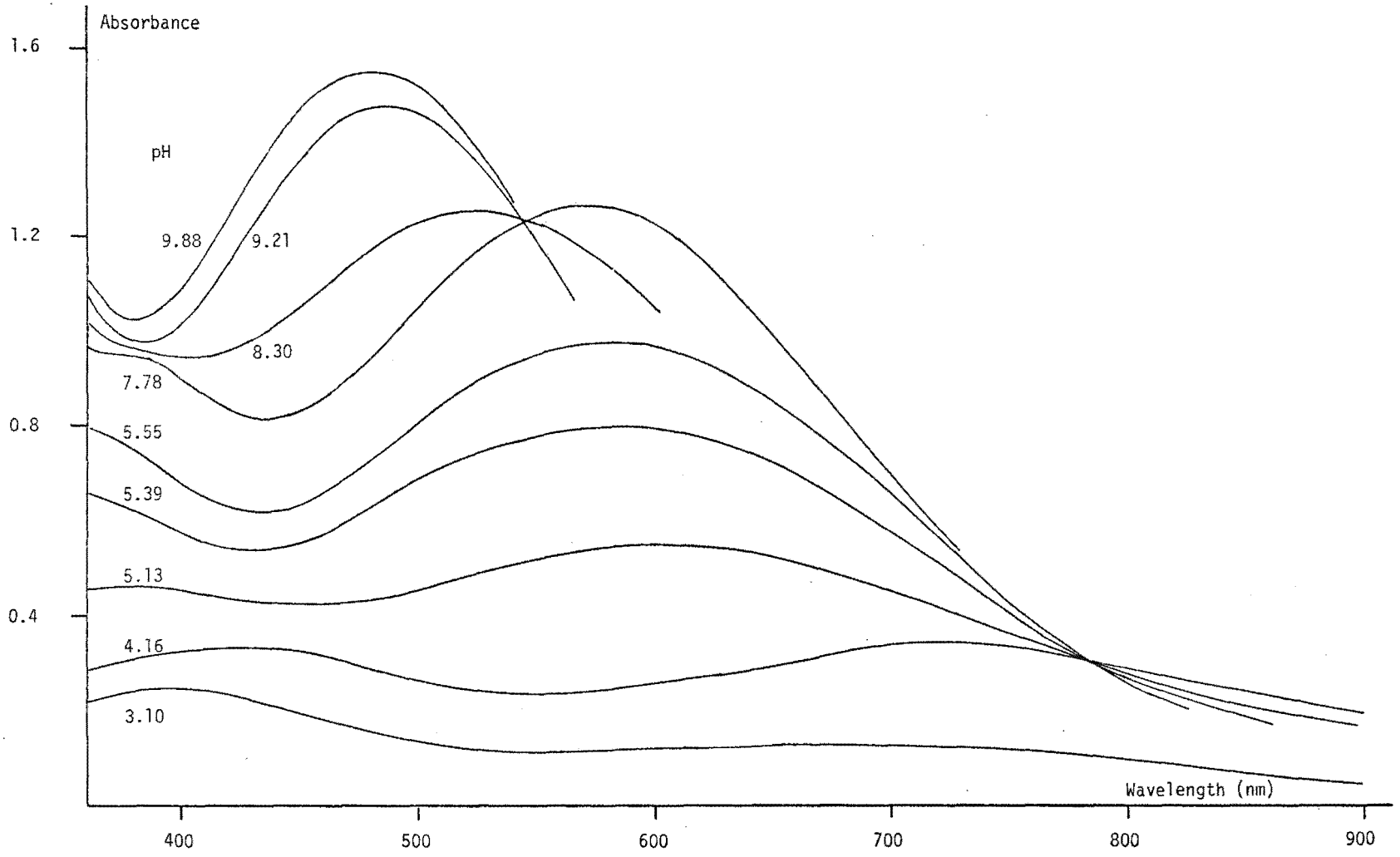

Figure 6.13 Spectrophotometric Data From Solutions of Catechol (1×10^{-3} M) and Ferric Ion, L/M 3:1

Table 6.6 Spectrophotometric Data For Solutions of Catechol and Ferric Iron (Ligand-Metal Ratio = 3:1)

pH	Description	Wavelength (nm)	ε (cm^{-1} l mol^{-1})	Species Involved
3.0	absorption maximum	388 ± 3	1340 ± 100	Q
4.5	absorption maximum	714 ± 5	2100 ± 100 *(a)*	FeL^+
4.8 - 6.2	isosbestic point	760 ± 5		FeL^+ / FeL_2^-
7.2	absorption maximum	573 ± 5	3530 ± 50	FeL_2^-
7.7 - 9.2	isosbestic point	540 ± 10		FeL_2^- / FeL_3^{3-}
9.8	absorption maximum	473 ± 7	4320 ± 100	FeL_3^{3-}

(a) This figure for ε assumes 50 % formation of FeL^+ at the first endpoint (refer to section 6.6.4).

6.6.4 Discussion

Catechol (E° 0.792 V) is slowly oxidised by ferric ion in acid solution (pH < 3.0). An absorption peak, characteristic of o-quinone, developed at 388 nm giving the solution a pale yellow colour. As was the case for gallic acid, the formation of a (complex) intermediate species

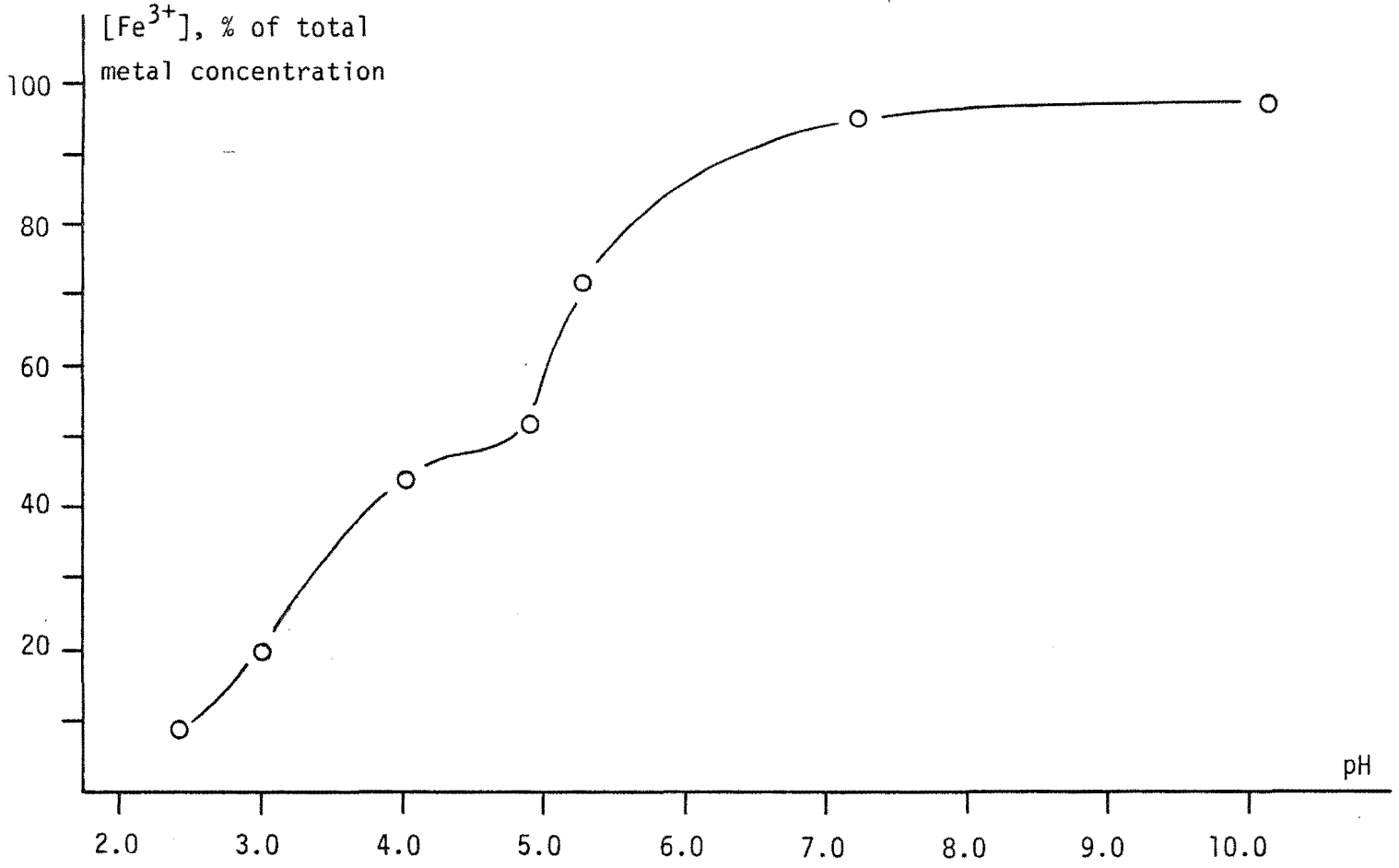

Figure 6.14 Ferric Ion Concentration in Solutions of Catechol (1×10^{-3} M) Versus pH, L/M 3:1

was observed in the redox process. This was evident as a transitory sea-green colour in solution. This same colour was observed in titrations of ferric ion and catechol in the pH range, 3.0 - 4.5. The visible spectrum in this pH region showed a maximum at 714 nm. These observations confirm earlier work done by Mentasti et al [58,66] who characterised the intermediate as FeL^+. Using a stopped-flow spectrophotometer they recorded the visible spectrum of this complex: λ_{max} = 700 nm, ϵ = 1250 cm^{-1} 1 mol^{-1}. The same workers also suggested that the redox process involving Fe^{3+} and catechol could be written as:

$$Fe^{3+} + \tfrac{1}{2}LH_2 \rightleftharpoons Fe^{2+} + \tfrac{1}{2}qno + H^+ \qquad (6.17)$$

where LH_2 denotes catechol and qno, the corresponding ortho-quinone. They found that the o-quinone product had a maximum absorbance in the visible spectrum at 390 nm, ϵ = 1460 cm^{-1} 1 mol^{-1}. Their proposed mechanism for this redox process has been discussed in section 6.4.6. Data presented here are consistent with the findings of Mentasti et al.

The titrations of solutions of catechol and ferric ion, in the absence of oxygen, showed that little or no complex formation occurs below pH 7.7. The inflexion in the titration curve at a = 1 was consistent with the titration of the proton released by the redox process 6.17. The appearance of pale green and purple colours in solution below pH 7.7, and the occurrence of a second endpoint within ½ mole of alkali of the first inflexion, suggests the presence of a trace of Fe^{3+} in solution.

Above pH 7.7 the development of a wine-red colour in solution suggested the formation of a ferrous-catechol complex (see section 6.2).

In titrations of catechol and Fe^{3+} at 3:1 stoichiometry where oxygen was present, three distinct buffer regions were observed. In the pH range, 3.0 - 7.2, dissolved oxygen oxidised Fe^{2+} (formed by reaction 6.17) to Fe^{3+}. This redox reaction was favoured by the formation of stable

Fe(III) - catechol complexes. The inflexion at the end of the first buffer region corresponded to the addition of approximately 1½ moles of alkali per mole of metal ions. The complete formation of the 1:1 complex, FeL^+, however required the titration of 2 moles of protons:

$$Fe^{3+} + H_2L \rightleftharpoons FeL^+ + 2H^+$$

Analytical data at the first endpoint showed that ca. 50 % of iron in solution was present as Fe^{2+}. Hence, assuming a = 1½, the overall reaction in this first buffer region could be represented as follows:

$$Fe^{3+} + 3H_2L + 1/8\ O_2 \longrightarrow \tfrac{1}{2}Fe^{2+} + \tfrac{1}{2}FeL^+ + \tfrac{1}{2}qno + 2H_2L + \tfrac{1}{4}H_2O + 1\tfrac{1}{2}H^+$$

Complex stoichiometry was also inferred from the position of endpoints (pH ca. 7.2) in partially de-oxygenated solutions. For two such solutions inflexions at ca. 2.5 and 3.5 moles of alkali per mole of metal ions were recorded for an equilibrium reaction expected to release 4 protons per metal ion, i.e.:

$$Fe^{3+} + 2H_2L \rightleftharpoons FeL_2^- + 4H^+$$

Introducing oxygen into these titration solutions lowered the pH to that observed in the aerobic systems for the same volume of added alkali. Explanation for these unexpected endpoints in titrations involving ferric iron and catechol appears to lie in the incomplete oxidation of Fe(II) to Fe(III) caused by insufficient concentrations of dissolved oxygen.

Spectrophotometric and potentiometric data are consistent with the formation of a tris complex at high pH. However, as was noted for gallic acid, ca. 1/6 of the ligand will be present in oxidised form for 3:1 metal-ligand stoichiometries.

Avdeef et al [54] have measured stability constants for Fe(III)-catechol complexes and have given spectrophotometric data for complexes of 2:1 and 3:1 stoichiometries (refer to table 1.1). They also noted the presence of a redox reaction between Fe^{3+} and catechol at low pH but indicated that this was reversible over short periods of time with the addition of base. No evidence was found in this work to support this latter observation of Avdeef et al. It is the opinion of this writer that atmospheric oxygen was responsible for any conversion of Fe^{2+} to Fe^{3+} observed by these workers. Hence their stability constant data must also be called into question since no account was taken of important redox processes.

6.7 Protocatechuic Acid

6.7.1 Potentiometric Data

Potentiometric data for the titration of solutions of protocatechuic acid and ferric iron (ligand:metal = 3:1) are given in figure 6.15. In the presence of oxygen a well-defined inflexion occurred around pH 7.3, corresponding to a = 7. At pH > 4.0 a blue-green colour was observed in solution which became dark blue by pH 7.3. At higher pHs a red-mauve colour developed.

In oxygen-free solutions, an endpoint in the titration curve was observed at pH ca. 7 corresponding to a = 6. The observed colour changes were similar to those for the aerated system.

6.7.2 Discussion

The complexing of Fe^{3+} with protocatechuic acid has been studied by Migal and Ivanov [63]. They reported evidence for three metal-ligand complexes, FeL, FeL_2^{3-}, FeL_3^{6-}, in the pH ranges, 3.0 - 4.5, 4.5 - 6.5, and

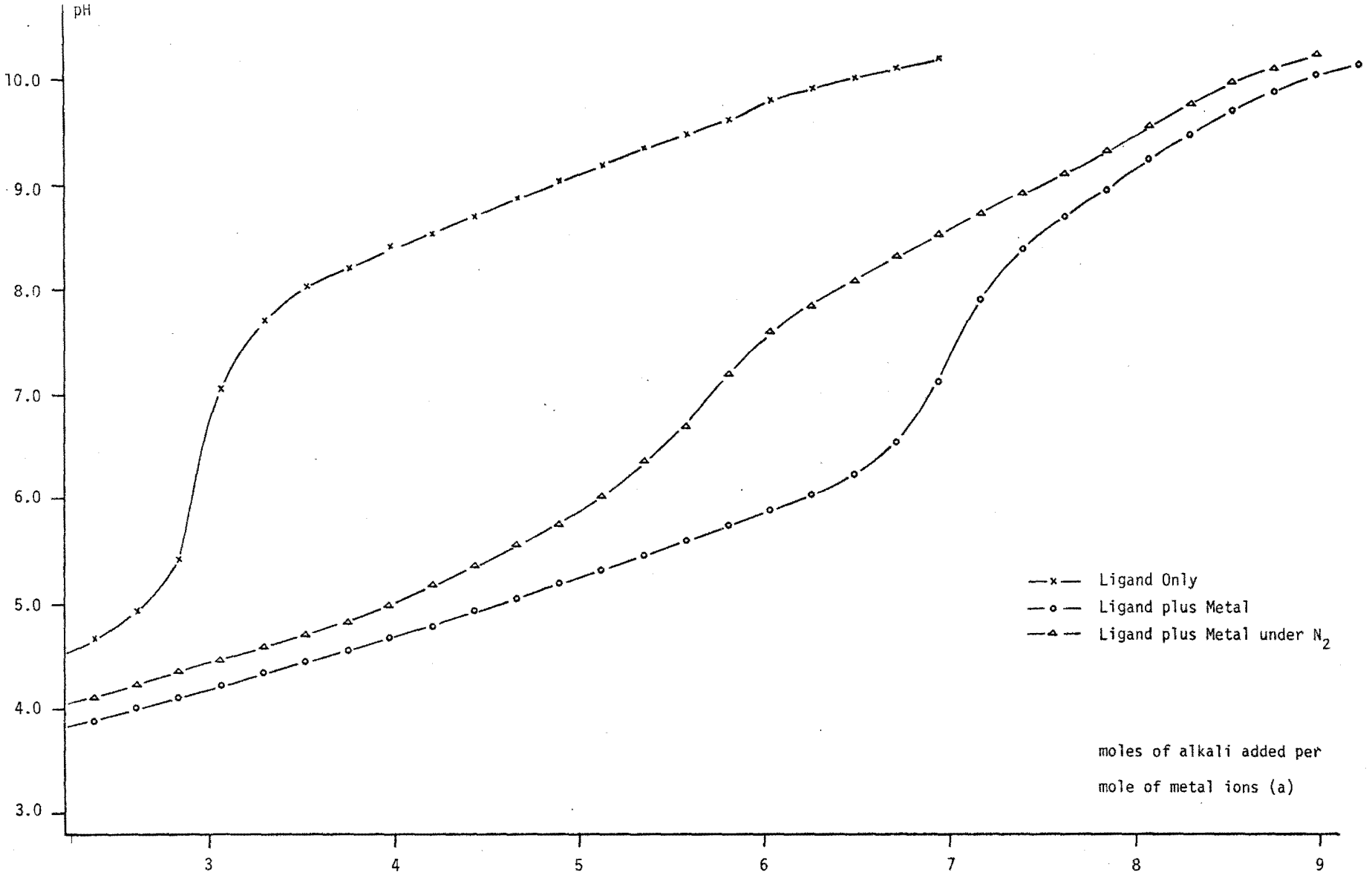

Figure 6.15 Potentiometric Data From Solutions of Protocatechuic Acid (1×10^{-3} M) and Ferric Ion at 25 °C, L/M 3:1

> 7.0 respectively. Spectrophotometric and stability constant data from their study appear in table 1.1.

Data presented here for aerobic systems is mostly consistent with this earlier work. The inflexion observed in the pH titration curve (pH 7.3) corresponds to the removal of a proton from the carboxylate function of the ligand plus the equivalent of 4 protons per metal ion, i.e.:

$$Fe^{3+} + 2LH_2^- \rightleftharpoons FeL_2^{3-} + 4H^+$$

Also, the observed colour changes match those reported earlier.

Previously it has been reported that protocatechuic acid is not oxidised by ferric ion in acid solutions [61]. This was ascribed to the larger reduction potential of the quinone/ligand couple ($E° = 0.885$ V) relative to those for other o-dihydroxy ligands investigated. Migal and Ivanov have also assumed that no complicating redox processes are present and took no account of them in their calculation of consecutive stability constants of the complexes. However, preliminary data presented here, for solutions of protocatechuic acid and ferric ion in the absence of oxygen, indicate that a redox equilibrium, such as reaction 6.18, may be important:

$$Fe^{3+} + \tfrac{1}{2}LH_3 \rightleftharpoons H_{qno} + Fe^{2+} + H^+ \qquad (6.18)$$

It is evident from the colours observed in the solution during an anaerobic titration that a significant proportion of the iron in solution is present as Fe(III); but from the position of the inflexion in the anaerobic titration (see figure 6.15) it is inferred that approximately 25 % of the iron is present as Fe^{2+} at pH < 7. In other words, reaction 6.18 is not reversed as the pH is increased.

6.8 Tiron

6.8.1 Potentiometric Data

Three separate buffer regions were observed in the titration of solutions of ferric iron and tiron exposed to the atmosphere (see figure 6.16). The formation of three distinct metal-ligand complexes was evident from the colour changes in these buffer regions. A blue-green colour developed in solution on mixing tiron with Fe^{3+} in the pH range < 4.0. At pH 4.0 an inflexion in the titration curve occurred, corresponding to a = 2. In the second buffer region a rich purple-blue colour developed. A sharp inflexion occurred at pH 6.3, corresponding to a = 4. Between pH 6.3 and 9.2 (the third buffer region) the solution became bright red in colour. A third inflexion, rather less well defined, was observed at a = 6. Titrations carried out in an atmosphere of nitrogen gave identical results to the aerobic system below pH 6.3 but at higher pHs a slight deviation was observed (see figure 6.16).

6.8.2 Discussion

The formation of ferric complexes with tiron has been studied in some detail [57, 60]. Potentiometric data, presented here are consistent with previous observations of the formation of three separate metal-ligand complexes; FeL^{+}, FeL_2^{-} and FeL_3^{3-} (see also table 1.1). The following equilibria can be ascribed to the three buffer regions observed (sulphonate groups have been ignored):

$$pH < 4.0 \qquad Fe^{3+} + LH_2 \rightleftharpoons FeL^{+} + 2H^{+}$$

$$4.0 < pH < 6.3 \qquad FeL^{+} + LH_2 \rightleftharpoons FeL_2^{-} + 2H^{+}$$

$$6.3 < pH < 9.2 \qquad FeL_2^{-} + LH_2 \rightleftharpoons FeL_3^{3-} + 2H^{+}$$

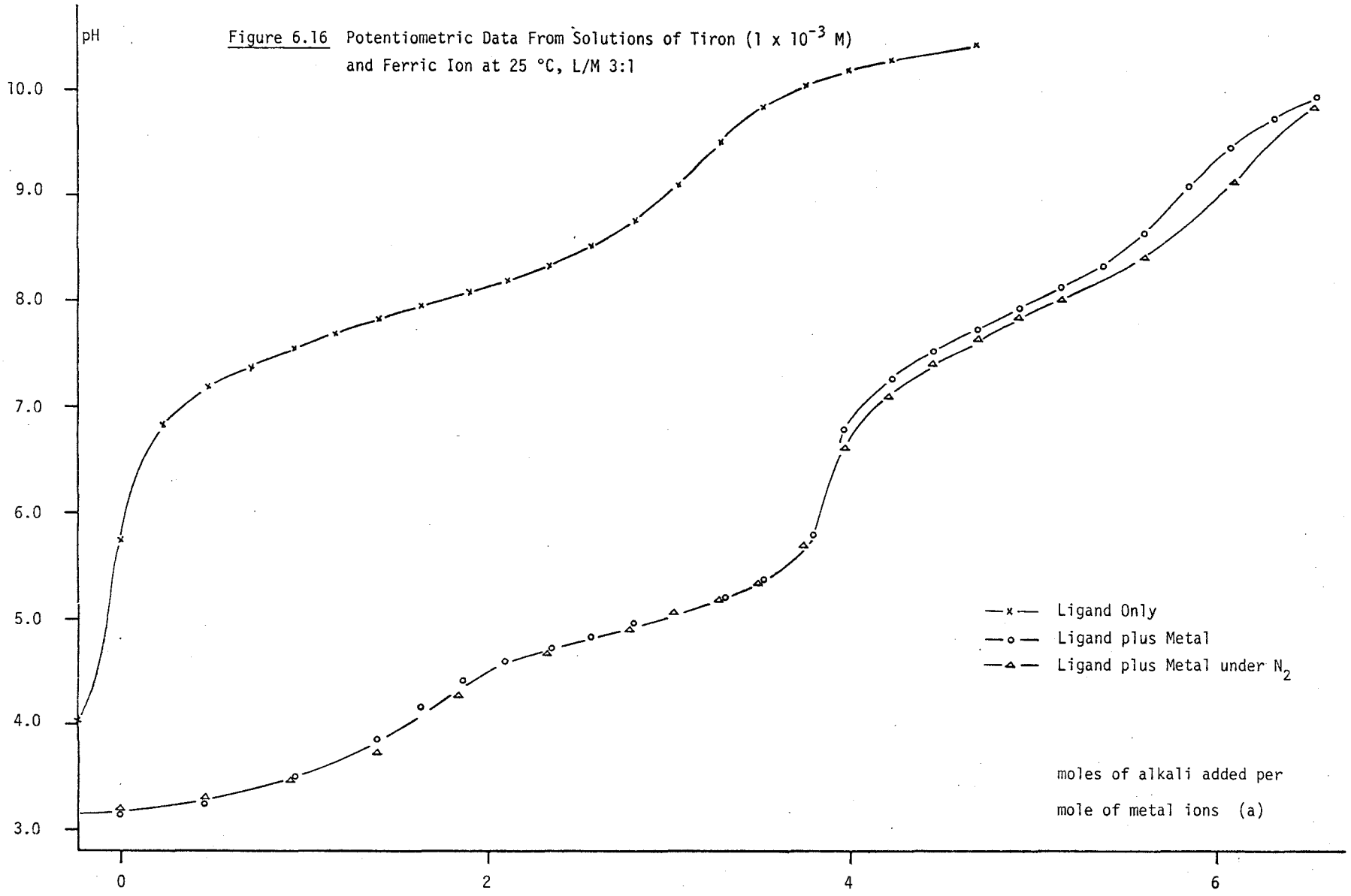

Figure 6.16 Potentiometric Data From Solutions of Tiron (1×10^{-3} M) and Ferric Ion at 25 °C, L/M 3:1

No evidence of a metal-ligand redox process was found. Presumably the rather larger reduction potential of tiron (E° = 0.955 V), and the formation of stable metal-ligand complexes at low pH excludes this possibility. At higher pHs (> 6.3), however, preliminary data indicate that metal-ligand complex formation may be affected by the presence of atmospheric oxygen. Oxidation of the ligand by oxygen in this pH region, may account for the observed deviation of the titration curves. Further work is required to substantiate this observation.

6.9 Summary

Of the ligands studied, only tiron (E° = 0.955 V) was found to be stable against oxidation by ferric ions in acidic solution. For the other ligands (E° = < 0.9 V), there was evidence for the following redox equilibrium below pH ca. 3.0:

$$Fe^{3+} + \tfrac{1}{2}LH_n \rightleftharpoons Fe^{2+} + \tfrac{1}{2}H_{n-2}\ \text{qno} \qquad (6.19)$$

where LH_n represents the ligand and H_{n-2} qno represents the corresponding o-quinone. Spectrophotometric absorptions due to o-quinones were found at 370 - 390 nm. For gallic acid and catechol (E° ca. 0.8 V), a metal-ligand complex intermediate was observed in the redox process. Pyrogallol, which has a relatively lower reduction potential (E° = 0.713 V at 30 °C), rapidly reduced ferric ion in solution, while protocatechuic acid (E° = 0.885 V) effected only a partial conversion of Fe^{3+} to Fe^{2+}.

Buffle and Martell [71], in their study of complexes of Fe(III) and the o-dihydroxy compound, 1,2-dihydroxynapthalene-4-sulphonate, suggested that an initial redox reaction (analogous to 6.19) was reversed as the pH was raised from 3 to 4. Metal-ligand complexes of stoichiometry 1:1 (green) and 2:1 (blue) were observed at higher pH. Their reaction conditions were reported to be oxygen-free. In this work, however, no

complex formation was observed below pH 7 for pyrogallol, catechol and gallic acid when titrations were carried out in an oxygen-free environment. The inflexion that occurred in the titration curves near this pH corresponded to the titration of protons released by reaction 6.19. At higher pHs excess ligand formed pale-coloured ferrous complexes. Hence, for the ligands studied in this work no reversal of reaction 6.19 was observed. An explanation for the difference between this result and that of Buffle and Martell (assuming their reaction conditions precluded the possibility of oxidation of Fe^{3+} by dissolved oxygen), may lie in the respective ligand structures. The "simple" o-dihydroxybenzenes may be involved in secondary coupling reactions upon oxidation, (see section 5.6), that don't occur for the fused ring compound studied by Buffle and Martell.

In the presence of oxygen, all ligands studied formed intense blue-coloured complexes. Their formation was accompanied by an inflexion in the titration curve at pHs between 6.3 and 7.4 after the addition of 4 moles of alkali per mole of metal ion (L:M > 2:1). These observations were attributed to the formation of a 2:1 complex between the unoxidised ligand and ferric ion (after oxidation of Fe^{2+} by oxygen). Co-ordination of the iron is thought to take place via two ortho-O^- groups on the ligand thus forming a five-membered chelate ring.

$$2LH_n + Fe^{3+} \rightleftharpoons Fe(LH_{n-2})_2^- + 4H^+$$

In addition to the 2:1 complex, 1:1 ferric-ligand complexes (green in colour) were formed for tiron, catechol and protocatechuic acid below pH 4.5. Some evidence for the formation of tris complexes at high pH was also found for each ligand studied. Endpoints at non-integral values of "a" were observed in the titration of Fe^{3+}/catechol solutions in air (pH 4.8) and protocatechuic acid with Fe^{3+} under

nitrogen (pH 7.3). These were attributed to mixed Fe^{3+}/Fe^{2+} systems. The proposed scheme of reactions is illustrated in figure 6.17.

No evidence was found for Fe^{3+}-catalysed oxidation of the ligands by dissolved oxygen below pH 7.0. It would appear that the formation of very stable Fe(III)-ligand complexes, plus the relatively high reduction potentials of the ligands compared with say ascorbic acid (E° = 0.412 V), for which such oxidation has been observed, eliminates this possibility.

Data presented here, along with information already known about the interaction of Fe^{3+} with o-dihydroxy substituted benzene ligands, (see section 1.2), form a basis from which predictions can be made about the behaviour of certain Fe(III) complexes in the soil system (see section C following).

C. CONCLUSIONS

As indicated in the introduction to this thesis, the mechanism for the podzolization process in soil has been variously explained. Attention has been mainly focussed on the interaction between iron, aluminium and organic matter, and many workers would concur with Peterson who, in a comprehensive treatise on podzolization [141], stated: "Without at this stage attempting to rule out any of the possible podzolization mechanisms ... , it seems that the one involving dissolution of iron and aluminium by organic complexing molecules and their subsequent precipitation due to overloading of the complexes with the metals, especially aluminium, would be in accordance with many of the known properties of podzols and give the most satisfactory answers to the questions asked (concerning the translocation of iron, aluminium and organic matter within the soil profile) ... "

Work for this thesis has concentrated on characterizing water-soluble iron-phenolic complexes formed in the pH range 2 - 11 under aerobic and anaerobic conditions. The following observations were made along with possible conclusions:

(1) Complex formation between ferrous ion and four of the model phenolic ligands studied did not occur below pH 7.

Some workers have suggested mobilization of iron in podzolization involves reduction of Fe(III) to Fe(II) by polyphenols, followed by complexing of Fe(II) (see Introduction). From the results presented here, and known formation constants for ferrous complexes with organic acids (e.g. citric and oxalic) [57], it is inferred that complexing of Fe(II), with organic compounds affording OH and/or COOH functional groups, does not occur at pHs typical of podzols.

(2) The formation of stable complexes between ferric iron and polyphenols is dependent on pH. Iron(III) was observed to form 2:1 ligand-metal complexes (total ligand concentration ca. 10^{-3} M) with the model ligands used in this work in the pH range 4.5 - 7.2 (4.0 - 6.0 tiron). 1:1 complexes formed in a distinguishable step below pH 4.5 for catechol and protocatechuic acids (< 4.0 for tiron). Fe^{3+} forms a very stable chelate bond with the ortho-dihydroxy function of the phenolic ligand. The logarithm of the stability constant for 1:1 Fe(III)-phenolate complexes is approximately 18 (e.g. tiron 17.6, protocatechuic acid 19.0; refer also to table 1.1) and that for a 2:1 complex is approximately 15 (e.g. tiron 14.9, protocatechuic acid 14.3). Stability constants for other o-dihydroxy chelates are likely to be similar. The pH range in which complex formation will occur depends, however, on the acidity of the co-ordinating ligand hydroxyl groups. Those ligands with strongly electron withdrawing constituents impinging on the o-dihydroxy function (e.g. tiron) will form complexes with Fe^{3+} at a lower pH than those without (e.g. catechol, pyrogallol).

(3) Model ligands used in this study for which E° was less than ca. 0.9 V, were oxidised by ferric ion in acid solution (pH < 3). For these ligands, complex formation was critically dependant on oxygen concentration as well as pH. With increasing pH, Fe(III)-ligand complexes were formed as ferrous ion, a product of the initial ligand-metal redox reaction, was oxidised by dissolved oxygen (equation 6.20)

$$Fe^{2+} + \tfrac{1}{4}O_2 + H^+ \rightleftharpoons Fe^{3+} + \tfrac{1}{2}H_2O \qquad (6.20)$$

$$E^\circ = 0.48 \text{ V}$$

Titration solutions exposed to oxygen behaved as a mixed Fe^{3+} / Fe^{2+} system and for solutions purged of oxygen, iron remained in the +2 state.

In the presence of a continuing supply of readily oxidisable organic matter ($E° < 0.9$ V), strong reducing conditions may conceivably prevail in the soil, especially if the latter remains waterlogged. In this environment any oxygen present would be rapidly consumed by the organic matter and the oxidation of ferrous ion may be limited. This would therefore represent a non equilibrium situation. Even under these conditions, as noted before, iron(II), if mobilized, is not likely to be in complex form, if organic acids and polyphenols are the complexing agents.

The e.m.f. of reaction 6.20 indicates that at equilibrium the +3 state for iron is favoured at low pH. The formation of stable hydroxy and/or ligand compounds with Fe^{3+} favours the +3 state in the weakly acidic - alkaline pH range. The fact that Fe^{2+} is stable in solutions of low pH is attributed to a low rate of oxidation. In the weakly acidic to neutral pH range the rate of oxidation of Fe^{2+} is considerably higher. The rate law expression in this pH region is a function of pH [142]:

$$\frac{d}{dt}[Fe^{3+}] = k\,[Fe^{2+}][O_2][OH]^2$$

Hence in the soil environment, if thermodynamic equilibrium is reached in which oxygen is present, it can be expected that iron will be present in the ferric oxidation state. (It should be noted that very little oxygen is required to maintain iron in the +3 state. Qualitative results from this work showed that minute traces of oxygen were sufficient to oxidise ferrous to ferric ion at pH > 4. Peterson has shown [141] that at equilibrium, at pH 4.7, an oxygen partial pressure as low as 10^{-14} atmospheres is sufficient to maintain the ratio of $[Fe(OH)_2^+] + [Fe(OH)^{++}]$ (the major iron(III) hydroxy species at this pH) to $[Fe^{++}]$ at greater than 100. In the presence of organic ligands capable of forming a stable Fe(III)-complex even less oxygen would be required. For example, consider

a catechol-type ligand (LH_2):

$$LH_2 + Fe^{2+} + \tfrac{1}{4}O_2 \rightleftharpoons FeL^+ + \tfrac{1}{2}H_2O + H^+$$

$$K = [FeL^+][H^+] / [Fe^{2+}][O_2]^{\frac{1}{4}}[LH_2]$$

$$= K_R K_{f1} = 8.7 \times 10^5$$

where $\log K_R = (E^\circ_{O_2/H_2O} - E^\circ_{Fe^{3+}/Fe^{2+}}) / 0.059 = 7.3$

and K_{f1} = formation constant for FeL^+ = 4.35×10^{-2} [66]

Hence, for pH = 4.7, total ligand concentration ca. 5×10^{-4} M,

$$\frac{[FeL^+]}{[Fe^{2+}]} = 100 \text{ when } [O_2] = 5 \times 10^{-22} \text{ atm}).$$

(4) Ferric hydroxide was not precipitated from metal-ligand solutions prepared in the course of this work. This shows that the metal-ligand complexes formed are of sufficient stability to keep the free metal concentration below $K_{sp}/[OH]^3$ (total metal concentration typically 5×10^{-4} M, total ligand 5×10^{-4} - 5×10^{-3} M). In other words, phenolic-ligand complexing stabilizes the ferric state to a greater extent than does the formation of ferric hydroxy species. This suggests that certain phenolics, if present in the soil, are capable of dissolving $Fe(OH)_3$, a reaction observed by workers using bark and leaf extracts (see Introduction).

(5) Ferric ion catalysed auto-oxidation of the ligands studied was not observed within the time-scale of the titrations carried out (i.e. hours). However, results from solutions of gallic acid and ferric ion (L/M > 3:1) indicated that if the pH was alternatively raised and lowered, in the region 3 - 10, eventually the blue and red colours characteristic of complex formation (see section 6.4) were no longer

apparent and red-grey colours predominated. A similar effect was noted from solutions of gallic acid and ferric ion (pH ca. 5) allowed to stand for several days, suggesting that the ligand had been completely oxidised. Whereas other workers have postulated oxidation of the metal to explain deposition of iron in the B horizon, perhaps slow Fe^{3+}-catalysed oxidation of the ligand may contribute to the deposition mechanism?

In summary, results presented here are consistent with a podzolization mechanism involving the translocation of iron in the +3 state, co-ordinated in chelate form with polyphenols. Other ligand types will be important complexing agents for Fe^{3+}. A computer simulation of the competitive formation of complexes between Fe^{3+} and several organic acids, such as citric and oxalic, and the polyphenol, tiron, has been described by Powell and Taylor [143]. This indicated that from a selection of simple model compounds, the most effective in dissolving $Fe(OH)_3$ at pH 4.0 are citric acid > pyrophosphate > tiron > oxalic acid.

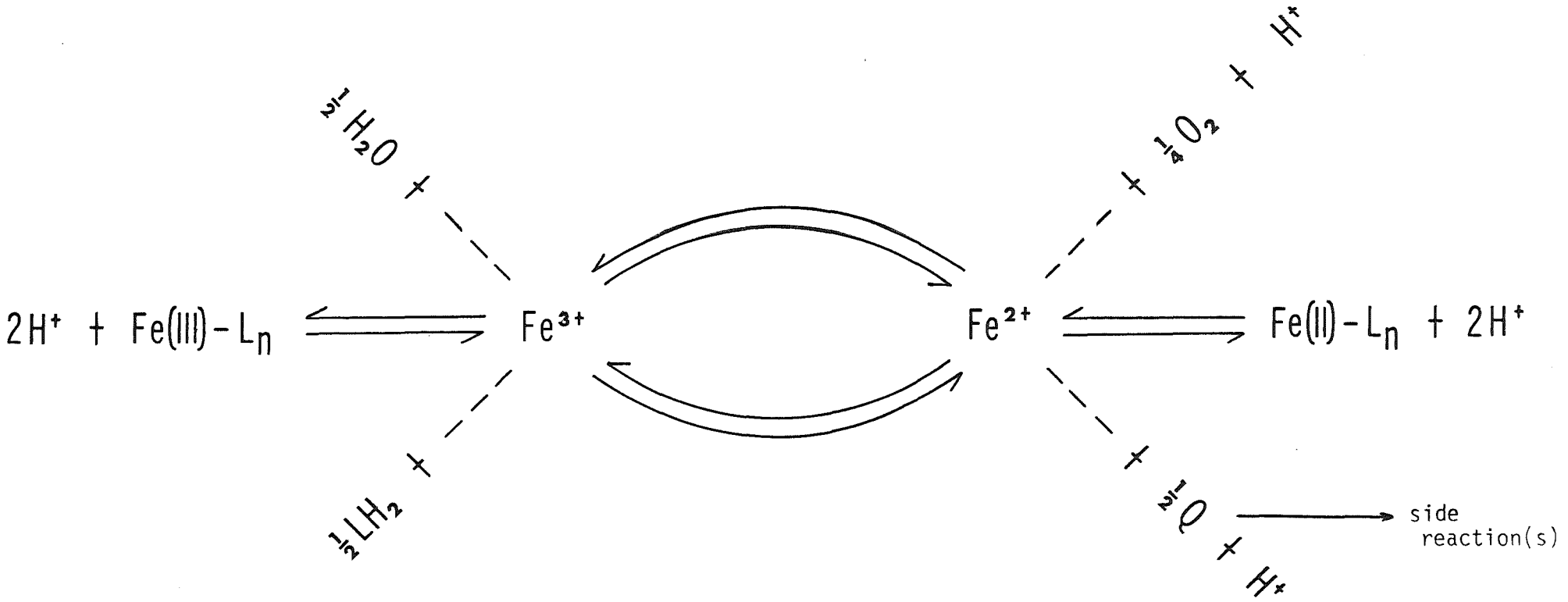

Figure 6.17 Schematic Representation of Reactions of Iron and Polyphenols in Aqueous Solution

PART B

THE STUDY OF A MAIMAI SOIL IN THE PAKIHI LANDS OF THE WEST COAST, SOUTH ISLAND, N.Z.

CHAPTER 7

PREFACE TO PART B

7.1 Pakihi Soils of the West Coast

7.1.1 Geomorphology and Soil Parent Materials

The wet podzolized soils of the West Coast of the South Island, New Zealand extend across the Buller, Inangahua, Grey and Westland counties. The term *pakihi* , a Maori word meaning "clearing in the forest or bush", has been used to describe the extensive area of swampy, unused land that is underlain by many of these podzolized soils.

The West Coast is a mountainous region with a narrow strip of lowland between the Tasman Sea and the Southern Alps. A major crustal fracture called the Alpine Fault [144], marked by a line of steep bluffs, stretches from the coast of Milford Sound in the south, north east to the northern extremity of the South Island. The mountains consist mainly of schist, greywacke and argillite, with outlines of granite. The lowlands west of the Fault, where extensive areas are under pakihi soils, form river flats, terraces, basins and hills. Phases of glaciation which occurred about 14 000 to 22 300 years ago (Otira,Kumara - 2 and Kumara - 3) led to huge morainic depositions [145]. The parent material of the podzolized soils are in many instances derived from the resultant morainic outwash gravels, sands and silts of greywacke, granite, sandstone, mudstone and some schist composition. On some of these outwash materials there is a covering of silt or fine sandy material, thought to be a loessial deposit [146].

7.1.2 Climate and Vegetation

The climate in this region is mild and humid with an annual

rainfall in excess of 2500 mm. Precipitation is greatest in areas close to the mountain ranges. Below 1000 m, the natural vegetation is forest with fairly thick undergrowth. In the central Westland and southern Nelson area forests are mixed podocarp-beech below ca. 915 m; elsewhere they are mostly mixed beech and podocarp-hardwood. Swampy soils of the low terraces supported species such as kahikatea, silver pine, rimu and kamahi. In many places there is evidence of early felling and milling of this timber while some areas of forest have been extensively burnt off. The present pakihi vegetation consists of typical swamp species such as sphagnum moss, wiwi rush, sedges and coarse ferns.

7.1.3 Classification and Description of the Wet Land Soils

The country with pakihi vegetation falls into two broad categories [147]. The first of these categories includes parts of the low glacial outwash terraces and moraine, with annual precipitation usually in excess of 3810 mm. The second group comprises intermediate and high glacial outwash terraces as well as some alluvial terraces and old dunes, often covered with fine-textured silty or fine sandy material thought to be loess. Within these categories a number of newly recognised soil series have recently been defined [148]. Collectively they have become known as "wet land soils".

In the Grey and Buller counties (the area relevant to this work) some of the soil series characterized have been: *Okarito*, a gley podzol, which is found on the highest glacial outwash terraces under pakihi vegetation; *Mawhera*, a gleyed soil related to Okarito, still found mainly under forests; *Hukarere*, a predominantly gleyed soil similar to Okarito and Mawhera but with iron or humus pans in the upper parts of the solum; *Kumara*, a shallow gley podzol, developed originally under podocarp forests; *Flagstaff*, a shallow gleyed soil formed on rolling moraine with iron pans common at the moraine interface; *Maimai*, a gley,

shallow, humic and extremely wet soil, formed on low glacial outwash terraces; *Addison,* a gley podzol, similar to Maimai in appearance but much thicker and more bouldery with massive iron pans under wet humic horizons; *Charleston,* a shallow gley podzol developed from cemented sand on old dunes and *Waiuta*, described as a true podzol. Soil "type sites" have been established for each soil series. These afford representative profiles from which chemical and physical data have been collected [149] and provide "in-field" demonstrations of typical series characteristics [150].

Although these soils vary in parent material, age, relief, texture, degree of podzolization and chemical and physical properties, two important features are common to them. Firstly, many of the soils are waterlogged for substantial portions of the year. In several soils this is due to the presence of compacted, structureless, silty horizons, impeding vertical water movement. This is often aggravated by impervious iron or humus iron pans lower in the profile, overlaying compact C - horizons. Secondly, under high annual rainfall, substantial leaching of the topsoil has left major deficiencies of many plant nutrients. Acidic conditions prevail in the upper horizons and extensive accumulation of undecomposed organic matter at the surface is common.

7.1.4 Utilization of Pakihi Soils

Approximately half of the total land area potentially suitable for farming on the West Coast is represented by pakihi soils, an estimated area of 200 000 ha. No more than 3 % of this large area is being farmed at present [151]. The fact that development of these lands could double the area of West Coast farmlands establishes their important economic potential. In recent years both forestry and agricultural interests have been represented in research and development programmes. Many such programmes have been expensive and time-consuming as the soils in question are waterlogged and impoverished. Considerable investment in

drainage and fertilizer has been required and the long term economic viability of such development is yet to be firmly established.

7.2 The Main Study Region

7.2.1 General Description

The region chosen for study was a Department of Lands and Survey agricultural development farm at Ruru, about 10 km north-east of Lake Brunner, 150 m above sea level. This was known as the "Bell Hill Land Development Block". This and other Lands and Survey development blocks are depicted in figure 7.1. The total area under development covers 5700 ha of which ca. 2400 ha have been developed to date. The elevated northern, western and southern parts of this block had been previously developed for sheep and cattle farming but a poorly-drained flat central basin (ca. 1000 ha) adjacent to the small township of Ruru had remained largely untouched before commencement of this work. Several experimental farm units have now been established on this swampy basin and more are planned for the future.

The parent material is mostly greywacke, sandstone, granite, gravels and sands, part of glacial moraine or outwash gravels resulting from the Kumara - 2 phase of the Otira glaciation [145]. The high annual rainfall, ca. 2700 mm, once supported a forest of white, silver and red pines, but these were cut over and burnt some 50 - 60 years ago. Since then regrowth has resulted in a vegetative cover of sphagnum moss, tangle ferns, and wiwi rush amidst fallen logs. Early soil mapping showed the area as a complex of Okarito fine sandy loam and Waiuta loam [152], but now it has been re-mapped as Maimai soils. It is characterised by sandy texture, iron-pan formation, poor drainage and high organic matter in the topsoil in a flat outwash terrace situation.

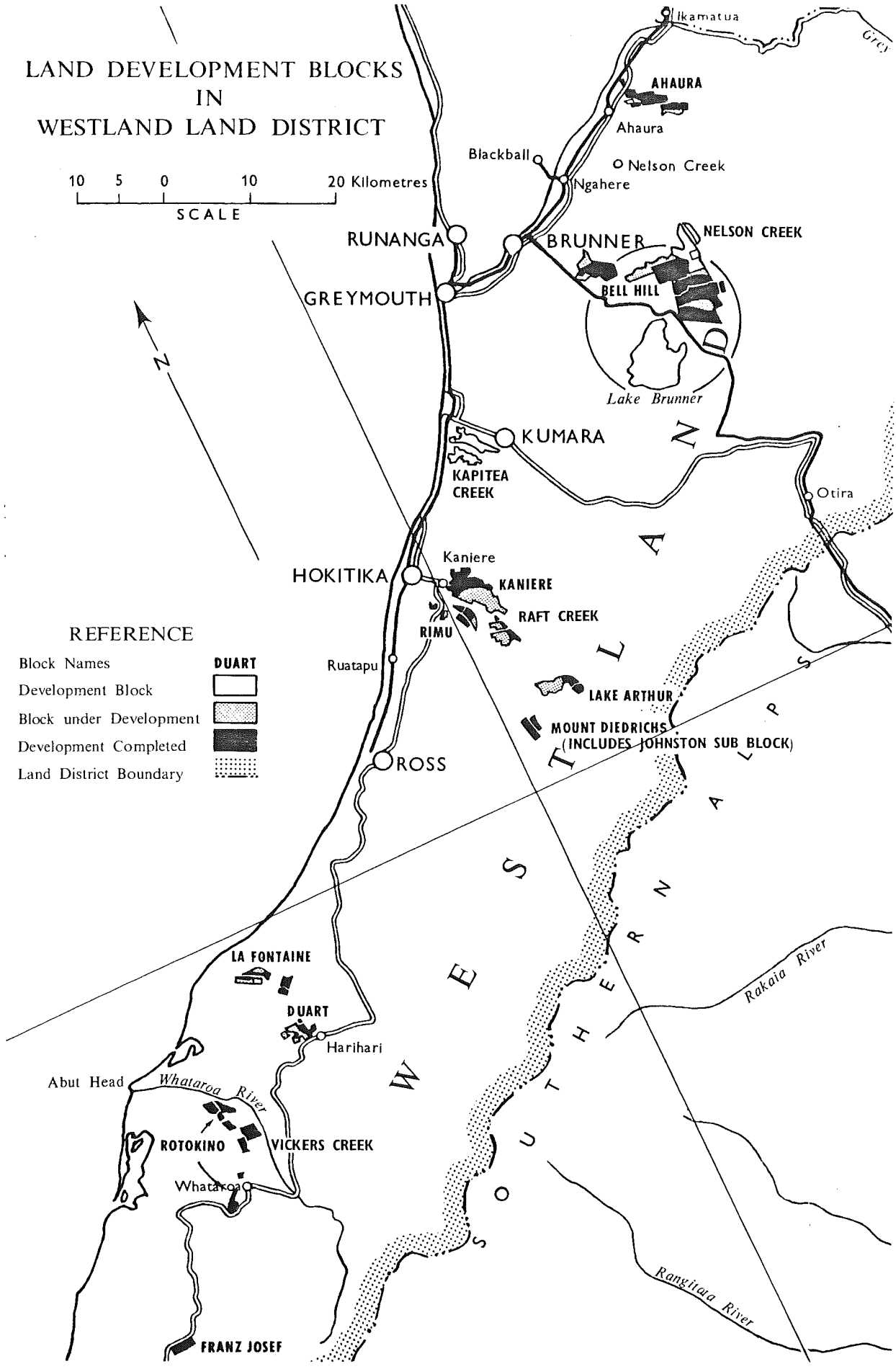
LAND DEVELOPMENT BLOCKS
IN
WESTLAND LAND DISTRICT
10 5 0 10 20 Kilometres
SCALE
N
REFERENCE
Block Names
Development Block
Block under Development
Development Completed
Land District Boundary
DUART
Ikamatua
Grey
AHAURA
Ahaura
Blackball
Nelson Creek
Ngahere
RUNANGA
BRUNNER
NELSON CREEK
GREYMOUTH
BELL HILL
Lake Brunner
KUMARA
KAPITEA CREEK
Otira
Kaniere
HOKITIKA
KANIERE
RAFT CREEK
RIMU
Ruatapu
LAKE ARTHUR
MOUNT DIEDRICHS
(INCLUDES JOHNSTON SUB BLOCK)
ROSS
WESTERN SOUTHERN ALPS
LA FONTAINE
DUART
Harihari
Rakaia River
Abut Head
Whataroa River
ROTOKINO
VICKERS CREEK
Whataroa
Rangitata River
FRANZ JOSEF

Figure 7.1

7.2.2 Soil Profiles

A typical soil profile from the study region is illustrated in figure 7.3. At the surface a dark moist humic horizon (A_{1g}), containing many fine roots and semi-decomposed organic matter, is evident. Beneath this is an horizon of eluviation (relative loss) marked by a characteristic pale grey colour due to podzolization and gleying processes (G). At a depth of ca. 25 cm traces of an "iron-stone" pan overlie an horizon of illuviation (relative accumulation) marked by a distinct orange - brown colour characteristic of iron oxides and humus (B_3). This horizon was frequently immediately above an additional iron-pan which had formed in or on well-aerated underlying gravels and sands (C - horizon). The presence of these pans was considered to be partly responsible for poor vertical drainage of water. The extents of podzolization and gleying in the sampled areas were quite variable and markedly affected profiles over short distances, as observed along drain sections for example.

Detailed profile descriptions of two sites within the study area are given in section 9.1.

7.2.3 The Sampling Areas

Three main areas were sampled within the central swampy basin of the Bell Hill block. These were as follows (refer to figure 7.2):

(1) An 82 hectare farm unit on the eastern side of the Lands and Survey development block. The majority of this unit was oversown in 1968 and the remainder in February, 1974. It supported beef cattle during 1974-5 and was later converted to a dairy farm. This will be referred to as the "Dairy Unit".

(2) Two smaller areas ca. 100 m from the perimeter fence lines of the Dairy Unit on undeveloped pakihi land. These will be referred to as the "Bell Hill Undeveloped" area. Samples were collected from these areas

Figure 7.2 Sampling Areas: Ruru (RR), Dairy Unit (DU) and Bell Hill Undeveloped (BU) Within the Bell Hill Land Development Block

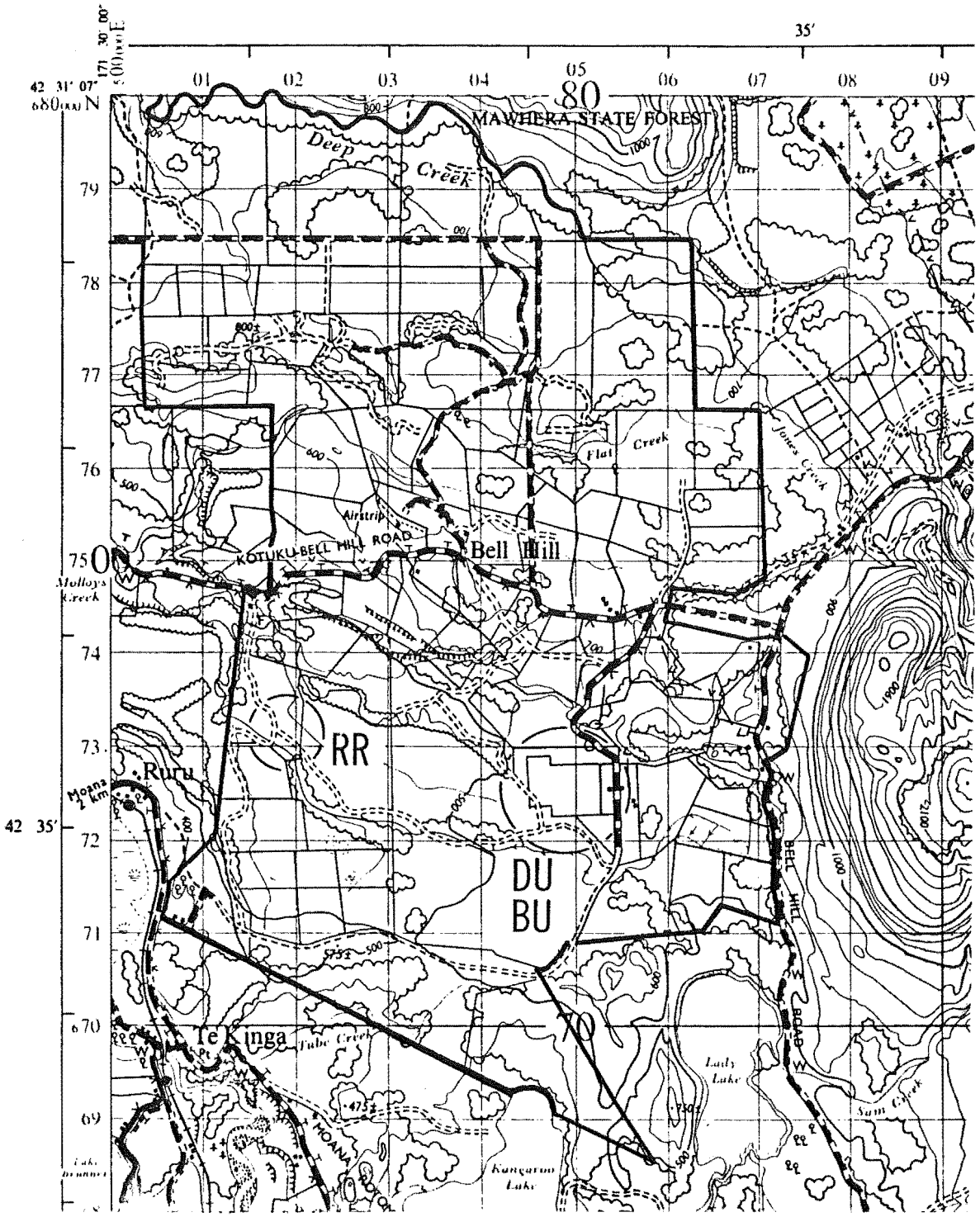

Bell Hill Block : ☐ Scale : 1:63 360

to provide estimated baseline data for the development of the adjacent Dairy Unit.

(3) A one hectare area in the southwest corner of a 50 ha block approximately 2.5 km west of the Dairy Unit. This area was sampled before development began in 1976 and thereafter samples were collected regularly during the initial stages of pasture development. This will be referred to as the "Ruru" area.

In addition to the Bell Hill area, samples from eight soil series were analysed for cobalt. These series were: Maimai, Addison, Charleston, Flagstaff, Hukarere, Okarito, Kumara and Mawhera.

More detailed information about sample collections is given in chapter 8.

7.2.4 The Programme for Agricultural Development

The pasture development programme has followed an established pattern for pakihi soils, viz liming followed by special mix fertilizer, oversowing with mixed clover and grass seeds, fencing and stocking. Figure 7.4 shows a typical view across the study region. This photograph was taken in the Ruru area and shows the contrast between pakihi land in its natural state and that under agricultural development. Tables 7.1 and 7.2 summarize the development stages of the Bell Hill and Ruru units including the timing of sample collections.

7.3 Objectives

The major objectives of the overall study within the Bell Hill block were:

(1) To measure physical and chemical properties of the soil in the study region (including two main soil profile studies) and to describe both the soil and the pedological changes that have occurred since its

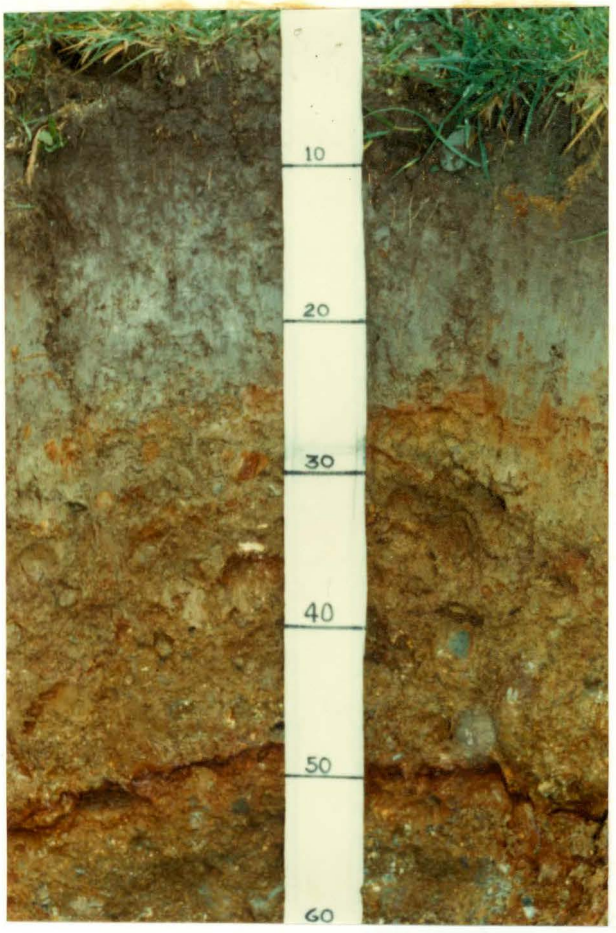

Figure 7.3 Soil Profile from the Study Region

Figure 7.4 View Across Part of the Ruru Study Area

formation.

(2) To compare the nutrient levels and other properties of the developed land with those of the undeveloped soils in the Bell Hill area to determine (a) the fertilizer requirements of the undeveloped Ruru area, (b) the effect of the development programmes in the Ruru and Dairy Unit areas.

(3) To estimate net soil nutrient losses (K, Ca, P, S) by study of the nutrient balance (leaching, fertilizer application, precipitation etc) in the developed Dairy Unit.

(4) To analyse pasture herbage from the developed land for plant nutrients (P, S, Ca, K, Mg, B, Cu, Co) and dry matter yield, to monitor seasonal variations, and to provide data for correlation with measured availability of these nutrients in the soil.

The work presented in part B of this thesis relates in part to each of these objectives but has specific emphasis on the first two.

7.4 Scope of Part B

In order to provide statistically meaningful results for analyses of soil samples a comprehensive sampling plan was required. This and aspects of the various analytical procedures used are summarized in chapter 8.

Various mineralogical and chemical properties, as well as detailed profile descriptions of two sites chosen to represent the Maimai soil of the study region in its undeveloped state, are discussed in chapter 9.

The agricultural development of two farm units within the Lands and Survey Bell Hill block is the subject of chapter 10. The results of a soil-nutrient variability study are presented along with estimates of fertilizer requirements for land development and a review of this development with specific regard to nutrient levels in soil, herbage and

run-off water. The cobalt status of the Bell Hill block and a number of other wet land soils from the West Coast, is also included in this chapter.

Table 7.1 Development of the "Dairy Unit"

Date	Details
1968	Initial development of 60 ha block: Lime, 3.75 tonne ha^{-1} Special mix fertilizer, comprising 619 kg superphosphate, 5.6 kg $CuSO_4$, 0.14 kg Na_2MoO_4, 0.35 kg $CoSO_4$ per hectare Oversown with clover and grass seed mix, comprising 10 kg *Ruanui* rye, 4 kg *Manawa* rye, 3.5 kg *Apanui* cocksfoot, 3.5 kg *Huia* white clover and 2.25 kg *Tunoa* red clover per hectare
1969-1974	Annual maintenance applications of 30 % potassic superphosphate, 500 kg ha^{-1} plus 0.7 kg ha^{-1} $CoSO_4$
1974	
March-June	82 ha block fenced off into 40 paddocks (included ca. 20 ha of a second land area incorporated for the first time)
May	Regular grazing with beef cattle begun
October	82 ha block limed, 2.5 tonne ha^{-1} The second block of 20 ha oversown with clover, grass, special mix superphosphate at same rates used for the larger block.
1975	
January	
Sampling	
February	Maintenance application of 30 % K - superphosphate 500 kg ha^{-1} plus $CoSO_4$, 0.7 kg ha^{-1}

April	
Sampling	
September	Stocking was 150 - 190 2 yr beef heifers and 11 dairy
Sampling	cows, held on 4 paddocks over winter - changed to rotational grazing (12 hours per paddock)
November	375 ha^{-1} 30 % potassic superphosphate plus 0.7 kg ha^{-1} $CoSO_4$ applied
1976	
February	Beef stock removed and replaced with 92 in-calf dairy heifers and one Jersey bull (put on 24 h/paddock rotational grazing until winter)
March	"Spinner" drains following natural contours of the land were dug
April	
Sampling	
September	Ammonium sulphate applied to 6 of the paddocks as a trial (2 at 250 kg ha^{-1} and 4 at 125 kg ha^{-1})
October	
Sampling	
November	First of a split application of 30 % potassic superphosphate applied 375 kg ha^{-1}. 12 h/paddock rotational grazing of dairy stock
1977	
February	375 kg ha^{-1} superphosphate plus $CoSO_4$ 0.7 kg ha^{-1} plus 20 % elemental sulphur (following Ministry of Agriculture trials)
April	
Sampling	

September	Paddocks 2 - 9 and 31 - 40 oversown with grass and clover
	Paddocks 31 - 40 had 5 tonne ha^{-1} lime applied
	Paddocks 13 - 30 had 2.5 tonne ha^{-1} lime applied
	Whole unit had 375 kg ha^{-1} 30 % - K, 10 % - S, superphosphate + Co as before
September	Stocking was 110 dairy heifers plus 20 yearlings
Sampling	
1978	
February	375 kg ha^{-1} superphosphate, 30 % - K, 7 % - S + Co as before
April	Maintenance application of lime, 1 tonne ha^{-1} over 1/3 of block
September	375 kg ha^{-1} superphosphate, 30 % - K, 7 % - S + Co as before
	Stocking was 120 dairy heifers plus 40 yearlings
1979	
February	375 kg ha^{-1} superphosphate, 30 % - K, 7 % - S + Co as before
August	
Sampling	

Table 7.2 Development of the Ruru Area

Date	Details
1975	
September	Undeveloped pakihi land
Sampling	
1976	
September-	Initial development of 40 ha block:
October	Lime, 3.75 tonne ha^{-1}
	Special mix fertilizer, 625 kg ha^{-1}, clover and grass seed, 23 kg ha^{-1}, of similar composition to that used for initial oversowing in the Dairy Unit (refer to table 7.1)
1977	
	"On-off" mob stock (beef cattle) throughout 1977 - 1979
March-April	500 kg ha^{-1} 30 % potassic superphosphate + Co, 0.7 kg ha^{-1}
April	
Sampling	
September	
Sampling	
October	450 kg ha^{-1} 30 % potassic superphosphate + Co as before
December	2.5 tonne ha^{-1} lime applied

1978	
September	450 kg ha^{-1} K - superphosphate + Co as before
	+ 20 % S
October	
Sampling	
1979	
August	
Sampling	
August-	450 kg ha^{-1} K - superphosphate + Co as before
September	+ 7 % S
	Lime, 2.5 tonne ha^{-1}

CHAPTER 8

EXPERIMENTAL

A. COLLECTION OF FIELD SAMPLES

8.1 Selection of Sample Sites

8.1.1 Soil

Soil sample sites were carefully chosen in order to give maximum significance to the subsequent physical and chemical analytical results within the practical limits of extensive sample collection and analysis.

Three main sampling areas were established within the study region, viz "Dairy Unit" (DU), "Bell Hill Undeveloped" (BU), and "Ruru" (RR) (see section 7.2.3). Area DU was subdivided into two parts corresponding to different times of development; viz DU-68 and DU-74 denote areas first oversown in 1968 and 1974 respectively. This subdivision and other features of the Dairy Unit are illustrated in figure 8.1.

To characterize undeveloped Maimai soil in the study region, samples were collected from two soil profiles at sites thought to be representative of the soil in those areas. The first of these profiles was located in the Bell Hill Undeveloped area, ca. 100 m west of the western perimeter fenceline of the Dairy Unit (see figure 8.1). This site will be referred to as BU 101. The second profile was sampled from a site in the south east corner of the Ruru area and will be referred to as RR 112.

To provide information about agricultural development in the study region a chronological series of topsoil samples was collected in two of the sampling areas (viz DU, RR). Each sample in the series

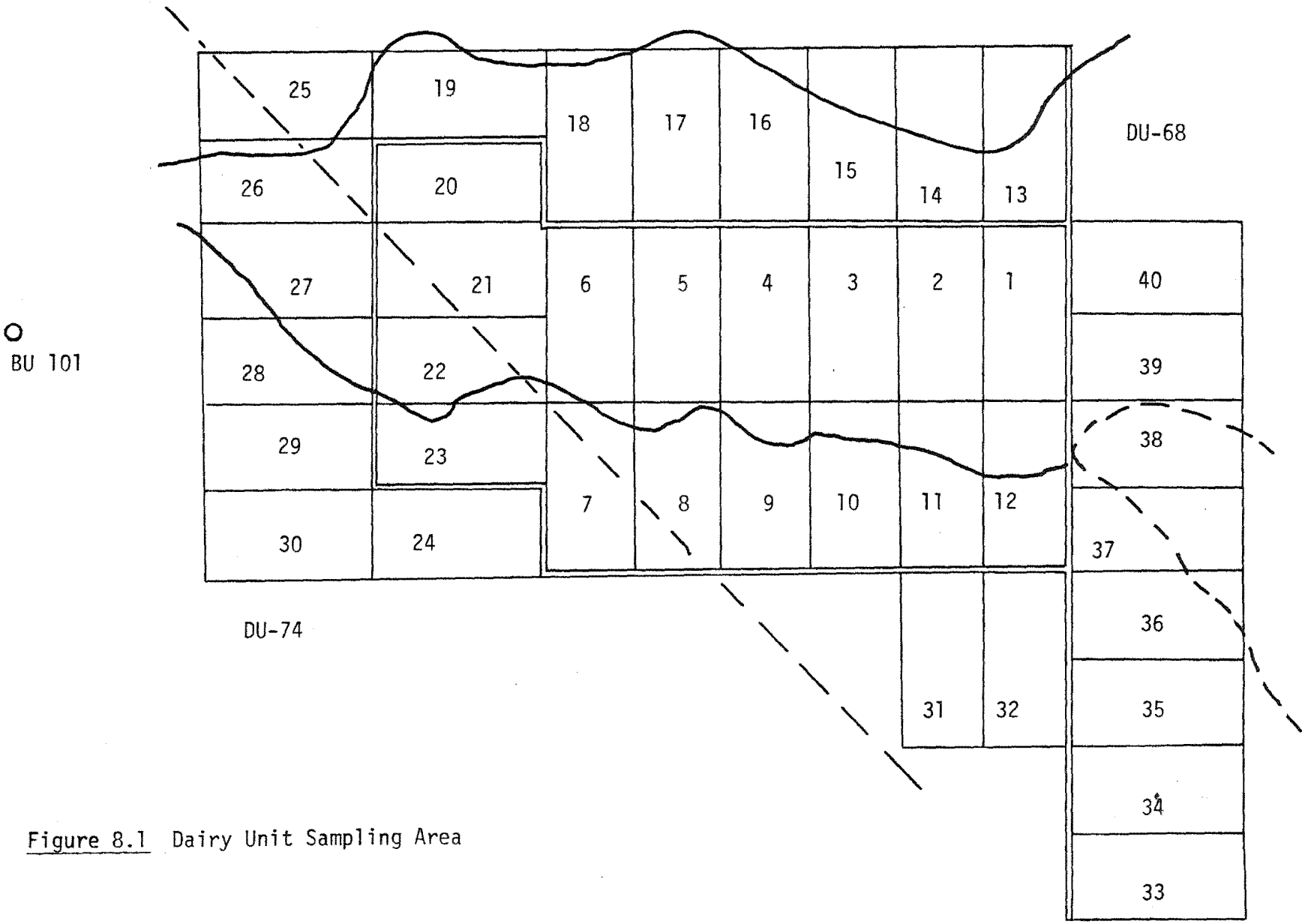

Figure 8.1 Dairy Unit Sampling Area

consisted of a number of sampling units (small soil cores) collected from over the sampling area and then pooled for analysis. Each collection in the series will be referred to as "survey sample". The location of the individual soil cores was determined by a combination of simple random and systematic sampling methods. (This is discussed in detail in section 8.3). The Bell Hill Undeveloped area was sampled on two occassions, firstly by selecting "representative" sites and later by systematic collection of soil cores. Data from these two survey samples were used to estimate the condition of the Dairy Unit prior to development (no samples from DU before 1974 were available). Table 8.1 summarizes information about soil samples.

Samples of other wet land soils were kindly provided by R. Lee of the New Zealand Soil Bureau, D.S.I.R., Taita. Full description of these soil samples has been given by Mew [150]. Various chemical and physical properties have been determined by Lee [149].

8.1.2 Water

In conjunction with E.S. Lee, H.K.J. Powell and N.Y. Tsao, a survey of nutrient levels in surface run-off from the Dairy Unit was conducted in the 1975/76 season. The nutrients Ca, K, S and P were monitored and losses were evaluated relative to accessions via rain-water and fertiliser. Experimental details and results have been published [153,154]. Appendix 16 summarizes the content of this work.

8.1.3 Herbage

Hay used for feeding stock in winter months was analysed for cobalt. A sample of lucerne hay originating from the east coast of the South Island, New Zealand, was collected from a hay barn within the Bell Hill block for this purpose. This sample was collected to provide information about additional sources of cobalt intake for stock.

Table 8.1 Details of Soil Sampling

(I) Survey Samples

Sampling Area	Time of Sampling	Sample Designation	Sampling Method *(a)*	Average Depth of Soil Cores (cm)	Number of Cores per Sample
Dairy Unit (DU)					
DU-74	Apr '75	DU-74/AP75	R	7.6	2
	Sept '75	DU-74/SP75	SR	"	9 *(b)*
	Apr '76	DU-74/AP76	SR	"	26
	Oct '76	DU-74/OC76	S	"	38
	Apr '77	DU-74/AP77	S	"	26
	Sept '77	DU-74/SP77	S	"	26
	Aug '79	DU-74/AG79	S	"	23
DU-68	Jan '75	DU-68/JA75	R	7.6	7
	Apr '75	DU-68/AP75	R	"	8
	Sept '75	DU-68/SP75	SR	"	31 *(b)*
	Apr '76	DU-68/AP76	SR	"	76
	Oct '76	DU-68/OC76	S	"	117
	Apr '77	DU-68/AP77	S	"	79
	Aug '79	DU-68/AG79	S	"	74
Bell Hill Undeveloped (BU)	Sept '75	BU/SP75 *(c)*	R	12.7	10
	Jan '76	BU/JA76 *(c)*	S	11.3	36

Ruru					
(RR)	Sept '75	RR/SP75 *(c)*	S	14.9	36
	Apr '77	RR/AP77	S	11.4	"
	Sept '77	RR/SP77	S	"	"
	Oct '78	RR/OC78	S	"	"
	Aug '79	RR/AG79	S	"	"

(II) Profile Samples

Sampling Area	Time of Sampling	Site Designation	Sampling Method *(a)*	Profile Depth (cm)	Soil Horizons
BU	May '75	BU 101 *(c)*	R	33.0	4
RR	Sept '75	RR 112 *(c)*	R	33.0	3

(a) *The various sampling methods are designated as follows:*

R = "representative" selection of sample sites

SR = simple random selection of sample sites

S = systematic selection of sample sites.

(b) *An additional 50 sample cores were collected over the entire Dairy Unit area (i.e. both DU-68 and DU-74) and pooled for analysis.*

(c) *These data refer to undeveloped pakihi soil.*

Herbage samples from the Dairy Unit were collected by N.Y. Tsao and E.S. Lee. A full description of this sampling has been given [155].

8.2 Sampling Techniques and Sample Preparation

8.2.1 Soil

For the collection of samples from soil profiles, pits were dug with a spade to a depth of ca. 55 cm. The soil horizons were examined on a freshly cut face on one side of the pit, and samples collected from this face. Subsequent treatment of moist samples was identical to that described later in this section for "core" samples.

An aluminium "core-sampler" was employed in the collection of topsoil survey samples (figure 8.2). The sampler consisted of a hollow stainless steel cylinder of diameter 3.5 cm, with depth graduations on the outside and sharpened at one end. A solid detachable plunger as well as a small T-handle, fitted snuggly within the cylinder, facilitating both the insertion of the cylinder into the ground and removal of the soil core forced into the cylinder on insertion. It was found that on very hard or very wet soils sample collection was quite difficult. Fortunately the great majority of sites afforded moist soil of the right consistency for easy sampling. The core sampler was able to collect soil cores of up to 20 cm in depth under good conditions; most samples required a depth of between 5 and 16 cm.

Early survey sampling (September 1975) in the Dairy Unit consisted of two cores per sampling site. Subsequent sampling showed that one core per site, when pooled, gave sufficient soil material for all the analyses. Soil cores collected after recent application of fertilizer had ca. 3 mm trimmed off the top to avoid contamination of soil by fertilizer granules. In most cases this represented removal of surface pasture roots only. Soil cores were transferred in labelled,

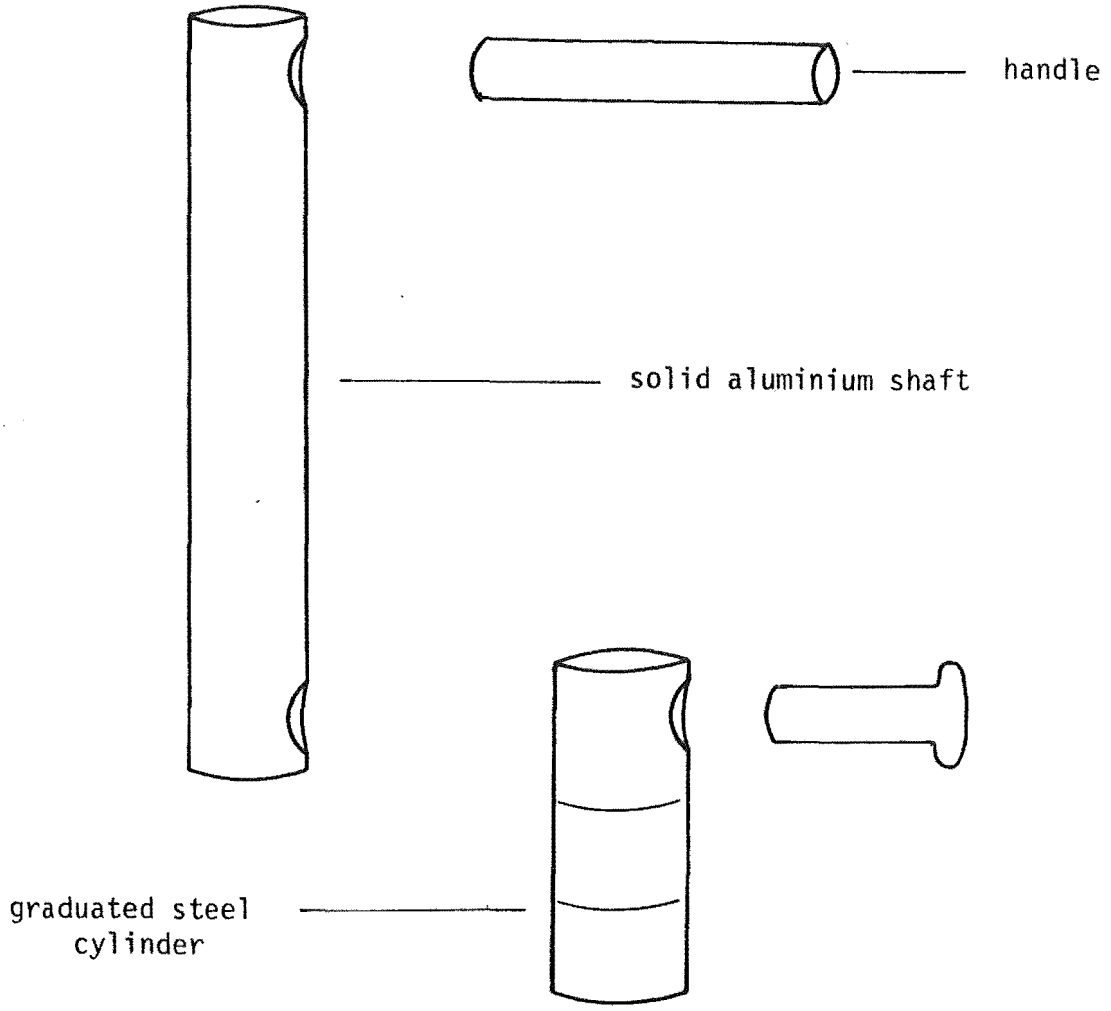

Figure 8.2 Core-sampler

sealed plastic bags. Once in the laboratory a small section of soil was cut longitudinally from each moist core and pooled for pH determination. The remaining soil was air-dried at ca. 30 °C over several days. Once dried, samples were ground with a stainless steel roller to pass through a 2 mm sieve, pooled where appropriate, and mixed thoroughly to ensure homogeneity. Stones, twigs and coarse fibrous material < 2 mm were discarded. A portion of the sieved material was ground further, using a "Gilco" ring mill, to pass through a 60-mesh sieve (0.25 mm). For most samples the weights of soil at each stage of sample preparation were recorded for bulk density and moisture content measurements. Prepared samples were stored in plastic bags or small plastic jars with screw lids. Table 8.1 summarizes additional details from the soil samplings.

8.3 Sampling Methods and Statistical Analysis for Survey Samples

8.3.1 Sampling Plan

To help fulfill objective (2) of this soil study (see section 7.3), a sampling plan was required that would give statistically significant results for the soil in the study region. Only sampling methods involving some form of random selection of the sampling units enable the calculation of errors inherent in the sampling procedure. (A detailed background summary of elementary sampling theory, including definitions of various statistical terms used in this chapter, is given in Appendix 15). "Random sampling" is by definition free from selection bias, but is no guarantee of the "representativeness" of a sample. "Systematic sampling", where sampling units are chosen according to some pre-specified pattern, is often a more precise and more accurate (if bias is absent) estimate of the true population mean, than a random sample of the same size. However, estimation of the sampling errors of a

systematic survey is more difficult. The sampling plan used in this work capitalized on advantages of both these approaches and can be summarized as follows:

(1) An indication of the inherent variability of population attributes was obtained.

(2) The numerical size for a simple random sample, to be collected over the entire sampling region, was calculated.

(3) The population variability was reassessed and sampling errors were calculated for future samplings.

The individual steps of this plan and results obtained are discussed in detail in the following sections.

8.3.2 Population Variability

Some prior knowledge of the inherent variability of the population is required to determine the numerical size of the sample to be collected. In the context of this study, the inherent variability of the population is the variation among all possible sampling units in the sampling area of the particular chemical or physical attribute being measured.

Results obtained by Lee [156] and Tsao [157] from a small number of "representative" soil sites, sampled in the Dairy Unit during 1975, were available. Since no random selection process was involved in collection of these samples, estimates of the population parameters, mean ($\bar{X}$) and variance (V), were likely to be biased. However, some useful preliminary information was obtained. Table 8.2 summarizes data calculated from Lee's and Tsao's results. Soil chemical attributes listed in the first half of the table were those most relevant to the evaluation of fertilizer application. Data in the second half of the table have been calculated from relatively fewer sample sites and must therefore be regarded as

Table 8.2 Preliminary Population Estimates from the Dairy Unit - "Representative" Sampling Sites.

Soil Analysis (a)	Sample Size (n) (b)	Sample Mean ($\bar{x}$)	Standard Deviation(s)	Coefficient of Variation (C%)	n'
Soil pH (H_2O)	19	5.38	0.33	6.2	3
Soil pH ($CaCl_2$)	19	4.43	0.40	8.9	5
Ca_{ex}	19	12.6	7.1	57	89
Mg_{ex}	19	1.20	0.69	58	92
K_{ex}	19	0.42	0.22	53	78
Σ cat_{ex}	19	14.2	7.7	54	81
% BS	19	46.9	22.4	48	64
CEC	19	30.7	13.2	43	52
% C	19	12.2	3.8	31	28
% N	19	0.79	0.42	53	78
C/N	19	16.8	2.8	17	11
Truog-P	35	5.19	3.68	71	137
Total K	6	1.35	0.22	16	10
Total Mg	6	1.80	0.39	22	15
K_c	6	0.16	0.04	26	21
Mg_r	5	0.62	0.63	101	200
P-retn	11	26.0	8.8	34	33
Org-P	11	51.1	26.3	51	72
0.5 M H_2SO_4-P	15	28.9	26.4	91	200
Total P	8	79.0	35.8	45	57
Tamms-Fe	5	0.29	0.15	53	78

(...contd)

Table 8.2 (contd)

	n	$\bar{x}$	s	C(%)	n'
Tamms-Al	5	0.20	0.11	56	86
Boron	6	18.5	6.22	34	33

(a) Methods of analysis are detailed in section B of this chapter.

(b) Terms C, s, n, n' and $\bar{x}$ are explained and/or defined in the text (sections 8.3.2 and 8.3.3).

very approximate only. Values of s^2 (the square of the standard deviation of a sample of size n) were used as preliminary estimates of the population variance. (It was convenient to express this variation as C, the "coefficient of variation", which is defined by:

$$C = 100\ s\ /\ \bar{x} \qquad (8.1)$$

and is simply the variation within the sample expressed as a percentage of the sample mean ($\bar{x}$). This definition facilitates comparisons of variability among samples with different sized means).

8.3.3 Determination of Sample Size

In order to estimate population parameters, $\bar{X}$ and V, for any given chemical or physical property, a random sample of size n, mean $\bar{x}$ and variance s^2 is chosen. Sample parameters $\bar{x}$ and s^2 are taken as unbiased estimates of $\bar{X}$ and V respectively. It was assumed that the distribution of all possible sample means $\bar{x}_i$ about the unknown population mean $\bar{X}$ followed a Normal or Gaussian curve (see figure 1, Appendix 15), with a variance that was estimated by $v = s^2 / n$. This assumption was found to be reasonable by Adams and Wilde [158].

Errors in sample data arising from chance selection are referred to here as "sampling errors". These are more commonly expressed in terms of the "standard error", $se(\bar{x})$, which represents the standard deviation of sample means, and is estimated by:

$$se(\bar{x}) = s\, n^{-\frac{1}{2}} \qquad (8.2)$$

Sampling errors are a function of (1) the inherent variability of the population (estimated by s) and (2) the sample size, n.

If the sample means are normally distributed, the probability of any one sample mean ($\bar{x}_i$) falling within certain limits of the true but unknown population mean ($\bar{X}$), is given by the "Students" t - Distribution (see Appendix 15). These limits are a function of the standard error ($se(\bar{x})$). For example, for a sample of size n = 121, there is a 95 % probability that the sample mean lies within about two standard errors of the population mean. In this example the parameter t, of the t - distribution, is equal to 1.98. The required limit of deviation of $\bar{x}$ from $\bar{X}$, or degree of required "sampling precision", is denoted by "D". If D is chosen, then the sample size required to give a sample mean that will lie within ±D of the population mean with some specified probability, or "confidence level", is given by:

$$n' = t^2 s^2 / D^2 \qquad (8.3)$$

This expression is more conveniently written as:

$$n' = t^2 C^2 / E^2 \qquad (8.4)$$

Where $E = 100\ D / \bar{x}$.

The calculation of n by equations (8.3 or 8.4) is an iterative procedure since the value assigned to t, itself depends on n.

For this study a sampling precision (E) of not greater than 12 % and a probability level of 95 % were chosen. A graphical relationship between C, the coefficient of variation and n' was established (see figure 3, Appendix 15) from which values of n' could be derived for each population attribute, to be measured (see table 8.2). The size of the simple random sample to be collected over the Dairy Unit was chosen to give a satisfactory compromise between high sampling precision for each attribute and exhaustive sample collection and analysis. On the basis of preliminary data, summarized in table 8.2, a sample size of about 100 was chosen. This ensured a sampling error of ca. 14 % for Truog-P and < 12 % for the other measurements listed in the first half of the table.

8.3.4 Sampling Procedure: Part I - A Simple Random Sample

A simple random sampling method was designed for the Dairy Unit as follows. The sampling area was given co-ordinates (x, y) defined in terms of "paces"; one pace was ca. 0.67 m. From a table of random numbers [159], pairs of co-ordinates were chosen. Each random number used had five digits and, since the maximum co-ordinates of the sampling area were (1800, 1200), the last digit of each random number was omitted. If the first digit was odd, it was changed to 1; if even or zero, it was changed to zero. This convention minimised the rejection of numbers

(because of size) without destroying their random properties. Each consecutive pair of random numbers, reading down the columns, was taken to represent an (x, y) co-ordinate for a sampling site. For convenience, each co-ordinate pair was re-defined relative to an origin located in the north-west corner of the appropriate paddock.

Two soil cores were collected from each of 125 defined sampling sites in the first sampling (Sept '75). Sampling sites located in drains, soakage pits, raceways or tree stumps were deemed to be outside the sampling area and were rejected. A total of 35 sites from this first random sample were rejected on this basis.

Soil cores from the first 40 sampling sites, as defined by the random numbers table, were analysed individually in order to determine an unbiased estimate of the population variance. The remaining 50 were pooled for analysis. Table 8.3 summarizes results from the analysis of the 40 individual soil cores. The coefficients of variation from the data in table 8.2 are included for comparison. Values of n' representing the number of sampling units required to give 12 % sampling precision (95 % confidence level) are also tabulated.

The values of C from this random survey were taken as unbiased estimates of the inherent variability of each population attribute. Comparison of C values showed that previous results from non-randomly located sites (table 8.2) tended to over-estimate the natural variability of population attributes. The most notable exception to this was for the determination of "exchangeable calcium" (C for random sample 72 %, cf. representative sample, 57 %). A more detailed discussion of variability of these population attributes is reserved for section 10.1.

On the basis of these results a sample size of at least 100 (excluding those rejected during sampling) was considered to be desirable for subsequent samplings.

Table 8.3 Population Estimates from the Dairy Unit - Random Selection of Sampling Sites

Analysis *(a)*	Sample Size (n) *(b)*	Sample Mean ($\bar{x}$)	Standard Deviation (s)	Coefficients of Variation		n'
				Random Sample	"Representative" Sample (Table 8.2)	
Ca_{ex}	40	11.3	8.2	72	57	145
Mg_{ex}	40	1.15	0.65	57	58	89
K_{ex}	40	0.37	0.15	41	53	48
Na_{ex}	40	0.21	0.12	60		99
Σcat_{ex}	40	13.1	8.7	67	54	122
CEC	40	30.7	13.4	44	43	55
% BS	40	41.0	14.0	34	48	33
% C	10	13.6	4.0	29	31	25
% N	10	0.79	0.21	26	53	21
C/N	10	17.3	1.9	11	17	6
Troug-P	47	4.2	3.0	70	71	133

(a) *Methods of analysis are detailed in section B of this chapter.*

(b) *Terms C (coefficient of variation), s, n, n' and $\bar{x}$ are explained and/or defined in the text (sections 8.3.2 and 8.3.3).*

8.3.5 Sampling Procedure: Part II - Other Survey Samples Collected

After one further sampling of the Dairy Unit area on a simple random basis (with pooling of sample cores for analysis) it was decided to capitalize on the advantages afforded by a systematic approach to sampling. A random choice must be involved at some stage of a systematic survey to ensure that the mean of a systematic sample is an unbiased estimate of the population mean (see Appendix 15). In practice this involved a random siting of the first sampling unit from which a rectangular sampling grid was established over the entire sampling area. The spacing of the intersection points on this grid was calculated to generate at least 100 sampling units. The mean of a systematic sample is likely to be a more precise estimate of the population mean. Hence the sample variance (s^2) calculated from the first simple random sample was used as an estimate of the population variance for systematic samples collected. In other words, it was assumed that the sampling error associated with the systematic samples was no greater than that calculated for a simple random sample of the same size. This will be a valid assumption when any periodic trends in the population do not coincide with the spacing of the systematic sampling grid. No periodic trends were found in the sampling areas surveyed but, as an added precaution, it was ensured that the spacing of the sampling grid used in the Dairy Unit did not coincide with the dimensions of the established paddocks.

For samples collected from areas BU and RR, it was also assumed that the sample variance (s^2) derived from the random sample in the Dairy Unit would not under-estimate the respective population variances. Where samples from areas BU or RR represented pakihi soil in an undeveloped state it was expected that the calculated sampling errors ($s\ n^{-\frac{1}{2}}$) based on this assumption would in fact be over-estimated, since

many population attributes (especially soil chemical properties) were observed to be rather uniform (and low) under these conditions. Systematic samples, with a random siting of the first grid point, were collected from these two areas (other details are given in table 8.1). Sample sizes in these surveys were lower (n = 36) than those collected in the DU area and consequently the corresponding sampling errors calculated were higher (e.g. Troug-P: $se(\bar{x})$ = 0.37 for n = 100, 0.61 for n = 36).

B. ANALYTICAL METHODS

Analytical results described in this section were initially calculated in units such as mg / 100 g soil, milli-equivalents (me) / 100 g soil etc. These units were retained from New Zealand Soil Bureau methods [160] for convenience and to facilitate comparison with published data for other New Zealand soils. However, for the purposes of assessing trends in soil chemical properties within soil profiles and estimating fertilizer requirements, it was considered more appropriate to use concentration units expressed in volume terms. Thus, units such as kilograms per hectare per centimetre horizon (kg ha^{-1} cm $horz^{-1}$) and milli-equivalents per hectare per centimetre horizon (me ha^{-1} cm $horz^{-1}$) have been used in the presentation and discussion of data.

8.4 Soil Analyses - Physical Properties

8.4.1 Volume - Weight Data

(a) Average Moisture Content. Samples collected in the field were weighed before and after drying and again after sieving to 2 mm. The average moisture content was calculated as:

$$\left(1 - \frac{\text{total mass of air-dried soil}}{\text{total mass of field moist soil}}\right) \times 100$$

(b) Rejected Material. The amount of sample material > 2 mm was expressed as a percentage of the total mass of air-dried soil.

(c) Dry Bulk Density. The depth of each soil core was recorded and the total volume of soil collected was calculated. From this an average dry bulk density was determined as:

$$\frac{\text{total mass of air-dried soil (g)}}{\text{total volume of soil collected (cm}^3\text{)}}$$

8.4.2 Particle Size Distribution

The relative proportions of clay (< .002 mm), silt (.002 - .02 mm) and sand (> .02 mm) were measured after separation by repeated dispersion and flocculation steps (see section 8.4.3).

8.4.3 Clay Mineralogy

Preparation of samples for mineralogical analysis and X-ray diffraction studies were based on methods described by Jackson [161]. The method is designed for soils that do not contain much allophane or other poorly ordered alumino-silicates. Removal of carbonates and soluble salts was considered unnecessary for these acid, water-logged soils.

(a) Oxidation of Organic Matter. Ten gram samples of air-dried soil, ground to< 2 mm, were oxidised in three successive treatments with 20 ml of 100 vol. hydrogen peroxide in tall-form 800 ml beakers. Excessive frothing was not encountered. Organic material was converted to carbon dioxide in this step and topsoil samples were observed to decolourize (brown - to khaki -grey), while subsoil samples became grey with an orange tint (G - horizon) or slightly more intense orange-brown (B_3 - horizon). Samples were centrifuged at 2500 rpm for 15 - 30 min with a few drops of acetone and 1 M hydrochloric acid to flocculate the fine clay particles.

(b) Removal of Cementing and Coating Materials. "Coating" and "cementing" materials were then removed with a citrate / dithionite extraction. A citrate reagent (30 ml), comprising sodium citrate buffered to pH 7.3 with citric acid, was added along with 5 ml of 1 M sodium bicarbonate. The soil / solution mixtures were heated to 80 °C

on a water bath and sodium dithionite (ca. 1 g) was added to dissolve insoluble iron(III) oxides. This process was repeated.

The efficiency of the iron extraction was assessed by recording concentrations of Fe^{2+} in the supernatants from successive centrifuging steps. Fe^{2+} was determined colorimetrically as an o-phenanthroline complex, the absorbance being measured at 510 nm. Results indicated that after two treatments with citrate-dithionite approximately 96.5 % of the "iron" was extracted and after three treatments close to 100 % removed. Two treatments were considered sufficient for the purposes of the analysis.

Filtrates and washings from the citrate-dithionite treatment were kept for analysis for Fe and Al (see section 8.5.10).

(c) Separating the Clay Fraction. Soil samples with organic matter, iron and aluminium removed were then subjected to a series of dispersion and separation steps to isolate silt, sand and clay fractions. Soil samples were transferred to 100 ml centrifuge tubes with distilled water (to 10 cm above the sediment layer) and shaken thoroughly to disperse clay-sized material. The mixtures were centrifuged at 500 rpm for 10 minutes and the supernatant suspensions were siphoned off. This process was repeated 9 times by which stage the supernatants were essentially clear. The dispersing reagent "Calgon" was added to aid the clay dispersion during the 9th and 10th stages. The suspensions of clay material separated in this process were centrifuged at 1700 - 2000 rpm for 5 - 7 minutes and the bulk of the water removed. Small quantities of saturated sodium chloride solution were added to aid flocculation.

Clay was dispersed again with vigorous shaking in 50 ml of distilled water and the suspensions were made up to 80 ml. Aliquots (10 ml) from each sample were pipetted into clean, weighed, oven-dried beakers (25 ml) and left to evaporate overnight under infra-red lamps. The residual clay fractions were dried to constant weight and the proportion

of clay material (i.e. < .002 mm) in each soil sample was calculated.

(d) Silt and Sand Fractions. Silt and sand residues remaining in the centrifuge tubes were separated as follows. The residues were dispersed with distilled water and allowed to stand for 5 min. The supernatant suspensions were siphoned off and the process repeated until the supernatants were clear. The silt material (.002 - .02 mm) thus collected was allowed to settle out overnight. Water was decanted off and the silt material was washed with ethanol and acetone and dried at 50 °C. The remaining sand fractions (> .02 mm) were oven-dried at 100 °C overnight.

(e) Preparation of Clay Samples for X-ray Studies. Sufficient clay suspension was taken to make two 10 ml portions of a 1 % suspension for each soil sample. These suspensions were saturated with potassium and magnesium chloride solutions respectively. After four thorough mixing and centrifuging steps, (1500 rpm, 5 - 7 minutes) each sample was washed 2 - 3 times with distilled water until dispersion occurred. Approximately 2 ml of magnesium and potassium-saturated clay suspensions were carefully pipetted onto the surface of small glass slides. The bubble of liquid was allowed to dry overnight leaving a thin film of clay material coating the glass slide. A second batch of samples was prepared using porous tiles. Approximately 6 ml of potassium-saturated suspension was pipetted onto a tile and water was drawn through the tile by suction. Tiles coated with magnesium-saturated suspensions also had ca. 4 ml of a 1 % glycerol solution deposited under suction.

Magnesium-saturated clays were also sprayed three times with glycerol spray immediately before X-ray treatment, allowing no time for drying or contraction of clay minerals. Samples on porous tiles were used for X-ray analysis (glass slides used as a back-up if necessary).

After initial X-ray analysis, potassium-saturated samples were heated in an oven for 2 hours at 350 °C, X-rayed again; heated further at 550 °C for 1 - 1½ hours and X-rayed for a third time. X-ray diffractometry (2θ ranging from 2° to 40° for FeKα radiation) was used to identify the crystalline mineral species. A Phillips PW 1310 generator and PW 1050 / 25 goniometer were used in this analysis.

8.5 Soil Analyses - Chemical Properties

Methods for chemical analyses of soil samples for exchangeable cations (Ca, Mg, K, Na), potassium and magnesium reserves, phosphate, carbon, nitrogen and soil pH, closely followed the procedures recommended by the New Zealand Soil Bureau [160]. For these analyses, a brief description of the method along with any modifications used and observations made are detailed in this section. In each analysis appropriate "blanks" were also analysed. Analytical grade chemicals were used where possible. A Varian Techtron A.A.5 spectrophotometer was used for all analyses by atomic absorption. Colorimetric analyses utilized Bausch and Lomb Spectronic 20 and Shimadzu MPS-50L spectrophotometers.

8.5.1 Soil pH

Measurements were made at a soil solution suspension ratio of 1:2.5, using field moist soil samples which had been stirred vigorously with distilled water and/or 0.01 M calcium chloride solution. A combination glass/calomel electrode was calibrated with at least two NBS standard buffers at pH 4.01 (phthalate), 6.86 (phosphate), or 9.18 (borax). This electrode coupled with a low sensitivity (± 0.05 pH unit) pH-meter was used to record pH data. In some experiments pH values were recorded with and without stirring after initial mixing and standing procedures [162]. More reproducible results were obtained for samples

that were stirred during the recording of pH. Replicate determinations established a reproducibility of ± 0.1 pH unit.

8.5.2 Determination of Exchangeable Cations

"Exchangeable cations", Ca^{2+}, Mg^{2+}, K^{+} and Na^{+}, were determined by leaching soil (< 2 mm) mixed with acid-washed silica sand (soil:sand ratio 1:2) with ammonium acetate (1 M, buffered to pH 7.0 ± 0.1). Ammonium ions displaced exchangeable cations from cationic exchange sites in the soil as well as occupying any vacant sites. Leachates were analysed for individual cations by atomic absorption spectroscopy (A.A.), after 1:1 dilution with a solution of strontium nitrate (final concentration 1200 ppm Sr), caesium chloride (final concentration 3200 ppm Cs), hydrochloric acid and ammonium acetate. Leachates from some topsoil samples required 1:4 dilution. Multiple working stock standards contained all four cations as well as the same concentrations of background components as the diluent solutions. Table 8.4 summarizes the instrumental parameters and working conditions used in the analyses by A.A.

8.5.3 Cation Exchange Capacity

Soil samples, after leaching with ammonium acetate, were rinsed with ethanol before a final leaching with 1 M sodium chloride solution. The leachate, displacing ammonium ions from the soil exchange sites, was analysed for ammonia using a modified Parnas-Wagner distillation apparatus. Concentrated sodium hydroxide solution, sufficient to give a solution pH of ca. 9.5 but not enough to hydrolyse organic nitrogen compounds, ensured complete recovery of ammonia. Distilled ammonia was collected in 1 % boric acid and titrated with standardised hydrochloric acid using bromocresol green-methyl red indicator. Cation exchange capacity (CEC) was determined from the leachate ammonia concentration.

Table 8.4 A.A. Operating Parameters for Determination of Exchangeable Cations

	Ca	Mg	K	Na
Lamp Current (mA)	3	3	5	5
Slit Width (nm)	0.1	0.1	0.3	0.2
Wavelength (nm)	422.3	285.0	766.3	588.8
Fuel/Support		Acetylene/air		
Flame Stoichiometry	Oxidising (O)	Reducing (R)	R	R
Scale Expansion	1	1	1	5
Concentration Range (mol dm^{-3})	0 - 1 x 10^{-3}	0 - 1 x 10^{-4}	0 - 1 x 10^{-4}	0 - 1 x 10^{-4}

8.5.4 Percentage Base Saturation

Total exchangeable bases (Σcat_{ex}) was calculated by summing the concentrations of the individual exchangeable cations (i.e. Ca, Mg, K and Na). Percentage base saturation (% BS) was calculated as:

$$\% \text{ BS} = \Sigma cat_{ex} \times 100 / \text{CEC}$$

8.5.5 Potassium and Magnesium Reserves

(a) Potassium Reserve. Readily soluble potassium was removed from samples of air-dried soil (< 2 mm) by boiling with 1 M nitric acid at a high acid:soil ratio (200 ml: 2 g). This extract was discarded and three further successive extractions at a lower ratio (25 ml: 2 g) were made. These extracts were analysed for potassium by A.A. and from the average solution concentration, K_c, which represents the long-term potassium-supplying power of the soil(as defined by Metson et al [163]), was calculated. A blank determination consisting of 25 ml 1 M HNO_3 boiled for 20 min gave zero absorbance for potassium. Operating conditions for analysis by A.A. were the same as used for the determination of exchangeable potassium; the concentration working range used in this analysis was 0 - 5 x 10^{-4} M. Successive extractions with HNO_3 gave potassium levels constant to within 3 %.

(b) Magnesium Reserve. Magnesium reserve (Mg_r) is taken to represent the acid soluble "reserve" magnesium of the soil [164] and was calculated as follows. Magnesium soluble in boiling dilute (1 M) hydrochloric acid (Mg_{as}) was determined and the exchangeable magnesium (Mg_{ex}), obtained by leaching with ammonium acetate (section 8.5.2), was subtracted to give Mg_r:

$$Mg_r = Mg_{as} - Mg_{ex}$$

The digestion with HCl was carried out under reflux to prevent concentration of the acid by evaporation. Samples were analysed for Mg in a manner similar to that used for exchangeable cation determination (see section 8.5.2).

8.5.6 Liming Experiment

In an experiment designed to simulate topdressing of undeveloped pakihi soil with lime, 100 g of air-dried soil (< 2 mm) was moistened to average field moisture (57 %) with distilled water. The soil used was from a pooled sample collected in the Ruru area before development. Reagent grade calcium carbonate was added to five separate subsamples according to the quantities given in table 8.5. Limed soil samples were sealed in plastic bags for six weeks at room temperature, air-dried, crushed and sieved to< 2 mm ready for analysis. Analyses for soil pH (on moist samples), phosphate and sulphate retention and magnesium reserve were performed on limed samples according to methods described in this chapter.

Table 8.5 Details of Liming Experiment

Sample Designation	Quantity of $CaCO_3$ added per 100 g air-dried soil		% BS
	grams	me	*(a)*
RR5L	0.5	10	47
RR8L	0.8	16	71
RR11L	1.1	22	95
RR14L	1.4	28	100
RR17L	1.7	34	100

(a) *Expected percentage base saturation if all added Ca^{2+} became "exchangeable".*

8.5.7 Determination of Phosphorus

(a) Total Phosphorus was determined by fusing samples of finely ground (< .25 mm) soil with sodium carbonate. This was followed by digestion with ca. 4.6 M sulphuric acid and removal of silicic acid by filtration.

(b) "0.5 M H_2SO_4- Soluble" Phosphorus was determined as phosphate soluble in 0.5 M H_2SO_4 with 16 hours extraction time at room temperature.

(c) "Organic" Phosphorus was determined in a similar manner to 0.5 M H_2SO_4-soluble P, the soil samples being ignited at 550 °C for ca. 1 h prior to extraction. Calcium acetate was added as 0.5 ml of a 20 % aqueous solution, to prevent loss of P on ignition. In practice it was found that more than 0.5 ml was required to adequately moisten soil (especially topsoil samples). "Organic" P was defined as:

org-P = ignited / 0.5 M H_2SO_4-soluble P - 0.5 M H_2SO_4-soluble P

Both 0.5 M H_2SO_4-soluble P and organic-P measurements used finely ground (< .25 mm) soil samples.

(d) "Inorganic" P was defined as:

inorg-P = total P - org-P

(e) "Truog" Phosphorus was determined as phosphate soluble in 0.001 M H_2SO_4 buffered to pH 3.0 with ammonium sulphate (Truog's method). Extraction time was crucial to the level of phosphorus recorded. This time was kept as close as possible to 30 minutes. Air-dried soil, < 2 mm, was used.

(f) "Phosphate Retention" was measured as the percentage of

added phosphate taken up by 5 g soil (< 2 mm) in 24 hours from an acetate buffer solution (pH 4.6) with an initial phosphate concentration of 0.03 M potassium hydrogen phosphate. Centrifuging to separate soil matter from the solution was effected at 3000 rpm for 15 - 20 minutes.

(g) Phosphate Sorption Isotherm. In an experiment designed to characterize the phosphate sorption properties of soil from the study region, and to estimate P-fertilizer requirements, a sorption isotherm was established. The method was based on that used by Fox and Kamprath[165] and has been described by Tsao[166] . A limed and washed soil sample (pH 6.3), from the Ruru area before pasture development, was equilibrated with 0.01 M $CaCl_2$ containing various quantities of $Ca(H_2PO_4)_2$. After six days equilibration at 25 °C, samples were centrifuged and phosphate in the supernatant was measured colorimetrically. P sorbed was plotted against P remaining in solution to give a sorption isotherm curve.

(h) Colorimetric Analysis. All phosphate measurements used the colorimetric procedure based on the method of Murphey and Riley, as adapted by Watanabe and Olsen[167] . This procedure involved the reduction of the phospho-molybdate complex by ascorbic acid in a reaction catalysed by antimony. The absorbance of the resulting dark-blue solution was measured at 882.5 nm. As many of the samples were very low in phosphorus the aliquots of extractant solution were often larger than those recommended by the New Zealand Soil Bureau[168] .

8.5.8 Sulphate Retention

The method used to determine sulphate retention was adapted from the procedure described by During and Martin[169] . This involved measuring the pecentage of added sulphate taken up by 4 g soil (< 2 mm) in 48 hours from a 0.01 M calcium chloride solution containing 50 ppm

sulphate as the potassium salt. The soil-solution mixtures were shaken vigorously twice during the equilibration period. Samples were filtered through two thicknesses of Whatman No.50 filter paper and a 10 ml aliquot was evaporated to dryness over a steam bath. Sulphate was determined using the colorimetric method of Johnson and Nishita, described in New Zealand Soil Bureau's method for the determination of adsorbed sulphate [170]. This method involved the reduction of sulphate to hydrogen sulphide using a reduction mixture comprising hydroiodic acid (sp. gr. 1.7), hypophosphorus acid (50 % w/w) and formic acid (90 %). The hydrogen sulphide evolved was collected in a solution of zinc acetate with the aid of a stream of nitrogen gas. An "amino reagent" (NN-dimethyl-p-phenylenediamine sulphate) was added to form methylene blue with sulphide in a reaction catalysed by ferric ions. The methylene blue formed was measured colorimetrically; maximum absorbance was found to be 662.5 nm. Deionised water, prepared by passing distilled water through an AMBERLITE IRA-400 [Cl] (strongly basic) ion exchange resin, was used in the preparation and dilution of solutions.

8.5.9 Carbon - Nitrogen Ratio

(a) "Oxidisable Carbon" was determined using the colorimetric method recommended by New Zealand Soil Bureau for soils expected to contain more than 10 % C [171]. The method involved oxidation of organic carbon in the soil sample (< .25 mm) by chromium trioxide in concentrated sulphuric acid. Chromic ion formed in solution was determined colorimetrically at 600 nm. Colorimetric standards were prepared from weighed sucrose samples, chosen to give known amounts of carbon.

(b) "Total Nitrogen" was determined using the method recommended for soils expected to contain < 20 ppm (0.002 %) nitrate [172]. Finely crushed soil (< .25 mm) was boiled with 3 - 5 ml of concentrated

sulphuric acid, potassium sulphate and selenium dioxide crystals (catalyst), over a bunsen burner for up to 5 min in a Kjeldahl tube. Further digestion was carried out on a Kjeldahl rack for ca. 45 - 60 minutes to give pale green-brown solutions. After cooling, sufficient concentrated sodium hydroxide was added to precipitate ferric hydroxide and ammonia was distilled off using the procedure described for CEC determination (see section 8.5.3)

(c) Carbon-Nitrogen Ratio (C/N) was calculated as follows:

C/N = % organic carbon / % total nitrogen

8.5.10 Determination of Citrate-Dithionite Extractable Iron and Aluminium

Washings from citrate-dithionite extractions, collected during preparation of samples for mineralogical analysis (see section 8.4.3), were treated with sulphuric acid (final solution 1 M in H_2SO_4). Solutions were filtered (to remove small quantities of clay material) and made to 1 litre including 20 000 ppm potassium chloride (to suppress ionisation of aluminium in the acetylene/nitrous oxide flame used).

A standard stock solution containing 1000 ppm of both iron and aluminium was prepared as follows:
Citrate reagent (90 ml, as described in section 8.4.3), concentrated sulphuric acid (14 ml), saturated sodium chloride (20 ml), acetone (.5 ml), potassium chloride (38 g), ferrous ammonium sulphate (7.0217 g) and aluminium potassium sulphate (17.5820 g) were dissolved in 1 litre of distilled water to give a multiple standard stock solution of an approximately similar matrix to that of the test solutions. Working standards were prepared by taking respectively 0, 2, 4, 6, 8, 10, 15 and 20 ml of stock solution and making up to 200 ml with special diluent solution made up in the same manner as the stock solution but

excluding iron or aluminium.

Samples and standards were measured for Fe and Al using A.A. (Operating parameters are given in table 8.6).

Table 8.6 A.A. Operating Parameters for the Determination of Fe and Al

	Fe	Al
Lamp Current (mA)	5	5.5
Slit Width (nm)	0.1	0.1
Wavelength (nm)	371.8	309.0
Fuel/Support	Acetylene / Nitrous Oxide	
Flame Stoichiometry	oxidising	reducing
Scale Expansion	7.5	6.0
Concentration Range *(a)*	0 - 100 ppm Fe	0 - 100 ppm Al

(a) Calibration curves were linear in these ranges.

8.5.11 Cobalt

(a) Total Cobalt in Soils. The method used for the determination of "total" levels of soil cobalt has been adapted from the procedure described by Kidson [173]. Approximately 10 g of finely crushed * soil (< .25 mm) was weighed into acid-washed porcelain basins and ashed at 400 - 450 ° C in a muffle furnace for 16 - 20 hrs (overnight). The pale grey-brown ash was digested under reflux conditions in 50 ml of 50 % hydrochloric acid for ca. 45 minutes. Digests were filtered through Whatman GF/C glass-fibre paper into 100 ml beakers. The filtrates were then evaporated to ca. 20 ml on a steam bath and, after cooling, were transferred to 25 ml volumetric flasks and made to the mark. A standard stock solution of Co, analysed gravimetrically, was diluted to give four working standards in the concentration range 0.87 - 3.48 ppm Co. Each standard solution was 6 M with respect to hydrochloric acid. Sample and standard solutions were analysed for Co using A.A. Details of working parameters used are given in table 8.7. A blank, consisting of 100 ml 50 % HCl refluxed as per sample treatment and reduced to 50 ml, was also prepared. Distilled water used for all Co analyses was passed through an AMBERLITE IR 120 (H) strongly acidic exchange resin which had been previously washed with 50 ml of 1 M hydrochloric acid and rinsed thoroughly with distilled water.

In addition to a direct calibration approach, a method of standard additions was used to check the presence of any matrix effects. Aliquots of each test solution (5 ml) were "spiked" with small volumes (0.02 - 0.24 ml) of concentrated Co stock solution. The mass of added Co was in proportion to the expected solution concentration. For

---

* *No Co contamination from the "Gilco" ring mill, used to prepare this sample, was found.*

Table 8.7 A.A. Operating Parameters for Co Analysis

Lamp Current	5 mA
Slit Width	0.025 nm
Wavelength	240.7 nm
Fuel / Support	acetylene / air
Flame Stoichiometry	oxidising
Scale Expansion	8 - 9
Concentration Range	0 - 3.48 ppm Co (calibration curve linear in this range)

example, four aliquots of a test solution, expected to contain ca. 0.7 ppm Co, were spiked with 0.7, 1.4, 2.1 and 2.8 ppm Co respectively.

The test solution (unspiked), a blank and four spiked test solutions were each analysed for Co. The Co concentration of these solutions was given by:

$$\text{concn (ppm)} = \frac{5x}{5 + v} + \frac{Cv}{5 + v}$$

where x represents the unknown concentration of the test solution to which v ml of stock solution (C ppm) has been added to 5 ml aliquots. If Beer's law is obeyed in the concentration range employed then:

$$(5 + v)\, A / 5 = \epsilon\, l\, (x + Cv / 5)$$

where A, ϵ and l have their conventional meanings in the Beer-Lambert relationship. Since the product ϵ l is constant through any series of measurements then a plot of (5 + v) A / 5 against Cv / 5 should give a straight line with an intercept corresponding to minus x.

Cobalt concentrations in 12 soil samples were calculated by the direct calibration and spiking methods. Results from the direct calibration approach, where matrix effects are largely ignored, were, on average, 33 % lower than those determined by the method of additions. Mitchell et al[174] also noted matrix interference in the determination of soil Co by A.A. Subsequent analyses of total Co levels in soils invoked the method of additions procedure.

(b) "Available" Co in Soils. Various methods have been used for determination of "available" Co in soils [175, 176] . The following method was used in this work. Samples (ca. 4 g) of air-dried soil (< 2 mm) were shaken vigorously overnight with 80 ml of 2.5 % acetic acid (prepared with deionised distilled water) in 250 ml conical flasks with plastic covered bungs. Samples were filtered through Whatman No. 42 filter paper into 100 ml beakers. Filtrates were reduced to 10 ml on a steam bath and, when cool, transferred to 10 ml volumetric flasks, and made to the mark.

Samples were analysed for Co using flameless atomic absorption spectroscopy (F.A.A.) A Varian Techtron Model 63 Carbon Rod Atomizer was used in conjunction with a Varian Techtron A.A. 5 Spectrophotometer. The instrumental parameters used in the determination of Co are summarized in table 8.8. A comparison of direct calibration and spiking methods showed agreement within experimental error. This was taken as justification for ignoring matrix effects which are presumably reduced by the ashing phase of the furnace cycle. A direct calibration approach was therefore used in conjunction with F.A.A. determination of Co. The presence of any non-atomic absorption was checked with the aid of a deuterium lamp.

(c) Co in Herbage. Samples containing up to 10 g of finely ground plant material were gently charred in a porcelin basin over a

Table 8.8 F.A.A. Operating Parameters for Co Analysis

Water Supply	flow rate ca. 0.5 l / min *(a)*
Mains Voltage	15 A supply *(b)*
Lamp Current	6 mA
Slit Width	0.15 nm
Wavelength	240.7 nm
Recorder	Yokogawa variable voltage chart recorder on 10 mV (direct reading) or 5 mV range
Sample Dispenser *(c)*	Oxford micropipette (5 μl) with disposable tip
Carbon Furnace Mode	STEP
Drying Phase *(d)*	4.0 / 60 sec
Ashing Phase *(d)*	7.5 / 15 sec
Atomizing Phase *(d)*	8.5 / 1.0 sec
Purging Gas *(e)*	Nitrogen (with Hydrogen diffusion flame during atomization)
Concentration Range	0 - 0.35 ppm Co (calibration curve linear in this range)

(a) *A constant flow rate was found to aid reproducibility.*

(b) *Minor fluctuations only were observed in the mains current.*

(c) *Originally an S.G.E. 5 μl syringe with an extractable metal needle was used; this was found to be the source of significant contamination.*

(d) *The furnace temperature was controlled by voltage steps calibrated in arbitary units.*

(e) *Commercially available "oxygen-free" nitrogen was found to prolong furnace life-times.*

low bunsen flame. Once charring was complete the samples were ashed at ca. 400 °C for 4 hrs and then digested with up to 50 ml 50 % HCl, 70 % $HClO_4$ (3:2 mixture) for 5 hours. Samples were then filtered through Whatman glass fibre filter paper into 100 ml beakers and reduced to minimum volume on a steambath. Once cooled, solutions were transferred to 25 or 50 ml volumetric flasks and made to the mark.

Standards used were those prepared for "available" Co. For herbage samples a Varian 775 double beam Atomic Absorption spectrophotometer was available. This also featured an automatic deuterium background corrector. The instrument was used in a direct concentration mode after initial calibration. Operating parameters were similar to those listed in table 8.8. No recorder was used however, advantage being taken of automatic integrating facilities in the instrument. Peak height mode was used with an integrating time of 20 seconds.

CHAPTER 9

STATUS OF THE UNDEVELOPED PAKIHI SOIL

In order to characterise the Maimai soil in the Bell Hill region in its "natural" state several chemical and mineralogical analyses were performed on soil samples. Except where stated, these samples were collected from areas prior to agricultural development. Analytical results are presented and discussed here as a background to aspects of this development outlined in chapter 10 as well as to highlight any important soil-forming processes.

A PHYSICAL PROPERTIES

9.1 Soil Description

9.1.1 Soil Classification

Two soil profiles, considered to be representative of the Maimai soil in the sampling region in its undeveloped state, were sampled to a depth of ca. 33 cm. The location of these profiles is described in section 8.1.1. Soil in close proximity to these two sites was classified by Mew [177] as Maimai fine sandy loam and Maimai silt loam. Tables 9.1 and 9.2 list the detailed profile descriptions made by Mew.

9.1.2 Volume-Weight Properties

Table 9.3 summarizes the results of physical measurements made on the two soil profiles studied, along with some data from survey samples (refer to table 8.1 for sampling details).

Average moisture content in the topsoil was high (46 - 67 % depending on time of sampling), confirming visual evidence of waterlogging

Table 9.1 Soil Profile from "Dairy Unit" Area

Classification: Maimai Fine Sandy Loam

Horizon Designation	Depth	Description
A_{1g}	0-14 cm (14 cm)	Brown to dark brown (7.5 YR 4/2) fine sandy loam; friable; weakly developed medium and fine crumb structure; abundant fine roots; indistinct smooth boundary,
G	14-32 cm (18 cm)	greyish brown (2.5 Y 5/2) silt loam; slightly sticky, non-plastic; massive; few medium prominent yellowish brown (10 YR 5/8) pseudo-mottles representing weathered greywacke stones; many fine roots; distinct irregular boundary,
Bfe	32-34 cm (2 cm)	red (2.5 YR 4/6) massive iron pan; indistinct irregular boundary,
B_3	34-52 cm (18 cm)	yellowish brown (10 YR 5/4) stony coarse sand; slightly firm; massive; many medium non-weathered greywacke, granite and some schist stones; indistinct wavy boundary,
C_1	on	olive grey (5 Y 4/2) stony sand; loose; single grain; many to abundant medium stones, as above.

Note: The profile site from which samples were collected for analysis differed only in horizon depths and in degree of formation of the iron pan.

Table 9.2 Soil Profile from "Ruru" Sampling Area

Classification: Maimai Silt Loam

Horizon Designation	Depth	Description
A_{1g}	0-19 cm (19 cm)	Dark greyish brown (10 YR 4/2) silt loam; friable; weakly developed fine crumb structure; slight iron mottling down root channels; abundant fine and few medium roots; indistinct smooth boundary,
G	19-51 cm (32 cm)	light brownish grey (2.5 Y 6/2) gritty silt loam; slightly sticky,slightly plastic; massive but soft and mushy; few small weakly weathered greywacke stones, strong brown (7.5 YR 5/8) in colour giving pseudomottled appearance; few fine and medium roots; distinct wavy boundary,
Bfe	51-51.4 cm (0.4 cm)	dark reddish brown (2.5 YR 3/4) massive cemented iron pan; indistinct irregular boundary,
C_1	on	olive brown (2.5 Y 4/4) compact stony moraine, mainly greywacke.

Note: The profile site from which samples were collected for analysis differed only in horizon depths and in degree of formation of the iron pan.

Table 9.3 Volume-Weight Properties

Sampling Area	Horizon	Depth	Ave. Moisture Content	Material > 2 mm	Dry Bulk Density
		(cm)	(%)	(%)	(g cm^{-3})
Bell Hill Undeveloped (Site BU 101)	A_{1g}	0 -12.7	56 *(a)*	6 *(b)*	0.49 *(b)*
	G	12.7-17.8	20		0.70
	B_3	17.8-33.0	26		1.04
Ruru (Site RR 112)	A_{1g}	0 -17.8	57	4	0.46 *(c)*
	G	17.8-23.0		65	
		23.0-33.0		39	

(a) *This figure represents an average value from several survey samples collected from the developed Dairy Unit; range observed during seasonal variations was 46 - 67 %.*

(b) *Data determined from survey sample BU/JA76, collected from the Bell Hill Undeveloped area, 0 - 11.3 cm (see also table 8.1).*

(c) *Figure determined from survey sample RR/SP75, collected from the Ruru area before development, 0 - 14.9 cm (see also table 8.1).*

throughout substantial periods of the year. The average dry bulk density of the topsoil was low (< 0.5 g cm^{-3}) consistent with the presence of significant amounts of relatively undecomposed organic matter. In the lower horizons the presence of weakly-weathered gravels accounts for the rather larger proportion of material > 2 mm. The stony texture of the G horizon, especially in the Ruru area, suggests that despite prolonged waterlogging, once pasture is established, the soil could support stock without the severe pugging observed on other West Coast wetland soils. (Field observations in the developed Dairy Unit area, which has supported cattle since 1974, generally confirmed this).

9.2 Clay Mineralogy

9.2.1 Particle Size Analysis

Clay - (< .002 mm), silt - (.002 mm - .02 mm) and sand - (> .02 mm) sized fractions were separated from deferrated soil samples in the course of mineralogical analysis (see section 8.4). Table 9.4 summarizes relevant particle size data (on a weight/weight basis) from the soil profile studied in the Bell Hill Undeveloped area, some topsoil samples from the same area and the Ruru soil before development. Figure 9.1 presents these data on a weight/volume basis.

Soils may be classified into textural classes by their particle size distributions [178]. On this basis the topsoil in the Dairy Unit was designated as a "loamy sand" or a "sandy loam" while that in the Ruru area corresponded to a "silt loam".

A relatively larger proportion of clay was found in the topsoil of the Ruru sample (20 %) compared with the soil from the Bell Hill Undeveloped area (9 - 14 %). Clay contents, expressed in weight/volume terms, increased with depth in the profile studied (figure 9.1).

Table 9.4 Particle Size Analysis

Sampling Area	Horizon	% Sand > .02 mm	% Silt .002 - .02 mm	% Clay < .002 mm
Bell Hill Undeveloped (Site BU 101)	A_{1g} (0 - 7.6 cm)	65.4	25.4	9.2
	A_{1g} (7.6 - 12.7 cm)	62.4	26.6	11.0
	G (12.7 - 17.8 cm)	66.3	24.7	9.0
	B_3 (17.8 - 33.0 cm)	60.3	25.0	14.7
Bell Hill Undeveloped (BU/SP75) *(a)*	A_{1g} (0 - 12.7 cm)	54.2	32.0	13.8
	A_{1g} (0 - 12.7 cm)	46.7	40.8	12.5
Ruru (RR/SP75) *(b)*	A_{1g} (0 - 15.2 cm)	47.0	32.8	20.2

(a) *"Representative" selection of sample sites (see also table 8.1).*

(b) *Survey sample collected from the Ruru area prior to development.*

It is generally considered that increasing clay content is associated with increasing soil weathering[179] . The observed trend in clay contents with profile depth points to a well developed soil in which clay from the upper horizon has been removed. A fluctuating water-table regulating the translocation of clay through leaching may account for this removal. Campbell, however, has suggested clay destruction in the presence of "organic chelates" and low pH conditions, occurring over a long time period, was responsible for low clay contents (5 - 10 %) of the

Figure 9.1 Clay Contents of "Bell Hill Undeveloped" Profile

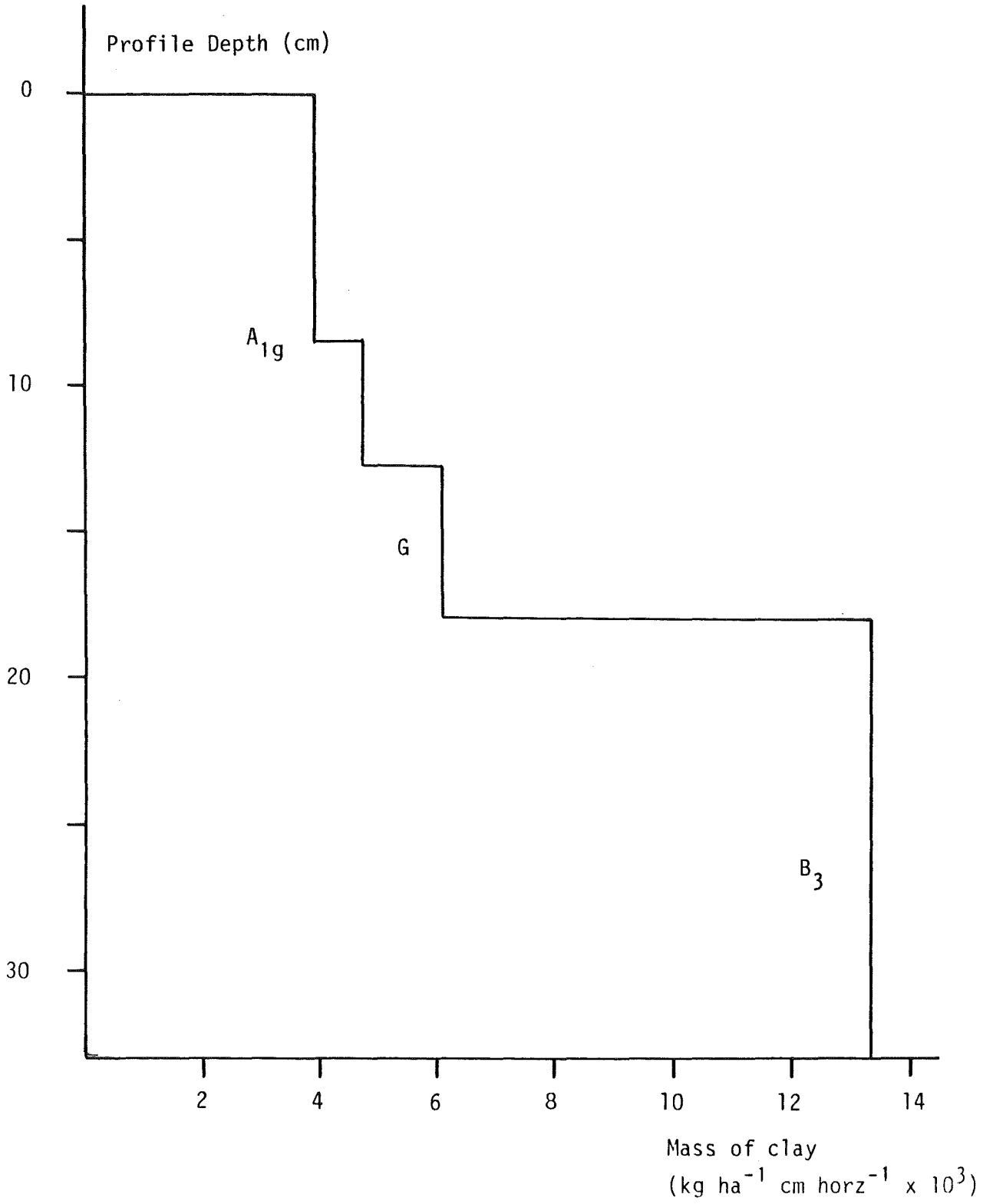

poorly-drained gley podzols Okarito and Kumara [179]. Increasing clay content with depth was observed in profiles of these two soil types also.

9.2.2 Clay Mineral Types

The soil samples listed in table 9.4 were studied by X-ray diffraction to determine principal clay minerals. Diffraction patterns for four of these samples (A_{1g}, G and B_3 horizons of the "Bell Hill Undeveloped" profile and A_{1g} horizon from the Ruru area) are illustrated in figure 9.2.

Diffraction patterns of clays from A horizons showed two main broad reflections corresponding to basal spacings of between 1.0 and 1.4 nm (typically ca. 1.26 nm) and between 1.4 and 1.8 nm (typically ca. 1.6 nm) respectively, when saturated with Mg^{++} and solvated with 1 % glycerol solution. Saturating these clays with K^+ at room temperature resulted in relatively sharp reflections at 1.0 nm (intense) and 5.0 nm (weak). This pattern was attributed to the presence of mica-vermiculite (the shorter wavelength) and vermiculite-montmorillonite interstratified minerals. Reflections between 2.5 and 3.5 nm indicated some regularity in the stratification. A weaker reflection at 1.0 nm in Mg^{++} saturated/glycerol solvated clays indicated the presence of the non-expanding illite mineral (mica). Clay from the Ruru area contained some kaolinite evidenced by a weak reflection corresponding to a basal spacing of ca. 0.715 nm, which disappeared on heating to 550 °C. Quartz, with reflections at 0.425 and 0.336 nm was observed in all clay samples studied.

A similar pattern of reflections was observed in subsoil samples (horizons G and B_3) with two additional features being apparent. Firstly, a weak reflection corresponding to a basal spacing of 1.4 nm in K^+-saturated clay from the G horizon sharpened and intensified on heating to 550 °C, indicating the presence of primary chlorite in this horizon. In clay from the B_3 horizon, a very sharp intense peak in the diffractogram was observed

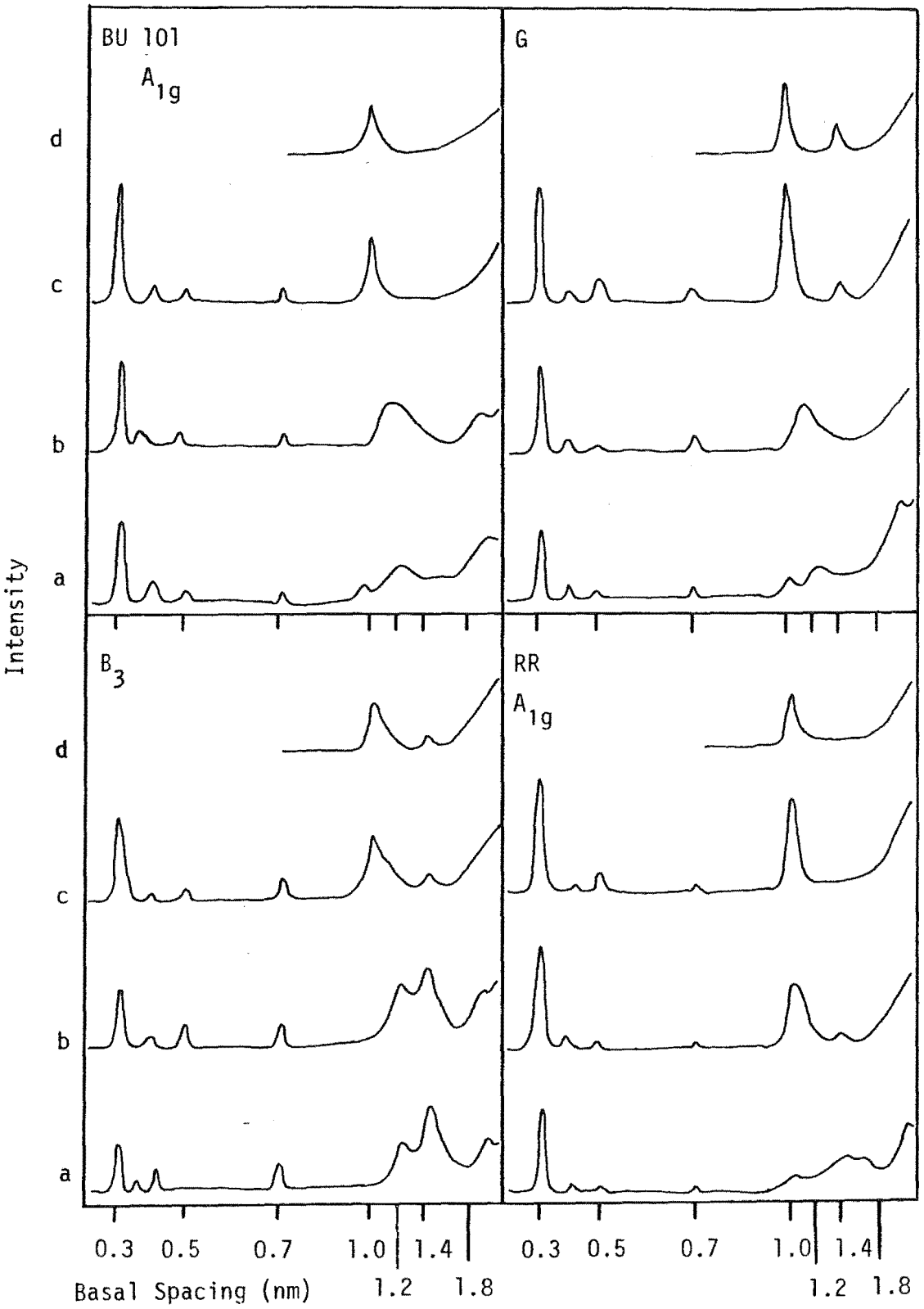

Figure 9.2 Diffractograms of Clay Fractions from BU and RR Areas

(a) Mg-satd/glycerol (b) K-satd, 20 °C
(c) K-satd, 350 °C (d) K-satd, 550 °C

at a basal spacing of ca. 1.4 nm. This reflection gradually weakened on saturation with K^+ and heating to 550 °C, with a corresponding gain in intensity at 1.0 nm. A small peak at 1.4 nm remained after heating to 550 °C suggesting a 2:1 - 2:2 Al-intergrade (otherwise known as pedogenic chlorite or chloritised vermiculite). The properties of this intergrade are intermediate between those of vermiculite and chlorite and its resistance to collapse on heating results from the presence of hydroxyalumina polymers in the interlayer spaces. No mica was observed in the B_3 horizon.

Results presented here are consistent with the weathering of mica and primary chlorite to vermiculite intergrades and pedogenic chlorite. Since weathering intensity normally decreases with depth, the presence of pedogenic chlorite in the B_3 horizon and its absence from the upper horizons suggests an additional process operating. In his study of gley podzols of the West Coast Campbell[180] concluded that the onset of a combination of low pH conditions (< 4.5) and high organic matter levels (often associated with the growth of individual red beech trees) can initiate a secondary weathering cycle . In this process, soil profiles developing towards laterites, with a relative accumulation of Fe and Al over Si in the upper horizons, undergo rapid loss of these two metals under the influence of soil organic matter and intense acid leaching conditions. This leads to the destruction of allophane, gibbsite and ferromagnesian chlorite and the dealumination of pedogenic intergrades. The direction of weathering has thus been altered towards a podzolic end product.

The clay mineralogy of the Maimai profile described in this work is consistent with this model for podzolic development, although the weathering process observed by Campbell in other West Coast podzols, with end products of montmorillonite and kaolin, is not as far advanced in this soil. This may be due, in part, to the slightly higher pHs (4.5 - 4.9) prevailing in the topsoil compared with those considered ideal for podzolic development (< 4.5)[180] .

B CHEMICAL PROPERTIES

9.3 Iron and Aluminium

Levels of iron and aluminium extracted by two commonly-used reagents have been determined as a background to the soil fertility study presented in chapter 10 (hydrated oxides of iron and aluminium are largely responsible for the retention of phosphate and sulphate in acid soils[181]) and to provide additional information about the nature and degree of the weathering processes that have been operating in this soil (the amount and distribution of various forms of iron and aluminium is a function of such processes as the weathering of primary minerals, crystallisation and resilication of amorphous iron and aluminium constituents, leaching and the organic cycle).

9.3.1 Amorphous Fe and Al

Amorphous compounds of iron and aluminium are thought to exist as coatings on crystalline particles or as separate identities [182]. Leaching of soil columns with an acid/oxalate solution (Tamm's solution) extracts amorphous iron and aluminium without extensively attacking the less soluble crystalline forms[183] . The oxalate ion, $C_2O_4^{=}$ complexes with Fe^{3+} and Al^{3+} at the pH of extraction (ca. 3.3). Table 9.5 summarizes data for Tamm's oxalate-extractable Fe and Al for soil from the Dairy Unit and the Bell Hill Undeveloped areas, including the profile sampled in that region.

9.3.2 Crystalline Fe and Al

Both microcrystalline and amorphous compounds of iron and aluminium are considered to be extracted when soil samples are the subject of strong reducing conditions (dithionite) in the presence of a citrate

complexing agent [183]. Results of citrate-dithionite extractions are included in table 9.5. Also included in table 9.5 are results for total iron as determined by Hennessy [184] using X-ray fluorescence.

9.3.3 Discussion

Evidence of substantial leaching of Fe and Al from the upper horizons of the soil profile and possible deposition in the B_3 horizon was found for the soil profile studied. The yellow-brown colour of the B_3 horizon (which persisted after ashing at 400 °C) was attributed to the presence of iron oxides whereas Lee[185] suggested humic staining was responsible for the colour of the B_3 horizon of a soil profile in the Dairy Unit.

Recently it has been suggested[186] that a level for Tamm's extractable Al of > 0.6 % is a suitable diagnostic criterion for a podzol B_f horizon. The horizon designated B_3 in profile 101 meets this requirement.

Total iron increased down the soil profile. Indications were that a larger fraction of total Fe was in the amorphous form in the upper horizons whereas more crystalline Fe was present in the G and B_3 horizons (see table 9.5). This suggests that with comparatively rapid movement of iron from the upper horizons extensive crystallization has been restricted in these horizons.

Levels of citrate-dithionite extractable iron and aluminium in the topsoil from the Ruru area (0.34 and 0.17 kg ha^{-1} cm $horz^{-1}$ x 10^3 resp.) were higher than those from the corresponding horizons in the Bell Hill Undeveloped area (0.06 and 0.02 kg ha^{-1} cm $horz^{-1}$ x 10^3 resp.). These data suggest that the translocation of iron in the Ruru area has not been sufficient to substantially hinder the crystallization process. This is consistent with field observations where it was noted that typical podzolization features, such as iron-pan formation, were generally

Table 9.5 Iron and Aluminium in Undeveloped Pakihi Soil

Sampling Area	Horizon	Total-Fe (Fe_T)	Tamm's-extractable			Citrate-Dithionite extractable		
		(a)	Fe *(a)*	% of Fe_T	Al *(a)*	Fe *(a)*	% of Fe_T	Al *(a)*
Bell Hill Undeveloped (Site BU 101)	A_{1g} (0 - 7.6 cm)	0.30	0.17	53	0.05	0.06	19	0.02
	A_{1g} (7.6 - 12.7 cm)	0.32	0.17	52	0.05	0.11	35	0.02
	G (12.7 - 17.8 cm)	0.88	0.13	15	0.07	0.60	68	0.10
	B_3 (17.8 - 33.0 cm)	3.64	1.01	28	0.98	1.97	54	0.84
Bell Hill Undeveloped (BU/SP75)	A_{1g} (0 - 12.7 cm)					0.30		0.05
Dairy Unit (DU-68/SP75)	A_{1g} (0 - 7.5 cm)		0.21		0.11			
Ruru (RR/SP75)	A_{1g} (0 - 15.2 cm)		0.24		0.11	0.34		0.17

(a) *Units of kg ha^{-1} cm $horz^{-1}$ x 10^3 have been used throughout.*

Note *Tamm's Fe and Al analyses performed by Tsao [187], Fe_T by Hennesey [184].*

less well developed in the Ruru area compared with the Dairy Unit or Bell Hill Undeveloped areas. One important consequence of this was the higher P-retention predicted for the topsoil of the Ruru area (see also section 9.5). Levels of Fe and Al and hence phosphate adsorption in this Maimai soil were found to be higher than many of the other wetland soils analysed by Lee [149].

9.4 Carbon, Nitrogen

Table 9.6 summarizes data from the determination of oxidisable carbon (oxidimetric chromic-acid procedure) and nitrogen (micro-Kjeldahl procedure) from two soil profiles and two survey samples covering both undeveloped pakihi areas in the study region. These data are presented both on a weight/weight and a weight/volume basis.

Carbon and nitrogen levels in topsoil samples were medium to medium-high by New Zealand Soil Bureau ratings[188] and decreased steadily down the soil profiles. Carbon-nitrogen ratios were consistently high throughout the soil profile (typical of the wetland soils [189]), ranging from 16.4 (A_{1g} horizon) to 22.0 (B_3 horizon). Under acid, waterlogged conditions where microbial activity is inhibited, slow decomposition of litter of low base status has resulted in these high C/N ratios.

Subsurface accumulation of organic matter, a feature of some podzols, was not observed in the two profiles studied, although Lee reported increased organic-carbon levels in the B_3 horizon of a profile within the Dairy Unit [185].

9.5 Phosphorus, Sulphur

Table 9.7 summarizes phosphorus and sulphur data from undeveloped soils in the study region.

Total-P in the soils studied ranged from 7 to 30 kg ha^{-1} cm $horz^{-1}$.

Table 9.6 Carbon and Nitrogen Levels in Undeveloped Pakihi Soil

Sampling Area	Horizon	Carbon		Nitrogen		C/N
		(%)	*(a)*	(%)	*(a)*	
Bell Hill Undeveloped Area (Site BU 101)	A_{1g} (0 - 7.6 cm)	7.4	3.63	0.45	0.22	16.4
	A_{1g} (7.6 - 12.7 cm)	5.3	2.60	0.31	0.15	17.3
	G (12.7 - 17.8 cm)	2.4	1.68	0.12	0.08	19.7
	B_3 (17.8 - 33.0 cm)	2.2	2.29	0.10	0.10	22.0
Bell Hill Undeveloped (BU/JA76)	A_{1g} (0 - 12.7 cm)	9.0		0.52		
Ruru (Site RR 112) *(b)*	A_{1g} (0 - 17.8 cm)	7.1	3.27	0.41	0.19	17.3
	G (17.8 - 23.0 cm)	2.8	1.96	0.15	0.10	18.7
	G (23.0 - 33.0 cm)	2.9	2.03	0.15	0.10	19.3
Ruru (RR/SP75)	A_{1g} (0 - 15.2 cm)	9.8	4.51	0.50	0.23	19.6

(a) *Units of kg ha^{-1} cm $horz^{-1}$ x 10^3.*

(b) *Volume-weight data calculated using bulk density data estimated from the Bell Hill profile.*

The P-content of the B_3 horizon was greater than that of the topsoil and this reflects the high levels of Fe and Al in this lower horizon.

Organically-bound phosphorus represents between 60 and 90 % of the total-P content of the A_{1g} horizon. This is consistent with the accumulation of organic matter and extensive leaching of inorganic forms of phosphorus typical of a podzolised soil.

Phosphate in the inorganic fraction is largely associated with iron and aluminium in soils of pH below 6.5. Sorption occurs at positively charged sites on the surface of iron and aluminium hydrous oxides attached to clay particles. Results for soils taken in the sampling region indicated a close relationship between phosphate retention and Fe and Al extracted by Tamm's oxalate reagent (see figure 9.3). A similar correlation has been observed by other workers[190]. The phosphate sorption properties of the subsoil were observed to be higher than those of the upper horizons. This is consistent with relatively higher levels of iron and aluminium lower in the profile - a feature of podzolized soils.

Phosphate retention of the topsoil of the Ruru sampling area (40 - 50 %) was higher than that from the Bell Hill Undeveloped region (19 - 34 %). This is again related to higher levels of iron and aluminium which, in this soil, appear to be related to the higher clay content of the Ruru soil (20 % cf. 9 - 14 % in the Bell Hill area). This suggests that the P-fertilizer requirements for pasture development would be higher for this area.

The proportion of inorganic P soluble in 0.5 M H_2SO_4 (representing poorly ordered phosphate species weakly bound to the surface of clay particles) decreases with increasing weathering due to the slow occlusion of "crystalline" phosphate within the amorphous clay colloids (fixation). This proportion can range from 5 % - 100 %[181]. A-horizons showed 50 - 60 % indicating a moderate degree of weathering, whereas lower in the profile this fraction was typically 22 - 27 %. With lower P-retention in the A horizon, phosphate has been removed from the upper horizons before significant occlusion has taken place. Phosphorus extracted by Truog's reagent (10^{-3} M H_2SO_4) providing a measure of plant available-P, was very low in A_{1g} horizons.

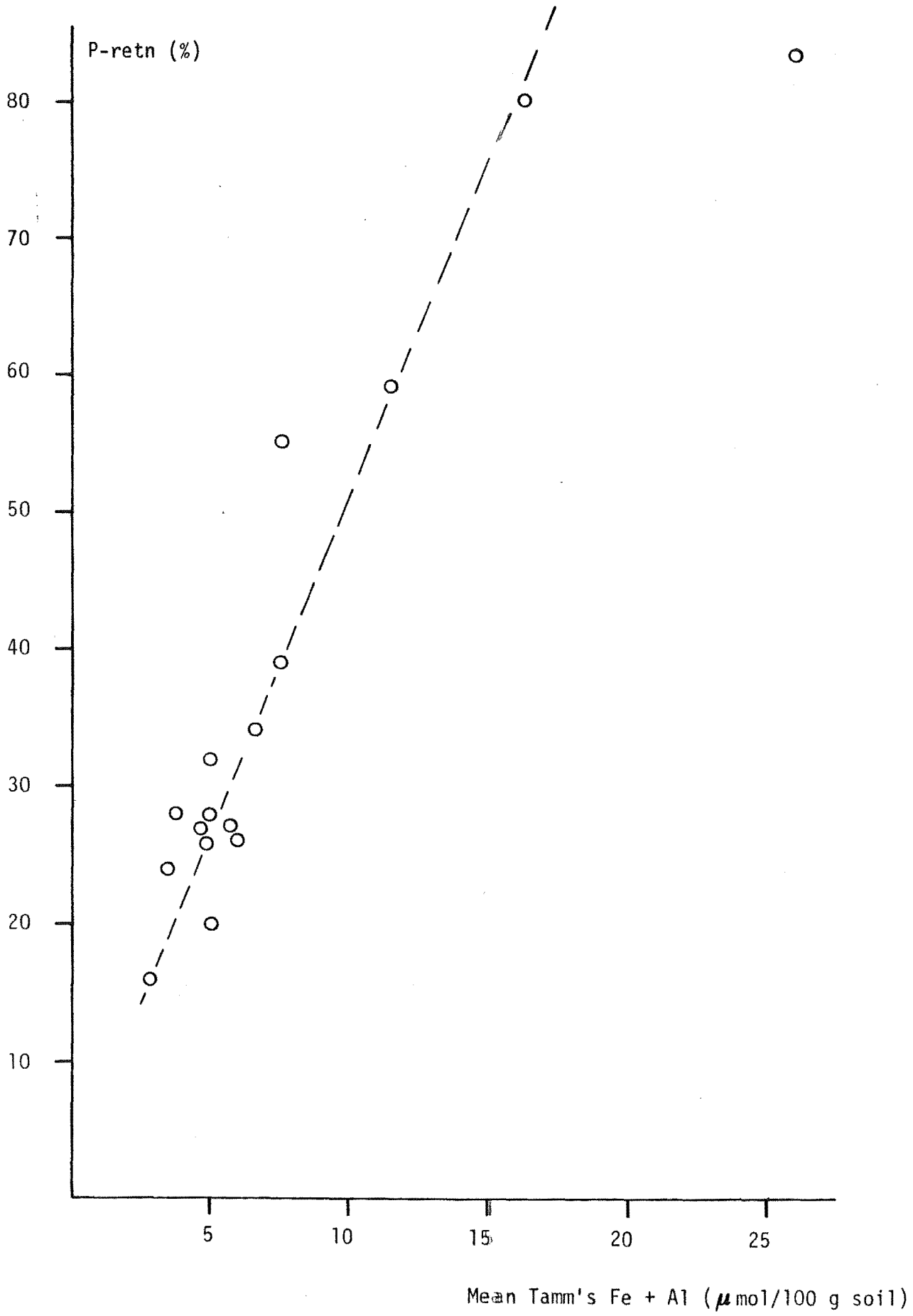

Figure 9.3 Correlation Between Mean "Tamm's" Fe + Al and P-retention

Table 9.7 Phosphate and Sulphate Data From Undeveloped Pakihi Soil

Sampling Area	Horizon (Depth (cm))	Total-P (a)	Org-P	Inorg-P	0.5 M H_2SO_4 sol-P	% Acid-sol/Inorg	% Org/Total	Truog-P	P-retn	Ad SO_4-S (b)	S-retn
Bell Hill Undeveloped (Site BU 101)	A_{1g} (0 - 7.6)	11.5	7.25	4.26	2.40	56	63	0.59	19.6	0.73	
	A_{1g} (7.6 - 12.7)	7.06	5.00	2.06	1.23	59	71	0.15	31.6	0.30	12
	G (12.7 - 17.8)	9.67	4.69	4.97	1.33	27	49	0.35	24.2	0.57	8
	B_3 (17.8 - 33.0)	29.0	14.6	14.5	3.64	25	50	1.04	82.8	3.1	75
Bell Hill Undeveloped (BU/JA76)	A_{1g} (0 - 11.3)	18.6	14.2	4.40	3.45	79	76	0.44	33.5		4
Ruru (Site RR 112)	A_{1g} (0 - 17.8)	13.5	12.0	1.43	0.97	68	89	0.18	39.5		22
	G (17.8 - 23.0)	16.5	10.4	6.09	1.33	22	63	0.02	48.5		
Ruru (RRSP/75)	A_{1g} (0 - 15.2)	14.4	10.0	4.37	1.38	32	70	0.23	50.0		

(a) Apart from percentage data, units used throughout are kg ha^{-1} cm $horz^{-1}$.

(b) Adsorbed sulphate-sulphur data determined by E.S. Lee[156].

Sulphate adsorption in soils is thought to be effected by oxides of iron and aluminium, especially aluminium [191]. Levels of adsorbed sulphate in the sampling region were generally low as might be expected of a strongly podzolised acid soil. The lower horizon, B_3, showed the largest concentration of SO_4-S and this is consistent with the higher concentrations of iron and aluminium already noted for this horizon.

Sulphate retention was very low in the upper horizon of the Bell Hill profile (4 - 12 %) but higher in the Ruru soil (22 %) where levels of iron and aluminium (and clay content) are higher.

9.6 Cation Exchange Properties

Various cation exchange properties for the two soil profiles studied, as well as several topsoil samples, are summarized in table 9.8.

Low pH values (< 5.0) were observed in A_{1g} horizons consistent with extensive leaching under high rainfall and acidic litter. A slight rise in soil pH was observed down the soil profile.

Levels of exchangeable bases were low to very low by New Zealand Soil Bureau ratings[188] (viz Σcat_{ex} < 5 me/100 g soil), again consistent with extensive leaching of the soil. A decrease in total exchangeable bases was observed down the soil profile with a slight increase in the B_3 horizon.

Cation exchange capacities (CEC) were medium to high (viz > 20 me/100 g soil), reflecting the relatively large surface accumulations of organic matter. The high cation exchange capacity of the B_3 horizon probably reflects an increase in clay content in this horizon. Cation exchange capacities have been significantly correlated with clay and organic matter contents [192]. Trends noted in this work suggest that CECs of surface horizons are primarily a function of organic matter while those of lower

Table 9.8 Exchangeable Cation Status of Undeveloped Pakihi Soil

Sampling Area	Horizon (Depth (cm))	K_c (a)	Mg_r	Soil pH H_2O	Soil pH $CaCl_2$	Ca_{ex}	Mg_{ex}	K_{ex}	Na_{ex}	Σcat_{ex}	CEC	% BS
Bell Hill	A_{1g} (0 - 7.6)	0.074	0.15	4.9	3.7	0.88	0.44	0.18	0.14	1.64	10.5	15.5
Undeveloped	A_{1g} (7.6 - 12.7)	0.078	0.17	4.7	3.7	0.38	0.22	0.07	0.10	0.78	9.5	8.2
(Site BU 101)	G (12.7 - 17.8)	0.160	3.29	5.0	4.0	0.08	0.08	0.04	0.08	0.29	8.4	3.4
	B_3 (17.8 - 33.0)	0.400	13.20	5.5	4.5	0.07	0.09	0.07	0.19	0.43	18.2	2.3
Bell Hill												
Undeveloped	A_{1g} (0 - 11.3)	0.063	0.95	4.6	3.5	1.52	0.47	0.09	0.02	2.10	11.3	18.3
(BU/JA76, BU/SP75)												
Ruru	A_{1g} (0 - 17.8)			4.8	4.3	0.25	0.23	0.08	0.02	0.58	12.3	4.7
(Site RR 112)	G (17.8 - 23.0)					0.12	0.10	0.04	0.04	0.30	11.1	2.7
	G (23.0 - 33.0)					0.04	0.10	0.02	0.04	0.20	11.3	1.8
Ruru	A_{1g} (0 - 15.2)	0.14	1.20	4.8	4.3	0.35	0.26	0.09	0.02	0.71	11.4	6.2
(RR/SP75)												

(a) Apart from soil pH, units used throughout are me ha^{-1} cm $horz^{-1}$ x 10^6.

horizons depend to a greater extent on clay content and type.

Values of K_c, representing the long-term potassium supplying potential of the soil[163], increased with depth. With the predominance of mica and vermiculite intergrades (clay types capable of fixing potassium) throughout the soil profile, this trend was expected from the relative clay contents of each horizon (see figure 9.1).

Magnesium reserves, represented by Mg_r values [164], followed a similar pattern with relatively high levels observed in the G and B_3 horizons. This trend is consistent with the presence of magnesium-bearing chlorite minerals observed in the lower horizons.

Soil from the Ruru sampling area showed higher reserves of both potassium and magnesium in the A_{1g} horizon (viz 0.14 and 1.20 respectively cf. Bell Hill Undeveloped 0.07, 0.15 - 0.95 x 10^6 me ha^{-1} cm $horz^{-1}$). This probably reflects the larger clay content of the soil in this area. However, values for K_c and Mg_r were not particularly high (relative to New Zealand Bureau ratings [160]) for soil from either of these sampling areas and it was expected that supplements of these two elements would be required for adequate pasture growth and stock health (this is discussed further in chapter 10).

9.7 Summary

The physical and chemical properties of the Maimai soil studied reflect many of the features of a moderately weathered podzolic soil. Extensive leaching of the topsoil has left impoverished and acidic A_{1g} and G horizons with surface accumulation of organic matter. The presence of compact horizons as well as impervious iron-pans, has resulted in extensively waterlogged flat-land soils.

Clay contents increased with depth with pedogenic chlorite (a 2:1 - 2:2 Al-intergrade) noticeable in the B_3 horizon. A larger fraction of total iron was present in micro-crystalline form in the lower horizons

whereas amorphous forms dominated the A_{1g} horizon. The proportion of inorganic phosphate soluble in 0.5 M H_2SO_4 decreased with soil depth. These observations are consistent with the influence of secondary weathering effects, involving dissolution and/or destruction of crystalline clay minerals and the translocation of iron and aluminium from surface horizons under intense leaching in the presence of acidic organic litter.

The topsoil has been largely depleted of many important plant nutrients. This, combined with low reserves of potassium and magnesium and relatively high phosphate fixing properties (Ruru area in particular), suggests a comprehensive fertilizer programme for adequate pasture development. The combination of high rainfall and poor drainage presents a further major hurdle to viable agriculture on this soil.

CHAPTER 10

AGRICULTURAL DEVELOPMENT OF A MAIMAI SOIL

Two farm blocks within the Bell Hill region, namely the "Dairy Unit" and "Ruru" areas, have been sampled prior to and during agricultural development and utilization. Results are presented here for levels of major nutrients in soil, herbage and water covering a time period of up to five years. The main emphasis is on the soil analyses. These levels are discussed in the light of proposed and actual fertilizer applications. The inherent spatial variability of various soil chemical properties is evaluated.

In most cases results are presented on a "per hectare centimetre horizon" (ha^{-1} cm $horz^{-1}$) basis and, except where otherwise stated, a soil depth of 7.6 cm has been assumed in calculating rates of fertilizer application. This depth is commonly taken to represent the zone of maximum root activity [193].

10.1 Variability of Soil Chemical Properties

In order to assess the significance of yearly changes in average nutrient levels in the topsoils of the study region, a simple random sample was collected from the Dairy Unit area (see chapter 8, section A). Up to forty individual soil cores were analysed for exchangeable cations, carbon, nitrogen and "Truog" - phosphorus in order to determine the inherent variability of these soil chemical properties in the study region. The results of these analyses are summarized in table 10.1 in the form of coefficients of variation C (the standard deviation of n sampling units expressed as a percentage of the mean). Coefficients of variation previously determined from "representative sites" (see section 8.3.2)

Table 10.1 Coefficients of Variation for Soil Chemical Properties

Analysis *(a)*	Dairy Unit Survey				Adams and Wilde	
	weight basis		volume basis		(%)	*(d)*
	(%)	*(b)*	(%)	*(c)*		
pH (0.01 M $CaCl_2$)	(9)				10	
Ca_{ex}	72		38		40	
Mg_{ex}	57		56		33	
K_{ex}	41		37		66	
Na_{ex}	60				49	
Σ cat_{ex}	67				34	
CEC	44		22		19	
% BS	34				25	
% C	29					
% N	26				23	
C/N	11					
Truog - P	70		81			
P - retn	(34)				25	
0.5 M H_2SO_4 - P	(91)				67	
Total Ca					16	
Total K	(16)				10	

(a) *Data in this table are based on analyses by Lee [156] and Tsao [157].*

(b) *Values in parentheses are from "representative" sites (data from table 8.2).*

(c) *Several analytical results were re-calculated on a per volume basis rather than a per weight basis using dry bulk density data.*

(d) *Data from a survey by Adams and Wilde [158] on Westmere silt loam are included. A total of 32 sampling sites over a single soil mapping unit (scale 1:31 680), 0 - 10 cm depth were used.*

as well as statistical data determined by Adams and Wilde [158] for soils in the Wanganui, New Zealand, district are included for comparison.

Data in table 10.1 illustrate the high natural variability typical of many soil chemical properties. Of those results re-calculated on a volume basis, exchangeable - Ca and cation exchange capacity values showed a marked reduction in variability. This reflects the variation in bulk density observed in the topsoils of the study region due mainly to accumulations of undecomposed organic matter.

Variability among sampling units depends very much on the particular soil chemical property measured as well as the size of the area surveyed. Factors contributing to this variability include variations in parent material, topography and soil management, and have been discussed by Beckett and Webster[194] . Summarizing a large number of studies, these authors separated soil properties into three groups of low, medium and high average variabilities respectively. Adams and Wilde[158] extended this classification by assigning ranges of C values to each group. Table 10.2 details these groups.

Table 10.2 Classification of Coefficients of Variation of Soil Chemical Properties

Group	Range of C (%)	Soil Properties
I	12 - 19	Total Ca, K
II	21 - 31	Total N, CEC, Σcat_{ex}, % BS, P - retn
III	36 - 111	Ca_{ex}, Mg_{ex}, Na_{ex}, K_{ex}, 0.5 M H_2SO_4- P

Results presented in this study show general agreement with this broad classification. In addition to the analyses described by Adams, the following additions to the various groups could be made: Group I, C/N ratio

(C ca. 11 %); Group II, % C (C ca. 29 %) and Group III, Truog - P (C ca. 70 %).

It should be noted that many of the variability studies presented in the literature have been based on non-random siting of sampling units and therefore cannot be strictly regarded as bias-free.

10.2 Sampling Errors

Once unbiased estimates of the population variance were found the sampling error, $se(\bar{x})$, for any mean nutrient level was calculated as a function of sampling size. From equation 8.2 we have:

$$se(\bar{x}) = sn^{-\frac{1}{2}}$$

Values of s, for analyses done on topsoil samples, are listed in table 8.3. These data along with the appropriate value of n, the sample size, were used to calculate $se(\bar{x})$ for each survey sample collected.

Variability in soil chemical attributes calculated in this study reflect the natural heterogeneity possessed by the soil itself as well as the effect of grazing stock in their irregular return of dung and urine [193]. The effect of seasonal variations in soil nutrient levels has not been distinguished. In addition to these sampling "errors" there were the usual uncertainties associated with the various analytical methods. In general these were less than the sampling error [195]. In the presentation of results, the larger of the errors is diagramatically represented by "error bars" in the appropriate figures (e.g. figures 10.2 - 10.4).

10.3 Estimating Fertilizer Requirements

The Ruru area was first sampled prior to planned pastural development. Hence the opportunity existed to estimate initial fertilizer

requirements. Several different methods can be used for making such estimates. The following sections consider some of these in the estimation of initial lime and phosphate application rates for the Ruru soil.

10.3.1 Lime

The application of lime for the development of many New Zealand soils has become standard practice. In most cases the desired effect is the raising of the soil pH and the increasing of levels of the major plant nutrient, calcium. Other important reasons have been summarised by Miller[196]. The acid wet land soils of the West Coast have required substantial quantities of lime for initial pasture development and in particular for the establishment of clover. The rate of application of lime depends on both the properties of the soil in question and the quality of the limestone itself. One method of determining initial lime-requirements involves the calculation of the amount of lime needed to raise the % BS of the soil to 60 %[188]. This amount often raises the soil pH to about 6[196].

The lime-requirements of the Ruru sampling area were calculated prior to pasture development. The CEC of this soil was found to be 25 me / 100 g soil, while % BS was 6 %. Hence, to raise % BS to 60 %, ca. 13.5 me / 100 g soil of Ca^{++} would be required if it is assumed that all added calcium becomes "available". This corresponds to approximately 3 tonnes of agricultural limestone (assumed to be 80 % $CaCO_3$) per hectare, 7.6 cm (ca. 3 inches) deep. This estimated lime-requirement takes no account of losses of Ca^{++} by leaching or other means.

During has formulated an empirical approach for the estimation of initial liming rates appropriate for three broad classes of soils[197]. For one of these classes, silt loams, he suggested that 2.5 tonne ha^{-1}

of lime will increase the soil pH by about 0.4 - 0.5 units in the top 7.6 cm. On this basis "expected" pH levels for the Ruru soil, following initial lime application of up to 7.4 tonne ha^{-1}, have been calculated (table 10.3). These data suggest that an application of approximately 6 tonnes of lime per hectare would be required on the undeveloped Ruru soil to raise the pH to 6.0.

The actual liming rates used and subsequent development of the Ruru area are considered in section 10.4

10.3.2 Phosphate

Phosphate requirements for pasture development depend on several factors. These include the phosphate - fertility of the virgin soil, phosphate - sorption characteristics of the soil and planned stocking rates.

One method for the determination of initial soil-phosphate requirements involves the establishment of a phosphate - sorption isotherm curve, from which the amount of phosphate required to sustain what is considered to be an optimum soil concentration of 0.2 ppm P [198] can be determined (see section 8.5.7*(g)*).

In a laboratory experiment, an artifically limed soil (rate of application equivalent to 6.1 tonne ha^{-1} lime; pH 6.3;i.e. sample RR 14L), from the Ruru sampling region, was incubated with calcium dihydrogen phosphate solution at various concentrations (see section 8.5.7). Figure 10.1 presents the results as phosphate sorbed plotted as a function of phosphate remaining in solution. At a soil solution concentration of 0.2 ppm P the equivalent of 120 kg P per 7.6 cm hectare was sorbed (or 1.2 tonne ha^{-1} superphosphate with 10 % P content [199]). The pH of the soil used in this experiment was higher than that of the Ruru soil following actual initial lime application (viz 6.3 cf. field pH 5.5). Since

Figure 10.1 P-Sorption Isotherm

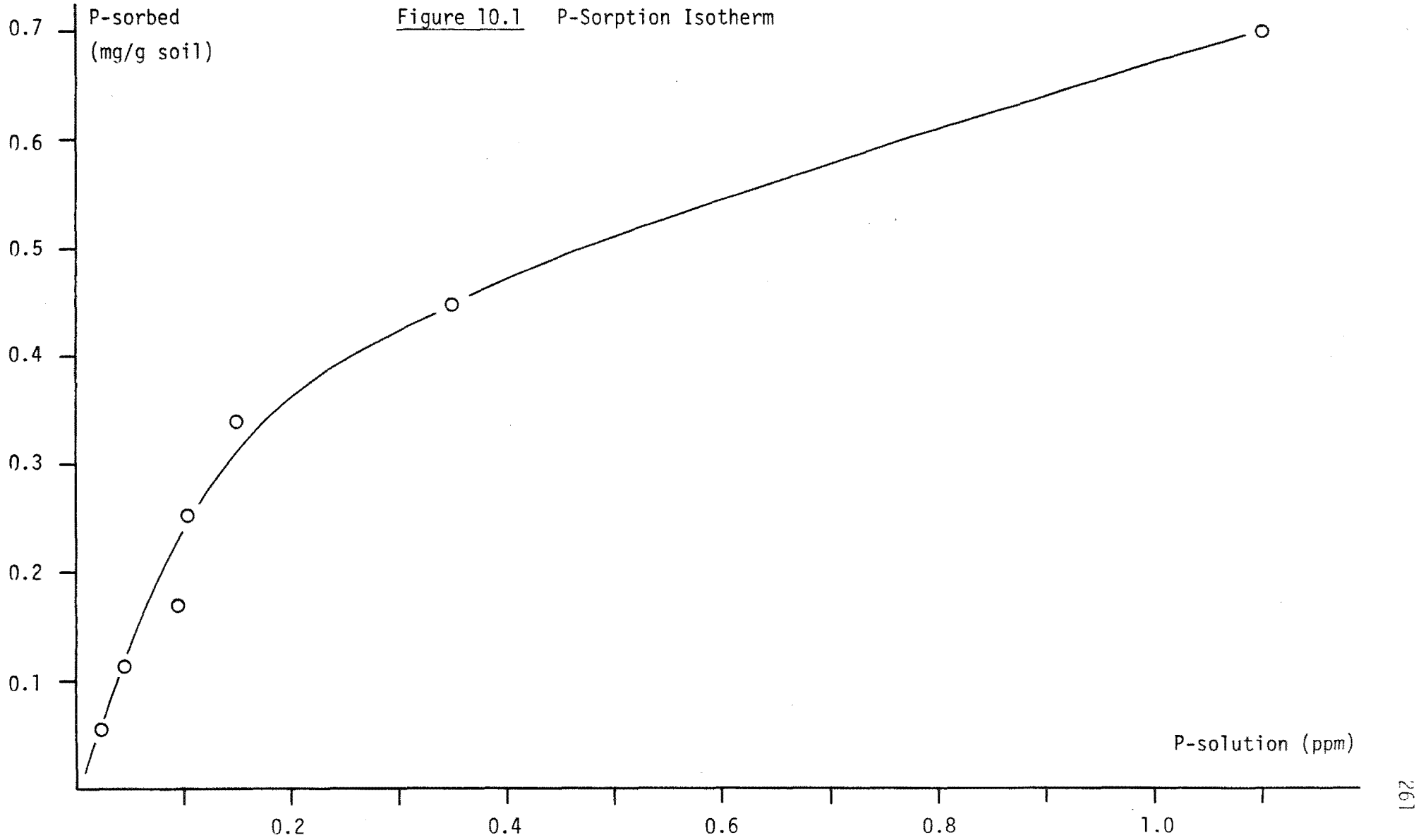

the phosphate-sorption properties of a soil tend to decrease with increasing pH (see section 10.4.3*b*), the initial application rate of 1.2 tonne ha^{-1} superphosphate suggested by the isotherm study represented an underestimation of phosphate requirements for this soil.

An alternative estimation of an initial P-application rate was based on an empirical approach described by During[200] . He suggested that high initial rates of phosphate topdressing followed by reasonably low annual maintenance applications (< 500 kg ha^{-1}) give vigorous clover growth in the first year and superior long term residual levels of P. On this basis, 1.3 tonne ha^{-1} superphosphate was recommended for medium P-sorbing soils on which a stocking rate of 20 "ewe equivalents" (i.e. one ewe with one lamb [201]) per hectare was planned.

Soil from the Ruru area was found to have medium P-retention properties by New Zealand Soil Bureau ratings[160] (P-retention 40 - 50 %, see also section 10.4.3). For a stocking rate of close to that reached on the Dairy Unit (see table 7.1), an initial application of about 850 kg ha^{-1} superphosphate was calculated for the Ruru area on the basis of During's formulation.

During has also suggested that 250 - 440 kg ha^{-1} superphosphate is an appropriate rate for annual maintenance applications for a pasture production capable of supporting 20 ewe equivalents per hectare[200] . On this basis 175 - 300 kg ha^{-1} would be required in the Ruru area if a stock rate similar to that reached in the Dairy Unit is planned.

The actual rates of phosphate fertilizer application used in the Ruru area and resulting phosphate levels in the soil as well as data from the Dairy Unit are discussed in section 10.4.3*b*.

10.4 Results of Pasture Development

10.4.1 Liming and Soil pH

In an experiment designed to simulate the addition of lime to the undeveloped Ruru soil, various quantities of $CaCO_3$ were added to field-moist soil samples (see section 8.5.6). Table 10.3 summarizes the expected and observed results (pH, % BS) as well as data from the field, following the initial application of lime to the Ruru area.

Lime was first applied to the Ruru area at a rate of 3.75 tonne ha^{-1}, close to that calculated as ideal for this soil (using Metson's method, section 10.3.1). However, field data after initial liming indicated that base saturation (31 %) had not increased as much as suggested by Metson's approach (viz 75 %). Soil pH (5.5) was slightly less than that predicted by the simulated liming experiment (viz 5.6 - 5.7), closer to that suggested by During's empirical approach (i.e. 5.4 - 5.6).

Exchangeable calcium levels in the Ruru soil rose from 7 to 78 kg ha^{-1} cm $horz^{-1}$ following initial lime application. Hence, of the 158 kg of calcium added per hectare approximately 55 % was rendered "non-exchangeable". This is consistent with calcium levels observed in surface run-off in the Dairy Unit area (see Appendix 16), where losses of this nutrient amounted to the equivalent of ca. 40 % of that applied in fertilizer over a six month period.

Hence the estimation of lime requirements using base saturation data or simulated liming in the laboratory as previously described, represented an oversimplification. These approaches took no account of leaching or immobilization of calcium.

The effect of liming has been to raise the soil pH from ca. 4.6 in the undeveloped soils to ca. 5.5 (see table 10.4 and figure 10.2).

Table 10.3 Data From the Liming of Ruru Soil

Sample Designation	$CaCO_3$ Added (me/100 g soil) (a)	Equivalent Quantity of Limestone (80 % $CaCO_3$) (tonne ha^{-1})	"Expected" Results		Observed Results		
			% BS (b)	pH (c)	pH LAB (d)	pH FIELD	% BS FIELD
RR/SP75	0	0				4.8	6
RR 5L	10	2.2	47	5.1-5.2	5.0		
RR 8L	16	3.5	71	5.3-5.5	5.6		
RR/AP77	(17.1)	3.75 (e)	75	5.4-5.6		5.5	31
RR 11L	22	4.8	95	5.6-5.8	5.8		
RR 14L	28	6.1	(102)	5.7-6.0	7.0		
RR 17L	34	7.4	(144)	6.2-6.6	7.1		

(a) *Data in this column refer to added amounts of $CaCO_3$ to soil samples in an artificial liming experiment (see section 8.5.6).*

(b) *This calculation assumes all added Ca^{++} becomes "available".*

(c) *pH ranges as calculated from estimates by During (reference 197).*

(d) *pH determined on artificially limed soil in laboratory.*

(e) *Lime at this rate was applied to the Ruru area as part of initial development in Oct 1976.*

Table 10.4 Bulk Density, Moisture Content and pH During Pasture Development

Sample Designation	Years of Development	Dry Bulk Density ($g\ cm^{-3}$)	Average Moisture Content (%)	pH (H_2O)	pH ($CaCl_2$)
Bell Hill					
Undeveloped					
BU/SP75 BU/JA76	0	0.49	63	4.6	3.5
Dairy Unit					
DU-74/AP75 *(a)*	½	(0.41) *(c)*		5.3	4.5
DU-74/AP76	1½	0.44	62	5.7	4.4
DU-74/OC76	2	0.36	57	5.2	4.9
DU-74/AP77	2½	0.42	60	5.6	
DU-74/SP77	3	(0.41) *(c)*			
DU-74/AG79 *(b)*	5	0.42		5.4	4.7
DU-68/JA75	7	(0.56) *(c)*		5.2	4.2
DU-68/AP75	7¼	(0.56) *(c)*		5.4	4.5
DU-68/SP75	7½	0.56			
DU-68/AP76	8	0.65	50	5.6	4.8
DU-68/OC76	8½	0.50	67		4.9
DU-68/AP77	9	0.54	46	5.6	4.7
DU-68/AG79 *(b)*	11½	0.46		5.7	5.1

Table 10.4 (continued)

Ruru					
RR/SP75	0	0.46	61	4.8 *(d)*	4.3 *(d)*
RR/AP77	½	0.59	43	5.5	4.5
RR/SP77	1	(0.59) *(c)*			
RR/OC78	2	(0.59) *(c)*		4.9	4.3
RR/AG79 *(b)*	3	0.35		5.6	4.9

(a) *data determined by E.S. Lee* [156]

(b) *data determined by H.K.J. Powell* [202]

(c) *dry bulk density data not determined; an average value assumed for subsequent calculations*

(d) *single samples only*

Although there were some fluctuations in pH with time no clear-cut pattern has emerged. The largest increase in soil pH occurred within the first year after initial liming; subsequent maintenance applications have held pH levels in the range 5.2 - 5.7 for almost the entire duration of development to date (i.e. up to 11½ years).

Figure 10.2 Variation In Soil pH With Time

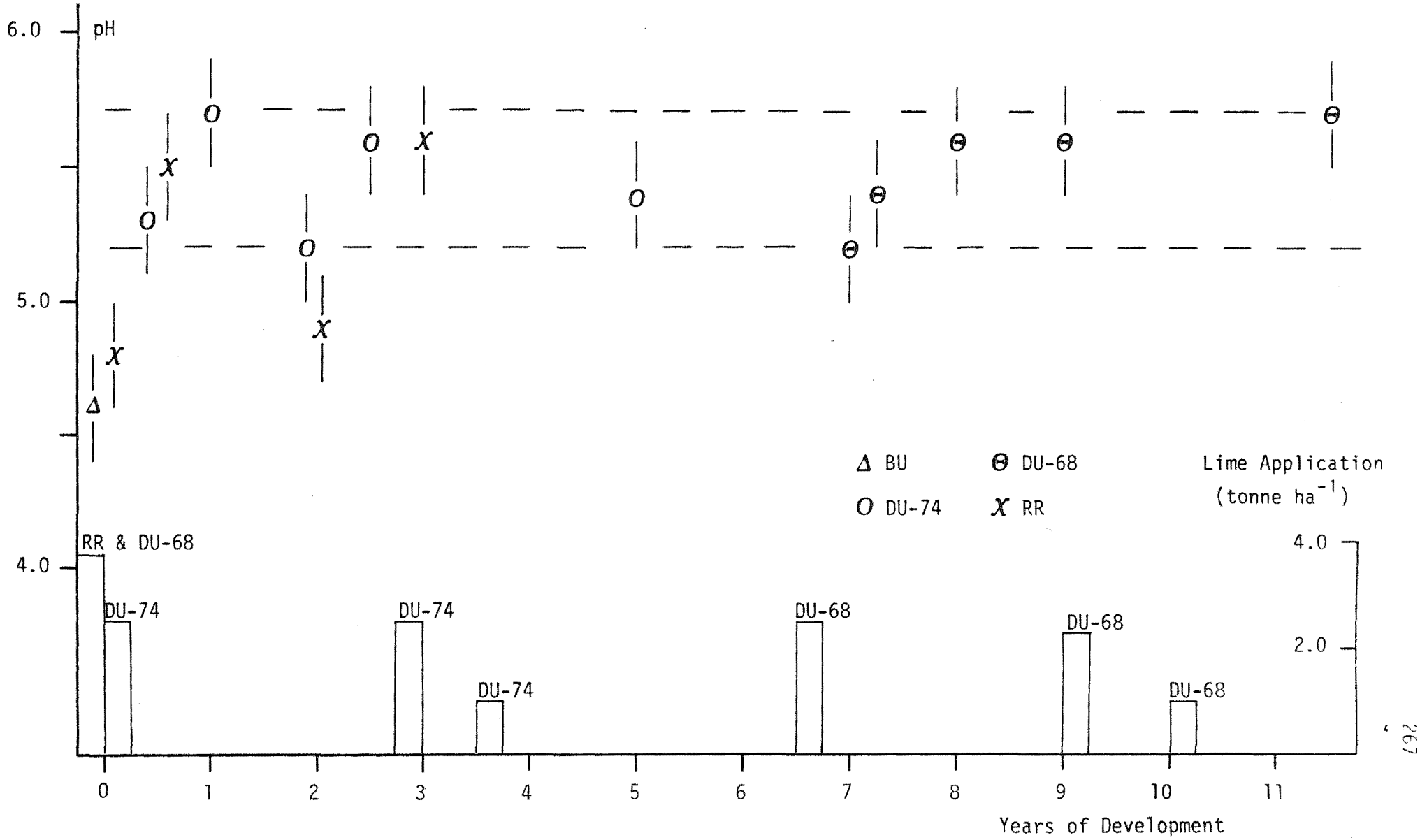

10.4.2 Exchangeable Cations

Table 10.5 lists data for levels of exchangeable cations Ca^{++}, K^{+}, Mg^{++} and Na^{+} for the Dairy Unit and Ruru areas since 1975. Figure 10.3 summarizes data for exchangeable calcium along with appropriate "error bars".

(a) Calcium. A steady increase in levels of exchangeable calcium was observed in the DU-74 and Ruru areas in the eighteen months following initial applications of lime and superphosphate. Subsequent maintenance additions of fertilizer have held these levels at ca. 7×10^{6} me Ca ha^{-1} cm $horz^{-1}$ for the Dairy Unit and ca. 4.5×10^{6} me Ca ha^{-1} cm $horz^{-1}$ for the Ruru soil. The high Ca level observed in the DU-74 area after 3 years development probably reflects the close proximity of this sample collection to fertilizer application in September 1977 (see also table 7.1).

Figure 10.3 suggests a deterioration in soil-calcium levels in the DU-68 area since 1976. While both soil pH and herbage-Ca levels have remained relatively constant during this period, continued high losses of Ca in run-off water, already mentioned, and the additional demands of dairy stock (first introduced in 1976), suggest that levels of this important nutrient, in both herbage and soil, should continue to be monitored closely.

(b) Potassium. Metson suggested [203] that pasture on soils with medium potassium reserves (i.e. K_c 0.20 - 0.35 me/100 g soil) is likely to respond to the addition of potassium when exchangeable-K is low. Those soils with low potassium reserves (i.e. $K_c < 0.20$ me/100 g soil) are regarded as consistently K-deficient. Potassium reserves in the Dairy Unit area were found to be uniformly low (K_c 0.07 - 0.21 me/100 g soil), suggesting that continued application of potassium will be

Table 10.5 Levels of Exchangeable Cations

Sample Designation	Years	Ca_{ex}	Mg_{ex}	K_{ex}	Na_{ex}	Σcat_{ex}	CEC	% BS
		(units: me ha^{-1} cm $horz^{-1}$ x 10^6)						
Bell Hill								
Undeveloped								
BU/JA76	0	1.52	0.47	0.09	0.02 *(a)*	2.10	11.3	19
Dairy Unit								
DU-74/AP75	½	2.72	0.26	0.09	0.02 *(a)*	3.09	9.9	31
DU-74/SP75	1	3.29	0.45	0.14	0.02 *(a)*	3.90	11.0	35
DU-74/AP76	1½	7.26	0.53	0.17	0.02	7.98	15.1	53
DU-74/OC76	2	6.62	0.54	0.14	0.02	7.34	14.0	52
DU-74/AP77	2½	6.64	0.55	0.18	0.03	7.39	15.2	49
DU-74/SP77	3	8.21	0.51	0.15	0.04	8.91	12.9	69
DU-74/AG79 *(b)*	5	6.13	0.55	0.11	0.03 *(a)*	6.82	14.4 *(a)*	48
DU-68/JA75	7	7.11	0.61	0.28	0.03	8.01	18.0	44
DU-68/AP75	7¼	6.05	0.78	0.26	0.03	7.11	16.7	43
DU-68/SP75	7½	6.89	0.65	0.21	0.03	7.78	17.8	44
DU-68/AP76	8	7.28	0.60	0.29	0.03	8.20	13.6	60
DU-68/OC76	8½	5.55	0.50	0.22	0.03	6.30	14.8	42
DU-68/AP77	9	5.89	0.45	0.26	0.03	6.59	14.9	44
DU-68/AG79	11½	5.42	0.41	0.22	0.03 *(a)*	6.08	16.0 *(a)*	38
Ruru								
RR/SP75	0	0.35	0.26	0.09	0.02	0.71	11.4	6
RR/AP77	½	5.02	0.38	0.12	0.03	5.55	17.8	31
RR/SP77	1	4.13	0.43	0.19	0.04	4.79	19.0	25
RR/OC78	2	4.62	0.22	0.19	0.04 *(a)*	5.07	17.2	29
RR/AG79 *(b)*	3	4.72	0.40	0.14	0.04 *(a)*	5.30	18.0 *(a)*	29

Footnotes for Table 10.5

(a) *data not determined - values estimated for calculation of* Σcat_{ex} *and % BS*

(b) *data determined by H.K.J. Powell* [202]

required to maintain adequate pasture production. Levels of potassium observed in surface run-off from the Dairy Unit, over a six month period in the 1975/76 season, reinforce this suggestion (see Appendix 16). The equivalent of 32 % of potassium applied as fertilizer was "lost" during this period.

Herbage analysis for the 1975/76 season[204] in the Dairy Unit indicated that potassium levels were in or just below the "critical" or pasture response range of 1.8 - 2.5 % [205], whereas recent data for the 1978/79 season show an excess of this element in grasses and clover [204].

Annual maintenance applications of potassium (via "potassic superphosphate") in the Dairy Unit amounted to the equivalent of 0.26 x 10^6 me K ha^{-1} cm $horz^{-1}$ up to 1976 and 0.39 x 10^6 me K ha^{-1} cm $horz^{-1}$ after the introduction of dairy cattle. Additions of fertilizer in the Dairy Unit have increased levels of exchangeable potassium in the soil from 0.09 (as measured in the Bell Hill Undeveloped area) to ca. 0.15 in the DU-74 area and 0.25 x 10^6 me ha^{-1} cm $horz^{-1}$ in the DU-68 area. These levels are low-medium by New Zealand Soil Bureau standards[188].

Levels of potassium in surface run-off suggest that continued extensive leaching of this mobile element is likely under the high rainfall typical of local conditions. Although potassium in herbage appears more than adequate, low potassium reserves and low-medium levels

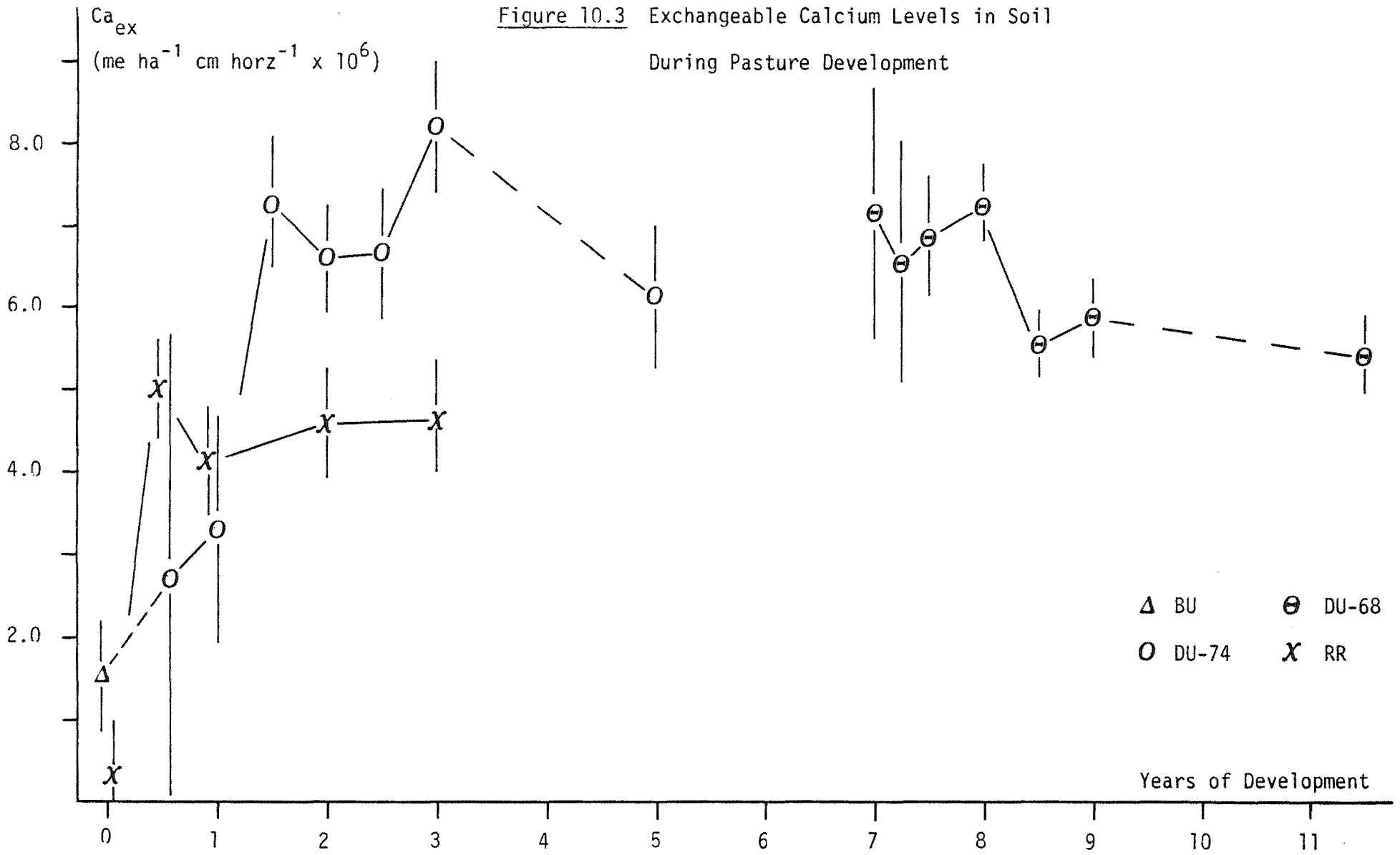

Figure 10.3 Exchangeable Calcium Levels in Soil During Pasture Development

in the soil suggest that pasture growth (as far as K is concerned) is largely dependant on whatever potassium is added by way of fertilizer to a rather thin horizon in the top few centimetres of the soil profile. K-fertilizer applications appear to be adequate for current pasture-yield conditions in the Dairy Unit. Should this yield be increased, by overcoming other nutrient deficiencies for example, the potassium-status of the herbage may become important.

A similar picture was observed for the Ruru area where levels of exchangeable-K in the soil are currently (i.e. up to 1979) around 0.19×10^6 me ha^{-1} cm $horz^{-1}$ (base level in undeveloped soil was 0.09×10^6 me ha^{-1} cm $horz^{-1}$). However, potassium reserves in this soil are higher (K_c 0.31 me/100 g soil) than those in the Dairy Unit and therefore the additions via fertilizer (0.23×10^6 me K ha^{-1} cm $horz^{-1}$) would appear to be adequate for the current stock program (refer to table 7.2).

(c) Magnesium and Sodium. These elements have not been added to the Bell Hill region in the fertilizer treatments and this is reflected in the rather uniform soil-levels of these two elements. Stock feed has been supplemented by the use of magnesium "cattle-licks". This has probably compensated for marginally low magnesium levels observed in herbage in the Dairy Unit[205] (viz seasonal means ca. 0.19 % cf. stock requirements 0.15 - 0.20 %[206]).

Overall, % BS figures showed a steady increase from 19 % to ca. 43 % in the Dairy Unit while an increase of a similar magnitude was observed in the Ruru area (6 % to ca. 28 %).

10.4.3 Carbon, Nitrogen, Phosphorus and Sulphur

Table 10.6 summarizes data for soil phosphorus, nitrogen and oxidisable carbon in the study areas.

(a) Carbon and Nitrogen. Carbon and nitrogen levels in both the

Table 10.6 Phosphate, Oxidisable Carbon and Soil Nitrogen With Pasture Development

Sample Designation	Years	Total P	Org P	Inorg P	Truog P	Truog P/ Total P	C *(a)*	N *(a)*	C/N
		(units: kg ha^{-1} cm $horz^{-1}$)				(%)			
Bell Hill									
Undeveloped									
BU/JA76	0	18.6	14.2	4.4	0.44	2.3	4.43	0.25	17.4
Dairy Unit									
DU-74/AP76	1½	26.8	18.6	8.2	1.57	5.9	5.66	0.30	18.9
DU-74/OC76	2				1.69		4.46	0.29	15.3
DU-74/AP77	2½				2.07		5.15	0.30	17.0
DU-74/SP77	3				2.36		4.12	0.24	17.1
DU-74/AG79 *(b)*	5	23.0	13.6	7.5	2.00	8.7		0.23	
DU-68/JA75	7	44.2	28.6	15.6	2.91	6.6	6.80	0.44	16.8
DU-68/SP75	7½	47.8	36.4	11.4	3.70	7.7		0.40	
DU-68/AP76	8	48.9	31.5	17.4	4.25	8.7	6.45	0.40	16.0
DU-68/OC76	8½						5.35	0.31	17.1
DU-68/AP77	9				3.94		5.29	0.35	15.1
Ruru									
RR/SP75	0	14.4	10.0	4.4	0.23	1.6	4.49	0.23	19.5
RR/AP77	½				2.15		6.48	0.32	20.2
RR/SP77	1				2.26		6.81	0.32	21.3
RR/OC78 *(b)*	2	23.6	18.8	4.8	2.07	8.8	6.67	0.35	19.0
RR/AG79 *(b)*	3	28.9	21.2	7.7	1.53	5.3		0.30	

(a) *units: kg ha^{-1} cm $horz^{-1}$ x 10^3*

(b) *data determined by H.K.J. Powell* [202]

Dairy Unit and Ruru areas have remained relatively constant during pasture development with the exception of the first year of development where small increases in both elements were apparent in each sampling area. Although total nitrogen levels in the soil were medium to high by New Zealand Soil Bureau ratings [188], analysis of herbage collected from the Dairy Unit during the 1975/6 season [204] indicated marginally deficient N-levels in clover (3.8 - 4.2 %) and marked N- deficiency in grasses (2.2 - 2.9 % cf. deficient range < 4.0 % [205]). Some improvement in these levels was noted in the 1978/9 season, attributable in part to increased stock rotation. However, nitrogen in grasses remained deficient. This may be largely a problem of continuing poor drainage and water-logging, limiting microbial activity.

(b) Phosphate. It is well known that only a small proportion of the total phosphorus content of the soil is available to plants and that large quantities of phosphate added by way of fertilizers are quickly rendered unavailable to growing plants, so-called phosphorus fixation. It is generally accepted that phosphate mobility in soils is largely controlled by sorption-desorption reactions, but the mechanisms of these reactions are not well understood. Iron and aluminium compounds, especially short range order (amorphous) hydrated oxides, are involved and often there is a good correlation between measures of P-sorption and iron and aluminium concentrations in the soil[190] (see also section 9.5, figure 9.3). Ryden and Syers[207] have suggested reactions such as 10.1 as being important in the sorption process

$$M - OH_2^+ + H_2PO_4^- \rightleftharpoons M - H_2PO_4 + H_2O \quad (10.1)$$

M represents Fe, Al.

The addition of lime generally lowers the P-retention of the soil as the net charge on the hydroxy aluminium or iron species is lowered with

increasing pH. (In a laboratory experiment addition of $CaCO_3$, equivalent to 6.1 tonnes ha^{-1} lime, was found to reduce the P-retention of the undeveloped Ruru soil from 50 to 41 %).

As has already been noted (section 9.5) soil from the undeveloped Ruru area with relatively higher levels of iron and aluminium, showed a greater propensity to sorb added phosphate than that from the Bell Hill Undeveloped or Dairy Unit areas. Hence the initial rate of application of 0.6 tonnes superphosphate per hectare, applied to the Dairy Unit, was considered insufficient for the development of the Ruru block. An initial rate of 0.85 - 1.2 tonne ha^{-1} was recommended by the author (see section 10.3.2). In practice 1.1 tonne ha^{-1} superphosphate was applied at Ruru in the first year of pasture development. After three years, soil-P levels (as measured by Truog's test) were similar to those in the Dairy Unit at a comparable stage of development. Relatively large annual maintenance applications (viz 315 kg ha^{-1} superphosphate) with low stocking rates appear to have provided additional compensation for the extra phosphate needs of the Ruru area. The long term P-status of the soil and herbage of this region has yet to be evaluated.

The Dairy Unit had an initial application of 625 kg ha^{-1} special mix superphosphate followed by maintenance applications of the equivalent of 315 kg ha^{-1} superphosphate annually (refer to table 7.1). This area initially supported up to 200 cattle. With their replacement by up to 120 dairy cows in 1976, the annual rate of phosphate added was increased to the equivalent of 525 kg ha^{-1} of superphosphate. In the light of the estimated fertilizer requirements discussed in section 10.3.2*b* this program for the Dairy Unit seems more than adequate for pasture and stock needs.

As might be expected with annual applications of 300 - 500 kg/ha superphosphate and relatively small losses in surface run-off (see Appendix 16), total soil P-levels have increased steadily over the

development years in the Dairy Unit. There has been a corresponding increase in "available-P", as measured by the Truog extraction, as well as a gradual increase in the size of the available-P fraction. This fraction was ca. 2 % of total soil-P before development and has increased to nearly 9 % after 8 years. This is consistent with a gradual lowering of P-sorption properties of the soil upon liming and repeated phosphate additions. Figure 10.4 summarizes Truog-P data for the study region.

The ratio Organic-P/Total-P has remained in the 0.6 - 0.7 range for most of the development years despite improvements in drainage and soil pH. Hence there has been a corresponding build-up in the organic-P fraction of soil where limited microbial activity has meant low rates of mineralisation.

Phosphorus levels in herbage from the Dairy Unit were found to be adequate (> 0.35 %)[204] and generally above that for which fertilizer application would improve the pasture yield (i.e. the "critical level"). This suggests that for the current yield of pasture production in the Dairy Unit phosphate additions are in excess.

(c) Sulphate. The mechanism of sulphate sorption in soil is thought to be similar to that for phosphate, with aluminium implicated in particular [191]. Hence a decrease in sulphate retention is expected following liming (see section 10.4.3*b*). This was shown to be the case for the Ruru soil. In an artificial liming experiment, previously discussed (section 10.4.1), sulphate retention in a sample of Ruru topsoil (RR 14L) was reduced from 22 % to less than 1 % with the addition of lime equivalent of 6.1 tonne ha^{-1} (cf. 6.25 tonne ha^{-1} added to the Ruru block in the first development year). Sulphate retention of the soil is also expected to decrease following the application of superphosphate[208], with the more strongly sorbed phosphate ions displacing sulphate from the sorption sites. This is consistent with the rather higher levels of

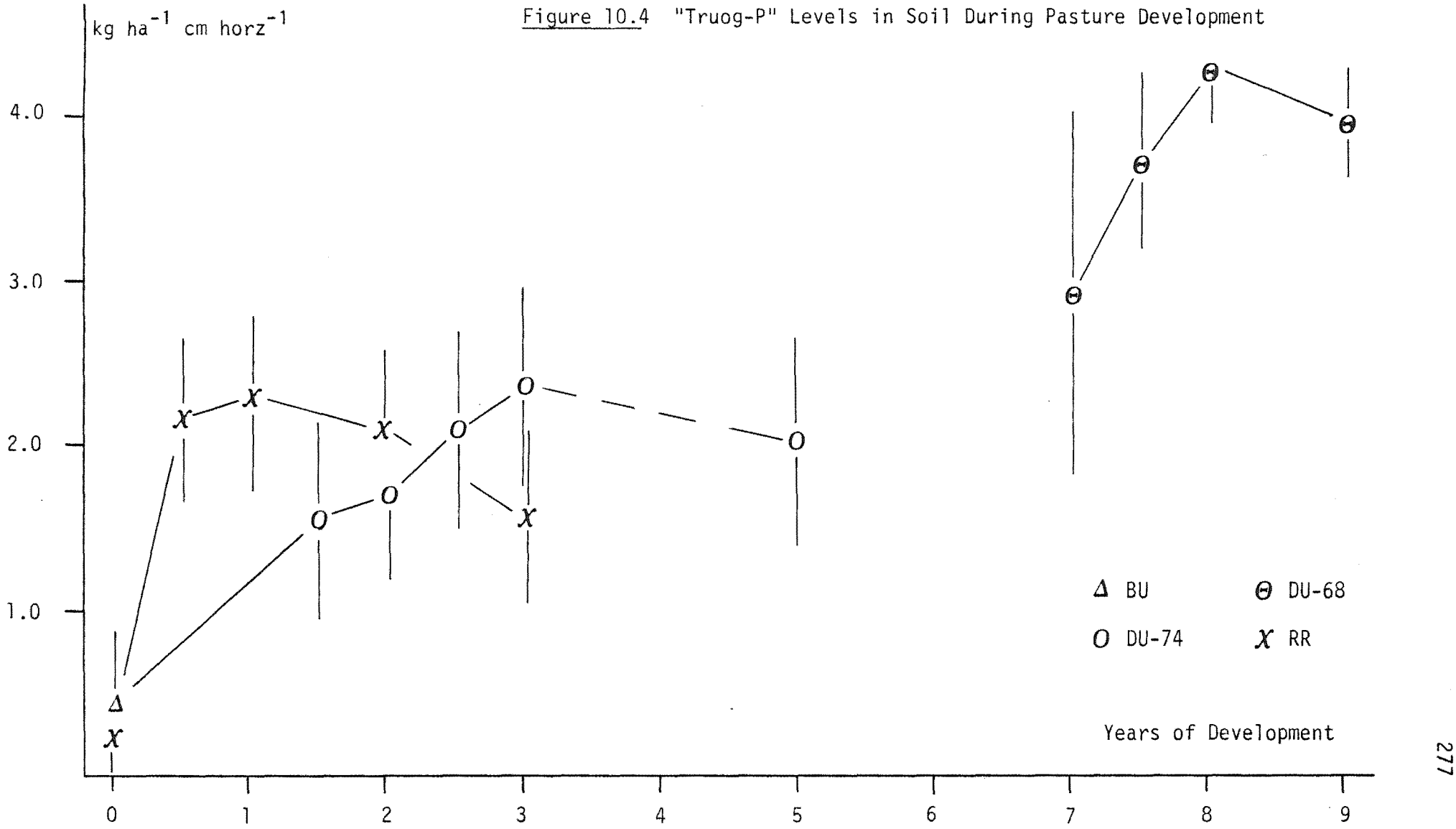

Figure 10.4 "Truog-P" Levels in Soil During Pasture Development

sulphur observed in surface run-off from the Dairy Unit (losses of sulphate amounted to the equivalent of ca. 37 % of that applied in fertilizer over a six month period, cf. phosphate ca. 6 % - see Appendix 16).

Although adsorbed sulphate-S levels in soil from the Dairy Unit were found[156] to be in the medium range (1.5 - 5 mg/100 g soil, N.Z. Soil Bureau ratings [160]), deficiencies in herbage sulphur (< 0.25 % [204]) were observed in the 1975/6 season and again in the 1978/9 season, after the introduction of elemental sulphur with annual fertilizer application (equivalent to 75 kg ha^{-1} from 1977).

10.4.4 Cobalt

It has been recognised for some time that a widespread cobalt deficiency exists in New Zealand soils. Kidson[173] surveyed a large number of New Zealand soils and found that, although soil Co levels (measured as total-Co) are not necessarily a reliable guide in predicting stock ailments such as "bush-sickness", those soils where there were significant signs of unthriftiness in stock had total-Co levels of less than 2 ppm. Mitchell[209] quotes a level of 0.3 ppm of acetic acid – extractable Co as necessary to support healthy sheep. Levels of below 0.07 ppm in pasture are thought to give rise to Co-deficiencies in sheep and this deficiency becomes serious below 0.04 ppm [210]. Concentrations of 0.04 ppm in herbage appear to be adequate for cattle[210] .

Tables 10.7 and 10.8 summarize data for "total" cobalt and acetic acid-extractable cobalt (HAc-Co) determined for the study region and also for eight wetland soils from the Buller and Grey Valley districts. Acetic acid-extractable cobalt representing "available" Co (see section 8.5.11*b*) was found to be approximately 10 % of total cobalt (range 2 - 35 %).

Inclusion of cobalt in fertilizer mixtures has been standard practice in the study region with annual applications of 0.7 - 1.4 kg $CoSO_4$ per ha (equivalent to 0.6 - 1.2 ppm Co for 7.6 cm soil depth). A

Table 10.7 Soil Cobalt Levels in Wet Land Soils

Soil Series	Typesite Designation	Horizon (a)		HAc-Co (ppm)	Total-Co (ppm)
Maimai	MA1	A_{1g}	(0 - 20 cm)	0.17	1.4
	MA2	A_{1g}	(0 - 16 cm)	0.08	1.3
Kumara	KU1	A_{1g}	(0 - 16 cm)	0.19	1.6
	KU2	A_{1g}	(0 - 17 cm)	0.15	1.5
Hukarere	H1	A_{1g}	(0 - 12 cm)	0.20	1.2
	H2	A_{11} & A_{12}	(0 - 14 cm)	0.43	1.2
Okarito	OK1	A_{11}	(0 - 14 cm)	0.02	0.9
	OK2	A_{11}	(0 - 27 cm)	0.05	0.6
Mawhera	MW1	A_{11}	(0 - 11 cm)	0.12	1.8
	MW2	A_{11}	(0 - 10 cm)	0.06	1.3
Flagstaff	FL1	A_1	(0 - 14 cm)	0.23	2.0
	FL2	A_1	(0 - 8 cm)	0.13	2.2
Charleston	CH1	A_1	(0 - 18 cm)	0.19	1.3
	CH2	A_1	(0 - 19 cm)	0.16	2.2
Addison	AD1	A_{11} & A_{12}	(0 - 18 cm)	0.08	0.7
	AD2	A_{11} & A_{12}	(0 - 15 cm)	0.06	0.7

(a) A full description of these soil samples has been given by Mew [150].

rise in HAc-Co was observed in the Ruru and Dairy Unit developments with time, with levels reaching 0.3 and 0.5 ppm respectively.

In general the wet land topsoils studied in this work were low in total-Co (most less than 2 ppm; Okarito and Addison soils < 1 ppm). With the exception of one sample, corresponding HAc-Co levels were less than 0.3 ppm. Co-deficiency may therefore be a problem on these soils especially for the Okarito and Addison series sampled. Further sampling and determination of herbage levels of Co would be required to confirm this suggestion.

Undeveloped Maimai soil from the study region showed higher levels of total-Co (2.0 - 4.9 ppm) and HAc-Co (0.15 - 0.32 ppm) than either of the Maimai typesites (cf. 1.3 - 1.4 ppm and 0.08 - 0.17 ppm respectively). Fertilizer application has accentuated this difference. The cobalt content of pasture in the Dairy Unit and in lucerne used to feed stock in winter months appears to be adequate for stock needs. Co-deficiencies in stock have not been noted at Ruru and this is consistent with measured Co levels in soil and plant material (see also table 10.9).

Kidson[173] noted that soil samples taken from Bald Hill, Westport (Addison soil) showed low total-Co (0.3 - 1.0 ppm) yet stock were healthy. This may point to the unreliability of using total-Co data to predict deficiencies (whereas HAc-Co is known to be correlated with plant-Co on many soils[176]). Alternatively, other sources of cobalt, such as winter feed, which were not mentioned by Kidson, may account for good stock health.

10.4.5 Other Trace Elements

Herbage from the Dairy Unit has been analysed for boron, copper, iron, manganese, molybdenum and zinc[204]. The levels of these trace elements were found to be adequate for stock requirements and beyond reported critical response levels[205]. Observed concentrations (ppm) in clover

Table 10.8 Soil Cobalt Levels in the Bell Hill Region

Sample Designation	Horizon	Stage of Development	HAc-Co (ppm)	Total-Co (ppm)
BU 101	A_{1g} (0 - 7.6 cm)	Undeveloped	0.30	2.0
	A_{1g} (7.6 - 12.7 cm)	"	0.17	2.9
	G (12.7 - 17.8 cm)	"	0.15	5.1
	B_3 (17.8 - 33.0 cm)	"	0.17	8.7
BU/JA76	A_{1g} (0 - 11.3 cm)	"	0.32	4.4
DU-74/AP76	A_{1g} (0 - 7.6 cm)	1½ years	0.35	4.4
DU-68/AP76	A_{1g} (0 - 7.6 cm)	8 years	0.50	4.9
RR/SP75	A_{1g} (0 - 14.9 cm)	Undeveloped	0.15	4.9
RR/AP77	A_{1g} (0 - 11.4 cm)	½ year	0.25	
RR/SP77	A_{1g} (0 - 11.4 cm)	1 year	0.31	

were (critical values[205] in parentheses) B 33 - 45 (25 - 35); Cu 9 (4 - 6); Fe 120 - 170 (60); Mn 60 - 70 (25 - 30); Mo 1; Zn 80 - 120 (12 - 18).

Table 10.9 Herbage Cobalt Levels in the Dairy Unit

Sample	Description	Co (ppm)
Grass	pasture developed 1½ yrs	0.057
Grass	" " 8 yrs	0.083
Clover	pasture developed 1½ yrs	0.082
Clover	" " 8 yrs	0.087
Lucerne	grown in Canterbury (used to feed stock at Bell Hill during winter months)	0.075

10.5 Summary

Substantial quantities of fertilizer added to the two main sampling areas in the study region during the development period to date have done much to compensate for the naturally-impoverished Maimai topsoil. Levels in the soil and herbage, of the "macro" nutrients potassium, calcium and phosphate, appear to be adequate under present yield conditions, while deficiencies in sulphur and nitrogen have been noted in herbage analyses. Currently, the Dairy Unit area supports over 100 dairy cows.

While appropriate "chemical adjustments" to the nutrient status of the soil have been and can be made, "physical" and "biological" changes

are also required for productive farming on the pakihi soils. Although these latter two factors have not been studied in any detail in this work, field observations in the study region have suggested that poor drainage under high rainfall conditions continues to be a major limitation to the establishment of permanent high-quality pasture. With low reserves of several nutrients, relatively high losses in surface run-off and low rates of mineralisation, present pasture appears to be heavily dependant on annual additions via fertilizer.

Finally, it should be noted that, while similar conclusions have been reached for other pakihi soils of the West Coast [211], important differences in physical and chemical properties, both within and between the various soil series, are evident. Hence, effective long-term utilization of the Bell Hill Development Block will depend on the continued critical evaluation of the current farming methods being employed in the light of the specific features of this region.

APPENDIX 1

PREPARATION OF STANDARD BUFFER SOLUTIONS AT 25 °C

Buffer	Buffer Substance(s)	Weight in air, per litre (g)	Solution Concentration (molal)	Drying Requirements	Distilled Water	pH(S)
Tetroxalate	$KH_3(C_2O_4)_2.2H_2O$	12.61	0.05	60 °C	air equilibrated	1.679
Tetroxalate	"	2.535	0.01	"	"	2.157
o-Phthalic Acid-	$C_6H_4(COOH)_2$	1.246	0.00757	40 °C	"	2.913
Phthalate	$KHC_6H_4(COO)_2$	1.018 *(a)*	0.00503	110 °C, 1-2 h		
Tartrate	$KHC_4H_4O_6$	Saturated solution	0.0341	"	"	3.557
Phthalate	$KHC_6H_4(COO)_2$	10.12	0.05	"	"	4.005

Acetate	CH_3COOH	*(b)*	0.01	—	purged of carbon dioxide	4.718
	$NaCH_3COO.3H_2O$	1.374	0.01	40 °C		
Phosphate (1:1)	KH_2PO_4	3.388	0.025	"	"	6.863
	Na_2HPO_4	3.533	0.025	"		
Phosphate (3.5:1)	KH_2PO_4	1.179	0.0087	"	"	7.415
	Na_2HPO_4	4.302	0.0304	"		
Tris (1:1)	$NH_2C(CH_2OH)_3.HCl$	7.768	0.05	40 °C	"	8.173
	$NH_2C(CH_2OH)_3$	5.970	0.05	80 °C		
Borax	$Na_2B_4O_7.10H_2O$	3.80	0.01	room temp, desiccator	"	9.183
Carbonate	$NaHCO_3$	2.092	0.025	"	"	10.014
	Na_2CO_3	2.640	0.025	275 °C, 2 h		
Hydroxide	$Ca(OH)_2$ *(c)*	Saturated solution	0.0203	110 °C, 1-2 h	air equilibrated	12.454

Footnotes for Appendix 1

(a) *KCl added to give solution concentration of 0.00505 m (0.373 g / litre).*

(b) *Required volume of an acetic acid stock solution calculated following standardisation against standard KOH.*

(c) *Calcium carbonate (washed) ignited at 1000 °C 45 min, boiled in water, filtered and dried.*

APPENDIX 2

ASSIGNMENT OF pH(S) VALUES TO BUFFER SOLUTIONS

2A.1 Tetroxalate Buffer (0.01 M)

In order to provide an additional reference buffer in the low pH region a potassium tetroxalate solution (0.01 m) was prepared. This buffer is not included in the NBS list of primary or secondary buffers but values of $p(a_H\ y_{Cl})^\circ$ have been tabulated[212]. Using the Bates-Guggenheim convention as described in section 3.2.2, a value for pH(S) of 2.157 was calculated for a temperature of 25 °C (ionic strength, I = 0.0180 M[212]; A = 0.5115[213]). A similar calculation for a 0.05 M tetroxalate solution gave pH(S) = 1.680 cf. NBS assignment of 1.679.

2A.2 o-Phthalic Acid/Hydrogen Phthalate Buffers

Hamer et al [80] have tabulated pH values for solutions with various concentrations of o-phthalic acid, potassium hydrogen phthalate and potassium chloride. These data can be regarded as pa_H values, although the convention implicit in the derivation of such numbers was different to that used in the NBS standard scale.

In this work a solution comprising H_2Ph (0.00743 m), KHPh (0.00503 m) and KCl(0.00505 m) was prepared and assigned a pH(S) value of 2.913 by interpolation of Hamer's data.

2A.3 o-Phthalic Acid/KOH Titrations

Hamer and Acree [83] have derived an empirical relationship which gives the pH of phthalate solutions as a function of the molality of potassium chloride:

$$pH = (pH)^\circ + \alpha_1 m_{KCl} + \alpha_2 m_{KCl}^2 + \alpha_3 m_{KCl}^3 \quad (2A.1)$$

Values of $(pH)^\circ$, α_1, α_2 and α_3 are listed for various concentrations of potassium hydrogen phthalate (KHPh)at given ratios of KHPh to K_2Ph.

In this work pH(S) values, computed by equation 2A.1, were assigned to appropriate points in the titrations of o-phthalic acid with standard potassium hydroxide solution. The measured pH (pH_m) was noted at these points enabling the determination of pH_m - pH(S). Data from up to four titrations of H_2Ph were averaged before recording in table 3.3.

APPENDIX 3

CORRECTIONS FOR LIQUID JUNCTION EFFECTS AT HIGH AND LOW pH

The following equation was used to modify the measured pH (pH_m) with deviations (Δ) due to liquid junction effects:

$$pH' = pH_m + \Delta$$

pH_m	Δ	pH_m	Δ
1.77	0.036	2.41 - 2.44	0.018
1.77 - 1.78	0.035	2.45 - 2.48	0.017
1.79 - 1.80	0.034	2.49 - 2.52	0.016
1.81 - 1.84	0.033	2.53 - 2.60	0.015
1.85 - 1.88	0.032	2.61 - 2.64	0.014
1.89 - 1.92	0.031	2.65 - 2.68	0.013
1.93 - 1.96	0.030	2.69 - 2.76	0.012
1.97 - 2.00	0.029	2.77 - 2.82	0.011
2.01 - 2.04	0.028	2.83 - 2.88	0.010
2.05 - 2.08	0.027	2.89 - 2.94	0.009
2.09 - 2.12	0.026	2.95 - 3.00	0.008
2.13 - 2.16	0.025	3.01 - 3.08	0.007
2.17 - 2.20	0.024	3.09 - 3.16	0.006
2.21 - 2.24	0.023	3.17 - 3.23	0.005
2.25 - 2.28	0.022	3.24 - 3.30	0.004
2.29 - 2.32	0.021	3.31 - 3.36	0.003
2.33 - 2.36	0.020	3.37 - 3.47	0.002
2.37 - 2.40	0.019	3.48 - 3.57	0.001

pH_m	Δ	pH_m	Δ
3.58 - 9.55	0.000	10.96 - 11.09	0.011
		11.10 - 11.23	0.012
9.56 - 9.69	0.001	11.24 - 11.37	0.013
9.70 - 9.83	0.002	11.38 - 11.51	0.014
9.84 - 9.97	0.003	11.52 - 11.65	0.015
9.98 - 10.11	0.004	11.66 - 11.79	0.016
10.12 - 10.25	0.005	11.80 - 11.93	0.017
10.26 - 10.39	0.006	11.94 - 12.07	0.018
10.40 - 10.53	0.007	12.08 - 12.21	0.019
10.54 - 10.67	0.008	12.22 - 12.35	0.020
10.68 - 10.81	0.009	12.36 - 12.49	0.021
10.82 - 10.95	0.010		

APPENDIX 4

FORTRAN PROGRAM TO CALCULATE HYDROGEN ION CONCENTRATIONS IN o-PHTHALIC ACID BUFFER SOLUTIONS

```
      SUBROUTINE PRELIM(Y,X,KD)
C     PROGRAM TO CALIBRATE DIHYDROGEN PHTHALATE BUFFER SYSTEMS
C     AK1 AND AK2 ARE ASSOCIATION CONSTANTS
      DIMENSION Y(200),X(2,200),V(200)
      DIMENSION CL(200),CHL(200),CH2L(200)
   24 FORMAT(' TITRATION NO.: ',I3,'     NUMBER OF DATA POINTS = ',I3/)
   64 FORMAT(' TITRE   P(H+)      PHTH        HPHTH       H2PHTH      NBAR
     1      BETA'/)
   65 FORMAT(F6.3,2X,F5.3,2X,3(E10.3,2X),2X,F5.3,2X,E10.3)
   71 FORMAT(E10.4,F10.4,2X,I3,F10.3,E10.4,2X,F5.1,X,I3,2F8.5)
   72 FORMAT(2F10.4)
   73 FORMAT(F8.4,3(2X,F7.4),2(3X,I2),6(3X,E10.4)/)
   74 FORMAT(7X,37HDATA FOR CALIB CURVE FOR PHTH BUFFERS/)
   75 FORMAT(' TITRE      PH       P(H+)     DELTA      N     MN       F(H)
     1      F(HL)       F(L)       IONSTR       CK1          CK2'/)
   78 FORMAT(3F7.3,2E10.4,E10.3,F7.4,E10.4,F6.3)
      READ(5,78)BTHL,BTL,BTH,AK1,AK2,AI,XA,XB,GAMMA
      KD=0
   99 READ(5,71,END=100)TBI,ALKI,ZKODE,TV,CKCL,TEMP,KL,DKOH,DSOLN
      IF(ZKODE)100,100,81
   81 KN=KD+1
      KD=KD+KL
      READ(5,72) (V(J),Y(J),J=KN,KD)
      WRITE(6,74)
      WRITE(6,24)ZKODE,KL
      WRITE(6,75)
C     ALL CONCENTRATIONS CONVERTED TO MOLALITY
      DSOLU=CKCL*7.456E-2+TBI*0.16614
      DSOLV=DSOLN-DSOLU
      TM=TV*DSOLV
      TBL=TBI/DSOLV
      CKCL=CKCL/DSOLV
      DO 13 J=KN,KD
      AM=V(J)*DKOH
      Q=TM/(TM+AM)
      TB=TBL*Q
      CCKCL=CKCL*Q
      ALK=(V(J)*ALKI)/(TM+AM)
      MN=0
C     CALCN OF SOLN STOICHIOMETRY TO GET INITIAL ESTIMATE OF IONIC STR
      ACID=2.*TB-ALK
      ZPH=(Y(J)-0.086)/0.995
      YH=10.0**(-ZPH)
      HYD=1.007E-14/(GAMMA*YH)
      R=ACID/TB
      IF(R-1)20,20,21
   20 MHL=R*TB
      ML=(1.-R)*TB
      GO TO 50
   21 MHL=(2.-R)*TB
      ML=0.0
   50 YIST=(CCKCL+3.*ML+MHL)
C     CALCN OF ACTIVITY COEFF EXPRESSIONS
   22 Z=XA*SQRT(YIST)/(1.+XB*AI*SQRT(YIST))
      N=1
      AHL=10.**(-(Z+BTHL*MHL))
      AL=10.**(-(4.*Z+BTL*ML))
    7 AH=10.**(-(Z+BTH*YH))
C     CALCN OF CONCENTRATION CONSTANTS FROM GIVEN EQUILIBRIUM ACTIVITY
C     CONSTANTS
      GFN1=1./(AH*AHL)
      GFN2=AHL/(AH*AL)
      CK1=AK1/GFN1
      CK2=AK2/GFN2
C     CALCN & REFINEMENT OF HYDROGEN ION CONCENTRATION
      A=CK1*CK2
      D=ACID+HYD
      B=2.*A*TB+CK2-A*D
      C=CK2*(TB-D)+1.
      FX=A*YH**3+B*YH**2+C*YH-D
      FXP=3.*A*YH**2+2.*B*YH+C
      XH=YH-FX/FXP
      IF(XH)8,8,9
    9 PXH=-ALOG10(XH)
      PYH=-ALOG10(YH)
      G=PXH-PYH
```

```
      IF(ABS(G)-.005)5,5,6
    6 YH=XH
      HYD=(1.007E-14)/(GAMMA*YH)
      N=N+1
      IF(N-20)7,7,5
C     CALCN & REFINEMENT OF IONIC STRENGTH
    5 MN=MN+1
      DF=1.+CK2*XH+A*XH**2
      CL(J)=TB/DF
      CHL(J)=CK2*XH*CL(J)
      CH2L(J)=A*(XH**2.)*TB/DF
      XIST=(CCKCL+3.*CL(J)+CHL(J))
      GI=YIST-XIST
      IF(ABS(GI)-.0005)51,51,43
   43 YIST=XIST
      IF(MN-20)22,22,51
    8 PXH=1.0
C     CONVERSION OF MOLALITY BACK TO MOLARITY AT 25C
   51 X(1,J)=PXH-ALOG((TM*AM)/(1.000485*(TV+V(J))))
C     ADJUSTMENT FOR NON-NERNSTIAN RESPONSE
      Y(J)=Y(J)*(-0.00699)+0.0479)
      DELTA=Y(J)-X(1,J)
      WRITE(6,73)V(J),Y(J),X(1,J),DELTA,N,MN,AH,AHL,AL,XIST,CK1,CK2
   13 CONTINUE
      WRITE(6,64)
C     CALCN OF NBAR & BUFFER CAPACITY
      DO 16 J=KN,KD
      H=10**(-X(1,J))
      XNBAR=(2.*TBI-ALKI*V(J)/TV-(TV+V(J))*H/TV)/TBI
      J1=J-1
      IF(J1)60,60,61
   60 BETA=0.0
      GO TO 14
   61 BETA=(V(J)-V(J1))*ALKI/((TV+V(J))*(X(1,J)-X(1,J1)))
   14 WRITE(6,65)V(J),X(1,J),CL(J),CHL(J),CH2L(J),XNBAR,BETA
   16 CONTINUE
      GO TO 99
  100 RETURN
      END
      006:0152:2  IS THE LOCATION FOR EXCEPTIONAL ACTION ON THE I/O STATEMENT AT S
```

```
      SUBROUTINE CALC(I,X,Y,P)
      DIMENSION X(2,200),P(2)
      Y=P(1)*X(1,I)+P(2)
      RETURN
      END
```

APPENDIX 5

FORTRAN PROGRAM TO CALCULATE HYDROGEN ION CONCENTRATIONS IN DILUTE SOLUTIONS OF HCl

```
      SUBROUTINE PRELI2(Y,X,KD)
C     PROGRAM TO CALIBRATE HCL/KOH SYSTEMS
      DIMENSION Y(200),X(2,200),V(200)
   24 FORMAT(' ITRATION NO.: ',I3,'    NUMBER OF DATA POINTS = ',I3,'
     1  ENDPOINT = ',F10.4/)
   71 FORMAT(2F10.4,2X,I3,F10.3,2X,F5.1,X,I3,F6.3)
   72 FORMAT(2F10.4)
   74 FORMAT(X,40HDATA FOR CALIB CURVE FOR HCL/KOH SYSTEMS/)
   99 READ(5,71,END=100)VE,ALKI,ZKODE,TV,TEMP,KL,AISTR

      IF(ZKODE)100,100,81
   81 KN=KD+1
      KD=KL+KD
      READ(5,72) (V(J),Y(J),J=KN,KD)
      WRITE(6,74)

      WRITE(6,24)ZKODE,KL,VE
      DO 13 J=KN,KD
      XH=ALKI*(VE-V(J))/(TV+V(J))
      X(1,J)=-ALOG10(XH)
      Y(J)=Y(J)-(Y(J)*(-0.00699)+0.0479)
   13 CONTINUE
      GO TO 99
  100 RETURN
      END
      002:005:12  IS THE LOCATION FOR EXCEPTIONAL ACTION ON THE I/O STATEMENT AT
                                                                              S
```

APPENDIX 6

FORTRAN PROGRAM TO CALCULATE HYDROGEN ION CONCENTRATIONS IN DILUTE SOLUTIONS OF KOH

```
      SUBROUTINE PRELI3(Y,X,KD)
C     PROGRAM TO CALIBRATE KCL/KOH SYSTEMS
      DIMENSION Y(200),X(2,200),V(200)
   74 FORMAT(X,40HDATA FOR CALIB CURVE FOR KCL/KOH SYSTEMS/)
   24 FORMAT(' TITRATION NO.: ',I3,'    NUMBER OF DATA POINTS = ',I3/)
   71 FORMAT(F10.4,2X,I3,F10.3,X,I3,F6.3,2X,F8.6)
   72 FORMAT(2F10.4)
   99 READ(5,71,END=100)ALKI,ZKODE,TV,KL,AISTR,CKCL
      IF(ZKODE)100,100,81
   81 KN=KD+1
      KD=KL+KD
      READ(5,72) (V(J),Y(J),J=KN,KD)
      WRITE(6,74)
      WRITE(6,24)ZKODE,KL
      DO 13 J=KN,KD
      XOH=ALKI*V(J)/(TV+V(J))
      XIST=CKCL+XOH
      GFN=(-1.0132*SQRT(XIST))/(1+1.1836*SQRT(XIST))+0.279*(XIST)-0.0472
     1*(XIST)**1.5
      GFN=10**(GFN)
      XH=1.0E-14/(XOH*GFN)
      X(1,J)=-ALOG10(XH)
      Y(J)=Y(J)-(Y(J)*(-0.00699)+0.0479)
      X(1,J)=10**(-X(1,J))
      Y(J)=10**(-Y(J))
   13 CONTINUE
      GO TO 99
  100 RETURN
      END
      00A:0074:2  IS THE LOCATION FOR EXCEPTIONAL ACTION ON THE I/O STATEMENT AT
```

APPENDIX 7

REPRESENTATIVE DATA FROM TITRATIONS OF o-PHTHALIC ACID WITH STANDARD POTASSIUM HYDROXIDE AT 25 °C, IONIC STRENGTHS 0.04, 0.15 AND 0.20 M

7A.1 Ionic Strength 0.04 M

Titre (ml) *(a)*	pH' *(b)*	pc_H	Titre (ml)	pH'	pc_H
0.0000	3.2188	3.1529	0.0580	4.3224	4.2457
0.0100	3.3054	3.2437	0.0620	4.4705	4.3988
0.0140	3.3446	3.2851	0.0660	4.6145	4.5445
0.0180	3.3930	3.3299	0.0700	4.7514	4.6800
0.0220	3.4464	3.3790	0.0740	4.8853	4.8065
0.0260	3.5027	3.4331	0.0780	5.0082	4.9268
0.0300	3.5682	3.4934	0.0820	5.1290	5.0441
0.0340	3.6467	3.5613	0.0860	5.2579	5.1620
0.0380	3.7303	3.6388	0.0900	5.3757	5.2844
0.0420	3.8270	3.7282	0.0940	5.5208	5.4165
0.0460	3.9358	3.8325	0.0980	5.6748	5.5665
0.0500	4.0536	3.9545	0.1020	5.8581	5.7502
0.0540	4.1805	4.0940	0.1040	5.9558	5.8648

(a) *Cumulative volume of 0.8893 M KOH added to 49.93 ml of titration solution, initially comprising o-phthalic acid (9.873×10^{-4} M), KCl (0.0385 M).*

(b) *pH' corresponds to measured pH (pH_m) corrected for liquid junction deviations (see section 4.4.3).*

7A.2 Ionic Strength 0.15 M

Titre (ml) *(a)*	pH' *(b)*	pc_H	Titre (ml)	pH'	pc_H
0.0000	2.8694	2.7803	0.1600	3.9287	3.7995
0.0150	2.9207	2.8299	0.1700	4.0798	3.9381
0.0250	2.9580	2.8653	0.1800	4.2207	4.0795
0.0300	2.9781	2.8838	0.1900	4.3537	4.2155
0.0400	3.0184	2.9226	0.2000	4.4624	4.3421
0.0500	3.0577	2.9638	0.2100	4.5782	4.4590
0.0600	3.1050	3.0081	0.2200	4.6940	4.5681
0.0700	3.1563	3.0557	0.2250	4.7474	4.6204
0.0800	3.2117	3.1073	0.2350	4.8481	4.7217
0.0900	3.2721	3.1635	0.2450	4.9407	4.8206
0.1000	3.3306	3.2254	0.2550	5.0364	4.9192
0.1100	3.4031	3.2940	0.2650	5.1482	5.0198
0.1200	3.4886	3.3709	0.2700	5.2046	5.0718
0.1300	3.5843	3.4581	0.2750	5.2620	5.1253
0.1400	3.6900	3.5576	0.2850	5.3828	5.2391
0.1500	3.7958	3.6713	0.3000	5.5832	5.4388

(a) *Cumulative volume of 0.8893 M KOH added to 49.93 ml of titration solution, initially comprising o-phthalic acid (2.9959×10^{-3} M), KCl (0.1470 M).*

(b) *pH' corresponds to measured pH (pH_m) corrected for liquid junction deviations (see section 4.4.3).*

7A.3 Ionic Strength 0.20 M

Titre (ml) *(a)*	pH' *(b)*	pc_H	Titre (ml)	pH'	pc_H
0.0000	2.8613	2.7722	0.1650	3.9680	3.8369
0.0150	2.9137	2.8212	0.1750	4.1170	3.9727
0.0250	2.9509	2.8561	0.1850	4.2509	4.1075
0.0350	2.9892	2.8932	0.1950	4.3678	4.2355
0.0450	3.0285	2.9327	0.2050	4.4765	4.3549
0.0550	3.0687	2.9749	0.2150	4.5953	4.4662
0.0650	3.1201	3.0201	0.2250	4.7061	4.5711
0.0750	3.1735	3.0690	0.2350	4.8048	4.6718
0.0850	3.2309	3.1221	0.2450	4.8964	4.7703
0.0950	3.2862	3.1802	0.2550	4.9891	4.8687
0.1050	3.3477	3.2443	0.2650	5.1018	4.9691
0.1150	3.4302	3.3157	0.2750	5.2166	5.0744
0.1250	3.5179	3.3959	0.2850	5.3415	5.1882
0.1350	3.6175	3.4869	0.2950	5.4684	5.3160
0.1450	3.7132	3.5905	0.3000	5.5399	5.3878

(a) *Cumulative volume of 0.8893 M KOH added to 49.93 ml of titration solution, initially comprising o-phthalic acid (2.9959×10^{-3} M), KCl (0.1970 M).*

(b) *pH' corresponds to measured pH (pH_m) corrected for liquid junction deviations (see section 4.4.3).*

APPENDIX 8

REPRESENTATIVE DATA FROM TITRATIONS OF HCl WITH STANDARD POTASSIUM HYDROXIDE AT 25 °C, IONIC STRENGTHS 0.04, 0.15 AND 0.20 M

8A.1 Ionic Strength 0.04 M

Titre (ml) *(a)*	pH' *(b)*	pc_H	Titre (ml)	pH'	pc_H
0.030	1.7979	1.7244	0.550	2.0658	1.9980
0.060	1.8160	1.7415	0.600	2.1050	2.0382
0.100	1.8372	1.7637	0.650	2.1483	2.0826
0.150	1.8603	1.7871	0.700	2.1957	2.1318
0.200	1.8845	1.8118	0.750	2.2501	2.1872
0.250	1.9107	1.8379	0.800	2.3125	2.2507
0.300	1.9369	1.8657	0.860	2.4011	2.3413
0.350	1.9651	1.8953	0.900	2.4706	2.4141
0.450	1.9973	1.9269	0.950	2.5844	2.5263
0.500	2.0305	1.9610	1.000	2.7324	2.6777

(a) *Cumulative volume of 0.8893 M KOH added to 49.93 ml of titration solution, initially comprising HCl (1.995×10^{-2} M), KCl (0.0200 M).*

(b) *pH' corresponds to measured pH (pH_m) corrected for liquid junction deviations (see section 4.4.3).*

8A.2 Ionic Strength 0.15 M

Titre (ml) (a)	pH' (b)	pc_H
0.000	1.7888	1.6982
0.100	1.8271	1.7395
0.200	1.8724	1.7849
0.300	1.9228	1.8355
0.350	1.9510	1.8630
0.400	1.9792	1.8924
0.450	2.0094	1.9239
0.500	2.0426	1.9578
0.550	2.0799	1.9944
0.600	2.1181	2.0343
0.650	2.1624	2.0782
0.700	2.2108	2.1270
0.750	2.2652	2.1818
0.800	2.3296	2.2443
0.850	2.4011	2.3173
0.900	2.4877	2.4049
0.950	2.5995	2.5145
1.000	2.7465	2.6610
1.050	2.9771	2.8833

(a) *Cumulative volume of 0.8993 M KOH added to 49.93 ml of titration solution, initially comprising HCl (2.003×10^{-2} M), KCl (0.1300 M).*

(b) *pH' corresponds to measured pH (pH_m) corrected for liquid junction deviations (see section 4.4.3).*

8A.3 Ionic Strength 0.20 M

Titre (ml) *(a)*	pH' *(b)*	pc_H
0.000	1.7949	1.7004
0.100	1.8352	1.7420
0.200	1.8805	1.7877
0.300	1.9298	1.8386
0.350	1.9570	1.8664
0.400	1.9872	1.8960
0.450	2.0184	1.9277
0.500	2.0517	1.9619
0.550	2.0879	1.9989
0.600	2.1282	2.0392
0.650	2.1725	2.0837
0.700	2.2229	2.1330
0.750	2.2772	2.1886
0.800	2.3417	2.2523
0.850	2.4162	2.3267
0.900	2.5068	2.4164
0.950	2.6216	2.5294
1.000	2.7757	2.6820
1.050	3.0234	2.9189

(a) *Cumulative volume of 0.8993 M KOH added to 49.93 ml of titration solution, initially comprising HCl (1.992×10^{-2} M), KCl (0.1800 M).*

(b) *pH' corresponds to measured pH (pH_m) corrected for liquid junction deviations (see section 4.4.3).*

APPENDIX 9

REPRESENTATIVE DATA FROM TITRATIONS OF KCl SOLUTION WITH STANDARD POTASSIUM HYDROXIDE AT 25 °C, IONIC STRENGTHS 0.04, 0.15 AND 0.20 M

9A.1 Ionic Strength 0.04 M

Titre (ml) *(a)*	pH' *(b)*	pc_H
0.080	10.9655	10.9499
0.100	11.0673	11.0462
0.120	11.1498	11.1247
0.160	11.2797	11.2484
0.200	11.3774	11.3441
0.250	11.4751	11.4394
0.300	11.5567	11.5171
0.350	11.6231	11.5825
0.400	11.6795	11.6390
0.450	11.7299	11.6887
0.500	11.7742	11.7330
0.600	11.8507	11.8093
0.700	11.9151	11.8735

(a) *Cumulative volume of 0.7826 M KOH added to 49.93 ml of titration solution, comprising KCl (0.0350 M).*

(b) *pH' corresponds to measured pH (pH_m) corrected for liquid junction deviations (see section 4.4.3).*

9A.2 Ionic Strength 0.15 M

Titre (ml) *(a)*	pH' *(b)*	pc_H
0.120	11.1095	11.0445
0.140	11.1911	11.1112
0.160	11.2395	11.1689
0.200	11.3452	11.2652
0.250	11.4459	11.3614
0.300	11.5275	11.4399
0.350	11.5959	11.5061
0.400	11.6553	11.5634
0.450	11.7067	11.6138
0.500	11.7530	11.6589
0.600	11.8316	11.7367
0.700	11.8980	11.8022

(a) *Cumulative volume of 0.7826 M KOH added to 49.93 of titration solution, comprising KCl (0.1450 M).*

(b) *pH' corresponds to measured pH (pH_m) corrected for liquid junction deviations (see section 4.4.3).*

9A.3 Ionic Strength 0.20 M

Titre (ml) *(a)*	pH' *(b)*	pc_H
0.160	11.2203	11.1538
0.200	11.3210	11.2502
0.250	11.4217	11.3465
0.300	11.4912	11.4251
0.350	11.5697	11.4914
0.400	11.6292	11.5488
0.450	11.6785	11.5993
0.500	11.7258	11.6445
0.600	11.8134	11.7224
0.700	11.8708	11.7882

(a) *Cumulative volume of 0.7826 M KOH added to 49.93 ml of titration solution, comprising KCl (0.1951 M).*

(b) *pH' corresponds to measured pH (pH_m) corrected for liquid junction deviations (see section 4.4.3).*

APPENDIX 10

THE "ACTIVITY COEFFICIENT FUNCTION" OF WATER

The use of the activity product of water (K_w) in the calculation of either hydrogen or hydroxide ion concentration involves the estimation of an "activity coefficient function", the term in parentheses in equation 4.39:

$$K_w = a_H\, a_{OH} / a_{H_2O} = m_H\, m_{OH} \cdot (f_H\, f_{OH} / a_{H_2O})$$

Harned and Owen [118] have described an empirical relationship to determine this function, viz:

$$\log (f_H\, f_{OH} / a_{H_2O}) = \frac{-2\, S\, I^{\frac{1}{2}}}{1 + A'\, I^{\frac{1}{2}}} + \beta I + C\, I^{1.5} \qquad (4A.1)$$

where

$$S = \frac{1.814 \times 10^6}{(DT)^{1.5}} \qquad (4A.2)$$

$$A' = 50.3\, a^\circ\, (DT)^{-\frac{1}{2}} \qquad (4A.3)$$

$$\beta = b^\circ + b_1\, t \qquad (4A.4)$$

$$C = c^\circ + c_1\, t \qquad (4A.5)$$

In this work the following values of the various parameters in equations 4A.1 - 4A.5 were used [(a)]:

DT *(b)*	2.341×10^{4} at 25 °C
a°	3.6
b°	0.266
c°	-0.035
b_1	5.2×10^{-4}
c_1	-4.88×10^{-4}
t *(c)*	25

(a) *From Harned and Owen's data for KCl at 25 °C*

(b) *D = dielectric constant, T = temperature °K*

(c) *t = temperature °C*

APPENDIX 11

FORTRAN PROGRAM TO CALCULATE $\bar{n}_H$ FOR TITRATIONS OF GALLIC ACID WITH KOH

```
      SUBROUTINE PRELIM(YO,X,NO,XKCL,HYDROL,TTL)
C
C       CALCULATION OF N-BAR,DEGREE OF PROTONATION OF THE LIGAND
      DIMENSION HYDROL(200),TTL(200),XKCL(200)
      DIMENSION YO(200),X(2,200)
   40 FORMAT(F10.4,F10.2,E10.4,F10.4)
   41 FORMAT(I1,F9.4,F10.4)
   43 FORMAT('1DATA FOR PROTONATION CONSTANTS OF GALLIC ACID'/)
   44 FORMAT('0TOTAL LIGAND CONCN = ',E11.4,5X,'ALKALI CONCN = ',F6.4,5X
     1,'TOTAL INITIAL VOL = ',F7.3,5X,'KCL = ',F6.4//)
   45 FORMAT('0 TITRE    PHOBS    P(H+)    I STR    NBAR     GA FN     HYDROL
     1       ACID'/)
   46 FORMAT(X,6(F6.3,2X),2(E10.4,3X))
      WRITE(6,43)
C     READ OBSERVATIONS TO SENTINEL
      NO=0
      J=0
  801    J=J+1
   99 READ(5,41,END=100) ISENT,YO(J),X(1,J)
      IF(ISENT)801,801,1101
 1101 KN=NO+1
      NO=J-1
      READ(5,40)ALKI,VOL,TLI,CKCL
      WRITE(6,44)TLI,ALKI,VOL,CKCL
      WRITE(6,45)
      GFN=0.6
      DO 2 I=KN,NO
      TR=YO(I)
C
C     CORRECTIONS FOR NON NERNSTIAN RESPONSE & PH/P(H+) RELATIONSHIP
      PH=X(1,I)
      X(1,I)=X(1,I)+(X(1,I)*0.00699-0.0479)
      X(1,I)=(X(1,I)-0.086)/1.0010
      H=10.0**(-X(1,I))
      XKCL(I)=CKCL*(VOL/(VOL+YO(I)))
      TL=TLI*VOL/(VOL+YO(I))
      ACID=4.0*TL-ALKI*YO(I)/(VOL+YO(I))
   60 GFN2=GFN
   59 AKW=1.008E-14/GFN
      HYDROL(I)=AKW/H
      TH=ACID+HYDROL(I)
      YO(I)=(TH-H)/TL
C
C     DETERMINATION OF IONIC STRENGTH
      IF(YO(I)-2.)50,51,51
   50 IF(YO(I)-1.)55,54,54
   51 IF(YO(I)-3.)53,52,52
   52 CLH3=(4.0-YO(I))*TL
      CLH2=0.0
      CLH=0.0
      CL=0.0
      GO TO 56
   53 CLH3=(YO(I)-2.0)*TL
      CLH2=(3.0-YO(I))*TL
      CLH=0.0
      CL=0.0
      GO TO 56
   54 CLH3=0.0
      CLH2=(YO(I)-1.0)*TL
      CLH=(2.0-YO(I))*TL
      CL=0.0
      GO TO 56
   55 CLH3=0.0
      CLH2=0.0
      CLH=(YO(I)-0.0)*TL
      CL=(1.0-YO(I))*TL
   56 XISTR=XKCL(I)+CLH3+3.0*CLH2+6.0*CLH+10.0*CL+HYDROL(I)
C
C     DETERMINATION & REFINEMENT OF IONIC PRODUCT OF WATER
   57 GFN=10**(-1.0124*SQRT(XISTR)/(1.+1.1833*SQRT(XISTR))+0.279*XISTR-0
     1.0472*(XISTR)**1.5)
      IF(ABS(GFN2-GFN)-0.001)58,58,60
   58 WRITE(6,46)TR,PH,X(1,I),XISTR,YO(I),GFN,HYDROL(I),ACID
      TTL(I)=TL
    2 CONTINUE
      GO TO 99
  100 RETURN
      END
```

```
      SUBROUTINE CALC(X,P,I,Y,CLH4,CLH3,CLH2,CLH,CL,XISTR,XKCL,HYDROL,TT
     1L)
C     CALCULATION OF N-BAR,CONCENTRATION OF LIGAND SPECIES & IONIC
C     STRENGTH BASED ON HYDROGEN ION CONCENTRATION & PROTONATION CONSTS
      DIMENSION HYDROL(200),TTL(200),XKCL(200)
      DIMENSION CLH4(200),CLH3(200),CLH2(200),CLH(200),CL(200)
      DIMENSION X(2,200),P(4)
      H=10.**(-X(1,I))
      D=1.0+P(1)*H+P(1)*P(2)*H**2.+P(3)*P(2)*P(1)*H**3.+P(1)*P(2)*P(3)*P
     1(4)*H**4.
      Y=(P(1)*H+2.0*P(2)*P(1)*H**2+3.*P(3)*P(2)*P(1)*H**3+4.*P(4)*P(3)*P
     1(2)*P(1)*H**4)/D
      CLH4(I)=(P(1)*P(2)*P(3)*P(4)*H**4.)*100.0/D
      CLH3(I)=(P(1)*P(2)*P(3)*H**3.)*100.0/D
      CLH2(I)=(P(1)*P(2)*H**2)*100.0/D
      CLH(I)=(P(1)*H**1.)*100.00/D
      CL(I)=100.00/D
      XISTR=XKCL(I)+(CLH3(I)+3.*CLH2(I)+6.*CLH(I)+10.*CL(I))*TTL(I)/100.
     1+HYDROL(I)
      RETURN
      END
```

APPENDIX 12

FORTRAN PROGRAM TO CALCULATE $\bar{n}_H$ FOR TITRATIONS OF CATECHOL WITH KOH

Program identical to that for gallic acid (Appendix 11) except for the following changes:

ACID = 2.0 * TL + AA - ALKI * YO(I)/(VOL + YO (I))

XISTR = XKCL (I) + CLH + 3.0 * CL + AA + HYDROL (I)

Note: AA denotes concentration of standard acid initially added to stock solutions of catechol

APPENDIX 13

FORTRAN PROGRAMS TO CALCULATE T_H FOR SOLUTIONS OF FERROUS ION AND GALLIC ACID & CATECHOL

13A.1 Gallic Acid

```
FILE  5(KIND=READER)
FILE  6(KIND=PRINTER)

      SUBROUTINE PRELIM(YO,X,NO,TL,TM,CKCL,XK)
C
      DIMENSION X(2,200),YO(200),TL(200),TM(200),CKCL(200),XK(20)
      WRITE(6,43)
C
C     READ OBSERVATIONS TO SENTINTEL
      NO=0
      J=0
  801 J=J+1
   99 READ(5,41,END=100)ISENT,YO(J),X(1,J)
      IF(ISENT)801,801,1101
 1101 KN=NO+1
      NO=J-1
C
C     READ INITIAL PARAMETERS
      READ(5,40)ALKI,VOL,XKCL,TLI,TMI,ACIDI
      READ(5,42)XK(1),XK(2),XK(3),XK(4)
      WRITE(6,44)ALKI,VOL,XKCL,TLI,TMI,ACIDI
C
C     LOOP TO CONVERT PH TO H CONCN
      DO 2 I=KN,NO
      X(1,I)=(X(1,I)-0.086)/1.0010
      X(1,I)=10.0**(-X(1,I))
C
C     CORRECTIONS FOR DILUTION
      Q=VOL/(VOL+YO(I))
      TL(I)=TLI*Q
      TM(I)=TMI*Q
      CKCL(I)=XKCL*Q
      ACID=ACIDI*Q
      YO(I)=4.*TL(I)+ACID-ALKI*YO(I)/(VOL+YO(I))
    2 CONTINUE
      GO TO 99
  100 RETURN
C
   40 FORMAT(F10.4,F10.2,F10.4,3E10.4)
   41 FORMAT(I1,F9.4,F10.4)
   42 FORMAT(5E10.4)
   44 FORMAT('0ALKALI CONCN = ',F6.4,5X,'TOTAL INITIAL VOL = ',F7.3,5X,'
     1KCL = ',F6.4//' TOTAL INITIAL LIGAND CONCN = ',E11.4,5X//' TOTAL
     2INITIAL METAL CONCN = ',E11.4,5X,'ADDED ACID = ',E11.4//)
   43 FORMAT('1'//'0CALCULATION OF IRON(II)-GALLIC ACID STABILITY CONSTANT
     1S'/)
      END
002:0083:2  IS THE LOCATION FOR EXCEPTIONAL ACTION ON THE I/O STATEMENT AT
```

```
      SUBROUTINE CALC(I,X,Y,P,FM,CKCL,TM,TL,XK,CFHL,CFHLB,CFHLD,CFHLO,CF
     1OH,XISTR,MN,N1,HL,XPHCON,SHL,HYDROL)
C
      DIMENSION P(20),X(2,200),CKCL(200),TM(200),TL(200),XK(20)
C
      H=X(1,I)
      MN=0
      E=XK(2)*XK(3)*XK(4)*H**3.+XK(2)*XK(3)*H**2.+XK(2)*H+1./(XK(1)*H)+1
C
C     BY-PASS TO CALCULATE INITIAL ESTIMATE OF HL & FE CONCENTRATIONS
      IF(I-1)1,1,3
    1 HL=TL(I)/E
      FM=TM(I)
      GO TO 10
C
C     CALCULATION & REFINEMENT OF HL CONCENTRATION
   12 SHL=HL
    3 C=2.*(P(2)*FM**2)/H+2.*(P(3)*FM**2)/H**2
      D=E+P(1)*FM+P(1)*P(4)*FM/H
   13 N=1
    7 FX=C*HL**2+D*HL-TL(I)
      FXP=2*C*HL+D
      XHL=HL-FX/FXP
      IF(ABS(XHL-HL).LE.0.005*HL)GO TO 5
    6 HL=XHL
      N=N+1
      IF(N-20)7,7,5
    5 IF(ABS(SHL-HL).LE.0.005*HL)GO TO 8
   10 MN=MN+1
      IF(MN-20)11,11,8
C
C     CALCULATION OF FREE METAL ION CONCENTRATION
   11 PB=1.+P(1)*HL+P(4)*P(1)*HL/H+P(5)/H
      PA=2.*(P(2)*HL**2)/H+2.*(P(3)*HL**2)/H**2
      NL=1
   22 FX2=PA*FM**2+PB*FM-TM(I)
      FXP2=2.*PA*FM+PB
      XFM=FM-FX2/FXP2
      IF(ABS(XFM-FM).LE.0.005*FM)GO TO 12
   21 FM=XFM
      NL=NL+1
      IF(NL-20)22,22,12
C
C     CALCULATION OF IONIC STRENGTH
    8 H3L=XK(2)*XK(3)*HL*H**2.
      H2L=XK(2)*HL*H
      YL=HL/(XK(1)*H)
      FHL=P(1)*FM*HL
      FHLB=(P(2)*(FM*HL)**2)/H
      FHLD=P(3)*(FM*HL/H)**2
      FHLO=P(4)*P(1)*FM*HL/H
      FOH=P(5)*FM/H
      XISTR=H3L+3.*H2L+6.*HL+10.*YL+FHL+6.*FHLB+10.*FHLD+FOH+4.*FM+CKCL(
     1I)
C
C     CALCULATION OF HYDROLYSIS
      GFN=10.**(-1.0124*SQRT(XISTR)/(1.+1.1833*SQRT(XISTR))+0.279*XISTR-
     10.0472*(XISTR)**1.5)
      AKW=1.0C6E-14/GFN
      HYDROL=AKW/H
C
C     CALCULATION OF TH
      Y=4.*XK(2)*XK(3)*XK(4)*HL*H**3+3.*H3L+2.*H2L+HL+FHL+FHLB-FOH+H-
     1HYDROL
C
C     CALCULATION OF CONCENTRATIONS OF INDIVIDUAL METAL LIGAND SPECIES
      CFHL=FHL*100./TM(I)
      CFHLB=2.*FHLB*100./TM(I)
      CFHLD=FHLD*100./TM(I)
      CFHLO=FHLO*100./TM(I)
      CFOH=FOH*100./TM(I)
      XPHCON=-ALOG10(X(1,I))
      N1=N
      RETURN
      END
```

13A.2 Catechol

```
      FILE  5(KIND=READER)
      FILE  6(KIND=PRINTER)
            SUBROUTINE PRELIM(YO,X,NO,TL,TM,CKCL,XK)
      C
            DIMENSION X(2,200),YO(200),TL(200),TM(200),CKCL(200),XK(20)
            WRITE(6,43)
      C
      C     READ OBSERVATIONS TO SENTINTEL
            NO=0
            J=0
        801 J=J+1
         99 READ(5,41,END=100)ISENT,YO(J),X(1,J)
            IF(ISENT)801,801,1101
       1101 KN=NO+1
            NO=J-1
      C
      C     READ INITIAL PARAMETERS
            READ(5,40)ALKI,VOL,XKCL,TLI,TMI,ACIDI
            READ(5,42)XK(1),XK(2)
            WRITE(6,44)ALKI,VOL,XKCL,TLI,TMI,ACIDI
      C
      C     LOOP TO CONVERT PH TO H CONCN
            DO 2 I=KN,NO
            X(1,I)=(X(1,I)-0.086)/1.0010
            X(1,I)=10.0**(-X(1,I))
      C
      C     CORRECTIONS FOR DILUTION
            Q=VOL/(VOL+YO(I))
            TL(I)=TLI*Q
            TM(I)=TMI*Q
            CKCL(I)=XKCL*Q
            ACID=ACIDI*Q
            YO(I)=2.*TL(I)+ACID-ALKI*YO(I)/(VOL+YO(I))-X(1,I)
          2 CONTINUE
            GO TO 99
        100 RETURN
      C
         40 FORMAT(F10.4,F10.2,F10.4,3E10.4)
         41 FORMAT(I1,F9.4,F10.4)
         42 FORMAT(2E10.4)
         44 FORMAT('0ALKALI CONCN = ',F6.4,5X,'TOTAL INITIAL VOL = ',F7.3,5X,'
           1KCL = ',F6.4//' TOTAL INITIAL LIGAND CONCN = ',E11.4,5X//' TOTAL
           2INITIAL METAL CONCN = ',E11.4,5X,'ADDED ACID = ',E11.4//)
         43 FORMAT(///'0 CALCULATION OF FE(II)-CATECHOL STABILITY CONSTANTS'/)
            END
            002:007F:2  IS THE LOCATION FOR EXCEPTIONAL ACTION ON THE I/O STATEMENT AT
```

```
      SUBROUTINE CALC(I,X,Y,P,FM,CKCL,TM,TL,XK,CFHL,CFHLB,CFHLD,CFHLO,CF
     1OH,XISTR,MN,N1,HL,XPHCON,SHL,HYDROL)
C
      DIMENSION P(20),X(2,200),CKCL(200),TM(200),TL(200),XK(20)
C
      H=X(1,I)
      MN=0
      E=XK(1)*XK(2)*H**2+XK(1)*H+1.
C
C     BY-PASS TO CALCULATE INITIAL ESTIMATE OF HL & FE CONCENTRATIONS
      IF(1-1)1,1,3
    1 HL=TL(I)/E
      FM=TM(I)
      GO TO 10
C
C     CALCULATION & REFINEMENT OF HL CONCENTRATION
   12 SHL=HL
    3 C=2.*P(2)*FM**2/H
      D=E+P(1)*FM
   13 N=1
    7 FX=C*HL**2+D*HL-TL(I)
      FXP=2*C*HL+D
      XHL=HL-FX/FXP
      IF(ABS(XHL-HL).LE.0.005*HL)GO TO 5
    6 HL=XHL
      N=N+1
      IF(N-20)7,7,5
    5 IF(ABS(SHL-HL).LE.0.005*HL)GO TO 8
   10 MN=MN+1
      IF(MN-20)11,11,8
C
C     CALCULATION OF FREE METAL ION CONCENTRATION
   11 PB=1.+P(1)*HL+P(5)/H
      PA=2.*P(2)*HL**2/H
      NL=1
   22 FX2=PA*FM**2+PB*FM-TM(I)
      FXP2=2.*PA*FM+PB
      XFM=FM-FX2/FXP2
      IF(ABS(XFM-FM).LE.0.005*FM)GO TO 12
   21 FM=XFM
      NL=NL+1
      IF(NL-20)22,22,12
C
C     CALCULATION OF IONIC STRENGTH
    8 H2L=XK(2)*XK(1)*HL*H**2
      H1L=XK(1)*HL*H
      FHL=P(1)*FM*HL
      FHLB=(P(2)*(FM*HL)**2)/H
      FHLD=P(3)*(FM*HL/H)**2
      FHLO=P(4)*P(1)*FM*HL/H
      FOH=P(5)*FM/H
      XISTR=H1L+3.*HL+3.*FM+CKCL(I)+FOH
C
C     CALCULATION OF HYDROLYSIS
      GFN=10.**(-1.0124*SQRT(XISTR)/(1.+1.1833*SQRT(XISTR))+0.279*XISTR-
     10.0472*(XISTR)**1.5)
      AKW=1.0086E-14/GFN
      HYDROL=AKW/H
C
C     CALCULATION OF TH
      Y=2.*H2L+H1L+H-FOH-HYDROL-FHLB
C
C     CALCULATION OF CONCENTRATIONS OF INDIVIDUAL METAL LIGAND SPECIES
      CFHL=FHL*100./TM(I)
      CFHLB=2.*FHLB*100./TM(I)
      CFHLD=FHLD*100./TM(I)
      CFHLO=FHLO*100./TM(I)
      CFOH=FOH*100./TM(I)
      XPHCON=-ALOG10(X(1,I))
      N1=N
      RETURN
      END
```

APPENDIX 14

BASIC THEORY OF "JOB VARIATION PLOTS"

Job variation plots have been used in this work for the determination of the stoichiometric composition of metal complexes (ML_n). If the ratio of the reacting species, say M and L, is continuously varied in a series of solutions such that the sum of the reactant concentrations is constant, then observation of the ratio at which the maximum amount of product is obtained allows the calculation of the ratio of M and L in the product formed.

In the simple case where the reactants, M and L form only one complex at a time the reaction may be written as:

$$M + nL \rightleftharpoons ML_n$$

If a series of solutions is prepared containing say $(1 - x)c_T$ moles per litre of M and xc_T moles per litre of L, then the equilibrium concentrations of M, L and ML_n are related as follows:

$$c_M = c_T (1 - x) - c_{ML}$$

$$c_L = c_T.x - nc_{ML}$$

Where c_T = total number of moles of reactants present per litre (constant) c_M, c_L, c_{ML} = equilibrium concentration of M, L and ML_n respectively, $x = 0 - 1.0$. Assuming constant activity coefficients, so that the law of mass action is valid in terms of concentrations, the equilibrium constant for the complexation reaction may be written as:

$$k = \frac{c_{ML}}{c_M.c_L^n}$$

Differentiation of this expression with respect to x allows the determination of the relationship between the maximum value of c_{ML} and x:

$$k \frac{dc_M}{dx} \cdot c_L^n + n c_L^{n-1} c_M \cdot \frac{dc_L}{dx} = \frac{dc_{ML}}{dx}$$

Setting $dc_{ML} / dx = 0$ and eliminating c_M, c_L and c_{ML} gives:

$$n = \frac{x}{1 - x}$$

Hence, by determining the value of x which corresponds to maximum formation of ML_n, (where $dc_{ML} / dx = 0$) the composition ratio, n, may be calculated.

The value of x is often determined from spectrophotometric measurements which follow the absorbance of ML at an appropriate wavelength. If the extinction coefficients of M, L and ML_n are ϵ_M, ϵ_L and ϵ_{ML} respectively at a given wavelength, the difference (Y) between the measured absorption and that predicted upon the assumption of no reaction is:

$$Y = l [c_M \epsilon_M + c_L \epsilon_L + c_{ML} \epsilon_{ML} - c_T (1 - x) \epsilon_M - c_T x \epsilon_L]$$

where l = optical path lenth. If $\epsilon_{ML} >> \epsilon_M + \epsilon_L$ it can be shown [214] that Y is a maximum when c_{ML} is a maximum.

A plot of Y against x will yield a very sharp maximum when a single very stable complex is formed. When a single complex of only moderate stability is formed, the maximum is broadened and usually of smaller magnitude.

APPENDIX 15

A BACKGROUND TO SURVEY SAMPLING

For reasons of reduced cost and greater speed and scope, information about a large field of study is often obtained from a "sample survey". A number of "sampling units" (identifiable parts of the "population", the measurements or attributes of which can be recorded) are collected together to form a "sample". Conclusions obtained from the sample are used to make inferences about the nature of the whole field of study, the "population" (which itself is a large assembly of sampling units).

15A.1 Estimation of Population Parameters

15A.1.1 Definitions

The total number of sampling units in the population surveyed determines the population size (N). Each sampling unit has associated with it a measurement or attribute (x) which, in general, will be unique to that unit. The population is surveyed to estimate the average value of x over all units of the population. This quantity is called the "population mean" ($\bar{X}$) and is defined as:

$$\bar{X} = \sum^{N} x / N$$

A measure of the inherent variability among individual sampling units in the population is given by the "population variance" (V) which is effectively a type of average of the deviations of each unit value, x, from their overall mean, $\bar{X}$. The population variance is given by:

$$V = \sum^{N} (x - \bar{X})^2 / (N - 1)$$

Similar definitions follow for sample parameters; mean ($\bar{x}$) and variance (s^2):

$$\bar{x} = \sum^{n} x / n$$

$$s^2 = \sum^{n} (x - \bar{x})^2 / (n - 1)$$

where n = size of sample.

15A.1.2 Use of Sample Data as Population Estimates

Since it is not practicable to measure each and every unit of the population, $\bar{X}$ and V are estimated from a chosen fraction of the whole population and this constitutes a sample.

For the population there exists a number of possible samples of size n, that could be chosen at any one time ($^{N}C_{n}$ in total), the composition of which depends on the method of selecting the individual sampling units. It can be shown [215] that, if all possible samples of size n have the same probability of being chosen from the population, then $\bar{x}_i$ (the mean of any one of these samples) is an unbiased estimate of $\bar{X}$. Also, under the same conditions, s_i^2 (the variance of any one sample) is an unbiased estimate of V. A "simple random sample" (see section 15A.2.2) meets these requirements. Indeed any sample selection method, that contains at some stage a random selection process, will provide an unbiased estimate of the population mean. Examples of these methods are "stratified random sampling", "multistage" or "cluster" sampling and "systematic" sampling with a random choice of the first unit (see also section 15A.2.3). However, for these methods, a valid estimate of the population variance may not always be possible from the sample itself.

Any completely non-random sampling method must lead to a biased estimate of the population mean and cannot provide a valid

estimate of sampling errors. For example, "representative sampling", in which sampling units in the opinion of the observer represent the population, will give biased results despite the assertion that 'this sample could have arisen by a random choice'.

15A.1.3 Precision of the Estimate

In general for any set of samples (regardless of selection procedure) there will exist a variation within the corresponding set of sample means which limits the precision of the population estimate. This variation is measured by the "sampling variance" (v), the square root of which is called the "standard error" (or "sampling error"), $se(\bar{x})$. If all possible samples of size n are equally probable then $se(\bar{x})$ is estimated by:

$$se(\bar{x}) = s / (1 - n/N)^{\frac{1}{2}}$$

Hence the variation among sample means depends on:

(1) The population variance, V, as estimated by s.

(2) The sample size, n: the larger the sample size for a given V, the less variable will be $\bar{x}$.

(3) The "sampling fraction", n/N: the larger the sampling fraction for a given population variance and sample size the less variable will be $\bar{x}$.

Note that where the sampling fraction is small (i.e. n is much less than N) its value is of little account in determining the precision of the sample mean as a population estimator. In this case the precision depends primarily on n and V and the standard error is estimated by:

$$se(\bar{x}) = s\, n^{-\frac{1}{2}}$$

To summarise; when surveying a population the following information is required:

(1) an estimate of the unknown population mean for the particular measurement or attribute under study. This estimate is provided by $\bar{x}$, the sample mean and is unbiased if all the possible samples, of size n, that could have been selected are equi-probable.

(2) the precision of the estimate of the population mean. This estimate is provided by the standard error of the sample mean and involves calculation of the sample variance.

(3) the limits within which it can be confidently stated that the population mean lies. This is the subject of the next section.

15A.1.4 Limits to the Estimate

The standard error measures the variability of the estimate $\bar{x}$ about the population mean ($\bar{X}$); thus a sample mean with a small standard error is less likely to differ greatly from the population mean than one with a large standard error. This idea can be made more precise by introducing the quantity:

$$t = (\bar{x} - \bar{X}) / se(\bar{x})$$

If $\bar{X}$ were known, values of t for any given sample, i, could be calculated and tabulated. As has been noted, the number of possible samples of size n that could be chosen from a population of size N is ${}^{N}C_{n}$. For example, if N = 25 (a very small population by normal standards) there are 53 130 possible samples of size 5 that could be chosen. Hence it can be seen that for most populations the number of possible samples and associated values of t is very large. The distributions of these values can usually be described, with only a small degree of approximation,

by continuous mathematical functions (distribution functions) that express the probability that t, for example, will be less than any chosen value T. Provided the sample is not very small these functions agree closely with two standard distribution functions; $\bar{x}_i$ following the "normal distribution" and t following the "students" t - distribution (a function depending only on n - 1, the degrees of freedom on which the estimated sampling variance is based).

Values of the t - distribution are tabulated with various degrees of freedom and for given probability levels. For example, for a sample of size n = 121 (i.e. 120 degress of freedom), t = 1.98 at the 95 % probability level. That is, there is a 95 % probability that the estimated population mean ($\bar{x}$) lies within about twice the standard error of the true population mean. From equation 15A.1:

$$\bar{x} - \bar{X} = 1.98\ (se(\bar{x}))$$

The values of $t.se(\bar{x})$ are known as "confidence limits" of the estimated population mean. The confidence limits for the above example can be expressed thus:

$$\bar{X} = \bar{x} \pm 1.98\ se(\bar{x}) \quad (95\ \%)$$

The 95 % probability level is generally adopted as providing a satisfactory compromise between a frequency of error that is too high and limits for the estimate of the population mean that are too imprecise.

The estimation of population parameters is illustrated in figures 1 and 2.

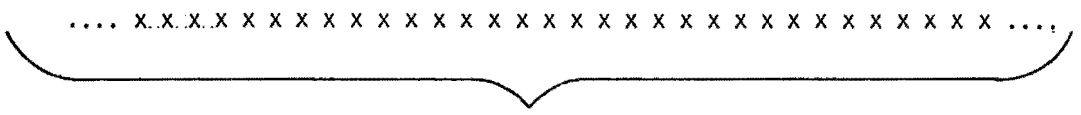

population of size N, mean X, and variance S^2 (= V)

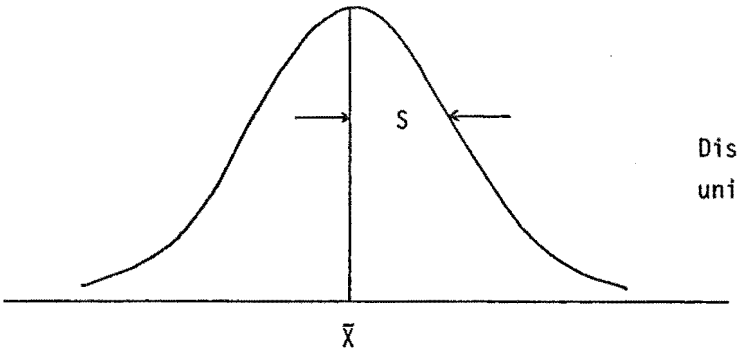

Distribution of all sampling units about population mean

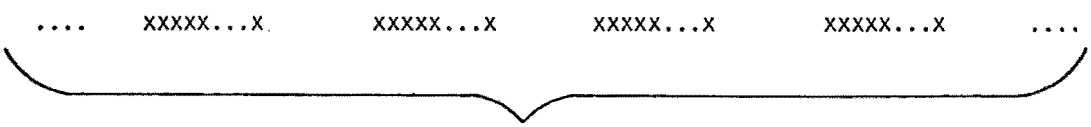

samples of size n, mean $\bar{x}_i$, and variance s_i^2

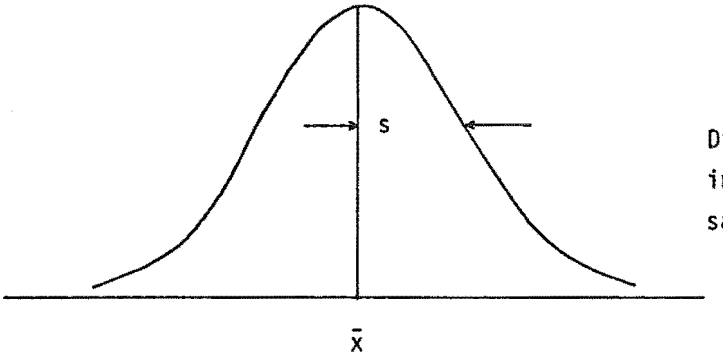

Distribution of n sampling units in a particular sample about the sample mean

$\bar{x}$ and s^2 provide the best unbiased estimate of X and V respectively

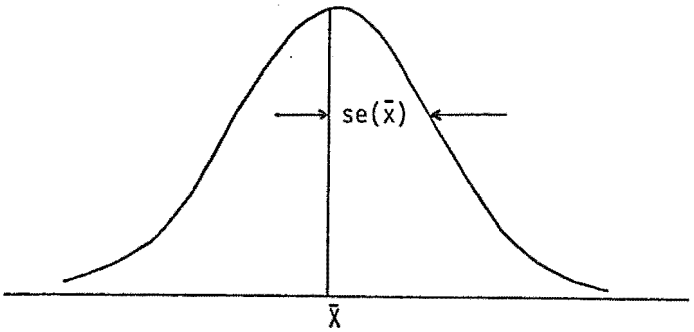

Distribution of sample means $\bar{x}_i$ about the unknown population mean X with a variance which is estimated by $v = s^2/n.(1-n/N)$

Figure 1 Estimating Population Parameters

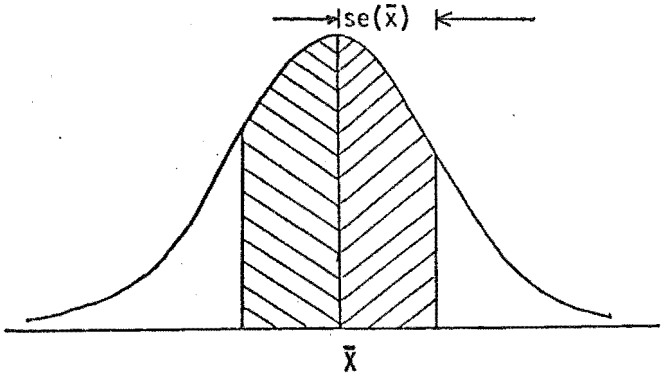

67 % probability level
t ca. 1
(denoted *)

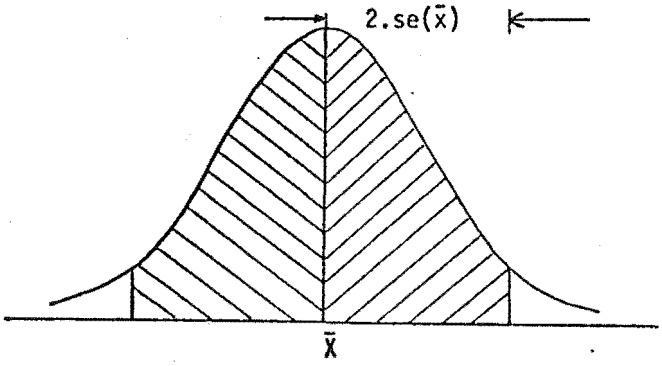

95 % probability level
t ca. 2
(denoted **)

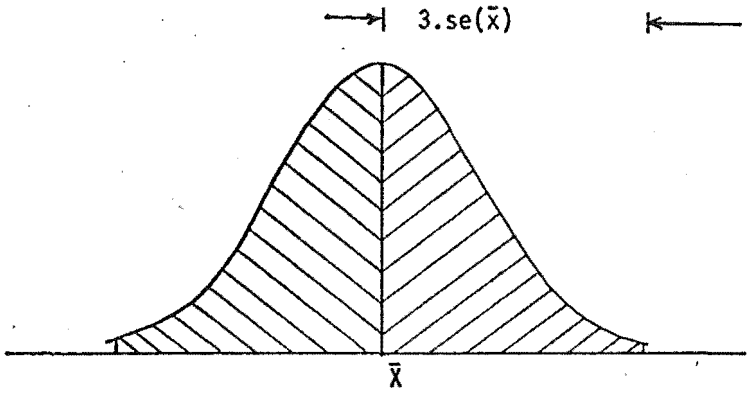

99 % probability level
t ca. 3
(denoted ***)

$\bar{x}$ lies within the shaded areas with the probability stated

Figure 2 Confidence Limits on the Estimate of the Population Mean

15A. 2 Sampling Method

15A.2.1 Determination of Sample Size

Natural variations among sampling units of the population restrict the precision of the estimate of the population mean. This precision is dependant in part on the size of the sample taken. In designing sample surveys the determination of the required sample size is of prime importance. In general a balance is required between the increase in precision obtained from a larger sample and the practicability of obtaining such a sample.

In order to answer the question 'How large a sample ought to be taken (i.e. the number of sampling units)?', the following information is required:

(1) the sampling design to be used

(2) the degree of precision required

(3) some estimate of the inherent variability of the population to be sampled.

Consider the case of a simple random sample from a large population. For a given degree of precision (D), an expression can be written for the number of sampling units required to give a sample mean that will lie with ± D of the true but unknown population mean at some stated probability level, viz :

$$n = t^2 s^2 / D^2 \qquad (15A.2)$$

Some prior knowledge of the inherent variability of the population is required. This can usually be obtained by one of four means:

(1) by the results of a pilot survey

(2) by previous sampling of the same or similar population

(3) by guesswork about the structure of the population, assisted by some mathematical results

(4) by taking the sample in two stages, the first being a sample of size n' (guessed) from which the value of s^2 and hence the required n may be determined.

The calculation of the appropriate sample size (n) is an iterative process since the value assigned to t, itself depends on the yet unknown value of n. In practice some initial value is guessed for n and the corresponding value for t is extracted from statistical tables. A new value of n is calculated and the process is repeated until no significant improvement in n is achieved.

Equation 15A.2 can be conveniently written:

$$n = t^2 C^2 / E^2$$

where $C = 100\ s / \bar{x}$, known as the "coefficient of variance (or variation)"

and $E = 100\ D / \bar{x}$

In this form a graphical relationship between n and C (for given t and E) that has more general applicability can be derived (see figure 3).

15A.2.2 Simple Random Sampling

The most straight-forward case of random sampling is that of "simple" random sampling. This method involves the selection entirely at random of a given number of sampling units from the population. This is commonly effected using a table of random numbers. Each unit in the population is given a number and the required number for the sample is selected by some sequential reading of the random numbers table. Sampling

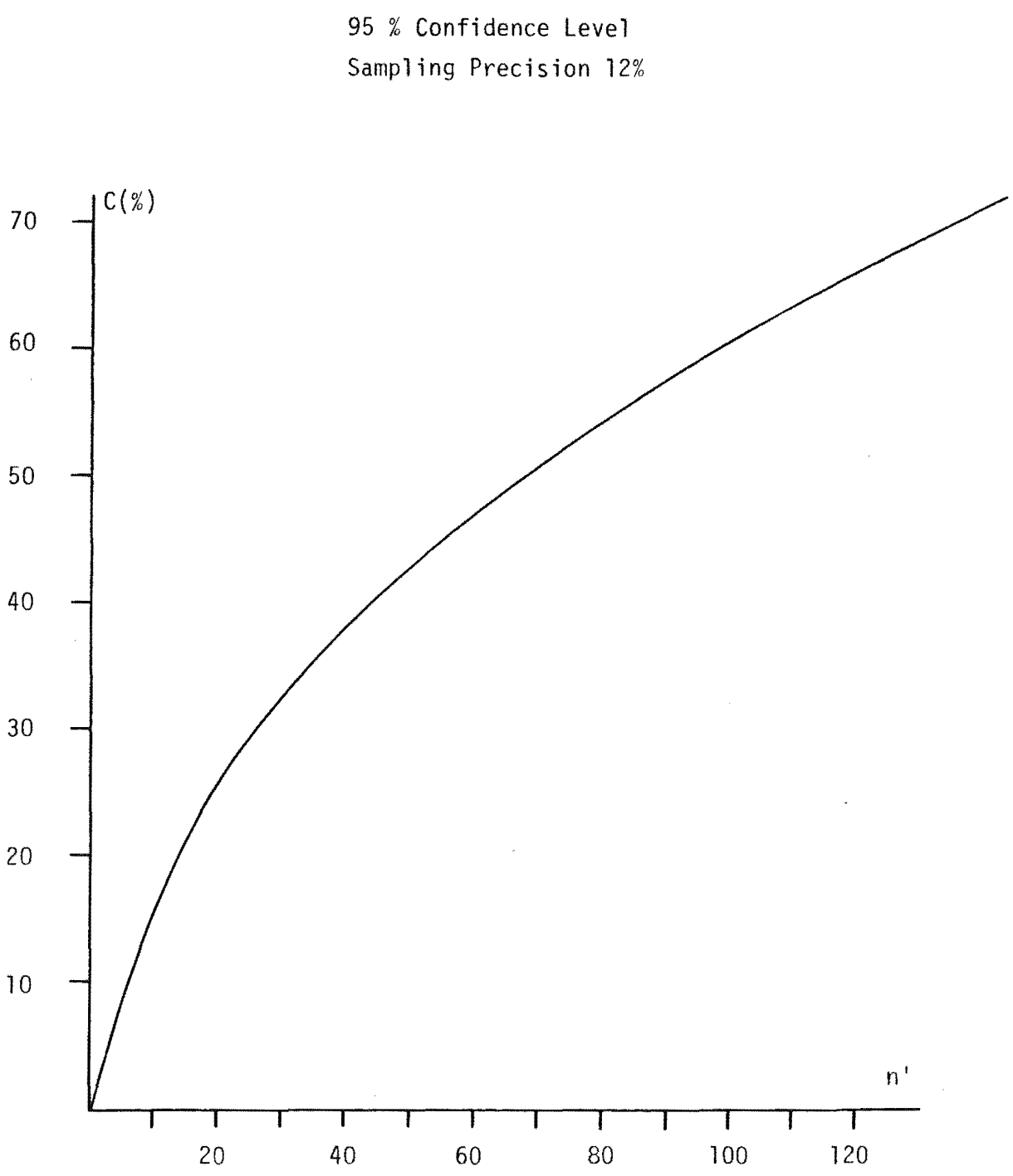

Figure 3 Coefficient of Variation as a Function of Sample Size

sites can be conveniently allocated by choosing cartesian coordinates from the table of random numbers.

15A.2.3 Systematic Sampling

Systematic sampling, where one of the first r units is selected and every rth subsequent unit of the population is then sampled, has the following advantages:

(1) It is quicker and easier (and therefore cheaper) than simple random sampling.

(2) The population size need not be known exactly before sampling can begin.

(3) Any trends or clumping of similar units in the population will tend to be more accurately represented in a systematic sample and hence a more precise estimate can be expected.

Thus the advantages of systematic sampling are considerable. The disadvantage that often outweighs them, is that no valid estimate of error can be calculated in a single systematic sample.

In order that the mean of a systematic sample should be an unbiased estimator of the population mean a random choice must be incorporated at some stage of the sampling procedure. Since the units of a particular sample are fixed by the use of a regular sampling interval the only randomisation possible is the random choice of one sample from a set of possible systematic samples. There are two possible ways of doing this:

Method 1

Choose every rth unit reading in both directions from a unit chosen at random from the whole population. In practice, a number between 1 and N (the population size) is chosen at random and divided by r (for a 1

in r sample) leaving a remainder j (say); then the sample consists of the units numbered:

$$j,\ j + r,\ j + 2r \ldots.$$

Method 2

Choose every rth unit from one of the first r units chosen at random.

The two methods may at first seem to be equivalant and it is true that they give rise to the same set of r possible samples.

In general if N is an exact multiple of r, all possible samples will contain N/r units and methods 1 and 2 are equivalent. If N is not an exact multiple of r, the size of the sample will be one of the two integers on either side of N/r. By method 1 the probability of selection of a particular sample will be given by its size divided by N, while by method 2 all samples will be equally probable. It can be shown[215] that by method 1 an unbiased estimate of the population mean may be obtained, but by method 2 bias is present. If the sample is reasonably large this bias is not usually serious. Method 2 must be used when the size of the population is not known before sampling begins but in general method 1 is to be preferred where possible.

A simple extension of this sampling system can be used for field experiments where sample plots can be sited with their centres at the intersection points of a regular rectangular grid.

In summary:

(1) the mean of a systematic sample can be expected to be a more precise estimate of the population mean than the mean of a random sample of the same size. For a sample of given size, the sampling variance of $\bar{x}$ will be less for systematic than for a random sample if the list from which the systematic sample is drawn shows a fairly

consistent trend or any appreciable grouping in values of x.

(2) no valid estimate of the sampling variance of the mean of a systematic sample can be based on variations within the sample. (The sampling variance depends in general on the set of all possible values that could be obtained from all possible samples. The set of all possible systematic samples is much smaller than the set of all possible random samples of the same size from the same population).

(3) An additional potential disadvantage in a systematic sample occurs when the population contains a periodic type of variation, and if the interval between successive units in the systematic sample happens to coincide with the wavelength (or a multiple of it) it is possible to obtain a sample that is badly biased.

APPENDIX 16

NUTRIENT CONCENTRATIONS IN RUN-OFF FROM A WET TERRACE LAND SOIL ON THE WEST COAST, SOUTH ISLAND *

H.K.J. Powell and M.C. Taylor

Dept. of Chemistry, Univ. of Canterbury, Christchurch, New Zealand

Loss of nutrient in "surface" run-off has been studied for a pasture developed on a Maimai silt loam under 2700 mm precipitation. The concentration of nutrients in run-off peaked significantly in the 3 months following fertilizer application (450 kg/ha of 30% potassic superphosphate), the relative concentrations being calcium > potassium > sulphur >> phosphorus.

By ignoring base levels of nutrient arising from previous applications and from soil weathering, and assuming 0.8 for the fraction of precipitation appearing as "surface" run-off, the estimated mass of nutrient lost (within 3 - 5 months of fertilizer application) was equivalent to 28% of potassium applied, 37% of sulphur, 40% of calcium and 6% of phosphorus.

INTRODUCTION

The wet terrace land soils on the West Coast of the South Island have a rainfall generally in excess of 2500 mm. In the region of the Grey and Taramakau river valleys, glacial outwash terraces and river terraces have carried indigenous podocarp vegetation. Under high rainfall soluble nutrients have been leached from the soil while canopy drip and/or humus has facilitated translocation of iron and aluminium down the soil profile. Clear felling of indigenous forest has left some 200,000 ha of these impoverished soils; some are being developed for forestry and/or agriculture.

Soils in this area fall into several distinct classes, but each is characterised by the development of iron pans at textural interfaces in the soil profile and/or the development of massive silty gleyed horizons. Both of these characteristics contribute to the problem of restricted vertical drainage.

The most important factors related to the development of quality pasture on these soils are considered to include (i) provision of surface drainage, (ii) adequate application of fertilizer, and (iii) stock management. The first two factors are interrelated and it was considered relevant to know how much nutrient is lost in surface run-off, both because of its loss from agriculture and its gain to rivers and lakes.

---

* *Soil Groups of New Zealand, Gley Podzols. N.Z. Soc. Soil Sci., 1980 (in print).*

The Study Area

The soil selected for study, Maimai loamy fine sand, is characterised by a shallow (14 cm) humic silt loam (A_{1g}) and a gravelly, massive gleyed horizon (14-32 cm). A dark red iron pan (32-34 cm) forms an indistinct irregular boundary over unweathered gravels. The topsoil (0-7.5 cm) had 12% clay, 32% silt and 56% sand, and a bulk density of 0.56 g/cm^3. The dominant clay minerals are vermiculite intergrades and interstratified smectites.

The site was on the Department of Lands and Survey "Ruru" block at Bell Hill on a poorly drained flat area of some 1000 ha of glacial outwash gravels. In their undeveloped state the soils support a secondary growth of tangle fern and rushes; indigenous forest was felled and burnt over early this century. Within this area an 80 ha unit (average longitudinal slope 0.7°) was limed (3.75 tonne/ha), top-dressed (625 kg superphosphate/ha, including Cu, Mo and Co) and oversown with perennial ryegrass and clover seed in 1968, and to 1975 had received annual maintenance applications of 450 kg/ha of 30% potassic superphosphate. Lime (2.5 tonne/ha) was applied again in October 1974. Stocking with cattle commenced in 1974. Surface drainage in this unit is facilitated by spinner drains and deeper drains (40-60 cm) following contour lines and flowing into soakage pits (2m x 2m) which run the length of one fence line in most of the 2 ha paddocks and which penetrate into the underlying gravels.

Sampling of Surface Run-off

The area under study had no single confluence for drainage water, thus the sampling was from open drains originating within the unit; sites were chosen to afford a representative sampling of the total drainage pattern over the 80 ha unit. Samples were collected at regular intervals following application of fertilizer (450 kg/ha) in November. Samples of surface run-off were collected within 24 h following periods of substantial precipitation, i.e. only flowing water was collected. Samples were analysed for potassium, calcium, phosphate-phosphorus and sulphur, both before and after filtration through 0.45μ membrane filters. Samples of run-off were also collected from two small catchments via troughs imbedded at 1 cm depth and coupled to a siphon fractionator described elsewhere (Dowling and Powell, 1979).

NUTRIENT CONCENTRATION IN RUN-OFF

Figure 1 shows the mean concentrations of calcium, potassium, sulphur and phosphate-phosphorus in run-off water as collected at ten sampling sites through 1975-6. The range of concentrations observed for each analysis was significant; for example, for samples collected in January 1976 the means and standard deviations were 11.8 ± 3.0, 3.2 ± 3.0, 2.6 ± 0.6, and 0.7 ± 0.25 for calcium, potassium, sulphur and phosphorus.

Filtration of samples through a 0.45μ millipore filter prior to analysis provided information on the transfer of nutrient contained in, or adsorbed on, suspended particulate matter. These measurements established that ca. 40% of PO_4^{3-}-P and 20% of S in the surface run-off water were associated with suspended solids (possibly as oxyanions adsorbed on clay, as insoluble particulates, or as a component(s) of humic material).

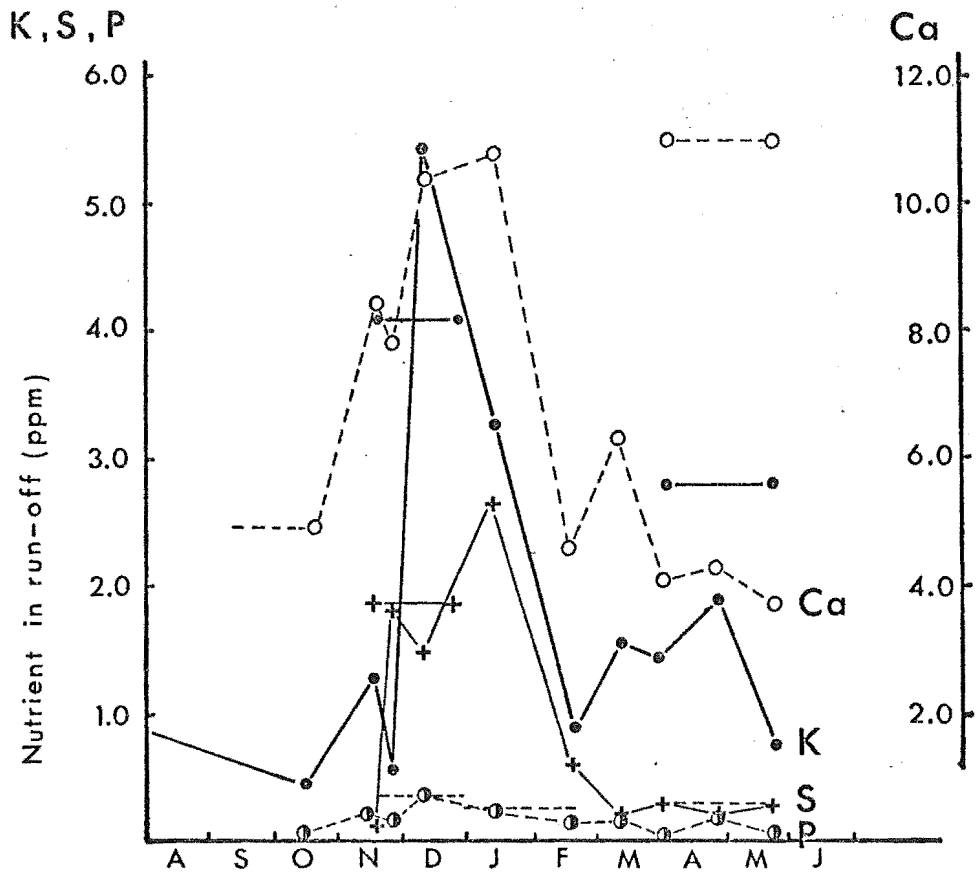

Fig. 1. Mean concentration of calcium O, potassium ●, sulphur +, and phosphorus ◑ in run-off water. Horizontal bars are for samples collected in catchment troughs.

In the first 4 months after topdressing high loadings of sulphur were observed in run-off. This is consistent with the mobility of the sulphate ion, and the decrease in sulphate-retentive property of the soil following application of superphosphate, (Saunders 1974).

The phosphate concentration in run-off is relatively low because of its marked tendency for adsorption onto poorly ordered hydrous oxides of iron and aluminium. However, this soil (0-7.5 cm) shows a significantly higher P-retention (39%) than other wet terrace land soils (e.g. Maimai type sites, 5%; Lee (1977)). This can be attributed to the presence of more poorly ordered iron and aluminium coatings (c.f. Maimai type site, Tamm's Fe and Al 0.04% and 0.03% respectively; this soil 0.4% and 0.2%).

The horizontal bars in Fig. 1 represent the mean levels of nutrient determined for samples collected over a period of weeks in catchment troughs imbedded in the field. In each case these concentrations are greater than or similar to the mean values determined for samples collected from running water in drains. It appears that surface water and near-surface water (to depth 1cm) which seep slowly into the troughs after the 'flood' of surface run-off has occurred carry a larger concentration of dissolved nutrient. In a subsequent year samples collected in troughs were analysed after heavy rainfall events. Nutrient concentrations were substantially higher than observed in drains and streams: potassium, up to 60 ppm; calcium, up to 28 ppm; phosphorus, up to 5 ppm. This is consistent with McColl's findings (1979). Results from small catchments can give a distorted picture of nutrient loss as there is no input of nutrients by surface flow from adjacent areas and the recorded volumes and concentrations may not represent values for water crossing a stream edge.

ESTIMATED LOSS OF NUTRIENT IN RUN-OFF

To calculate the total loss of nutrient in run-off it is necessary to also know (i) the percentage of precipitation appearing as surface run-off, and (ii) the input of nutrients in rainfall. The losses for each nutrient have been calculated from Fig. 1 by multiplying the average concentration of nutrient in run-off for the period between two samplings by the volume of run-off leaving the area. The volume of run-off from a catchment (assuming no vertical drainage) can be estimated as the difference between the known volume of precipitation, V_p, and the loss via evapotranspiration, V_e, if permanent saturation of the soil is assumed. The average Penman value of V_e for Hokitika is 708 mm/year (Coulter, 1977); a similar or smaller value would be applicable at Bell Hill. An estimated value of $V_p - V_e$ for the catchment for 1975-6, (2700-708 mm)would represent the minimum volume of run off expected (74% of V_p). Field measurements on two small catchments have indicated a run-off of 80 - 90% of precipitation. In this work the approximate figure of 80% was assumed.

The estimated losses of nutrient within 5 months of topdressing were sulphur 12 kg/ha, potassium 20 kg/ha, and phosphorus 2.5 kg/ha.

In these estimates no allowance was made for the input of nutrient via rainfall. This input was difficult to assess because of variation which we ascribed to the effects of wind-blown fertilizer originating from adjacent farming operations through spring and summer. Measurements reported by Campbell (1975) for the Taipo-Taramakau area indicate mean annual levels of 0.07 ppm K in rainfall (an accession of 1.5 kg/ha) and 0.04 ppm for Ca (1.1 kg/ha); these levels may be applicable in the study area.

ESTIMATED LOSS OF FERTILIZER

To estimate the loss of fertilizer in run-off it is necessary to subtract the "base-line" concentration of each nutrient, i.e. the concentration arising from soil weathering and from residues of fertilizer applied in previous years.

For potassium and sulphur the concentrations of nutrient in run-off (in winter and spring) prior to application of fertilizer were c 20% and 10% respectively of the maximum values attained after fertilizer was applied (Fig. 1). Thus a portion of the observed concentration did not arise from fertilizer applied immediately prior to sampling. There were insufficient data to allow accurate estimates of these "base-line" concentrations. However in terms of nutrient balance it is meaningful to express the cumulative loss as a percentage of the nutrient (fertilizer) applied in a given year.

Figure 2 shows the cumulative loss of each nutrient with time following topdressing, expressed as a percentage of the amount of each applied. The loss of sulphur was equivalent to c. 37% of applied sulphate-sulphur within 5 months of topdressing, the potassium loss was 28% and the phosphorus loss was equivalent to 6% of applied PO_4^{3-}-P. Loss of sulphur diminished abruptly after 4 months whereas loss of potassium continued steadily (to 32% after 6½ months).

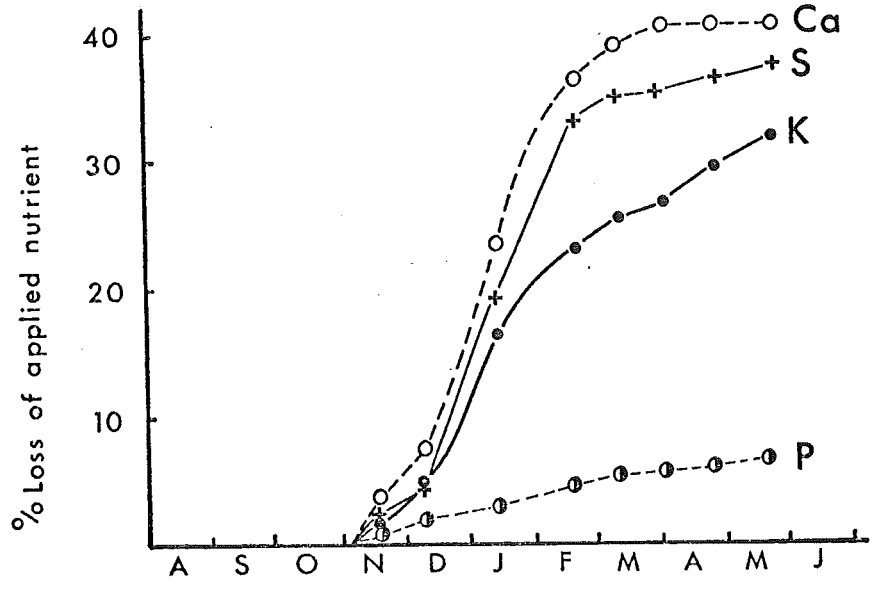

Fig. 2. Cumulative mass loss of nutrient in run-off expressed as a percentage of nutrient applied in fertilizer. Measurements commence at time of application (November).

In contrast the profile for calcium (Fig. 1) indicates appreciable concentration at all times, with an increased concentration following topdressing. However, superphosphate applied in early summer is a minor source of calcium relative to lime. When the concentration of calcium is referenced to the background level of c 4 ppm as observed in winter and spring (and assumed to derive from slow dissolution of lime) the percent loss of calcium applied in superphosphate is assessed as 40% in the first 5 months following topdressing (Fig. 2).

It is stressed that these results are valid only for the year and site of sampling. The concentration of nutrient in run-off will vary with the pattern and intensity of rainfall, with time and rate of application of fertilizer, and for individual soils grouped within the Maimai series. Estimation of nutrient concentration in run-off is limited by sampling. The estimation of total fertilizer loss is more difficult and is dependent on assumptions about total run-off and "base-line" concentrations of nutrient in run-off. However, these results do afford a basis for estimating losses from wet terrace land soils.

REFERENCES

Campbell, A.S. (1975). Chemical and mineralogical properties of a sequence of terrace soils near Reefton. Ph.D. Thesis. Lincoln College, University of Canterbury.

Coulter, J.D. (1977). Private communication.

Dowling, F. and Powell, H.K.J. (1979). A siphon device for fractionation of run-off samples. New Zealand Journal of Agricultural Research, in press

Lee, R. (1977). In Field demonstration and workshop on soils of West Coast wet terrace lands. Unpublished report, N.Z. Soil Bureau.

McColl, R.H.S. and Gibson, A.R. (1979). Downslope movement of nutrients in hill pasture, Taita, New Zealand. Parts I and II. N.Z. Journal of Agricultural Research, 22, 143-50, 151-61.

Mew, G., and Ross, C.W. (1975). Soils of the Grey Valley: Soil unit sheets. Unpublished report, N.Z. Soil Bureau.

Saunders, W.M.H. (1974). Effect of superphosphate topdressing on phosphate and sulphate retention. N.Z. Soil News, 22, 15-22.

R E F E R E N C E S

1. Jenny, H. Factors of Soil Formation. New York, McGraw-Hill, 1941.

2. Buckman, H.O.; Brady, N.C. The Nature and Properties of Soils. 6th Ed. New York, The Macmillan Company, 1960. p303.

3. Stobbe, P.C.; Wright, J.R. Soil Sci. Soc. Amer. Proc., 23:161 - 164. 1959.

4. Deb, B.C. J. Soil Sci., 1:112 - 122. 1949.

5. Jones, H.T.; Wilcox, J.S. J. Soc. Chem. Ind., 48:304T - 308T. 1929.

6. Rode, A.A. Pochvovedenie, 32:849 - 862. 1937. Referenced in: Joffe, J.S. Pedology. 2nd Ed. New Brunswick, Pedology Publications, 1949. p350.

7. Schnitzer, M. Soil Sci. Soc. Amer. Proc., 33:75 - 81. 1969.

8. Bloomfield, C. Proc. Easter Sch. Agr. Sci., Univ. Nottingham, 1964 (11):257 - 266.

9. Schnitzer, M.; DeLong, W.A. Sci. Agr., 32:680 - 681. 1952.

10. Bloomfield, C. Nature 170:540. 1952.

11. Bloomfield, C. J. Soil Sci., 4:5-16. 1953.

12. Bloomfield, C. J. Soil Sci., 4:17 - 23. 1953.

13. Bloomfield, C. J. Soil Sci., 5:39 - 45. 1954.

14. Bloomfield, C. J. Soil Sci., 5:46 - 49. 1954.

15. Bloomfield, C. J. Soil Sci., 5:50 - 56. 1954.

16. Bloomfield, C. J. Sci. Food Agric., 8:389 - 392. 1957.

17. Loissaint, P. Ann. Agron., Paris, 10:369 - 414; 493 - 542. 1959.

18. Coulsen, C.B.; Davies, R.I.; Lewis, D.A. J. Soil Sci., 11:30 - 44. 1960.

19. Hingston, F.J. Aust. J. Soil Res., 1:67 - 73. 1963.

20. Muir, J.W.; Logan, J.; Brown, C.J. J. Soil Sci., 15:226 - 237. 1964.

21. Ellis, R.C. J. Soil Sci., 22:8 - 12. 1971.

22. Bloomfield, C. Chem. Ind., 1958:259 - 260.

23. Bloomfield, C. Rothamsted Experimental Station, Hapenden, Herts., Report 1963. pp226 - 239.

24. Schnitzer, M.; DeLong, W.A. Can. J. Agr. Sci., 34:542 - 543. 1954.

25. Schnitzer, M.; Delong, W.A. Soil Sci. Soc. Amer. Proc., 19:360 - 368. 1955.

26. Schnitzer, M. Chem. Ind., 1957:1594 - 1595.

27. Fisher, R.F. Soil Sci. Soc. Amer. Proc., 36:492 - 495. 1972.

28. Bloomfield, C. Chem. Ind., 1955:1596 - 1597.

29. Schwarzenbach, G. Analyst, 80:713 - 729. 1955.

30. Schatz, A.; Schatz, V.; Schalscha, E.B.; Martin, J.J. Compost Sci., 4:25 - 28. 1964.

31. Barshad, I. Chemistry of the Soil. 2nd Ed. Ed. by Bear, F.E. New York, Reinhold, 1967. ppl - 70.

32. Swindale, L.D.; Jackson, M.L. Trans. Intern. Congr. Soil Sci. 6th Congr., Paris. E:233 - 239. 1956.

33. Atkinson, H.J.; Wright, J.R. Soil Sci., 84:1 - 11. 1957.

34. Mortensen, J.L. Soil Sci. Soc. Amer. Proc., 27:179 - 186. 1963.

35. Bate-Smith, E.C. Proc. Roy. Dublin Soc., 27:165 - 176. 1956.

36. Muir, J.W.; Morrison, R.I.; Brown, C.J.; Logan, J. J. Soil Sci., 15:220 - 225. 1964.

37. Morita, H. Proc. 3rd Int. Peat Congress, 1968. pp28-31.

38. Greenwood, D.J.; Lees, H. Plant and Soil, 12:69 - 80. 1960.

39. Swain, T.; Hillis, W.E. J. Sci. Food Agric., 10:63 - 68. 1959.

40. Putnam, H.D.; Schmidt, E.L. Soil Sci., 87:22 - 27. 1959.

41. Flaig, W. Soil Sci., 111:19 - 33. 1971.

42. Morita, H. Soil Sci., 120:112 - 116. 1975.

43. Coulsen, C.B.; Davies, R.I.; Lewis, D.A. J. Soil Sci., 11:20 - 29. 1960.

44. White, T. J. Sci. Food Agric., 8:377 - 385. 1957.

45. McHardy, W.J.; Thomson, A.P.; Goodman, B.A. J. Soil Sci., 25:471 - 483. 1974.

46. Rossotti, F.J.C.; Rossotti, H. The Determination of Stability Constants. New York, McGraw-Hill, 1961.

47. Tyson, C.A.; Martell, A.E. J. Amer. Chem. Soc., 90:3379 - 3386. 1968.

48. Ahrland, S.; Chat, J.; Davies, N.R. Quart. Revs., 12:265 - 276. 1958.

49. Hard and Soft Acids and Bases. Ed. by Pearson, R.G. Stroudsburg, Dowden, Hutchinson and Ross, 1973.

50. Wesp, E.F.; Brode, W.R. J. Amer. Chem. Soc., 56:1037 - 1042. 1934.

51. Ackermann, G.; Hesse, D. Z. Anorg. Allg. Chem., 375:77 - 86. 1970.

52. Mattil, K.F.; Filer, L.J. Ind. Eng. Chem., 16:427 - 429. 1944.

53. Yoe, J.H.; Jones, A.L. Ind. Eng. Chem. Anal. Ed., 16:111 - 115. 1944.

54. Avdeef, A.; Sofen, S.R.; Brengante, T.L.; Raymond, K.N. J. Amer. Chem. Soc., 100:5362 - 5370. 1978.

55. Harris, W.R.; Weitl, F.L.; Raymond, K.N. J. Chem. Soc. Chem. Comm., 1979:171 - 178.

56. Sylva, R.N. Rev. Pure Appl. Chem., 22:115 - 131. 1972.

57. Sillen, L.G.; Martell, A.E. Chem. Soc. Spec. Publ., No. 17. 1964.

58. Mentasti, E.; Pelizzetti, E.; Saini, G. J. Chem. Soc. Dal. Trans., 1973:2609 - 2614.

59. Shah, R.C. Chem. Abstr., 77:7072y. 1972.

60. McBryde, W.A.E. Can. J. Chem., 42:1917 - 1927. 1964.

61. Mentasti, E.; Pelizzetti, E.; Saini, G. J. Inorg. Nucl. Chem., 38:785 - 788. 1976.

62. Mentasti, E.; Pelizzetti, E.; Giraudi, G. Z. Phys. Chem., 100:17 - 23. 1976.

63. Migal, P.K.; Ivanov, V.A. Russ. J. Inorg. Chem., 18:536 - 540. 1973.

64. Jameson, R.F.; Neillie, W.F.S. J. Chem. Soc., 1965:2391 - 2395.

65. Gorton, J.E.; Jameson, R.F. J. Chem. Soc., 1968:2615 - 2618.

66. Mentasti, E.; Pelizzetti, E.; Saini, G. J. Chem. Soc. Dal. Trans., 1973:2605 - 2608.

67. Loginova, L.F.; Medyntsev, V.V.; Khomutov, B.I. Zh. Obsh. Khim., 42:739 - 742. 1972.

68. Ball, E.G.; Chen, T.T. J. Biol. Chem., 102:691 - 709. 1933.

69. Kortum, G.; Vogel, W.; Andrussow, K. Dissociation Constants of Organic Acids in Aqueous Solutions. London, Butterworths, 1961. pp190 - 535.

70. Koch, Von S.; Ackermann, G. Z. Anorg. Allg. Chem., 400:21 - 28. 1973.

71. Buffle, J.; Martell, A.E. Inorg. Chem., 16:2221 - 2229. 1977.

72. Boggess, R.K.; Martin, R.B. J Amer. Chem. Soc., 97:3076 - 3081. 1975.

73. Research pH Meter, Operating Instructions 1226 - B, Beckman Instruments Inc., California, 1963.

74. PHM64 Research pH Meter, Operating Instructions 7612C, Radiometer, Copenhagen.

75. Glass Electrodes, Operating Instructions 678 - D, Beckman Instruments Inc., California, 1966.

76. Combined Electrodes, Operating Instructions 7802F, Radiometer, Copenhagen.

77. Hedwig, G.R. Ph.D. Thesis. University of Canterbury, 1972. pp26 - 27.

78. Bates, R.G. Determination of pH, Theory and Practice. 2nd Ed. New York, J. Wiley & Sons, 1973. pp91 - 99.

79. Vogel, A.I. A Textbook of Quantitative Inorganic Analysis. 3rd Ed. London, Longmans Green & Co., 1961. p238.

80. Hamer, W.J.; Pinching, G.D.; Acree, S.F. J. Res. N.B.S., 35:539 - 564. 1945.

81. McBryde, W.A.E. Analyst, 94:337 - 346, 1969.

82. Russell, J.M.R. Ph.D. Thesis. University of Canterbury, 1977. p88.

83. Hamer, W.J.; Acree, S.F. J. Res. N.B.S., 35:381 - 416. 1945.

84. C.R.C. Handbook of Chemistry and Physics. 52nd Ed. 1971 - 2. pD205.

85. Reference 84, pF4.

86. Reference 82, p89.

87. Kee, T.S. M.Sc. Thesis. University of Canterbury, 1975. pp8 - 11.

88. Beckman 100802 Fieldlab Oxygen Analyser, Operating Instructions, Beckman Instruments Inc., California.

89. Reference 84, pD111.

90. Kozarek, W.J.; Fernando, Q. J. Chem. Ed., 49:202 - 204. 1972.

91. Reference 79, p196.

92. Reference 77, p24.

93. Sorensen, S.P.L. Biochem. Z., 21:131, 201. 1909.

94. Gold, V. pH Measurements, Their Theory and Practice. London, Methuen & Co. Ltd, 1956.

95. Sorensen, S.P.L., Linderstrom-Lang, K. Compt. Rend. Trav. Lab. Carlsberg., 15:No. 6. 1924.

96. Reference 78, p27.

97. Reference 78, p73.

98. Butikofer, H.P.; Covington, A.K. Anal. Chem. Acta, 108:179 - 191. 1979.

99. Durst, R.A. N.B.S. Spec. Publ. 260 - 53. 1975.

100. Reference 78, pp88 - 90.

101. Reference 78, pp85 - 86.

102. Morf, W.E. Talanta, 26:719 - 725. 1979.

103. Reference 78, pp377 - 384.

104. Reference 78, p23.

105. Bates, R.G., Pinching, G.D.; Smith, E.R. J. Res. N.B.S., 45:418 - 429. 1950.

106. Bates, R.G.; Bower, V.E.; Smith, E.R. J. Res. N.B.S., 56:305 - 312. 1956.

107. Reference 46, pp13 - 14.

108. Reference 78, pp256 - 257.

109. Albert, A.; Serjeant, E.P. Ionisation Constants of Acids and Bases. London, Methuen & Co. Ltd., 1962. p62.

110. Davies, C.W. J. Chem. Soc., 1938:2093 - 2098.

111. Reference 77, pp58 - 59.

112. McBryde, W.A.E. Analyst, 96:739 - 740. 1971.

113. Reference 78, pp262 - 263.

114. Powell, H.K.J.; Curtis, N.F. J. Chem. Soc. (B), 1966: 1205 - 1211.

115. Hedwig, G.R.; Powell, H.K.J. Anal. Chem., 43:1206 - 1212. 1971.

116. Avdeef, A.; Bucher, J.J. Anal. Chem., 50:2137 - 2142. 1978.

117. Manov, G.G.; Bates, R.G.; Hamer, W.J.; Acree, S.F. J. Amer. Chem. Soc., 65:1765 - 1767. 1943.

118. Harned, H.S.; Owen, B.B. The Physical Chemistry of Electrolyte Solutions. 2nd Ed. New York, Reinhold, 1950. pp485 - 489.

119. Reference 77, Appendices C and D.

120. Reference 82, pp110 - 114.

121. Vacca, A.; Sabatini, A.; Gristina, M.A. Coord. Chem. Rev., 8:45 - 53. 1972.

122. Reference 78, pp265 - 266.

123. Reference 78, p268.

124. Rossotti, F.J.C. Modern Co-ordination Chemistry. Ed. by Lewis, J.; Wilkins, R.G. New York, Interscience, 1970. ppl - 77.

125. Abichandani, C.J.; Jatkar, S.K.K. J. Ind. Inst. Sci., 21A:417 - 441. 1938.

126. Patel, D.C.; Bhattacharya, P.K. Ind. J. Chem., 8:835 - 837. 1970.

127. Agrawal, M.D.; Bhandari, C.S.; Dixit, M.K.; Sogani, N.C. Monat. Chem., 107:75 - 82. 1976.

128. Murakami, Y.; Nakamura, K.; Takunaga, M. Bull. Chem. Soc. Japan, 36:669 - 675. 1963.

129. L'Heureux, G.A.; Martell, A.E. J. Inorg. Nucl. Chem., 28:481 - 491. 1966.

130. Bartusek, M.; Zelinka, J. Coll. Czech. Chem. Comm., 32:992 - 1005. 1967.

131. Rodd's Chemistry of Carbon Compounds. 2nd Ed. Ed. by Coffey, S. Amsterdam, Elsevier Scientific Publishing Company, 1976. Vol 3, part D, pp194 - 195.

132. Grimshaw, J.; Haworth, R.D.; Pindred, H.K. J. Chem. Soc., 1955: 833 - 837.

133. Forbes, W.F. Interpretive Spectroscopy. Ed. by Freeman, S.K. New York, Reinhold, 1965. ppl - 25.

134. Scott, A.I. Interpretation of the Ultraviolet Spectra of Natural Products. Oxford, Pergamon Press, 1964. pp89 - 134.

135. Luessing, D.L.; Kolthoff, I.M. J. Amer. Chem. Soc., 75:2476 - 2479. 1953.

136. Mason, H.S. J. Biol. Chem., 181:803 - 812. 1949.

137. Vareille, L. Bull. Soc. Chim. France, 1955:870 - 872.

138. Job, P. Ann. Chim., 10:9 - 113. 1928.

139. Woldbye, F. Acta Chem. Scand., 9:299 - 309. 1955.

140. Laurence, G.S.; Ellis, K.J. J. Chem. Soc. Dal., 1972:1667 - 1670.

141. Petersen, L. Podzols and Podzolization. Copenhagen, DSR Forlag, 1976.

142. Ghosh, M.M. In Aqueous-Environmental Chemistry of Metals. Ed. by Rubin, A.J. Michigan, Ann Arbor, 1976. pp193 - 217.

143. Powell, H.K.J.; Taylor, M.C. In Soil Groups of New Zealand, Gley Podzols. N.Z. Soc. Soil Sci., 1980 (in print).

144. Wellman, H.W.; Willett, R.W. Trans. N.Z. Inst., 71:282 - 306. 1942.

145. Suggate, R.R. N.Z. Geol. Survey Bull., 77:48 - 51. 1965.

146. Young, D.J. N.Z. J. Geol. Geophysics, 10:647. 1967.

147. Mew, G. In Workshop on Gley Podzol Research, Lincoln College. Unpublished report, N.Z. Soil Bureau, Compiled by J.A. Adams. 1975.

148. Mew, G.; Ross, C.W. Soils of the Grey Valley: Soil unit sheets. Unpublished report, N.Z. Soil Bureau. 1975.

149. Lee, R. In Field Demonstration and Workshop on Soils of West Coast Wet Lands. Unpublished reports, N.Z. Soil Bureau. 1977, 1978.

150. Mew, G. Field Demonstration of West Coast Wet Land Soils, Tour Notes. 1977, 1978.

151. Smith, G.S.; Middleton, K.R.; Smith, R.G. N.Z. J. Exp. Agric., 4:423 - 427. 1976.

152. Gibbs, H.S.; Mercer, A.O.; Collie, T.W. D.S.I.R., Soil Bur. Bull., 2:Map No. 1. 1950.

153. Powell, H.K.J.; Taylor, M.C. In Soil Groups of New Zealand, Gley Podzols. N.Z. Soc. Soil Sci., 1980 (in print).

154. Lee, E.S.; Powell, H.K.J.; Taylor, M.C.; Tsao, N.Y. N.Z. J. Sci., 22:35 - 38. 1979.

155. Tsao, N.Y. M.Sc. Thesis. University of Canterbury, 1976. pp30 - 33.

156. Lee, E.S. M.Sc. Thesis. University of Canterbury, 1976. pp66 - 80.

157. Reference 155, pp37 - 72.

158. Adams, J.A.; Wilde, R.H. N.Z. J. Agric. Res., 19:435 - 442. 1976.

159. Langley, R. Practical Statistics, For Non-Mathematical People. London, Pan Books Ltd., 1968. p43.

160. Blackemore, L.C.; Searle, P.L.; Daly, B.K. N.Z. Soil Bureau Scientific Report, 10A. 1972.

161. Jackson, M.L. Soil Chemical Analysis - Advanced Course Univ. of Wisconsin, Madison, Wisconsin, 1956. pp31 - 188.

162. Reference 160, ppA1.1 - A1.5.

163. Metson, A.J.; Arbuckle, R.H.; Saunders, M.L. Trans. Int. Congr. Soil Sci. 6th, B:619 - 627. 1956.

164. Metson, A.J. In N.Z. Soil Bureau Bull., 26(2):76 - 82. 1968. (See also reference 160, pA7.B).

165. Fox, R.L.; Kamprath, E.J. Soil Sci. Soc. Amer. Proc., 34:902 - 907. 1970.

166. Reference 155, pp73 - 75.

167. Watanabe, F.S.; Olsen, S.R. Soil Sci. Soc. Amer. Proc., 29:677 - 678. 1965.

168. Reference 160, A5.1 - A5.11.

169. During, C.; Martin, D.J. N.Z. J. Agric. Res., 11:665 - 676. 1968.

170. Reference 160, A11.1 - A11.7.

171. Reference 160, A3.1 - A3.9.

172. Reference 160, A4.1 - A4.6.

173. Kidson, E.B. N.Z. J. Sci. Tech., 18:694 - 707. 1937.

174. Ure, A.M.; Mitchell, R.L. Spectrochimica Acta, 23B:79 - 96. 1967.

175. Mitchell, R.L. Atti Simp. Int. Agro - Chimica, 9:521 - 532. 1972.

176. Rana, S.K.; Ouellette, G.L. J. Ind. Soc. Soil Sci., 16:89 - 91. 1968.

177. Mew, G. private communication.

178. Taylor, N.H.; Pohlen, I.J. N.Z. Soil Bureau Bull., 25:82 - 89. 1970.

179. Campbell, A.S. PhD Thesis. Lincoln College, University of Canterbury, 1975. pp43 - 45.

180. Reference 179, pp201 - 202.

181. Saunders, W.M.H. In N.Z. Soil Bureau Bull., 26(2):95 - 103. 1968.

182. Deb, B.C. J. Soil Sci., 1:212 - 220. 1950.

183. Reference 141, pp77 - 109.

184. Hennessy, W. B.Sc. Hons. Project. University of Canterbury, 1975.

185. Reference 156, pp50 - 58.

186. McKeague, J.A.; Day, J.H. Can. J. Soil Sci., 49:161 - 163. 1969.

187. Reference 155, pp28 - 29, 49 - 53.

188. Metson, A.J. N.Z. Soil Bureau Bull., 12:168 - 175. 1971.

189. Young, A.W., private communication.

190. Saunders, W.M.H. N.Z. J. Agric. Res., 8:30 - 57. 1964.

191. Chao, T.T.; Harward, M.E.; Fang, S.C. Soil Sci. Amer. Proc., 26:234 - 237. 1962.

192. Reference 179, pp54 - 64.

193. During, C. Fertilizers and Soils in New Zealand. Wellington, N.Z. Dept. Agric. Bull. No. 409., 2nd Ed. 1972. pp159 - 161.

194. Beckett, P.H.T.; Webster, R. Soils and Fertilizers, 34:1 - 15. 1971.

195. Ball, D.F.; Williams, W.M. J. Soil Sci., 22:60 - 68. 1971.

196. Miller, R.B. In N.Z. Soil Bureau Bull. 26(2):72 - 75. 1968.

197. Reference 193, pp11 - 22.

198. Beckwith, R.S. Aust. J. Agric. An. Hus., 5:52 - 58. 1964.

199. Reference 193, pp23 - 49.

200. Reference 193, pp50 - 63.

201. Reference 193, pp1 - 10.

202. Powell, H.K.J., private communication.

203. Metson, A.J. Int. Congr. Soil Sci. 9th Trans., 2:621 - 629. 1968.

204. Powell, H.K.J.; Taylor, M.C. In Soil Groups of New Zealand, Gley Podzols. N.Z. Soc. Soil Sci., 1980 (in print).

205. McNaught, K.J. Proc. 11th Int. Grasslands Congr., 1970. pp334 - 338.

206. Reference 193, p90.

207 Ryden, J. C.; Syers, J.K. Nature 255:51 - 53. 1975.

208. Saunders, W.M.H. N.Z. Soil News, 22:15 - 22. 1974.

209. Mitchell, R.L. Neth. J. Agric. Sci., 22:295 - 304. 1974.

210. Wells, N. In Soils of New Zealand, Pt 2., Soil Bureau Bulletin 26(2):129. 1968.

211. O'Connor, M.B. Changes in Chemical and Physical Properties with Development on an Addison Gley Podzol, Westport. Unpublished Report. 1979.

212. Reference 78, p453.

213. Reference 78, p450

214. Jones, M.M. Elementary Coordination Chemistry. Englewood Cliffs, Prentice-Hall, Inc. 1964.

215. Sampford, M.R. An Introduction to Sampling Theory. London, Oliver and Boyd. 1962.